

**TORSIONAL BEHAVIOUR OF ELEVATED WATER TANKS
WITH REINFORCED CONCRETE FRAME-TYPE STAGINGS
DURING EARTHQUAKES**

A Thesis Submitted
in Partial Fulfillment of the Requirements
for the Degree of
DOCTOR OF PHILOSOPHY

by
SEKHAR CHANDRA DUTTA

to the
**DEPARTMENT OF CIVIL ENGINEERING
INDIAN INSTITUTE OF TECHNOLOGY KANPUR**
October 1995

23 JUL 1977
CENTRAL LIBRARY
I. I. T., KANPUR
Inv. No. A. 121910

CE - 1995 - D - DUT - TOR



A121910

CERTIFICATE

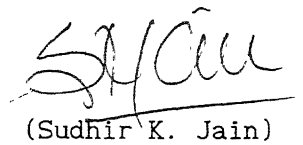
6/10/95
S.K.J.

It is certified that the work contained in the thesis entitled "Torsional Behaviour of Elevated Water Tanks with Reinforced Concrete Frame-Type Stagings During Earthquakes" by Mr. Sekhar Chandra Dutta, has been carried out under our supervision and that this work has not been submitted elsewhere for a degree.

October 1995


(C.V.R. Murty)

Assistant Professor


(Sudhir K. Jain)

Associate Professor

Department of Civil Engineering
Indian Institute of Technology Kanpur

ABSTRACT

Elevated water tanks have failed during past earthquakes owing to large torsional response. Considerable torsional response may occur due to accidental eccentricity if the uncoupled torsional and lateral natural periods of the tanks are closely spaced. Torsional response of RC elevated water tanks supported on axisymmetric frame-type stagings has been studied in this thesis.

Such stagings are idealized as one-storey lateral-torsional coupled systems consisting of two or four lateral force resisting elements, depending on the lateral-to-torsional stiffness ratio and lateral-to-torsional strength ratio of the staging. Linear and non-linear responses of these systems are studied due to earthquake ground motions. This study focusses attention on the maximum element displacement. Between two systems having the same lateral and torsional natural periods, normalized eccentricity and modal damping, the one with a lower torsional-to-lateral stiffness ratio, *i.e.*, tanks with small number of panels and columns, undergoes a larger torsional response. Also, in the elastic range the element displacement takes a minimum value at a torsional-to-lateral natural period ratio (τ) very close to 1.0 and a maximum value each on either side of this minimum. The range $0.7 < \tau < 1.25$ is found critical from torsion view point.

Nonlinear behaviour is studied through a simple strength-deteriorating hysteresis model. In general, the idealized two-element systems (*i.e.*, staging with low number of columns and

panels) are found more vulnerable than the four-element systems (*i.e.*, stagings with large number of columns and panels). The element displacements are found to be significantly larger than those of the corresponding symmetric systems, if the rate of strength deterioration is large or if the ductility reduction factor used in design is 2 or more.

The dynamic characteristics of usually constructed elevated water tanks on a circular row of columns and circumferential beams are studied. Approximate expressions for the torsional and lateral stiffnesses, and for the natural period ratio (τ) are derived. These tanks are found to generally have τ in the critical range identified in the linear study.

Four alternate staging configurations are studied: with radial beams, with radial beams and central column, with two circular rows of columns, and with diagonal braces. Expressions for estimating their lateral and torsional stiffnesses and natural period ratio (τ) are derived. First three of these configurations are found to have higher value of τ than that of the corresponding basic configuration, and the fourth configuration has a lower value. These configurations can be utilized to avoid large torsional response and to retrofit existing stagings.

panels) are found more vulnerable than the four-element systems (*i.e.*, stagings with large number of columns and panels). The element displacements are found to be significantly larger than those of the corresponding symmetric systems, if the rate of strength deterioration is large or if the ductility reduction factor used in design is 2 or more.

The dynamic characteristics of usually constructed elevated water tanks on a circular row of columns and circumferential beams are studied. Approximate expressions for the torsional and lateral stiffnesses, and for the natural period ratio (τ) are derived. These tanks are found to generally have τ in the critical range identified in the linear study.

Four alternate staging configurations are studied: with radial beams, with radial beams and central column, with two circular rows of columns, and with diagonal braces. Expressions for estimating their lateral and torsional stiffnesses and natural period ratio (τ) are derived. First three of these configurations are found to have higher value of τ than that of the corresponding basic configuration, and the fourth configuration has a lower value. These configurations can be utilized to avoid large torsional response and to retrofit existing stagings.

ACKNOWLEDGEMENTS

I sincerely express my deep sense of gratitude and sincere thanks to my thesis supervisors, Dr. Sudhir K. Jain and Dr. C.V.R. Murty for their valuable guidance, critical discussions, timely help of all kinds, continuous encouragement and kind-hearted affection throughout my association with them. It is their whole-hearted cooperation and meticulous scientific attitude which enabled me to complete this undertaking with ease and comfort. I also gratefully acknowledge the monetary support extended by them as and when required.

I also express my gratitude to other faculty members at I.I.T. Kanpur who taught me during the course work.

The friendship extended by my colleague Gehad Ez-Eldin Rashad is gratefully acknowledged. I would like to place on record my sincere thanks to Shri T. Sadagopan and Shri Moti Lal whose assistance throughout my doctoral program has enabled me to conduct many activities with relative ease. I am extremely thankful to Mr. J.V. Rao, Mr. G. Subrahmanyam and Mr. K.S.N Gupta for their help and mental support extended to me during the preparation of this thesis.

Sincere thanks are also due to the numerous students of I.I.T Kanpur, interaction with whom made my stay at I.I.T. Kanpur colourful and pleasing.

Finally, I wish to dedicate my thesis to my parents without whose inspiration and encouragement this thesis may never have been written.

TABLE OF CONTENTS

	Page No.
Abstract	(i)
Acknowledgements	(iii)
Table of Contents	(iv)
List of Tables	(ix)
List of Figures	(x)
List of Symbols	(xiv)

CHAPTER 1 : INTRODUCTION

1.1	General	1
1.2	Damages to Liquid Storage Tanks During Past Earthquakes	1
1.2.1	Shell Buckling of Steel Tank Container	2
1.2.2	Damage of Steel Tank Roof	2
1.2.3	Foundation Failure	2
1.2.4	Failure of Piping and Other Accessories	3
1.2.5	Failure of Tank Support System	3
1.2.6	Torsional Failure of Elevated Water Tanks	4
1.3	Past Research on Seismic Behavior of Elevated Water Tanks	5
1.3.1	Ground Supported Rigid Tanks	5
1.3.2	Ground Supported Flexible Tanks	6
1.3.3	Unanchored Tanks	7
1.3.4	Experimental Tests on Tanks	7
1.3.5	Tanks under Vertical Excitation	8
1.3.6	Effect of Soil-Structure Interaction on Seismic Response of Tanks	8
1.3.7	Elevated Water Tanks	9
1.4	Objectives of the Present Study	11
1.5	Organization of the Thesis	13
1.6	Sign Convention, Notation and Units	14
1.7	References	14
	Figures	20

CHAPTER 2 : LATERAL-TORSIONAL COUPLING IN THE LINEAR ELASTIC RESPONSE

2.1	Introduction	21
2.2	Modelling of Elevated Water Tanks	22
2.2.1	Idealization	22
2.2.2	Systems Considered	23
2.2.3	Equations of Motion	26

2.2.4	Response Quantities of Interest	26
2.3	Free Vibration Characteristics	28
2.4	Ground Motions Used	29
2.4.1	Harmonic Single-Frequency Synthetic Ground Motion	29
2.4.2	Spectrum-Consistent Synthetic Ground Motion	30
2.4.3	Ground Motions With Idealized Spectra	30
2.5	Damping	31
2.6	Parameters Considered	32
2.6.1	Uncoupled Lateral Natural Period, T_x	32
2.6.2	Uncoupled Natural Period Ratio, τ	32
2.6.3	Normalized Eccentricity	33
2.7	Study Under Harmonic Ground Motions	33
2.7.1	Analytical Derivation	33
2.7.2	Results and Discussion	36
2.8	Study Under Spectrum-consistent Synthetic Ground Motion	38
2.8.1	Numerical Analysis	38
2.8.2	Results and Discussion	38
2.8.2.1	Rotational Response	38
2.8.2.2	Element Displacement	39
2.9	Study Under Idealized Spectra	41
2.9.1	Analysis	41
2.9.2	Results and Discussion	42
2.10	Conclusions	44
2.11	References	45
	Figures	47

CHAPTER 3 : INELASTIC TORSIONAL RESPONSE

3.1	Introduction	62
3.2	Systems Considered	64
3.2.1	Nature of Eccentricity	66
3.3	Equations of Motion and Ground Motions Used	69
3.4	Hysteresis Model For Strength Deterioration	71
3.5	Ductility Reduction Factor, R_μ	75
3.6	Effect of Strength Deterioration	76
3.6.1	Study of Two-Element Systems	76
3.6.2	Study of Four-Element Systems	79
3.7	Behaviour of Elevated Water Tanks Located Near The Faults	82
3.7.1	Variation of Parameters	83
3.7.2	Results and Discussion	83
3.8	Conclusions	84
3.9	References	86
	Figures	89

CHAPTER 4 : DYNAMIC CHARACTERISTICS OF THE BASIC STAGING CONFIGURATION

4.1	Introduction	106
4.2	Analytical Expressions for Characteristic Quantities	107
4.2.1	Stiffness	107

4.2 1.1	Lateral Stiffness	108
4.2.1.2	Torsional Stiffness	112
4.2.2	Inertial Mass	113
4.2.3	Bending Moments and Shear Forces in Staging Members	114
4.2.3.1	Under Lateral Force	115
4.2.3.1.1	Beams	115
4.2.3.1.2	Columns	116
4.2.3.1.3	Bending Moments' and Shear Forces' Ratio	118
4.2.3.2	Under Torsional Moment	120
4.2.3.2.1	Beams	120
4.2.3.2.2	Columns	121
4.2.3.2.3	Bending Moments' and Shear Forces' Ratios	122
4.3	Numerical Study	122
4.3.1	Parameters Studied	122
4.3.1.1	Natural Period Ratio (τ)	122
4.3.1.2	Ratio of Member Forces' Ratios under Torsion and Lateral Force	124
4.3.1.2.1	Ratio of Bending Moments' Ratio	124
4.3.1.2.2	Ratio of Shear Forces' Ratios	125
4.3.2	Ranges of Parameters Studied	126
4 4	Results & Discussions	127
4.4.1	Study of Stiffness Ratio K_{θ}/K_x	127
4.4.2	Study of Natural Period Ratio (τ)	127
4.4.2.1	Effect of ρ	127
4.4.2.2	Effect of Depth of Water (h_w)	128
4.4.3	Effect of Different Design Parameters on τ	129
4.4.4	Adequacy Under Torsion, of Staging Members Designed for Lateral Force Alone	130
4.4.4.1	Adequacy of Design for Flexure	130
4.4.4.2	Adequacy of Design for Shear	130
4.5	Conclusions	131
4.6	References	132
	Tables	134
	Figures	137

CHAPTER 5 : ALTERNATE STAGING CONFIGURATIONS TO REDUCE TORSIONAL COUPLING

5.1	Introduction	145
5 2	Staging With Radial Beams	146
5.2.1	Lateral Stiffness	146
5.2.1.1	Due to Bending Deformation of Staging Members	146
5.2.1.2	Due to Axial Deformation of Staging Columns	147
5.2.2	Torsional Stiffness	147
5.2.3	Natural Period Ratio (τ_{rb})	148
5.2.4	Results and Discussion	149

5.3	Staging With Radial Beams and a Central Column	150
5.3.1	Lateral Stiffness	150
5.3.1.1	Due to Bending Deformation of Staging Members	150
5.3.1.2	Due to Axial Deformation of Columns	151
5.3.2	Torsional Stiffness	151
5.3.3	Natural Period Ratio (τ_{rbcc})	152
5.3.4	Results and Discussion	153
5.4	Staging With Two Concentric Rows of Columns With Circumferential and Radial Beams	153
5.4.1	Lateral Stiffness	154
5.4.1.1	Due to Bending Deformation of Staging Members	154
5.4.1.2	Due to Axial Deformation of Staging Columns	155
5.4.2	Torsional Stiffness	156
5.4.3	Natural Period Ratio (τ_{2crc})	156
5.4.4	Results and Discussion	157
5.5	Staging With Diagonal Braces	158
5.5.1	Stiffness Contributed by Truss Action of Staging Members	159
5.5.1.1	Lateral Stiffness	159
5.5.1.2	Torsional Stiffness	163
5.5.2	Total Stiffness of the Staging	165
5.5.2.1	Total Lateral Stiffness	165
5.5.2.2	Total Torsional Stiffness	165
5.5.3	Natural Period Ratio (τ_b)	165
5.5.4	Results and Discussions	166
5.5.4.1	Expressions for Stiffnesses	166
5.5.4.2	Effect of Addition of Diagonal Braces	167
5.6	Approach For Reducing Torsional Effects	168
5.7	Summary and Conclusions	170
5.8	References	171
	Tables	172
	Figures	175

CHAPTER 6 : SUMMARY AND CONCLUSIONS

6.1	Summary	183
6.2	Conclusions	184
6.3	Recommendations for Future Research in this Area	187

Appendix A : TORSIONAL-TO-LATERAL STRENGTH RATIO

A.1	General	189
A.2	Analysis	190
A.2.1	Derivation of Lateral Strength (S_x)	190
A.2.2	Derivation of Torsional Strength (S_θ)	191

A.3	Results	192
A.3.1	Design with $M_{pc} = M_{pb} \cos^2 \left(\frac{\pi}{N_c} \right)$	192
A.3.2	Design with $M_{pc} = M_{pb}$	193
A.3.3	Design with $M_{pc} = 0.5M_{pb}$	193
A.4	Comments	194
A.5	Reference	194
	Table	195
	Figures	196

LIST OF TABLES

Table No.	Title	Page No.
4.1	Details of the Tanks Analyzed.	134
4.2	Performance of Proposed Approximate Expressions in Predicting Stiffness for Basic Configuration (Fig.4.1).	134
4.3(a)	Performance of Proposed Approximate Expressions in Predicting Shear Forces and Bending Moments in Columns Under Applied Torsion Motion.	135
4.3 (b)	Performance of Proposed Approximate Expressions in Predicting Shear Forces and Bending Moments in Beams Under Applied Torsion Motion.	135
4.4	ϵ_M for Different Values of N_C and K_r (Values are Independent of N_p)	136
5.1	Performance of Proposed Approximate Expressions for Lateral Stiffness of Staging Radial Beams.	172
5.2	Performance of Approximate Expressions for Lateral Stiffness of Staging with Radial Beams and a Central Column.	172
5.3	Performance of Proposed Approximate Expressions for Stiffness of Staging with Two Concentric Rows of Columns with Circumferential and Radial Beams	173
5.4	Performance of Proposed Approximate Expressions for Stiffness of Staging with Diagonal Braces	174
A.1	Limiting Values of Strength Ratio (S_θ/S_x) for Different Designs Considered.	195

LIST OF FIGURES

Figure No.	Title	Page No.
1.1a	Collapse of a steel elevated tank in torsion (Steinbrugge, 1965).	20
1.1b	Collapse of a reinforced concrete elevated water tank in torsion (Jain et al, 1994).	20
2.1	Some commonly used stagings of elevated water tanks.	47
2.2	Schematic of the simplified idealization of an elevated water tank structure.	48
2.3	Idealized systems considered to model lateral-torsional coupling in elevated water tanks.	49
2.4	Definition of flexible and stiff elements in eccentric systems.	50
2.5	Spectrum-consistent synthetic ground motion	51
2.6	The three idealized acceleration spectra considered in the study.	52
2.7	Maximum normalized response of four-element system for single-frequency harmonic ground motion ($e/r=0.05$).	53
2.8	Maximum normalized element displacement of four-element system under single-frequency harmonic ground motion.	54
2.9	Envelopes of maximum response for different values of β (harmonic single-frequency ground motion).	55
2.10	Maximum normalized element displacement of four-element system under spectrum-consistent synthetic ground motion (a) $e/r=0.05$, (b) $e/D=0.05$, and (c) $e/D=0.20$.	56
2.11	Maximum normalized element displacement of two-element system ($e/D=0.05$) under spectrum-consistent synthetic ground motion.	57
2.12	Maximum normalized element displacement of four-element system ($e/r=0.05$) under spectrum-consistent synthetic ground motion.	58

2.13	Maximum normalized element displacement of four-element system ($e/D=0.05$) under idealized spectra.	59
2.14	Maximum normalized element displacement of four-element system ($e/D=0.20$) under idealized spectra.	60
2.15	Maximum normalized element displacement of four-element system ($e/D=0.05$) under idealized spectra.	61
3.1	Different types of eccentric systems in linear range.	89
3.2	Synthetic ground motion used along the axis of symmetry (a) generated acceleration-time history, (b) response spectrum generated by the time history (2% damping).	90
3.3	Simulated near-fault ground motion in directions parallel and normal to a strike-slip fault (Murty and Hall, 1994).	91
3.4	Accelerogram from port Hueneme earthquake, March 18, 1957 (NS Component) (Clough and Penzien, 1993).	92
3.5	General hysteresis loops based on the proposed simple strength-deteriorating hysteresis model.	93
3.6	Experimental load-deformation curve of a reinforced concrete member obtained under slow cyclic loading (Eshani and Wight, 1985).	94
3.7	Maximum normalized element displacement of stiffness-eccentric two-element system ($T = 0.5$ sec, $e/D=0.05$).	95
3.8	Maximum normalized element displacement of stiffness-eccentric two-element system ($T = 1$ sec, $e/D=0.05$).	96
3.9	Maximum normalized element displacement of stiffness-eccentric two-element system ($T=2$ sec, $e/D=0.05$).	97
3.10a	Maximum normalized element displacement of strength-eccentric two-element system ($T_x=0.5$ sec, $e_{\text{strength}}/D = 0.05$).	98

3.10b	Maximum normalized element displacement of strength-eccentric two-element system ($T_x = 0.5$ sec, $e_{\text{strength}}/D = 0.05$); enlarged view of the curves with some specific values of δ .	99
3.11	Maximum normalized element displacement of strength-eccentric two-element system ($T_x = 1$ sec, $e_{\text{strength}}/D = 0.05$).	100
3.12	Maximum normalized element displacement of strength-eccentric two-element system ($T_x = 2$ sec, $e_{\text{strength}}/D = 0.05$).	101
3.13	Maximum normalized element displacement of stiffness-eccentric four-element system under bi-directional & uni-directional ground motions.	102
3.14	Maximum normalized element displacement of stiffness-eccentric two-element system under fault-parallel ground motion ($e/D = 0.05$).	103
3.15	Maximum normalized element displacement of stiffness-eccentric two-element system under fault-normal ground motion ($e/D = 0.05$).	104
3.16	Variation of element displacement ductility demand under fault-parallel and fault-normal ground motions with different pulse durations.	105
4.1	A typical staging with basic configuration.	137
4.2	Staging sub-assemblages showing deflection between successive joints due to bending of beams and columns (Sameer and Jain, 1992).	138
4.3	Development of torsional resistance in typical frame-type staging.	139
4.4	Determination of shear forces in beams.	140
4.5	Critical direction for forces in beams and columns (Sameer and Jain, 1994).	141
4.6	Variation of natural period ratio, $\tau (= T_\theta/T_x)$, with $\rho (= R_{\text{egyr}}/R)$.	142

4.7	Variation of natural period ratio (τ) with depth of water, h_w . Natural period ratio (τ) is normalized with natural period ratio (τ_{empty}) at tank-empty condition. Water depth is normalized with radius of container (R_c).	143
4.8	Variation of nondimensional stiffness ratio parameter $R_s \sqrt{(K_x/K_\theta)}$ with N_c/N_p (a) $N_p=4$, (b) $N_p=6$, (c) $N_p=8$.	144
5.1	Plans of alternate staging configurations which increase natural period ratio, τ .	175
5.2	Alternate configuration which decreases natural period ratio, τ .	176
5.3	Effect of radial beams on natural period ratio.	177
5.4	Effect of radial beams and a central column on natural period ratio.	178
5.5	Effect of an additional inner row of columns on natural period ratio.	179
5.6	Relative deformation within a panel with diagonal braces.	180
5.7	Effect of diagonal braces on natural period ratio.	181
5.8	Schematic of τ - ρ space showing the possible cases of vulnerability under tank-full and tank-empty conditions.	182
A.1	Two possible mechanisms in tank stagings due to two different orientations of lateral load.	197
A.2	Two possible mechanisms in tank stagings due to torsional moment.	198

LIST OF SYMBOLS

Mathematical symbols have been defined where they first appear. They are summarized here in alphabetical order. Some symbols are given more than one meaning, when there is no question of confusion.

A_0	Cross sectional area of diagonal braces;
A_b	Cross sectional area of beams;
A_c	Cross sectional area of columns;
a_0	Peak ground acceleration in near-fault ground motion;
a_g	Peak ground acceleration in harmonic single-frequency synthetic ground motion;
b_j	Coordinate of element j oriented perpendicular to the direction of ground motion measured from centre of mass;
C	Axial compressive force in column (Eq.(5.25));
$[C]$	Damping matrix;
C_1, C_2	Parameters defined in Eq.(5.39);
CM	Centre of mass;
CS	Centre of stiffness;
D	Perpendicular distance between two lateral load resisting elements oriented in the same direction;
d_0	Peak displacement in near-fault ground motion;
d_i	Coordinate of element i oriented along the direction of ground motion measured from centre of mass;
E_0	Modulus of elasticity of diagonal braces;
E_c	Modulus of elasticity of columns;
E_b	Modulus of elasticity of beams;
e	Eccentricity between centre of mass and centre of stiffness;
e_{strength}	Eccentricity between centre of mass and centre of strength;
F	Lateral force carried by each bay in truss action due to a torque, T , applied at the top of the staging with diagonal braces;
F_1, F_2, F_3	Terms defined in Eqs.(5.26), (5.33) and (5.35), respectively;
F_b	Axial compression in beam due to a torque, T , applied at top of the staging with diagonal braces;

F_{ci}	Axial compressive force in a column in panel i due to a torque, T , applied at top of the staging with diagonal braces;
F_{cij}	Net axial compressive force in column j of panel i in truss action;
F_{dbi}	Axial force in diagonal brace in panel i under applied torsional moment;
F_{ij}	Axial force in column i in panel j ;
F_y	Yield strength of lateral load resisting elements,
H_i	Distance of applied lateral force from the point of contraflexure of panel i ;
H_j	Distance of point of inflection of column in panel j from applied lateral load;
h	Height of the panel;
h_0	Height at which the lateral force is applied measured from top of the staging;
h_a, h_b	Height of the panels above and below the panel under consideration;
h_i	Height of the i th panel;
h_w	Height of water in tank container;
I	Torsional mass moment of inertia of empty tank,
I_b	Moment of inertia of circumferential beam;
I_{br}	Moment of inertia of radial beams;
I_{bt}, I_{bb}	Moment of inertia of beams meeting the columns at top and bottom joints, respectively;
I_c	Moment of inertia of column;
I_s	Sum of moments of inertia of all the columns in a panel;
K	In-plane stiffness of each bay due to truss action in staging with diagonal bracings;
K_{arc}, K_{arb}	Relative axial stiffness of diagonal braces with respect to that of columns and beams, respectively, in staging with diagonal braces;
K_{axial}	Stiffness of the staging due to axial deformation of columns;
$K_{bx}, K_{b\theta}$	Lateral and torsional stiffness, respectively, of the staging with diagonal braces, due to combined effect of truss and frame actions;
$K_{cent.col.}$	Stiffness of central column in a single panel;
$K_{circ.col}$	Stiffness of all circumferential columns in a single panel;

K_{column}	Lateral stiffness of a column in a single panel;
$K_{\text{p(lateral)}}$	Lateral panel stiffness of staging of basic configuration;
$K_{\text{p(torsional)}}$	Torsional panel stiffness of staging of basic configuration;
$K_{\text{pi(lateral)}}$	Panel stiffness of the inner circular row of columns;
$K_{\text{po(lateral)}}$	Panel stiffness of the outer circular row of columns;
K_{r}	Relative stiffness of columns with respect to the beams;
K_{x}	Lateral stiffness of the system;
$K_{\text{srt}}, K_{\text{srb}}$	Sum of the rotational stiffnesses of all radial beams at all the joints at top and bottom of the panel, respectively;
K_{tx}	Lateral stiffness of staging with diagonal braces due to truss action only;
$K_{\text{t}\theta}$	Torsional stiffness of staging with diagonal braces due to truss action only;
$(K_{\text{x}})_{\text{rb}}$	Lateral stiffness of staging with radial beams;
$(K_{\text{x}})_{\text{rbcc}}$	Lateral stiffness of staging with radial beams and a central column;
$(K_{\text{x}})_{2\text{crc}}, (K_{\theta})_{2\text{crc}}$	Lateral and torsional stiffnesses, respectively, of stagings with two rows of columns;
K_{θ}	Torsional stiffness of structure about centre of mass;
$K_{\theta\text{t}}, K_{\theta\text{b}}$	Rotational stiffnesses of top and bottom joints, respectively;
$k_{\text{st}}, k_{\text{sb}}$	Summation of stiffnesses of all beams meeting at top and bottom joints of panel, respectively;
$\Sigma k_{\text{bt}}, \Sigma k_{\text{bb}}$	Summation of the stiffnesses of beams meeting at the top joint and bottom joint, respectively;
L	Span of circumferential beams;
L_{0i}	Length of diagonal braces in panel i;
L_{j}	Length of circumferential beams in panel j;
M_{be}	Design moment of beam in end panel under applied lateral force;
M_{bet}	Bending moment in beams of end panel under applied torsional moment;
M_{bjt}	Bending moment in the beams at level j under torsional moment;
M_{cb}	Design moment at the braced end of the critical

	column under applied lateral load;
M_{cj}	Design moment in column of panel j under applied lateral load;
M_{cjt}	Maximum column moment of panel j under applied torsional moment;
M_{cr}	Maximum moment of column at the restrained end of the end panel under applied lateral force;
M_{crt}	Bending moment at the restrained end of columns under applied torsional moment;
M_{empty}	Mass of the tank container (with one-third mass of the staging);
$M_{lateral}$	Mass which takes part in impulsive mode of vibration (consisting of the mass of container, one-third mass of staging and impulsive mass of the liquid);
M_{pb}	Plastic moment capacity of beams;
M_{pc}	Plastic moment capacity of columns;
$M_{torsional}$	Mass that participates in impulsive mode of torsional vibration;
M^*	Component of the plastic moment in columns acting on the vertical plane passing through the line of action of lateral force;
m	Mass of the system;
N_b	Number of beams meeting the column at the joint;
N_c	Number of columns in a staging;
	Number of columns in one circular row of staging in case of stagings with two rows of columns;
N_p	Number of panels;
P	Lateral load applied to the staging top;
	coefficient given by Eq.(2.16);
P_i	Participation factor for mode i ;
P_j	Force carried by bay j in the staging;
$\{p\}$	Stiffness-related resisting force vector;
Q	Coefficient given by Eq.(2.16);
R	Response reduction factor (defined as ratio of the maximum lateral force to be experienced if the structure were to remain elastic and the design lateral force);
	Coefficient given by Eq.(2.16);
R_c	Radius of container;
R_{egyr}	Effective radius of gyration of tank mass and its contents for impulsive mode of vibration;

R_{gyr}	Radius of gyration at tank-empty condition;
R_s	Radius of staging;
R_μ	Ductility reduction factor (defined as ratio of the maximum lateral force to be experienced if the structure were to remain elastic and the lateral yield force of the structure);
r	Radius of gyration about centre of mass;
r_{cgyr}	Radius of gyration of column cross-section;
S	Coefficient given by Eq.(2.16);
S_x	Lateral strength of the system;
S_θ	Torsional strength of the system;
SA	Spectral acceleration;
T	Natural period;
	Tensile force in column given in Eq.(5.26);
T_1	Duration of the near-fault pulses;
T_x	Uncoupled lateral natural time period;
T_θ	Uncoupled torsional natural time period;
t	Time (in seconds);
t_1	Time during which the ground motion builds up;
t_2	Time after which the ground motion starts decaying;
t_{total}	Total duration of spectrum-consistent synthetic ground motion;
U_b, U_c and U_{db}	Strain energy in all beams, columns and diagonal braces, respectively, due to truss action in staging;
U_t	Total strain energy of the staging due to applied torque, T , in truss action;
u	Lateral displacement of centre of mass of eccentric system relative to base;
\ddot{u}	Lateral acceleration of centre of mass relative to base;
u_0	Lateral displacement of symmetric system relative to base;
$\ddot{u}_g(t)$	Ground acceleration as a function of time;
V_{bj}	Design shear in beam at level j ,
\bar{V}_{bj}	Shear force in beams connected to the columns carrying design shear;
V_c	Column shear under lateral force;
V_{ct}	Design shear in column due to applied torsional moment;

v_0	Peak velocity in near-fault ground motion;
x_i	Distance of column i measured along the direction of lateral force from centre of staging;
y_j	Distance between the points of inflection of two consecutive panels;
\bar{y}	Distance of point of inflection of end panel from the braced end;
y_{jt}	Distance of point of inflection from the end of panel under applied torsional moment;
α	Angle the beam makes with direction of lateral force;
β	Ratio of the frequency of harmonic single-frequency synthetic ground motion (ω) to uncoupled lateral frequency (ω_x);
	Parameter used in Newmark's γ - β method;
β_i	Angle made by radial brace i with direction of lateral force;
γ	Parameter used in Newmark's γ - β method;
	Parameter which takes a value of 2 for intermediate panels and 1 for end panels in the panel stiffness expressions;
Δ_c	Lateral deflection of a column,
Δ_i	Lateral displacement of element i ;
Δ_f, Δ_s	Absolute value of displacements of flexible and stiff elements, respectively, in eccentric systems;
Δ_{fn}, Δ_{sn}	Absolute value of displacements of flexible and stiff elements, respectively, normalized with respect to displacement of the similar symmetric systems;
$\Delta_{fni}, \Delta_{sni}$	Normalized displacement of flexible and stiff elements, respectively, of the eccentric system;
δ	Rate of strength deterioration of the lateral load-resisting elements (defined as the fraction of original yield strength by which the strength deteriorates due to each cycle of yielding);
δ_0	Ratio of the moments of inertia of radial and circumferential beams in stagings;
δ_1	Ratio of moments of inertia of circumferential beams connected to columns of inner and outer circular rows in staging with two concentric rows of columns;
δ^*	Amount of unloading which takes place in Figure 3.5 immediately after the second yielding;
δ_{lt}	Lateral displacement of staging with diagonal braces due to truss action under lateral loading;
ε_M	Ratio of moment-ratio of columns and beams under torsion to that under lateral force;

ε_v	Ratio of shear-ratio of columns and beams under torsion to that under lateral force;
ζ	Modal damping ratio;
η	Ratio of moments of inertia of columns in inner and outer rows;
η_1	Ratio of cross-sectional areas of columns in inner and outer rows;
θ	Rotation of centre of mass relative to the ground;
$\ddot{\theta}$	Torsional acceleration of centre of mass relative to the ground;
θ_c	Rotation of column at braced end in end panel under applied lateral force;
θ_i	Inclination of diagonal brace with horizontal in panel i;
θ_n	Normalized rotation of centre of mass;
θ_t, θ_b	Rotations of top and bottom joints, respectively;
θ_t	Rotation in the horizontal plane due to a torque, T, applied at the top of the staging with diagonal braces, in truss action;
θ_v	Vertical angle of inclination of diagonal braces in all the panels of the stagings with diagonal braces;
μ	Ratio of radius of inner row of columns to that of outer row of columns;
ρ	Ratio of effective radius of gyration and that of staging;
τ	Natural period ratio (defined as ratio of torsional and lateral natural periods);
τ_b	Natural period ratio of staging with diagonal braces;
τ_{empty}	Natural period ratio at empty condition;
$\tau_{rb}, \tau_{rbcc}, \tau_{2crc}$	Natural period ratio of stagings with radial beams, with radial beams and a central column, and with two concentric rows of columns, respectively;
ϕ	Ratio of moments of inertia of central and circumferential columns in the staging with radial beams and a central column;
$\{\phi_1\}, \{\phi_2\}$	Mode shape vectors;
ϕ_j	Angle made by the plane of bay j with the direction of lateral force;
ω	Frequency of harmonic single-frequency synthetic ground motion;
ω_1, ω_2	Undamped natural frequencies of lateral-torsionally coupled systems;
ω_x, ω_θ	Uncoupled lateral and torsional natural frequencies, respectively;

CHAPTER 1

INTRODUCTION

1.1 GENERAL

The supply of drinking water is essential immediately after the destructive earthquakes. Also, without assured water supply, the uncontrolled fires subsequent to major earthquakes may cause more damage than the earthquakes themselves. Reports of the occurrence of such incidents are available from as early as the 1906 San Francisco earthquake. So, seismic performance of water tanks draws special significance, extending beyond the cost of the tanks and their contents.

Water supply systems in several countries rely primarily on elevated water tanks for storage and distribution. In major cities, the main supply scheme is augmented by individual distribution systems consisting of elevated water tanks. These structures are inherently vulnerable to damage under earthquakes, owing to the large mass concentrated at the top of a relatively slender supporting structure. Earthquake forces govern their design in severe seismic zones, owing to large mass and small exposed area to wind.

1.2 DAMAGES TO LIQUID STORAGE TANKS DURING PAST EARTHQUAKES

Although liquid containment structures have over the years performed reasonably well during earthquakes, a large number of them have been damaged and some have even collapsed. Some common types of failure or damage are briefly reviewed below.

1.2.1 Shell Buckling of Steel Tank Container

This common form of damage observed in ground supported steel water tanks, involves outward buckling of the bottom shell of the container, a phenomenon often termed as *elephant's foot* buckling. This phenomenon occurred on many tanks in the 1971 San Fernando earthquake (Jennings, 1971). This damage is more frequent in tanks which are full and have large height-to-diameter ratio. The vertical acceleration during earthquakes plays an important role in causing this failure. A recent study (Akiyama, 1992) addresses this problem along with that of the fracture of the bottom plate associated with the uplift, by equating input energy to the energy absorption capacity of the structure.

1.2.2 Damage of Steel Tank Roof

In tanks that are full or nearly full, resistance of the tank roof to free sloshing results in an upward pressure on the roof. This sometimes causes failure of the joints between walls and roofs, leading to spillage of the tank contents and buckling of the shell wall at the top.

1.2.3 Foundation Failure

If tanks are situated on cohesionless soil at sites close to harbours or rivers, soil liquefaction may occur under them, e.g., the 1964 Nigata earthquake. Base moments due to seismic lateral force caused considerable base rotation and settlements of the order of several metres during the 1964 Nigata earthquake (Kawasumi, 1964).

In tanks resting on firm foundations, fracture of container wall

and base plate welds are observed in unrestrained or inadequately restrained steel tanks.

An example of foundation failure of a reinforced concrete tank is also available in the literature (Jennings, 1971). A large underground reinforced concrete reservoir at the Balboa Water Treatment Plant suffered severe damage in the 1971 San Fernando Earthquake as a result of foundation failure (Priestley *et al.*, 1986).

1.2.4 Failure of Piping and Other Accessories

During earthquakes, some tanks are found to loose their contents due to fracture of inlet/outlet piping or other accessories at the connection to the tank. This generally results from large displacements of the tank.

1.2.5 Failure of Tank Support System

Steel and concrete elevated tanks have failed due to inadequacy of the supporting structural systems under lateral seismic forces generated during earthquakes. Damage of the staging systems of the steel elevated water tanks generally takes place due to stretching of ties; buckling of struts; tearing, warping and rupture of gusset plates at end connections; and separation of clevis, rivets and bolts. An instance of failure of the supporting structural system of a steel cement silo is also noted during the 1964 Alaska earthquake (Berg and Stratta, 1964).

Many reinforced concrete elevated water tanks have failed or severely damaged in the 1960 Chilean earthquake (Steinbrugge and Flores, 1963). Most of the reinforced concrete moment resisting frame supported

tanks sustained severe damage with similar damage patterns, while most of the shaft-supported tanks remained intact. Steinbrugge and Flores (1963) explained that failure sequence probably started with shear failure of the beams followed by plastic hinging at the columns ends, where bending moment is the largest. Collapse did not occur as the plastic hinges formed at the restrained joints dissipated the energy. Similar damage was also reported in a reinforced concrete elevated water tank at Khagaria during the 1988 Bihar-Nepal earthquake (Jain and Sameer, 1993).

1.2.6 Torsional Failure of Elevated Water Tanks

Steel elevated water tanks collapsed due to torsional vibrations during the 1952 Kern County, California earthquake (Steinbrugge, 1965; Steinbrugge and Moran, 1954). The orientation of the collapsed tank was approximately inverted and within the plan area of the supporting structure as shown in Figure 1.1a. The collapse in such tanks usually begins with the failure of a X-brace rod, creating severe torsional forces and thereby twisting the tank until eccentricity of the column load causes column failure. The tank then collapses vertically upon its standpipe. Inversion of the tank takes place owing to the unstable condition of a single support. This sequence of events leading to failure is shown in Figure 1.1a.

The evidence of torsional failure of a reinforced concrete elevated water tank is also available from the 1993 Killari earthquake (Jain *et al.*, 1994). The tank collapsed vertically downwards, burying the six supporting columns directly underneath the bottom slab of its container,

as shown in Figure 1.1b. This vertical collapse along with the evidence of an approximately 0.5 metre circumferential displacement suggests that torsional vibrations may have been the primary cause of its failure.

1.3 PAST RESEARCH ON SEISMIC BEHAVIOR OF ELEVATED WATER TANKS

There are standards, *e.g.*, ANSI/AWWA D100-84, which provide some specifications and guidelines for the seismic design and construction of elevated water tanks. Considerable research has been done on the different aspects of seismic behaviour of elevated water tanks. A comprehensive study (Pristley *et al*, 1986) helped in arriving at improved recommendations for seismic design of storage tanks and in identifying the areas where further research is needed. Past research in this area is briefly discussed in the following.

1.3.1 Ground Supported Rigid Tanks

Early developments of the seismic response theories on tanks assumed the containers to be rigid. An analytical formulation (Housner, 1963; USAEC, 1963) based on this assumption considered the hydrodynamic pressure of the contained liquid to be composed of two parts, namely (a) the impulsive pressure caused by the portion of the liquid accelerating with the tank, and (b) the convective pressure caused by the portion of the liquid sloshing in the tank. The model consists of equivalent springs and masses attached to the container at particular locations to simulate the forces and moments exerted by the liquid on the tank. In tanks with the commonly adopted proportions, the rigidly-attached component of the liquid contributes larger effects. In a recent study

(Veletsos and Shivakumar, 1993), the sloshing action of layered liquids in rigid cylindrical tanks has been investigated.

1.3.2 Ground Supported Flexible Tanks

Many flexible tanks were considerably damaged during the 1964 Alaska earthquake (Hanson, 1973). This pointed out the need to consider the non-rigid nature of the tank container. The finite element method was used to estimate the seismic stresses and displacements on circular cylindrical shells (Edward, 1969); the tank was regarded as anchored to its foundation and restrained against cross-section distortion. Similar studies by other researchers were also carried out. A simple procedure was proposed (Veletsos, 1974) for calculation of the hydrodynamic pressure distribution, base shears and overturning moments for the several assumed modes of vibration. This procedure assumed the tank to behave as a single degree of freedom system with an assumed mode of vibration and also assumed the cross section to remain circular during vibrations. A simplified formula was presented to obtain the fundamental natural frequencies of liquid-filled shells using Rayleigh-Ritz energy method.

A series of studies (Haroun, 1980; Haroun and Housner, 1981a; Haroun and Housner, 1981b; and Haroun and Housner, 1981c) was made on dynamic behaviour of deformable cylindrical tanks. These studies include detailed theoretical treatment of liquid-shell system, and an extensive experimental investigation of the dynamic characteristics of full-scale tanks. These studies led to the development of a mechanical model (Haroun, 1980) to estimate the seismic response taking into account the

deformation of the tank wall. Another study (Ungureanu and Negoita, 1992) addressed the wall flexibility effect on the earthquake response of the storage tanks. The paper proposed a "parametric parabola for the function of mode shapes, that takes into account in a better way the ratio between shear and moment".

1.3.3 Unanchored Tanks

Damage sustained by unanchored tanks during the 1979 Imperial Valley earthquake emphasized the need for more research in this direction (Haroun, 1981). Though the actual response is highly nonlinear, some approximate procedures have been developed to estimate the maximum stresses induced in the walls of unanchored tanks (Wozniak and Mitchell, 1973; Cambra, 1983). A computationally viable method was proposed to solve the local uplift problem of the tank wall in steel cylindrical tanks (Peek and Jennings, 1988; Peek, 1988). The behaviour of ground-supported unanchored metal cylindrical model tanks, placed on stiff foundations, was studied under static and earthquake-type dynamic lateral load (Manos, 1992). Another study concentrated on the dynamic uplift behaviour of unanchored cylindrical tanks subjected to ground acceleration (Lau *et al*, 1992). The study also compares the seismic behaviour of anchored and unanchored tanks.

1.3.4 Experimental Tests on Tanks

Experimental investigations on seismic behaviour of tanks include ambient and forced vibration tests on full-scale water storage tanks (Haroun, 1980); tests on small plastic models subjected to harmonic and

transient excitations at their base (Shih and Babcock, 1980; Shih and Babcock, 1984); tests on several aluminium tank models subjected to harmonic and transient excitations at their base (Clough, 1977, Niwa, 1978); and test on a full-scale wine storage tank of the type damaged during the 1980 earthquake in Livermore, California (Niwa and Clough, 1982). These experimental studies showed that the response under real earthquakes may exhibit considerable departure from the analytically predicted response. Higher order circumferential modes can be excited in the practical situation of an earthquake because of the initial irregularities in the shell radius. An approximate analysis of the effect of out-of-roundness on the dynamic response of tanks came as a consequence of an effort to interpret the results of these experiments (Veletsos and Turner, 1979).

1.3.5 Tanks under Vertical Excitation

In an early study, forced axial response of liquid storage tanks was studied by idealizing the tank shell as a system of rings stacked one on top of the other (Bleich, 1956). However, this model neglects the axial deformations as well as the bending rigidity of the tanks. Another simplified study emphasised the necessity of considering the effects of vertical acceleration on tanks (Marchaj, 1979). The effect of radial motion of water under vertical excitation in partly filled tanks, neglecting the axial deformation, was also studied (Kumar, 1981).

1.3.6 Effect of Soil-Structure Interaction on Seismic Response of Tanks

A study of circular cylindrical tanks under horizontal ground

shaking showed that soil-structure interaction might significantly reduce the impulsive components of response, but that it would have a negligible effect on the convective components (Veletsos and Yang, 1990). However, another study (Haroun and Abou-Izzeddine, 1992a; Haroun and Abou-Izzeddine, 1992b) showed that under horizontal ground motion, the hydrodynamic forces and moments exerted on the tank structure may be amplified owing to the effects of soil-structure interaction while under vertical ground motions, the soil-structure interaction effect reduces the tank response. The effect of soil structure interaction on X-braced elevated water tanks supported on isolated footings was also investigated (Haroun and Temraz, 1992); it was found that soil-structure interaction reduces member end actions, except at the base of the tower.

1.3.7 Elevated Water Tanks

Early shake table tests of scaled-model towers concluded the necessity of designing the elevated water tanks for dynamic response (Jacobson, 1929; Brown, 1934). Several studies were carried out on the seismic behaviour of cross-braced elevated tanks (Shepherd, 1973, Housner, 1963). The convective action of the liquid was allowed for by a two-mass representation of the storage tank and its contents.

The elevated water tanks supported on moment resisting frame staging were damaged, while those supported on shafts remained safe in 1960 Chilean earthquake (Steinbrugge and Flores, 1963). A simplified seismic response analysis of elevated water tanks was enabled by the two-mass idealization (Housner, 1963). The concept of two-mass idealization was widely accepted in the literature (Sonobe and

Nishikawa, 1969; Ifrim and Bratu, 1969; Shepherd, 1972; Boyce, 1973). On the other hand, a few researchers have also adopted the model of a single degree of freedom system (Chandrasekharan and Krishna, 1965; Ramaiah and Gupta, 1966).

A detailed finite element analysis of elevated tanks incorporating detailed shell behaviour of the container was also performed (Lee and Reddy, 1979). A series of studies were carried out to ascertain the relative importance of various factors which control dynamic forces exerted on the supporting structures (Haroun and Elliathy, 1985; Haroun, 1986; Haroun and Elliathy, 1986). It was observed that the fundamental mode of sloshing when combined with translation and rotation of the supporting tower structure provided maximum shearing force and moment on elastic supports in case of rigid tanks. For flexible tanks, the effect of wall flexibility needed to be accounted for. However, for small tanks, these effects may be negligible. A reliability-based design procedure has been proposed for reinforced concrete elevated water tanks under seismic action (Möller and Rubinstein, 1992). Meamari *et al.* (1992) have reported a study on the behaviour of reinforced concrete water towers during the 1990 earthquake in Iran.

Wandi and Hansen (1989) have investigated the behaviour of cross-braced steel elevated water tanks. The study involves three dimensional modeling of these structures inclusive of three dimensional modeling of the water motion with torsional effects and inelastic modeling of the structural members with appropriate hysteresis models. The study reported that torsional response was not dominant in the cases studied. It also found that towers with six columns exhibits less

torsional response than the towers with four columns.

1.4. OBJECTIVES OF THE PRESENT STUDY

The literature review shows that considerable research has been performed to understand, model and improve the design criteria for seismic performance of tanks. However, most of the effort was focused on seismic performance of ground-supported steel water tanks. Elevated water tanks are particularly vulnerable to earthquake forces due to the large mass supported on a slender supporting structure, called *staging*. The collapses of elevated water tanks during past earthquakes have been primarily attributed to failure of the stagings.

However, reports on some damages in past earthquakes suggest the occurrence of torsional vibration as a cause of failure (Jain *et al.*, 1994, Steinbrugge, 1965 and Steinbrugge and Moran, 1954). The elevated tanks, with their broadly axisymmetric structural geometry and mass distribution, do not appear to be prone to torsion. This is probably why torsional seismic response of elevated water tanks has not been much investigated. However, one study clearly noted that torsional response cannot be avoided in elevated water tanks (Shepherd, 1973). Asymmetric placement of ladders and water pipelines, sloshing of the water mass during shaking, and non-uniformity in construction, particularly of RC stagings, are some possible causes for developing small eccentricity in elevated water tanks. Besides, the ground motion itself can have a torsional component which can generate torsional motion in an otherwise symmetric structure.

Objective of the present study is to investigate in detail the

torsional behaviour of water tanks supported on reinforced concrete frame-type stagings during earthquakes. The basic staging studied consists of vertical columns located on perimeter of a circle. The columns are braced through horizontal circumferential beams at several levels. Such stagings have been modelled as simple two-element and four-element systems and the torsional response studied under elastic and inelastic regimes. Even though not much research is available to torsional response of elevated tanks, the subject of torsion in buildings due to earthquake ground motion has been extensively investigated in the past. Rutenberg (1992) has reviewed the literature on torsion in buildings. Hence, extensive review of torsion literature has not been made in this thesis. Study of torsion problem taken up in this thesis is limited to issues which are relevant to elevated tanks and which have not drawn enough attention; these include linear elastic response study with a focus on element displacement rather than behaviour of centre of mass, inelastic response under strength-deteriorating properties of material, and inelastic response caused by near-fault pulse-type earthquake ground motions. Important parameters affecting torsional response have been identified.

Subsequently, the dynamic characteristics of the basic staging have been studied; it is observed that most tanks of ordinary configuration may be quite vulnerable to large torsional response caused by accidental eccentricity. Alternative staging configurations have been studied with a view to reduce torsional vulnerability.

1.5. ORGANIZATION OF THE THESIS

The content of this thesis is presented in six relatively independent chapters. Chapter 1 introduces the subject matter of this thesis, and presents a brief literature survey of research on seismic behaviour of tanks. The need for conducting the present study is pointed out.

In Chapter 2, the linear torsional response of idealized models of elevated water tanks with small accidental eccentricity under a few representative ground motions is presented. The influence of torsional-to-lateral stiffness ratio and torsional-to-lateral natural period ratio on the torsional response of these systems in the linear range is discussed.

In Chapter 3, the implications of inelastic effects on the torsional response of idealized systems with small eccentricity are examined. The strength deteriorating property of reinforced concrete members under cyclic loads is modeled in a simplistic manner. An approximate analytical formulation is outlined in Chapter 4 to estimate the torsional and lateral stiffnesses, and hence, the torsional and lateral impulsive natural periods of elevated water tanks supported on frame-type stagings. A detailed parametric study is presented to arrive at the range of the natural period ratio for commonly constructed elevated water tanks.

In Chapter 5, four alternate staging configurations with less susceptibility to torsional effect are proposed. Again, an approximate analytical formulation for deriving their torsional and lateral stiffnesses, and hence their natural periods, is presented.

The summary and conclusions of the entire study and recommendations for future research in this area are presented in Chapter 6.

The literatures referred in different chapters are listed at the end of each chapter.

1.6 SIGN CONVENTION, NOTATION AND UNITS

Consistent sign convention and notations have been adopted throughout this thesis. Scalars are indicated by their variable names *e.g.*, u . Vectors are indicated by their variable names within chain brackets, *e.g.*, $\{p\}$, while the matrices are indicated by their variable names within square brackets, *e.g.*, $[M]$. The time derivative of any quantity is indicated with a dot over the variable name, *e.g.*, \dot{u} . In the numerical examples, SI units are adopted.

1.7 REFERENCES

- Akiyama,H., (1992), "Earthquake Resistant Limit State Design for Cylindrical Liquid Storage Tanks," *Proceedings of Tenth World Conference on Earthquake Engineering*, Vol.9, Madrid, Spain, pp 5001-5004.
- ANSI/AWWA D100-84, (1984) *AWWA Standard for Welded Steel Tanks for Water Storage*, approved by American Water Works Association, American Welding Society, New England Water Works Association and American National Standard Institute, American Water Works Association, Colorado, USA.
- Berg,G.V., and Stratta,J.L., (1964), "Anchorage and the Alaska Earthquake of March 27, 1964," *American Iron and Steel Institute*
- Brown,A.L., (1934), "Changed Elevated Tank Design Required for Safety Against Earthquake," *Engineering News-Record*, Vol.4, pp 424-425.
- Balendra,T., and Nash,W.A. (1978), "Finite Element Analysis of Seismically Excited Cylindrical Storage Tanks with Dome by Finite Element Method," *University of Massachusetts, Amherst*.
- Bleich,H.H., (1956), "Longitudinal Forced Vibrations of Cylindrical Fuel
-

- Tanks," *Jet Propulsion*, Vol.26, pp 109-111.
- Boyce,W.H., (1973), "Vibration Tests on a Simple Water Tower," *Proceedings of Fifth World Conference on Earthquake Engineering*, Rome, Italy, Vol.1, pp 220-225.
- Cambra,F.J., (1983), "A Study of Liquid Storage Tank Seismic Uplift Behavior," *Proceedings of Symposium on Lifeline Earthquake Engineering*, ASME, pp 37-46.
- Chandrasekharan,A.R., and Krishna,J., (1965), "Water Towers in Seismic Zones," *Proceedings of Third World Conference on Earthquake Engineering*, Auckland, New Zealand, Vol.4, pp 13-30.
- Clough,D.P., (1977), "Experimental Evaluation of Seismic Design Methods for Broad Cylindrical Tanks," *Report No: UCB/EERC 77-10*, Earthquake Engineering Research Centre, University of California, Berkeley, USA.
- Edward,N.W., (1969), "A Procedure for Dynamic Analysis of Thin Walled Cylindrical Liquid Storage Tanks Subjected to Lateral Ground Motions," *Ph. D. Thesis*, University of Michigan, Ann Arbor, USA.
- Hanson,R.D., (1973), "Behavior of Liquid Storage Tanks," *National Academy of Sciences*, pp 331-339.
- Haroun,M.A., (1980), "Seismic Design of Liquid Storage Tanks, *Report No: EERL 80-4*, Earthquake Engineering Research Laboratory, California Institute of Technology, Pasadena, USA.
- Haroun,M.A., (1981), "Behavior of Unanchored Oil Storage Tanks: Imperial Valley Earthquake," *Journal of Technical Topics in Civil Engineering*, ASCE, Vol.109, pp 22-40.
- Haroun,M.A., (1986), "Advances in the Seismic Analysis of Liquid Storage Tanks," *Proceedings of the Eighth Symposium on Earthquake Engineering*, Roorkee, Vol.1, pp 585-592.
- Haroun,M.A., and Abou-Izzeddine,W., (1992a), "Parametric Study of Seismic Soil-Tank Interaction I: Horizontal Excitation," *Journal of Structural Engineering*, ASCE, Vol.118, No.3, pp 783-797.
- Haroun,M.A., and Abou-Izzeddine,W., (1992b), "Parametric Study of Seismic Soil-Tank Interaction II: Vertical Excitation," *Journal of Structural Engineering*, ASCE, Vol.118, No.3, pp 798-812.
- Haroun,M.A., and Elliathy,H.M., (1985), "Seismically Induced Fluid Forces on Elevated Tanks," *Journal of the Technical Topics in Civil Engineering*, ASCE, pp 1-15.
- Haroun,M.A., and Elliathy,H.M., (1986), "Seismic Analysis of X Braced Elevated Tanks," *Proceedings of the Third U.S. National Conference*
-

on Earthquake Engineering, Vol.4, Charleston, S.C., USA.

Haroun,M.A., and Housner,G.W., (1981a), "Seismic Design of Liquid Storage Tanks," *Journal of Technical Councils, ASCE*, Vol.107, pp 191-207.

Haroun,M.A., and Housner,G.W., (1981b), "Earthquake Response of Deformable Liquid Storage Tanks," *Journal of Applied Mechanics, ASME*, Vol.48, pp 411-418.

Haroun,M.A., and Housner,G.W., (1981c), "Dynamic Interaction of Storage Tanks and Foundation Soil," *Proceedings of Second ASCE/EMD Conference on Dynamic Response of Structures*, Atlanta, USA, pp 346-360.

Haroun,M.A., and Temraz,M.K., (1992), "Effects of Soil-Structure Interaction on Seismic Response of Elevated Water Tanks," *Soil Dynamics and Earthquake Engineering*, Vol.11, pp 73-86.

Housner,G.W., (1957), "Dynamic Pressures on Accelerated Fluid Containers," *Bulletin of the Seismological Society of America*, Vol.47, pp 15-35.

Housner,G.W., (1963), "The Behavior of Inverted Pendulum Structures During Earthquakes," *Bulletin of the Seismological Society of America*, Vol.53, pp 403-417.

Ifrim,M. and Bratu,C., (1969), "The Effect of Seismic Action on the Dynamic Behavior of Elevated Water Tanks," *Proceedings of Fourth World Conference on Earthquake Engineering*, Santiago, Chile, Vol.B-4, pp 127-142.

Jacobsen,L.S., (1929), "Vibration Research at Stanford University," *Bulletin of the Seismological Society of America*, Vol.19, pp 1-27.

Jain,S.K., and Sameer,U.S., (1993), "A Review of Requirements in Indian Codes for Aseismic Design of Elevated Water Tanks," *The Bridge and Structural Engineer*, ING-IABSE, Vol.23, No.1, March, pp 1-16.

Jennings,P.C., (Editor), (1971), "Engineering Features of the San Fernando Earthquake of February 9, 1971," *Report EERL 71-02*, Earthquake Engineering Research Laboratory, California Institute of Technology, Pasadena, USA.

Kawasumi,H., (Editor), (1964), "General Report on the Nigata Earthquake of 1964," Tokyo Electrical Engineering College Press.

Kumar,A., (1981), "Studies of Dynamic and Static Response of Cylindrical Liquid Storage Tanks," *Ph.D. Thesis*, Rice University, Houston, USA.

Lau,D.T., Zeng,X., and Clough,R.W., (1992), "Dynamic Uplift Analysis of Unanchored Cylindrical Tanks," *Proceedings of Tenth World Conference*

- on Earthquake Engineering, Madrid, Spain, Vol.9, pp 5011-5016.
- Lee,S.C., and Reddy,D.V., (1979), "Seismic Response of Elevated Liquid Storage Tanks," **Proceedings of Second US National Conference on Earthquake Engineering**, Stanford, pp 193-199.
- Manos,G.C., (1992), "Study of the Vibratory Characteristics of Unanchored Cylindrical Liquid Storage Tank Models," **Proceedings of Tenth World Conference on Earthquake Engineering**, Madrid, Spain, Vol.9, pp 4969-4974.
- Meamari,A.M., Ahmadi,M.M. and Rezaee,B., (1992), "Behavior of Reinforced Concrete Water Towers During Manjil-Roudbar Earthquake," **Proceedings of Tenth World Conference on Earthquake Engineering**, Madrid, Spain, Vol.9, pp 4953-4959.
- Marchaj,T.J., (1979), "Importance of Vertical Acceleration in the Design of Liquid Containing Tanks," **Proceedings of the Second U.S. National Conference on Earthquake Engineering**, Stanford, USA.
- Möller,O., and Rubinstein,M., (1992), "Reliability-Based Design of R/C Water Tank Structures Under Seismic Action," **Earthquake Engineering and Structural Dynamics**, Vol.21, pp 665-678.
- Niwa,A., (1978), "Seismic Behavior of Tall Liquid Storage Tanks," **Report No: UCB/EERC 78-04**, Earthquake Engineering Research Centre, University of California, Berkeley.
- Niwa,A., and Clough,R.W., (1982), "Buckling of Cylindrical Liquid Storage Tanks Under Earthquake Loading," **Earthquake Engineering and Structural Dynamics**, Vol.10, pp 107-122.
- Peek,R., and Jennings,P.C., (1988), "Simplified Analysis of Unanchored Tanks," **Earthquake Engineering and Structural Dynamics**, Vol.16, pp 1073-1085.
- Peek,R., (1988), "Analysis of Unanchored Liquid Storage Tanks Under Lateral Loads," **Earthquake Engineering and Structural Dynamics**, Vol.16, pp 1087-1100.
- Priestley,M.J.N., Davidson,B.J., Honey,G.D., Hopkins,D.C., Martin,R.J., Ramsay,G., Vessey,J V., and Wood,J.H., (1986), "Seismic Design of Liquid Storage Tanks," **Recommendations of a Study Group of the New Zealand National Society for Earthquake Engineering**, New Zealand.
- Ramaiah,B.K., and Gupta,D.S.R.M., (1966), "Factors Effecting Seismic Design of Water Towers," **Journal of the Structural Division, Proceedings of ASCE**, Vol.92, No.ST4, pp 13-29.
- Rutenberg,A., (1992), "Nonlinear Response of Asymmetric Building Structures and Seismic Codes: A State of the Art Review," **European Earthquake Engineering**, Vol.6, No.2, pp 2-19.
-

- Shaaban,S.H., and Nash,W.A., (1975), "Finite Element Analysis of Seismically Excited Cylindrical Storage Tank, Ground Supported and Partially Filled with Liquid," University of Massachussetts, Amherst, USA.
- Shepherd,R., (1972), "Two Mass Representation of a Water Tower Structure," *Journal of Sound and Vibration*, Vol.23, No.3, PP 391-396.
- Shepherd,R., (1973), "The Seismic Response of Elevated Water Tanks Supported on Cross Braced Towers," *Proceedings of Fifth World Conference on Earthquake Engineering*, Rome, Italy, pp 640-649.
- Shih,C., and Babcock,C.D., (1980), "Scale Model Buckling Tests of a Fluid Tank Under Harmonic Excitation," *Preprint 80-C2/PVP/66*, PVP Conference, ASME, San Francisco.
- Shih,C., and Babcock,C.D., (1984), "Buckling of Oil Storage Tanks in SPPL Tank Farm During the 1979 Imperial Valley Earthquake," *Preprint 84-PVP-74*, PVP Conference, ASME, San Antonio.
- Sonobe,Y., and Nishikawa,T., (1969), "Study on the Earthquake Proof Design of Elevated Water Tanks," *Proceedings of Fourth World Conference on Earthquake Engineering*, Santiago, Chile, Vol.B-4, pp 11-24.
- Steinbrugge,K.V., (1965), "Earthquake Damage and Structural Performance in the United States," Chapter 9, *Earthquake Engineering*, Editor: Robert Wiegel, Prentice Hall, Inc., Englewood Cliffs, New Jersey.
- Steinbrugge,K.V., and Moran,D.F., (1954), "An Engineering Study of the South Californian Earthquake of July 21, 1952 and Its Aftershocks," *Bulletin of the Seismological Society of America*, Vol.44, Appendix R, pp 436-453.
- Steinbrugge,K.V., and Flores,R., (1963), "Engineering Report on the Chilean Earthquakes of May, 1960 - A Structural Engineering Viewpoint," *Bulletin of the Seismological Society of America*, Vol.53, No.2, pp 225-307.
- Ungureanu,N., and Negoita,A., (1992), "About the Earthquake Response of the Flexible Storage Tanks," *Proceedings of Tenth World Conference on Earthquake Engineering*, Madrid, Spain, Vol.9, pp 4989-4993.
- US Atomic Energy Commission, (1963), "Nuclear Reactors and Earthquakes," *TID-7024*, pp 367-390.
- Veletsos,A.S., (1974), "Seismic Effects in Flexible Liquid Storage Tanks," *Proceedings of Fifth World Conference on Earthquake Engineering*, Rome, Italy, Vol.1, pp 1-24.
- Veletsos,A.S., and Shivakumar,P., (1993), "Sloshing Response of Layered
-

Liquids in Rigid Tanks," **Earthquake Engineering and Structural Dynamics**, Vol.22, pp 801-821.

Veletsos,A.S., and Turner,J.W., (1979), "Dynamics of Out-of-Round Liquid Storage Tanks," **Proceedings of Third EMD Special Conference, ASCE**, pp 471-474.

Veletsos,A.S., and Yang,T., (1990), "Soil-Structure Interaction Effects for Laterally Excited Liquid Storage Tanks," **Earthquake Engineering and Structural Dynamics**, Vol.19, pp 473-496.

Wandi,A.M.A, and Hanson,R.D., (1989), "Nonlinear Seismic Response Behavior of Cross-Braced Steel Elevated Water Tanks," **Research Report**, Department of Civil Engineering, The University of Michigan, Ann Arbor, USA.

Wozniak,R.S., and Mitchell,W.W., (1978), "Basis of Seismic Design Provisions for Welded Steel Oil Storage Tanks," **Forty Third Meeting, API**, Toronto.

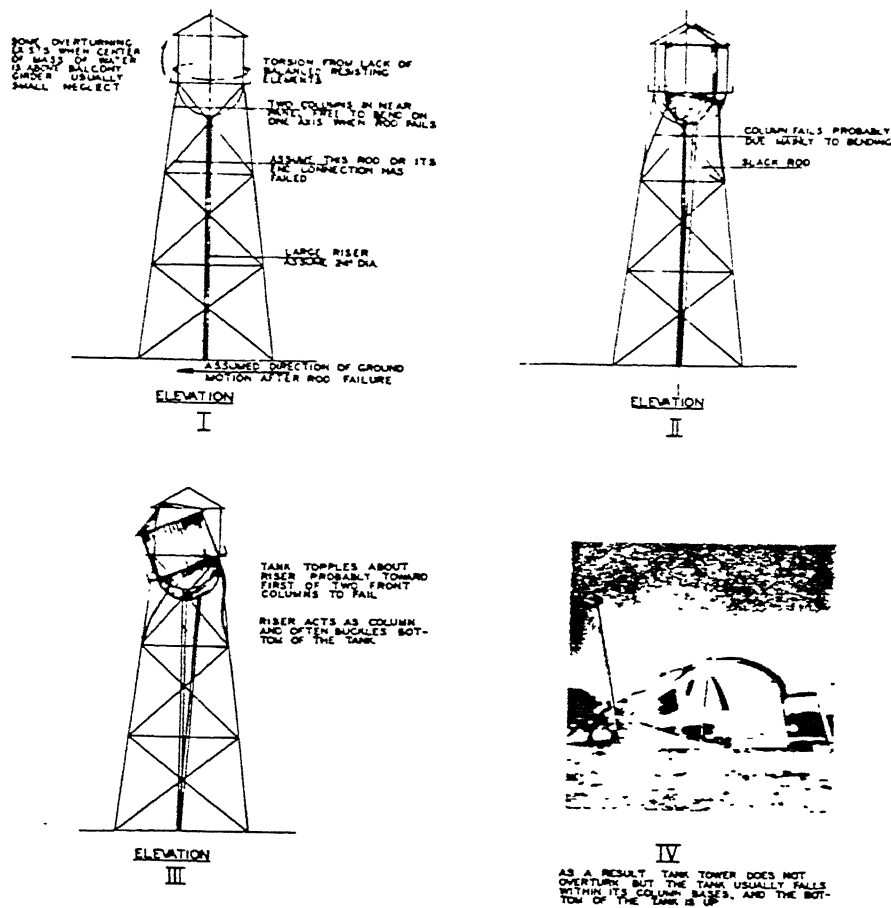


Figure 1.1a : Collapse of a steel elevated tank in torsion (Steinbrugge, 1965).

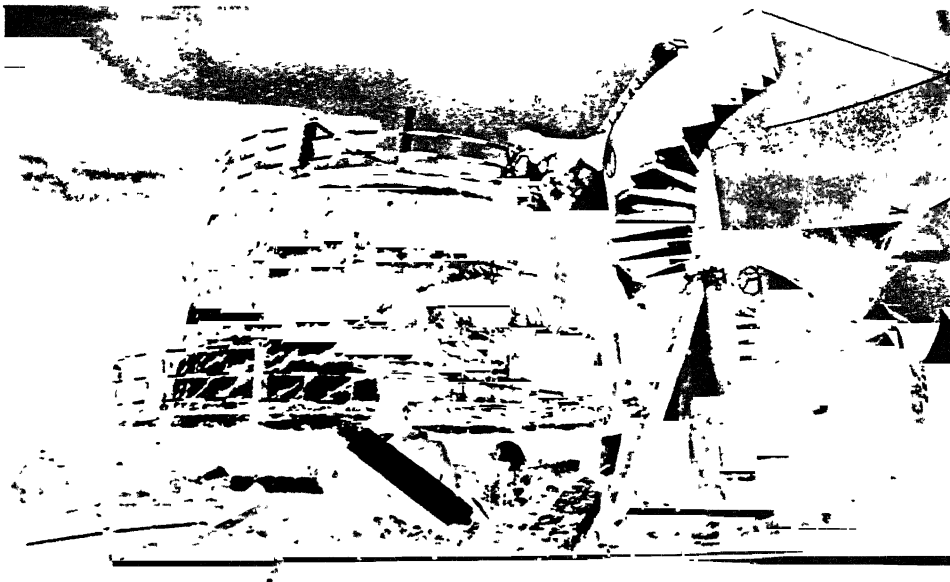


Figure 1.1b : Collapse of a reinforced concrete elevated water tank in torsion (Jain et al, 1994).

CHAPTER 2

LATERAL-TORSIONAL COUPLING IN THE LINEAR ELASTIC RESPONSE

2.1 INTRODUCTION

Structures, whose centres-of-stiffness (CS) do not coincide with the centres-of-mass (CM), are considered as torsionally unbalanced structures. They undergo rotation in the horizontal plane under a horizontal translatory movement of the ground. Elevated water tanks are seemingly symmetric structures. Usually, from the view point of stiffness and mass, they are at least bisymmetric, if not axisymmetric. Hence, their CS and CM tend to coincide. Even in such symmetric structures, instances arise at which a small eccentricity between CS and CM may be introduced. For instance, a geometrical imperfection in the columns could result in a small eccentricity between CS and CM. Sloshing of the water mass also may cause a shift in the CM, and thereby resulting in some eccentricity. Asymmetric placements of ladders, stairs and pipelines may be other sources of eccentricity.

The lateral and torsional motions of unsymmetric structures get coupled. The dynamic amplification of the rotational response is much larger, if the uncoupled lateral and torsional frequencies of a structure are close to each other (*e.g.*, Skinner and Skilton, 1965; Shepherd and Donald, 1967; Penzien, 1969; Hoerner, 1971; Kan and Chopra, 1977; Tso and Dempsey, 1980; Kan and Chopra, 1981; Chopra and Hejal, 1988). The above studies also conclude that this amplification effect is most pronounced when the eccentricity is small. Evidence of small

eccentric structures exhibiting considerable torsional response during earthquakes due to closely-spaced torsional and lateral natural periods is recorded in the literature (e.g., Lin and Papageorgiou, 1989).

Past studies on torsion have primarily focused on rotation about CM and the corresponding torque to evaluate the relative magnitude of torsional response. The study presented in this chapter discusses the linear lateral-torsional coupling behaviour of elevated water tanks, particularly in light of the displacement response along the perimeter columns of the frame stagings. It is seen that in addition to the various parameters identified in the past, the ratio of torsional stiffness to lateral stiffness also affects the torsional response.

2.2 MODELLING OF ELEVATED WATER TANKS

Elevated water tanks can be supported on various types of stagings, e.g., frame staging, concrete shaft staging, and masonry wall staging (see Figure 2.1). The tanks supported by masonry wall are called cisterns, and are usually of small capacity. However, this study addresses the torsional behaviour of tanks supported on frame stagings alone, even though the broad conclusions of this study are equally applicable to shaft supported tanks and cisterns.

2.2.1 Idealization

To understand its dynamic behaviour, a three-dimensional tank structure can be idealized as follows. Often, the tank mass is very much larger than that of the staging. As an accepted practice, the entire mass of the elevated water tank structure inclusive of one-third of the

staging mass can be considered to act at the top of the staging. Secondly, the staging, which offers lateral and torsional stiffness to the inertial forces generated at top of the staging under seismic ground motions, can itself be replaced by a set of equivalent elements each of which individually resists the lateral forces only.

Generally, elevated water tanks have two types of modes of lateral vibration namely, the impulsive and the sloshing modes of vibration. Similarly, impulsive and sloshing modes of vibration also exist under torsional motion. The natural periods of the sloshing modes of vibration of elevated water tanks are usually quite large in comparison with both the impulsive natural periods and the natural periods contained in the earthquake ground motions. Hence, only impulsive modes of vibration, in translation and torsion, are considered in this study. So, the structure is modelled as a single-storey system with two degrees of freedom namely, the lateral translation and the rotation of the CM in horizontal plane. The idealization of the tank structure used in this study is shown in Figure 2.2. The study as discussed in this chapter considers only unidirectional ground motion, say along x-direction, as marked in Figure 2.2. The lateral force-resisting elements 1 and 3 oriented in the direction of ground motion (*i.e.*, along x-direction) resist the lateral force and torsional moment, while elements 2 and 4 oriented in the direction perpendicular to that of the ground motion (*i.e.*, along y-direction) resist the torsional moment alone.

2.2.2 Systems Considered

The lateral and torsional behaviours of moment-resisting frame

stagings have been modelled by four-element and two-element systems shown in Figure 2.3. Elements in the idealized system are assumed to have zero out-of-plane stiffness. While four-element system models behaviour of stagings with large number of columns and panels, the two-element system represents the stagings with small number of columns (say, four) and small number of panels.

In the four element system, all the elements offer equal resistance to torsional moment like the columns in a staging. However, under lateral force due to ground motion, elements oriented in the direction of ground motion (elements 1 and 3 in Figure 2.3a) represent the columns located near bending axis of the staging; circumferential beams oriented at a small angle with the direction of lateral force make these columns share most of the lateral force. The elements oriented perpendicular to the ground motion direction (elements 2 and 4 in Figure 2.3a) represent columns located away from the bending axis of the staging; these columns do not contribute much in resisting the lateral force. In case of stagings with four columns, the orientation of circumferential beams are such that all the four columns equally participate in resisting the lateral force as well as torsional moment; therefore, two-element system (Figure 2.3b) in which all the elements equally resist both lateral force as well as torsional moment are able to model the resulting behaviour.

If D is the distance between two extreme end elements in either direction,

$$\frac{K_{\theta}}{K_x} = \begin{cases} D^2/4 & \text{for a two-element system,} \\ D^2/2 & \text{for a four-element system.} \end{cases} \quad (2.1a)$$

K_{θ}/K_x can be expressed in non-dimensionalized form as

$$\frac{K_{\theta}}{K_x D^2} = \begin{cases} 1/4 & \text{for a two-element system,} \\ 1/2 & \text{for a four-element system.} \end{cases} \quad (2.1b)$$

The ratio of torsional stiffness to lateral stiffness to lateral stiffness of stagings with large number of columns and panels is close to that for the four-element system. Similarly, this ratio for stagings with small number of columns (say, four) and panels is similar to that for the two-element systems. These observations have been shown in Chapter 4.

In this study, small eccentricity is introduced by providing one lateral load resisting element oriented in the direction of ground motion (x-direction) with slightly less stiffness and the other element oriented in the same direction with slightly more stiffness than the elements of the corresponding symmetric system. However, the total stiffness, K_x , of the eccentric system is kept same as that of its symmetric counterpart. So, the location of CS slightly shifts from that of CM which is geometric centre (GC) of the symmetric distribution of tank mass. The element in the eccentric system which has lesser lateral stiffness than the element in the corresponding symmetric system will hereinafter be called a flexible element. Similarly, the element which has larger lateral stiffness than the element in the corresponding symmetric system will hereinafter be called a stiff element. Figure 2.4 shows the same graphically.

In this chapter, four-element system has been studied extensively. Also, a limited study on the response of two-element systems with small eccentricity has been conducted.

2.2.3 Equations of Motion

The governing equations of motion of the undamped eccentric system in terms of the lateral displacement (u) and the rotation (θ) of the centre of mass relative to the ground, are

$$\begin{bmatrix} m & 0 \\ 0 & mr^2 \end{bmatrix} \begin{Bmatrix} \ddot{u} \\ \ddot{\theta} \end{Bmatrix} + \begin{bmatrix} K_x & K_x e \\ K_x e & K_\theta \end{bmatrix} \begin{Bmatrix} u \\ \theta \end{Bmatrix} = - \begin{bmatrix} m & 0 \\ 0 & mr^2 \end{bmatrix} \begin{Bmatrix} \ddot{u}_g(t) \\ 0 \end{Bmatrix}, \quad (2.2)$$

where m is the mass of the system; r is the radius of gyration of the mass about CM; K_x is the lateral stiffness of the systems in the x -direction; e is the eccentricity between CM and CS measured along the y -axis; K_θ is the torsional stiffness of the system about CM; and $\ddot{u}_g(t)$ is the ground acceleration at time t . \ddot{u} and $\ddot{\theta}$ are the lateral and torsional accelerations of CM relative to the ground

2.2.4 Response Quantities of Interest

In the past, discussions on lateral-torsional coupling in asymmetric systems have been primarily focused on the rotation about CM. The amplification of rotation due to torsional coupling is well documented in the literature. However, from the design view point, lateral force and lateral displacement of individual elements are of greater consequence. The lateral displacement Δ_i of element i oriented in x -direction arises from both the rotation, θ , and lateral displacement, u , of the CM of the system. If d_i is the distance of such an element i from CM, then

$$\Delta_i = u + d_i \theta. \quad (2.3)$$

Similarly, if b_j is the distance between CM and element j , oriented in

y-direction, then its lateral translation, Δ_j , is given by

$$\Delta_j = b_j \theta . \quad (2.4)$$

In the discussions that follow, Δ_i is used to denote displacement of the elements oriented in both x- and y-directions, without any loss of generality.

Failure is assumed to take place when individual resisting elements cross a specified design maximum displacement. This may be caused either by excessive translation or by excessive rotation of the entire structure. Thus, the absolute maximum element displacement, $|\Delta(t)|_{\max}$, of the elements oriented in the direction of ground motion and the absolute maximum rotation, $|\theta(t)|_{\max}$, of CM are of interest. The values of $|\Delta(t)|_{\max}$ are normalized with respect to the absolute maximum element displacement, $|u_0(t)|_{\max}$, of the corresponding symmetric system, having the same mass m and lateral stiffness K_x as those of the eccentric system considered.

In most of the past studies, $r\theta$ has been used as the measure of rotational response instead of the actual rotation, θ , of CM, where r is the radius of gyration of the mass about CM. Also, in order to non-dimensionalize the mode shape the governing equations of motion are often expressed in terms of u and $r\theta$, instead of u and θ . Focus of the present study is maximum element displacement and therefore choice of $r\theta$ is of no particular advantage over θ . Hence, in the present study, the equations of motion have been expressed in terms of u and θ .

Past studies have shown that when the uncoupled torsional natural period, T_θ , is close to the uncoupled lateral natural period, T_x , i.e., when $T_\theta/T_x \approx 1.0$, the rotation, θ , of the unsymmetric system is

amplified due to torsional coupling effect. This effect is largest at $T_\theta/T_x=1.0$. However, it appears that the element lateral displacement, Δ_1 , need not reach a maximum value at $T_\theta/T_x=1.0$, but may instead be amplified at some other values of natural period ratio, depending on the frequency content of the input ground motion. In fact, at times there could even be some de-amplification in the element lateral displacement Δ_1 , at the same T_θ/T_x where θ is amplified; such a trend is observed in a recent study (DeLallera and Chopra, 1994). Hence, this study clearly distinguishes between the two responses of interest, namely θ and Δ_1 .

2.3 FREE VIBRATION CHARACTERISTICS

The uncoupled lateral and torsional frequencies (ω_x and ω_θ), of the eccentric system are often defined as lateral and torsional frequencies, respectively, of the corresponding symmetric system. Hence, ω_x and ω_θ , and the corresponding uncoupled natural periods, T_x and T_θ , are

$$\omega_x = \frac{2\pi}{T_x} = \sqrt{\frac{K_x}{m}} \quad (2.5)$$

and

$$\omega_\theta = \frac{2\pi}{T_\theta} = \sqrt{\frac{K_\theta}{mr^2}} \quad (2.6)$$

Hereinafter, the ratio of the natural periods is denoted as τ , and is given by

$$\tau = \frac{T_\theta}{T_x} = \frac{\omega_x}{\omega_\theta} . \quad (2.7)$$

The eigen solution of the equations of motion, in Eq.(2.2), gives the two undamped natural frequencies, namely ω_1 and ω_2 , as:

$$\left(\frac{\omega_1}{\omega_x}\right)^2 = \frac{1}{2} \left(1 + \frac{1}{\tau^2}\right) - \sqrt{\frac{1}{4} \left(1 + \frac{1}{\tau^2}\right)^2 - \left(\frac{1}{\tau^2} - \frac{e^2}{r^2}\right)} , \quad (2.8)$$

and

$$\left(\frac{\omega_2}{\omega_x}\right)^2 = \frac{1}{2} \left(1 + \frac{1}{\tau^2}\right) + \sqrt{\frac{1}{4} \left(1 + \frac{1}{\tau^2}\right)^2 - \left(\frac{1}{\tau^2} - \frac{e^2}{r^2}\right)}. \quad (2.9)$$

The corresponding mode shape vectors, $\{\phi_1\}$, and $\{\phi_2\}$ are given by

$$\{\phi\}_i = \begin{Bmatrix} 1 \\ 2 \\ 1 - \left(\frac{\omega_i}{\omega_x}\right)^2 \\ -\frac{e}{r} \end{Bmatrix}, \quad \forall i = [1, 2]. \quad (2.10)$$

From Eq.(2.10), the mode shape vectors are dependent on the absolute value of eccentricity, e , and not directly on the normalized eccentricity, i.e., e/r or e/D . The mode shapes also depend on ω_1 , while ω_1 depends on τ and e/r . So, the mode shapes depend on τ , e/r and e . From Eq.(2.10), between two systems with same T_x , τ , e/r and damping, one with larger value of plan dimensions and larger absolute value of eccentricity will have lesser absolute value of rotation of CM.

2.4 GROUND MOTIONS USED

Three sets of ground motions are used in this study. They are discussed in the sub-sections below.

2.4.1 Harmonic Single-Frequency Synthetic Ground Motions

These ground motions are characterized in terms of the ratio of ground motion frequency (ω) to uncoupled lateral frequency of the structure (ω_x); this ratio has been denoted as β . In the present study, $\beta = \omega/\omega_x$ is varied from 0.5 to 1.5.

2.4.2 Spectrum-Consistent Synthetic Ground Motion

A ground motion consistent with a spectrum similar to the one given in Indian seismic code (IS:1893-1984) for 2% of critical damping, is generated by a procedure detailed in literature (Khan, 1987). The total duration of ground motion generated, t_{total} , is 20.48 seconds. The envelope function used to introduce the nonstationary characteristics in the synthetic ground motion is

$$E(t) = \begin{cases} (t/t_1)^2 & \text{for } t \leq t_1 \\ 1.0 & \text{for } t_1 \leq t \leq t_2 \\ \exp\{-0.2(t-t_2)\} & \text{for } t_2 \leq t \leq t_{\text{total}}, \end{cases} \quad (2.11)$$

where t is the time in seconds; t_1 is the time during which the ground motion builds up; and t_2 is the time after which motion starts decaying. The steady state duration of ground motion ($t_2 - t_1$) is taken as 9.0 sec. t_1 and t_2 are taken as 3.48 sec and 8 sec, respectively. The response spectrum regenerated from the synthetic ground motion time history has a maximum departure of around 10% from the target spectrum in the acceleration sensitive region (i.e., for natural periods between 0.0 and 0.5 second), as shown in Figure 2.5a. The generated time history is shown in Figure 2.5b.

2.4.3 Ground Motions With Idealized Spectra

The responses of systems under random ground motions are strongly contingent on the energy content in each of the frequencies. This means that a general consensus on the overall behaviour can only be gathered after considering a number of representative random ground motions. However, two extreme cases may be visualized encompassing most ground

motions, namely (i) flat acceleration spectrum, *i.e.*, the spectral acceleration, SA , is constant, and (ii) hyperbolic acceleration spectrum. Two variations are considered in the hyperbolic spectrum. namely $SA \propto 1/T$ and $SA \propto 1/T^{2/3}$, representing the actual and design spectra in the higher period region. The idealized spectra are shown in Figure 2.6.

2.5 DAMPING

For harmonic single-frequency ground motion, 2% of critical damping is considered in each mode of the corresponding uncoupled symmetric system. Such a simplification removes off-diagonal terms from the damping matrix. This is adopted to facilitate decoupling and arrive at an approximate, but closed-form, solution. Since, the objective of the present study is to better understand the behaviour of lateral-torsionally coupled system, such a closed-form expression will facilitate easy reference to the continuous variation of the response quantities with respect to the critical parameters of the problem. The damping matrix, thus, takes a simplified form as given below:

$$[C] = \begin{bmatrix} 2m\omega_x\zeta & 0 \\ 0 & 2mr^2\omega_\theta\zeta \end{bmatrix}, \quad (2.12)$$

where ω_x and ω_θ are the uncoupled lateral and torsional frequencies of the system, respectively, and ζ the modal damping ratio. In this study, ζ is taken as 0.02.

For synthetic spectrum-consistent ground motions, 2% of the critical damping is considered in each mode of the torsionally-coupled system and damping matrix is derived as per the procedure described in

the literature (Clough and Penzien, 1987).

Modal analysis is conducted to obtain response of the coupled system under the idealized flat and hyperbolic spectra of the ground motion. The modal responses are combined by the CQC method (Gupta, 1990). While combining the modal responses, a modal damping ratio of 2% of critical damping is used for each mode.

2.6 PARAMETERS CONSIDERED

The range of the parameters used in this study are briefly discussed below.

2.6.1 Uncoupled Lateral Natural Period, T_x

In the current study, responses are studied for systems with $T_x=0.5$ sec, 1.0 sec and 2.0 sec, representing the typical natural periods in acceleration-sensitive, velocity-sensitive and displacement-sensitive regions of response spectrum, respectively. These values of natural period are also good representation of realistic lateral periods of elevated tanks.

2.6.2 Uncoupled Natural Period Ratio, τ

Earlier studies have used T_x/T_θ as the influencing parameter for studying torsional response. However, in the present study, $\tau=T_\theta/T_x$ is used. The range of natural period ratio, τ , for elevated water tanks generally takes values between 0.4 and 1.5; this is shown in Chapter 4. So, in the parametric study presented in this chapter, τ is varied from 0.25 to 2.0. Systems with large τ refer to torsionally flexible systems

and, those with small τ refer to torsionally stiff systems.

2.6.3 Normalized Eccentricity

Normalized eccentricity is considered in two possible ways, namely (a) constant e/r , and (b) constant e/D . The radius of gyration, r , of the mass is a measure of its spread in plan. Hence, a constant value of e/r implies that eccentricity is a fixed percentage of the plan dimension of the mass. On the other hand, a constant value of e/D implies that eccentricity is a fixed percentage of the distance D between the extreme lateral force resisting elements. Since r is a quantity dependent on the geometric distribution of mass in plan, it is not easy to physically visualize the meaning of constant e/r . However, one can easily reflect on the meaning of constant e/D , since D is the physical distance between lateral force resisting elements

In the current study, small eccentricity cases of both $e/r = 0.05$, and $e/D = 0.05$ are considered to observe the difference in the trends of responses. A large eccentricity case of $e/D = 0.2$ is considered to observe the basic trends in the behaviour of large eccentricity systems.

2.7 STUDY UNDER HARMONIC GROUND MOTIONS

2.7.1 Analytical Derivation

The equations of motion, Eq.(2.2), under the harmonic single-frequency ground motion given by

$$\ddot{u}_g(t) = a_g \sin \omega t, \quad (2.13)$$

are solved analytically for a four-element system. The lateral displacement of CM of the damped system is

$$u(t) = - \frac{a_g}{\omega_x^2} \frac{(QR - PS)\cos \omega t + (PR + QS)\sin \omega t}{R^2 + S^2}, \quad (2.14)$$

the rotation of CM is

$$\theta(t) = \frac{a_g}{\omega_x^2} \frac{\left(\frac{e}{r}\right) (R \sin \omega t - S \cos \omega t) \left(\frac{1}{r}\right)}{R^2 + S^2}, \quad (2.15a)$$

and, the contribution of rotation to the element displacement is

$$\frac{D}{2} \theta(t) = \frac{a_g}{\omega_x^2} \frac{\left(\frac{e}{r}\right) (R \sin \omega t - S \cos \omega t) \left(\frac{D}{2r}\right)}{R^2 + S^2}, \quad (2.15b)$$

where

$$\begin{aligned} P &= \frac{1}{\tau^2} - \beta^2, \\ Q &= \frac{2\beta\zeta}{\tau}, \\ R &= (1-\beta^2)P - \frac{4\beta^2\zeta^2}{\tau} - \frac{e^2}{r^2}, \\ S &= 2\beta\zeta \left\{ P + \frac{1-\beta^2}{\tau} \right\} \end{aligned} \quad (2.16)$$

$$\text{and } \beta = \frac{\omega}{\omega_x}$$

In a four-element system (Figure 2.3a) with constant lateral natural period, T_x , decrease in non-dimensionalized stiffness ratio $K_\theta/(K_x D^2)$ due to removal of the two elements perpendicular to the ground motion will cause a decrease in r to maintain a constant value of τ . And, the system will reduce to a two-element system (Figure 2.3b). Since, the distance D between the resisting elements does not change, the ratio $D/(2r)$ in Eq.(2.15b) increases resulting an increase in the contribution of the rotation to the element displacement. So, between a four-element system representing stagings with many panels and columns and a two-element system representing stagings with less number of

panels and columns, the later will exhibit greater effect of torsional coupling, if both have same T_x , τ , e/r and modal damping. This shows the need of specifying non-dimensionalized stiffness ratio $K_\theta/(K_x D^2)$ in addition to the usual parameters required to define a linear eccentric system.

The flexible element displacement is

$$\Delta_f(t) = -\frac{a}{\omega_x^2} \frac{\left(QR-PS-\frac{eS}{r\tau\sqrt{2}}\right)\cos\omega t + \left(PR+QS+\frac{eR}{r\tau\sqrt{2}}\right)\sin\omega t}{R^2 + S^2} \quad (2.17)$$

and the stiff element displacement is

$$\Delta_s(t) = -\frac{a}{\omega_x^2} \frac{\left(QR-PS+\frac{eS}{r\tau\sqrt{2}}\right)\cos\omega t + \left(PR+QS-\frac{eR}{r\tau\sqrt{2}}\right)\sin\omega t}{R^2 + S^2} \quad (2.18)$$

The displacement of CM of the corresponding symmetric system is

$$u_0(t) = -\frac{a}{\omega_x^2} \frac{(1-\beta^2)\sin\omega t - (2\beta\zeta)\cos\omega t}{(1-\beta^2)^2 + (2\beta\zeta)^2} \quad (2.19)$$

Hence, the amplitude of element displacements, $\Delta_f(t)$ and $\Delta_s(t)$, normalized with respect to the amplitude of $u_0(t)$ is

$$\Delta_{fn} = \frac{\sqrt{\left(QR-PS-\frac{eS}{r\tau\sqrt{2}}\right)^2 + \left(PR+QS+\frac{eR}{r\tau\sqrt{2}}\right)^2}}{R^2 + S^2} \cdot \sqrt{(1-\beta^2)^2 + (2\beta\zeta)^2} \quad (2.20)$$

and

$$\Delta_{sn} = \frac{\sqrt{\left(QR-PS+\frac{eS}{r\tau\sqrt{2}}\right)^2 + \left(PR+QS-\frac{eR}{r\tau\sqrt{2}}\right)^2}}{R^2 + S^2} \cdot \sqrt{(1-\beta^2)^2 + (2\beta\zeta)^2} \quad (2.21)$$

$\theta(t)$ from Eq.(2.15) is normalized with $a_g\sqrt{2}/(D\omega_x^2)$, and the normalized rotation $\theta_n(t)$ is given by

$$\theta_n(t) = \frac{\theta(t)}{\left[\frac{a_g\sqrt{2}}{D\omega_x^2}\right]} \quad (2.22)$$

2.7.2 Results and Discussion

The absolute displacement of CM, u , absolute rotation about CM, θ , and absolute displacements of flexible and stiff elements, Δ_f and Δ_s , respectively, increase with lateral natural period, T_x , as seen from Eqs.(2.14), (2.15), (2.17) and (2.18). However, the normalized displacement of flexible and stiff elements, Δ_{fn} and Δ_{sn} , given by Eqs.(2.20) and (2.21), do not depend on lateral natural period, T_x , except through the frequency ratio β ($=\omega/\omega_x$).

The maximum normalized rotation of CM is shown in Figure 2.7a as a function of τ for different values of β . It is seen that the largest amplification occurs when β is close to $1/\tau$, i.e., when the natural period of the harmonic single-frequency ground motion is very close to the torsional natural period of the system. Further, the amplification is the largest when $\beta=1$ and $\tau=1$; this is because at these values the time period of the ground motion is equal to the lateral as well as the torsional natural periods. The amplification very sharply decreases as β moves away from 1 (e.g., for $\beta = 0.9$ or 1.1 , the peak amplification is about 50% of that for $\beta=1$).

The maximum lateral displacement of CM normalized with that of the corresponding symmetric system for different excitation frequency ratios, β , is shown in Figure 2.7b. Each curve corresponding to a particular value of β shows a maximum and a minimum, the location and magnitude of these vary with β . However, no maximum is found in the immediate neighbourhood of $\tau=1$, though for $\beta=1$ there is a minimum at $\tau=1$.

The maximum normalized flexible-element displacement, Δ_{fn} , is shown

in Fig.2.8a. In general, the peak in Δ_{fn} increases with decrease in β , except around $\beta=1$. A similar trend is noticed in the normalized stiff element displacement, Δ_{sn} , shown in Figure 2.8b.

The envelope of maximum rotation versus τ curves for different β is shown in Figure 2.9a. The figure also includes the envelope of the maximum $r\theta/(a_g/\omega_x^2)$ to show the difference in behaviour, if any, between θ and $r\theta$. It can be visualized from the figure that maximum value of θ and $r\theta$ show similar variation with τ upto $\tau=1.2$. For $\tau>1.2$, θ seems to be insensitive to change in τ while $r\theta$ weakly increases with τ . Note that in the present study, r increases with τ , and therefore, for a high value of τ , such increase in r is reflected in values of $r\theta$. Since, the peaks in maximum rotation occur at different values of τ for different β , in a real earthquake the exact value of τ at which the largest amplification will occur, depends upon the frequency content of the ground motion.

Envelopes of normalized maximum element displacement over the considered range of τ for different values of β are shown in Figure 2.9b. For $\tau>1$, the flexible element undergoes larger displacement than the stiff element; while for $\tau<1$, the stiff element undergoes larger displacement than the flexible element. In the following sections, an opposite trend is observed under the ground motion containing pulses of different frequencies. The general increase in maximum element displacement with increase in τ , as observed in Figure 2.9b, is owing to the increase in torsional flexibility of the system. Envelope is multivalued at some values of τ . This is owing to the fact that for two different values of β , the maximum displacements are different, though

they occur at the same τ .

2.8 STUDY UNDER SPECTRUM-CONSISTENT SYNTHETIC GROUND MOTION

2.8.1 Numerical Analysis

The equations of motion Eq.(2.2) are numerically solved for synthetic time-history using the Newmark's γ - β integration scheme (Bathe and Wilson, 1976) and the Gauss' elimination procedure. The Newmark's parameters, γ and β , are taken as 0.5 and 0.25, respectively, implying a constant average acceleration over the time step. The time step, Δt , is chosen as 0.01 seconds, which is sufficiently small in comparison to the natural periods T_θ and T_x of the systems considered.

2.8.2 Results and Discussion

2.8.2.1 Rotational Response

Many researchers (e.g., Kan and Chopra, 1977; Tso and Dempsey, 1980) have reported that rotation of CM is amplified in the neighbourhood of $\tau=1$. This is confirmed in the present study also. Further, this amplification in rotation of CM of systems with small eccentricity ($e/D=0.05$) is noted to be about 5 to 10 times the rotation at $\tau=0.25$ or that at $\tau=2$. For systems with large eccentricity ($e/D=0.2$), this effect is about 3 times. This reconfirms that the effect of torsional coupling is more dominant in systems with smaller eccentricity than those with large eccentricity. Since, the observations made regarding the rotational response only re-affirm the conclusions of the earlier studies, detailed numerical results are not presented here.

2.8.2.2 Element Displacement

The maximum normalized element displacements of four-element systems for $e/r=0.05$, $e/D=0.05$ and $e/D=0.2$ are presented in Figures 2.10a, b and c, respectively. The maximum element displacements of two element systems for $e/D=0.05$ are presented in Fig.2.11.

The element displacements of small-eccentricity systems show a clear minimum near $\tau=1$ accompanied by a local maximum each on either side of $\tau=1$, as seen in Figures 2.10a, 2.10b and 2.11. In the cases studied, these maxima are well within the range $0.7 < \tau < 1.25$. Beyond this range of $0.7 > \tau > 1.25$, the element displacements are less amplified and show a stabilizing trend. The de-amplification observed in element displacement of small-eccentricity systems around $\tau=1$ can be explained using system responses under harmonic single-frequency ground motions discussed in section 2.7.2. In Figure 2.7b, the de-amplification is most pronounced in systems with $\tau=1$ for $\beta=1$, while the ordinates due to other harmonics are small. So, under ground motions consisting of all frequencies, a minimum in element displacement will be expected due to de-amplification in lateral displacement of CM in systems with $\tau \approx 1$.

In Figures 2.10 and 2.11 the maximum element displacement in eccentric systems is only upto 20-40% more than that in the symmetric systems. Clearly, the effect of torsional coupling on maximum element displacements is quite subdued as against what one would expect on the basis of rotation alone.

Comparison of Figures 2.10b and 2.11 shows that the effect of torsion is more pronounced in the two-element systems as compared to that in the four-element systems. This is in line with observation made

in section 2.7.1 about the importance of $K_\theta/(K_x D^2)$ on torsional coupling. The two-element system has $K_\theta/(K_x D^2)$ equal to 0.25 as against 0.50 for the four-element system, and this causes more torsional coupling in two-element systems.

Consider the maximum normalized displacements of flexible and stiff elements given by Figures 2.12a and 2.12b, respectively. The flexible-element displacement is larger in the systems with $\tau < 1$, while stiff-element displacement is larger in the systems with $\tau > 1$. This is in contrast with the findings under harmonic ground motion in section 2.7.2 (Figure 2.9b) but in line with the response under idealized spectra discussed in section 2.9.2. Therefore, even though under single-frequency excitations the flexible element displacement dominates in systems with $\tau > 1$ (Fig.2.9b), the combined effect of different frequencies in the earthquake-type ground motion is such that stiff-element displacement is amplified in this range (Fig.2.12b), and vice versa.

In figures 2.10 and 2.11, the curves for $T_x = 0.5$ sec are generally higher than those for $T_x = 1.0$ sec and $T_x = 2.0$ sec. This implies that the effect of torsional coupling on element displacements is more prominent for stiff systems than that for flexible systems but with same value of τ . On the other hand, the study based on idealized shape of response spectrum, reported in the next section, shows that for a given value of τ the torsional coupling effect on element displacement is independent of T_x . This issue needs more detailed investigation in the future.

As one goes from $e/D = 0.05$ to $e/D = 0.20$, the eccentricity increases four folds while the maximum normalized element displacement increases

by only about two times (Figure 2.10b and 2.10c). Clearly, the effect of lateral-torsional coupling on element displacements is more prominent in small eccentricity systems than in large eccentricity systems.

The element displacement of a large eccentricity system with $e/D=0.2$ has a minimum at $\tau \approx 1$ in all cases of $T_x = 0.5$ sec, 1.0 sec and 2.0 sec (see Figure 2.10c). However, no clear trend is present on the existence of maxima on either side of this minimum, except when $T_x=0.5$ sec.

2.9 STUDY UNDER IDEALIZED SPECTRA

2.9.1 Analysis

The maximum element displacements are studied under three spectra, namely (i) flat spectrum, with spectral acceleration $SA = \text{constant}$, (ii) hyperbolic spectrum with SA varying as $1/T$, and (iii) hyperbolic spectrum with SA varying as $1/T^{2/3}$ (see Figure 2.6). From the governing equations of motion given by Eq.(2.3), the participation factor, P_i , for mode i of the two degree of freedom system is

$$P_i = \frac{\phi_{1i}}{\phi_{1i}^2 + \phi_{2i}^2 r^2}, \quad \forall i=[1,2] \quad (2.23)$$

where ϕ_{1i} and ϕ_{2i} are the elements corresponding to lateral and rotational degrees of freedom, respectively, in the i th mode shape vector. Displacement of the flexible element in mode i , normalized with that of the corresponding symmetric system, is

$$\Delta_{fni} = \begin{cases} (\phi_{1i} - \frac{D}{2} \phi_{2i}) P_i \left(\frac{\omega_x}{\omega_i} \right)^2 & ; \text{ for SA = constant;} \\ (\phi_{1i} - \frac{D}{2} \phi_{2i}) P_i \left(\frac{\omega_x}{\omega_i} \right)^{4/3} & ; \text{ for SA } \propto 1/T^{2/3}, \\ (\phi_{1i} - \frac{D}{2} \phi_{2i}) P_i \left(\frac{\omega_x}{\omega_i} \right) & ; \text{ for SA } \propto 1/T. \end{cases} \quad (2.24)$$

Similarly, the normalized displacement of the stiff side element is

$$\Delta_{sni} = \begin{cases} (\phi_{1i} + \frac{D}{2} \phi_{2i}) P_i \left(\frac{\omega_x}{\omega_i} \right)^2 & ; \text{ for SA = constant;} \\ (\phi_{1i} + \frac{D}{2} \phi_{2i}) P_i \left(\frac{\omega_x}{\omega_i} \right)^{4/3} & ; \text{ for SA } \propto 1/T^{2/3}; \\ (\phi_{1i} + \frac{D}{2} \phi_{2i}) P_i \left(\frac{\omega_x}{\omega_i} \right) & ; \text{ for SA } \propto 1/T. \end{cases} \quad (2.25)$$

From Eq.(2.24) and (2.25), the maximum normalized element displacement is a function of ω_x/ω_i and the mode shape vectors. From Eqs.(2.8), (2.9) and (2.10), these quantities are independent of T_x . So, the maximum normalized element displacement obtained under the three idealized spectra are independent of T_x .

2.9.2 Results and Discussion

The responses of four-element system with $e/D=0.05$ and $e/D=0.20$ under the three spectra are shown in Figures 2.13 and 2.14, respectively, and that of two-element system with $e/D=0.05$ are shown in Figure 2.15; these curves are independent of T_x . For small eccentricity systems, maximum normalized element displacement has a minimum near $\tau=1$, accompanied by a maximum each on either side at around $\tau=0.9$ and 1.1 (see Figures 2.13 and 2.15). This is consistent with the observation in systems subjected to synthetic ground motions. Also, a comparison of Figures 2.13 and 2.15 confirms that lateral-torsional coupling is

stronger in two-element systems than in four-element systems. In small-eccentricity systems, the maximum element displacements exceed those of the corresponding symmetric systems by upto about 15% and 30% for four-element and two-element systems, respectively. In large-eccentricity systems ($e/D=0.20$), this exceedance is by upto about 40% under flat spectrum and by upto about 30% under the two hyperbolic spectra. Thus, an increase in eccentricity from 5% to 20% does not significantly increase the effect of torsional coupling on maximum element displacement.

In all the cases studied here, the flexible element governs the maximum displacement when $\tau < 1$ and the stiff element governs when $\tau > 1$; this is similar to what was observed under synthetic spectrum-consistent ground motion. There is a general concern in the literature about systems which are torsionally very flexible, *i.e.*, value of τ is large. These systems may be expected to exhibit very high torsional response. This issue has been investigated by studying the response of systems with τ upto 50. No marked increase in maximum normalized element displacement is noted. This observation can be explained as follows. The participation Factor, P_i , given by Eq.(2.23), under lateral ground motion reduces with increase in τ , *i.e.*, with an increase in r . This implies that lateral excitations will not excite the torsional response if rotational moment of inertia is very high, unless very high rotational kinetic energy is supplied. If the ground motion contains significant torsional component, the system with large τ may be very easily excited in torsion. While, torsional ground motion is possible in long-plan buildings owing to spatial variation of earthquake time

history, in elevated water tanks, which have relatively small plan dimension, it is much more unlikely.

2.10 CONCLUSIONS

The following broad conclusions are available from the study presented in this chapter:

1. As per the published literature, torsional response of a linear eccentric system is governed by four parameters, namely T_x , τ , e/r and ζ . It is shown here that in addition to these four parameters, the stiffness ratio, $K_\theta/(K_x D^2)$, also has a very significant influence on the element displacements. For a given T_x , τ , e/r and ζ , maximum normalized element displacement of a two-element system is more than that of a four-element system since, the two-element system is having a lower non-dimensionalized stiffness ratio, $K_\theta/(K_x D^2)$ than that of a four-element system. The elevated water tanks with small number of panels and columns have a lower $K_\theta/(K_x D^2)$ and hence, they are more prone to the effect of torsional coupling.
 2. The maximum normalized element displacements of small eccentricity systems exhibits a minimum value at $\tau \approx 1$ and two local maxima, one on either side of $\tau = 1$. The two maxima lie within the range of $0.7 < \tau < 1.25$. Thus, the range $0.7 < \tau < 1.25$ may be considered to be critical from torsional coupling point of view.
 3. The effect of dynamic amplification due to torsional coupling on element responses is more prominent in small-eccentricity systems than in large-eccentricity systems. However, the effect of torsional coupling is less on maximum normalized element displacement than that
-

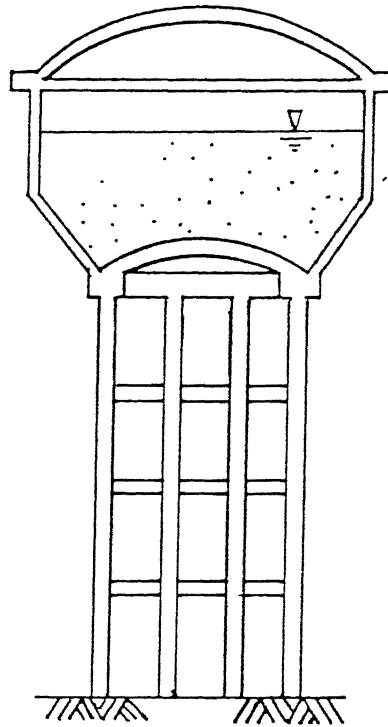
on the rotational response.

4. Under harmonic single-frequency ground motion, envelope of the maximum normalized stiff-element displacement curves for different values of β is having higher ordinates than that for flexible-element displacement curves in the region $\tau < 1$, and vice versa. On the contrary, under spectrum-consistent synthetic ground motion and idealized spectra, flexible element shows maximum displacement for $\tau < 1$, and hence govern the design, while the stiff element exhibits maximum displacement for $\tau > 1$. The contrast in the second case is perhaps due to the combined effect of all the frequencies.
5. Results of this chapter clearly show that elevated tanks should be configured such that the ratio of torsional period to lateral period (τ) does not lie in the range $0.7 < \tau < 1.25$; else, there may be significant torsional response even due to accidental eccentricity. Moreover, the tanks with small number of columns and panels, i.e., low value of $K_\theta / (K_x D^2)$, are more vulnerable to torsional response.

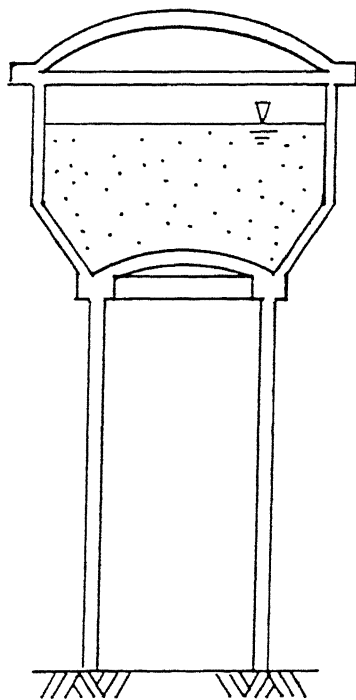
2.11 REFERENCES

- Bathe, J.K., and Wilson, E.L., (1976), **Numerical Methods in Finite Element Analysis**, Prentice-Hall, Inc., Englewood Cliffs, NJ, USA.
- Chopra, A.K., and Hejal, R., (1988), "Earthquake Response of Asymmetric Frame Buildings," **Proceedings of Ninth World Conference on Earthquake Engineering**, Vol.5, pp V31-V36, Tokyo-Kyoto, Japan.
- Clough, R.W., and Penzien, J., (1989), **Dynamics of Structures**, McGraw Hill Book Company, New York, USA.
- De Lallera, J.C., and Chopra, A.K., (1994), "Accidental Torsion in Buildings due to Stiffness Uncertainty," **Earthquake Engineering and Structural Dynamics**, Vol.23, pp 117-136.
- Gupta, A.K., (1990), **Response Spectrum Method**, Blackwell Scientific Publications, Cambridge, England.

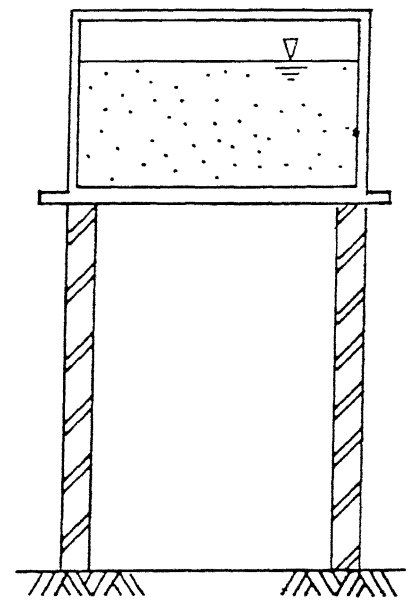
- Hoerner, J.B., (1971), "Modal Coupling and Earthquake Response of Tall Buildings," **Report No: EERL 71-07**, Earthquake Engineering Research Laboratory, California Institute of Technology, Pasadena, CA, USA.
- IS:1893-1984, **Indian Standard Criteria for Earthquake Resistant Design of Structures**, Bureau of Indian Standards, New Delhi, India.
- Kan, C.L., and Chopra, A.K., (1977), "Effects of Torsional Coupling on Earthquake Forces in Buildings," **Journal of Structural Division, ASCE**, Vol.103, No.ST4, pp 805-819.
- Kan, C.L., and Chopra, A.K., (1981), "Torsional Coupling and Earthquake Response of Simple Elastic and Inelastic Systems," **Journal of the Structural Engineering, ASCE**, Vol.107, No.ST8, pp 1569-1587
- Khan, M.R., (1987), "Improved Method of Generation of Artificial Time-Histories, Rich in All Frequencies, from Floor Spectra," **Earthquake Engineering and Structural Dynamics**, Vol.15, No.8, pp 985-992.
- Lin, B.C., and Papageorgiou, A.S., (1989), "Demonstration of Torsional Coupling Caused by Closely Spaced Periods - 1984 Morgan Hill Earthquake Response of the Santa Clara County Building," **Earthquake Spectra**, Vol.5, No.3, pp 539-556.
- Shepherd, R., and Donald, R.A.H., (1967), "Seismic Response of Torsionally Unbalanced Buildings," **Journal of Sound and Vibration**, Vol.6, No.1, pp 20-37.
- Skinner, R.I., Skilton, D.W.C., and Laws, D.A., (1965), "Unbalanced Buildings and Buildings with Light Towers under Earthquake Forces," **Proceedings of the Third World Conference on Earthquake Engineering**, Vol.2, Auckland and Wellington, New Zealand, pp 586-602.
- Penzien, J., (1969), "Earthquake Response of Irregularly Shaped Buildings," **Proceedings of the Fourth World Conference on Earthquake Engineering**, Vol.2, Santiago, Chile, pp A3-75 - A3-89.
- Tso, W.K., and Dempsey, K.M., (1980), "Seismic Torsional Provisions for Dynamic Eccentricity," **Earthquake Engineering and Structural Dynamics**, Vol.8, No.3, pp 275-289.
-



(a) Tank with frame staging



(b) Tank with shaft staging



(c) Cistern with wall staging

Figure 2.1 : Some commonly used stagings of elevated water tanks.

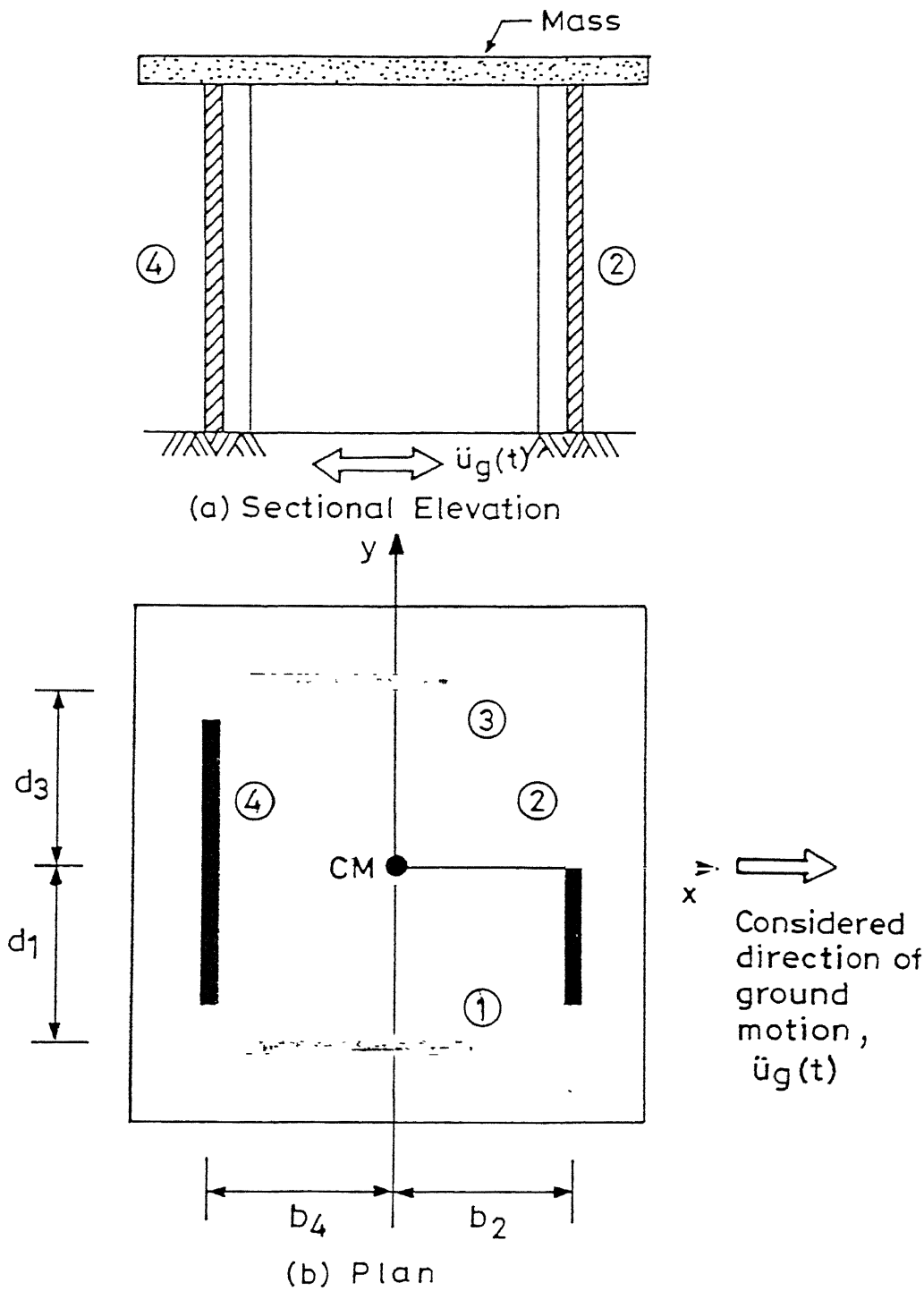
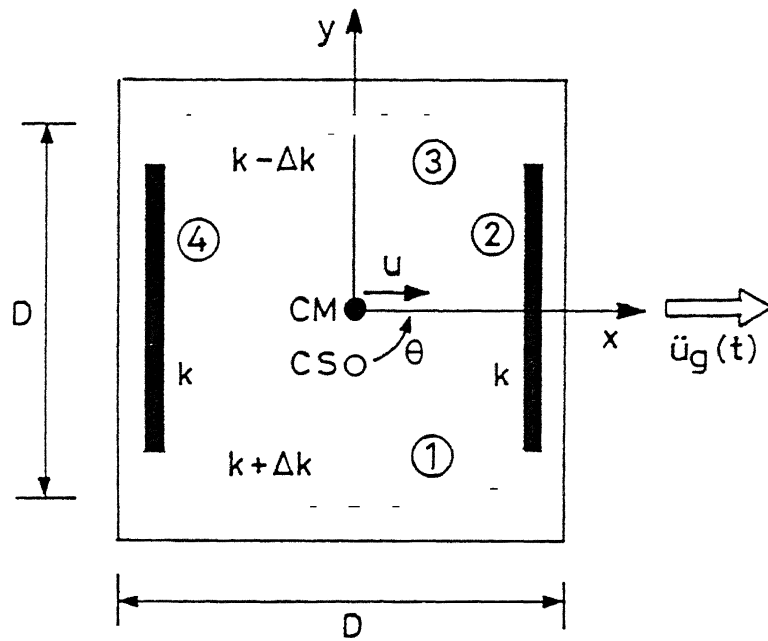
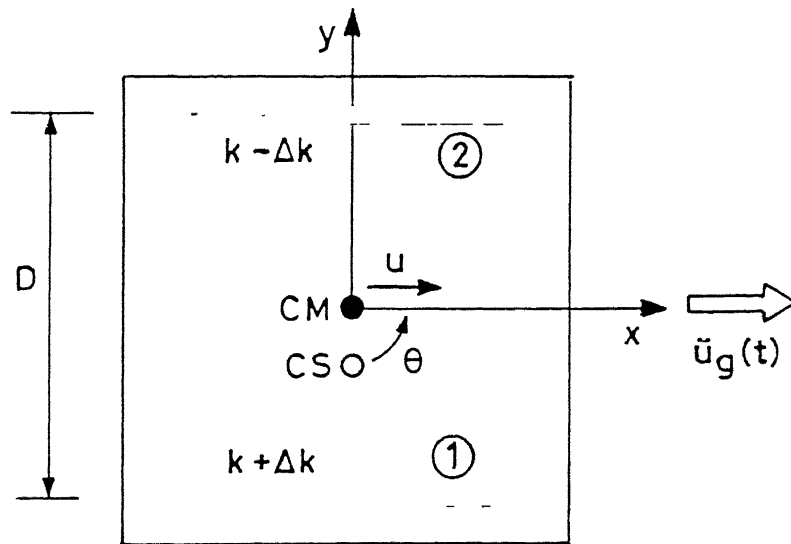


Figure 2.2 : Schematic of the simplified idealization of an elevated water tank structure.

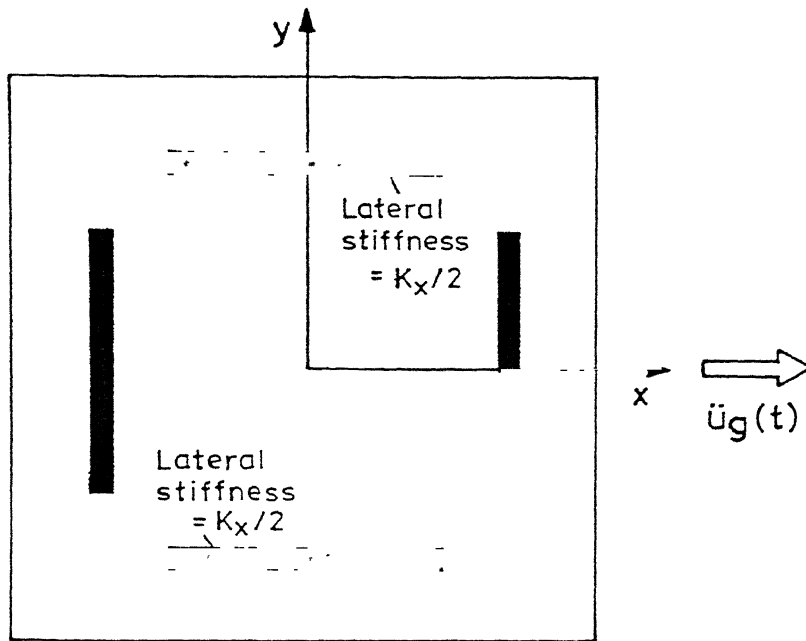


(a) Four-element system ($K_X = 2k$, $K_\theta = kD^2$)

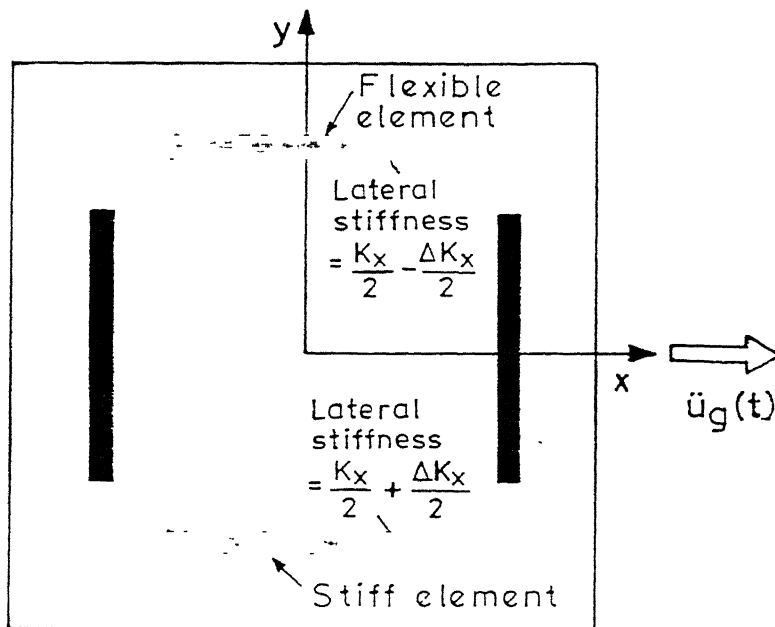


(b) Two-element system ($K_X = 2k$, $K_\theta = kD^2/2$)

Figure 2.3 : Idealized systems considered to model lateral-torsional coupling in elevated water tanks.



(a) Symmetric System



(b) Unsymmetric System

Figure 2.4 : Definition of flexible and stiff elements in eccentric systems.

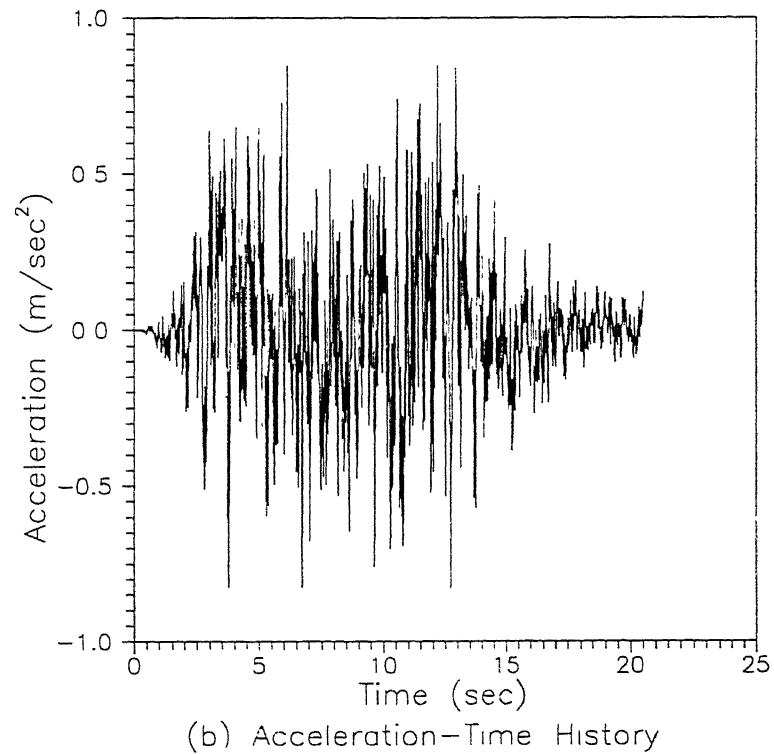
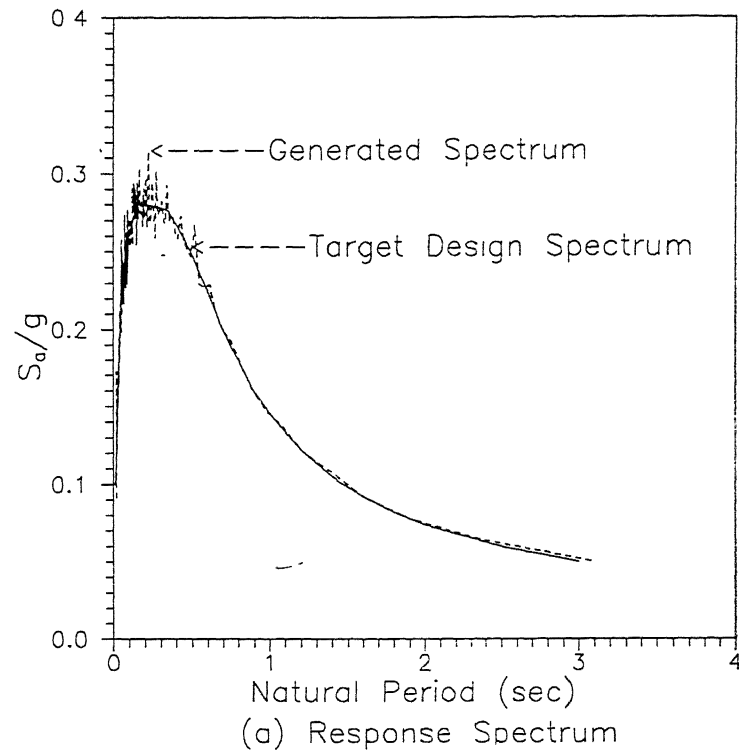


Figure 2.5: Spectrum-consistent synthetic ground motion.

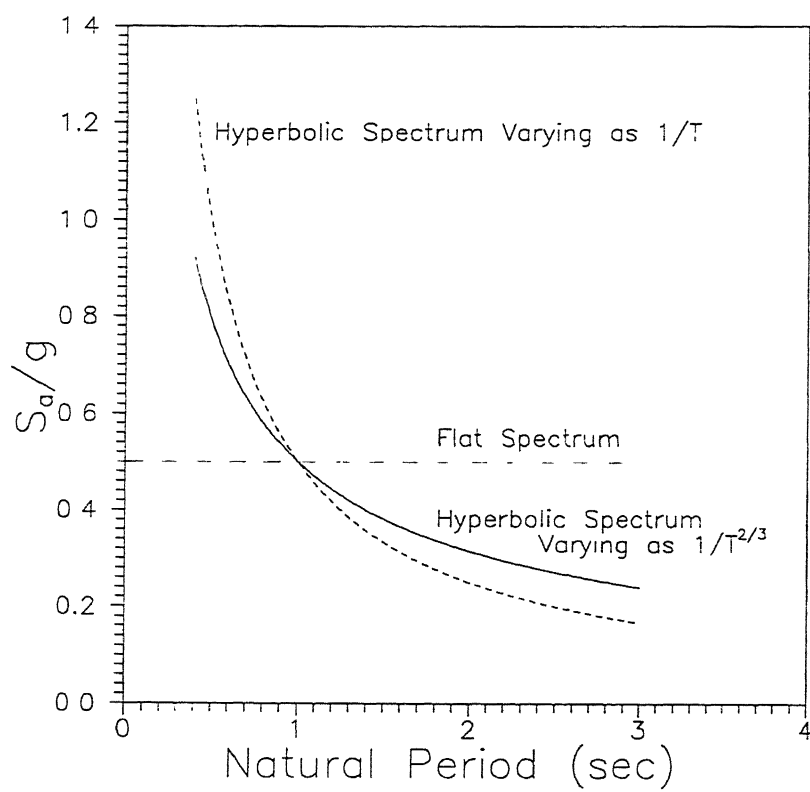
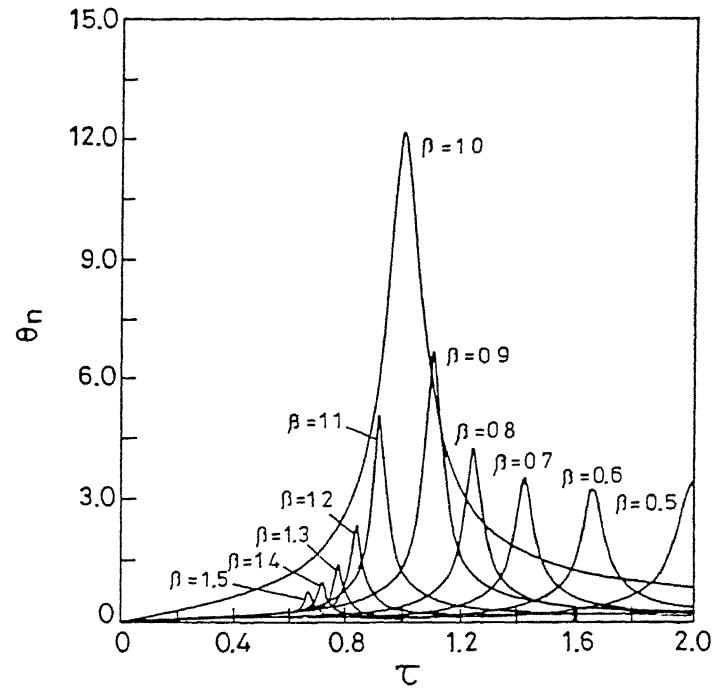
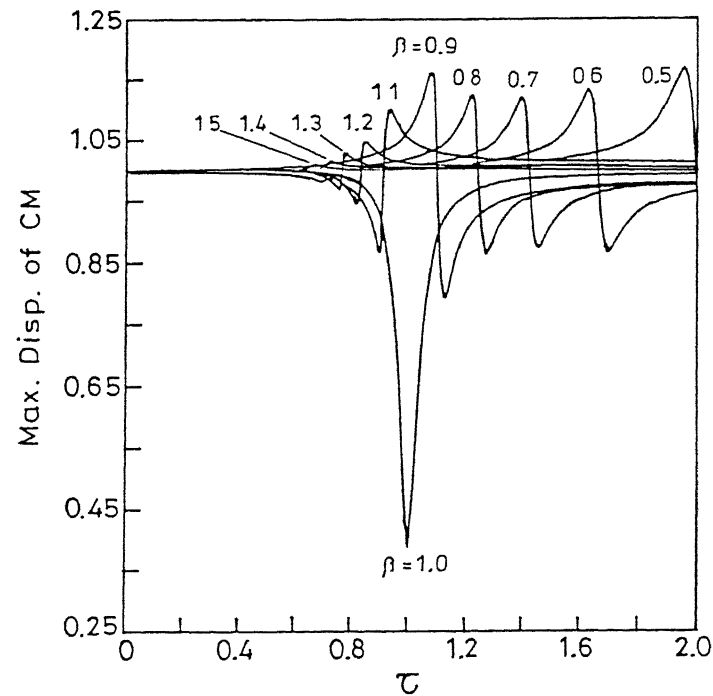


Figure 2.6: The three idealized acceleration spectra considered in the study.

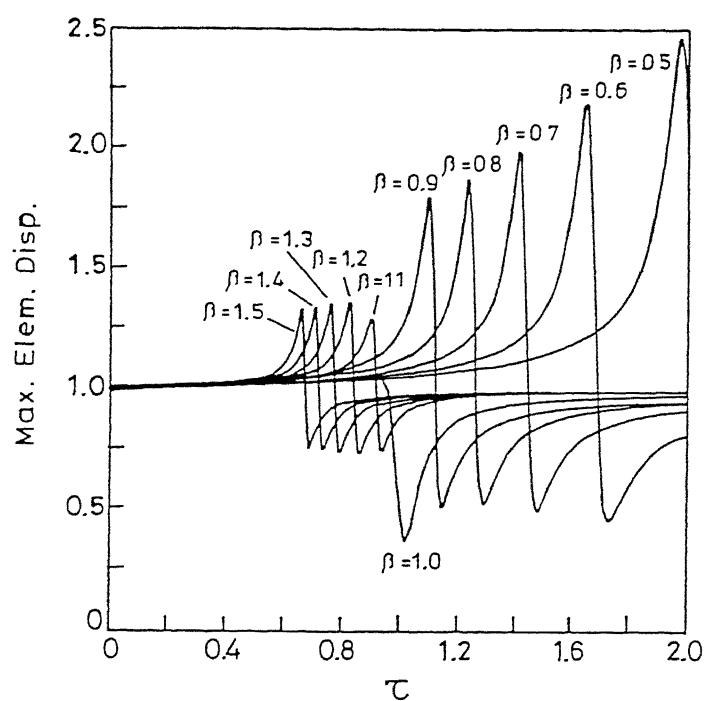


(a) Rotation of CM

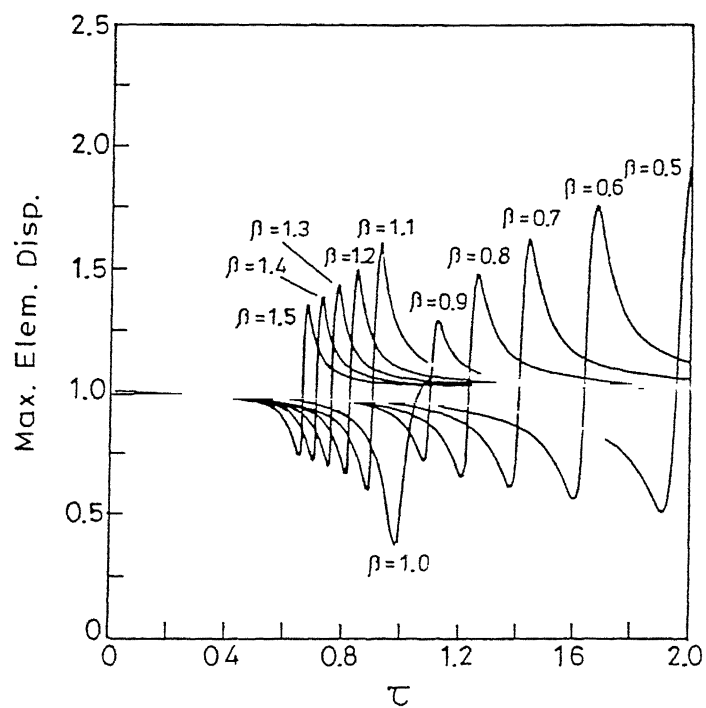


(b) Translation of CM

Figure 2.7 : Maximum normalized response of four-element system for single-frequency harmonic ground motion ($e/r=0.05$).

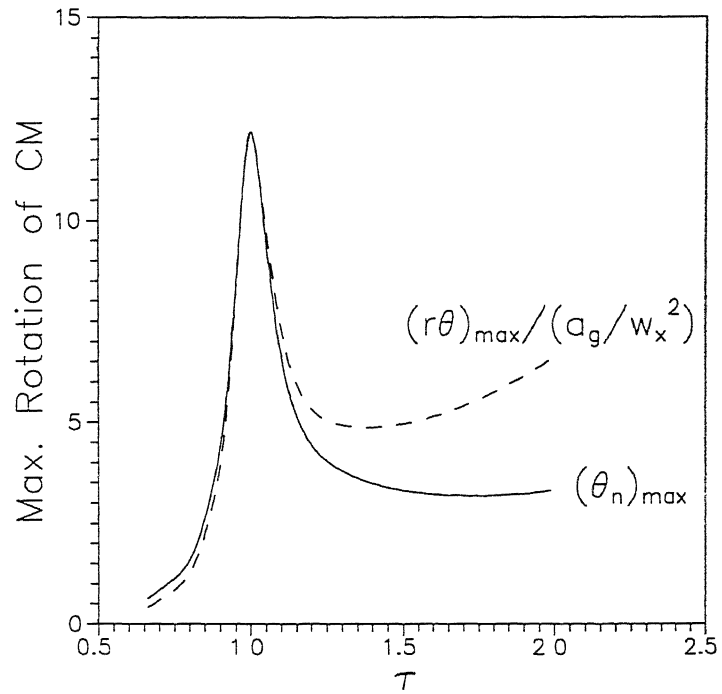


(a) Flexible element displacement

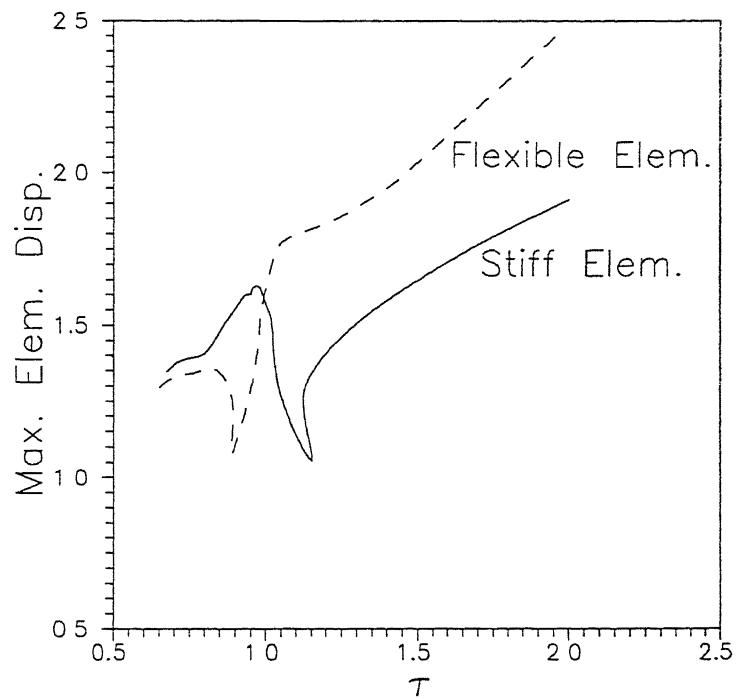


(b) Stiff element displacement

Figure 2.8 : Maximum normalized element displacement of four-element system under single-frequency harmonic ground motion.



(a) Rotation of CM



(b) Element Displacement

Figure 2.9 : Envelopes of maximum response for different values of β (harmonic single-frequency ground motion).

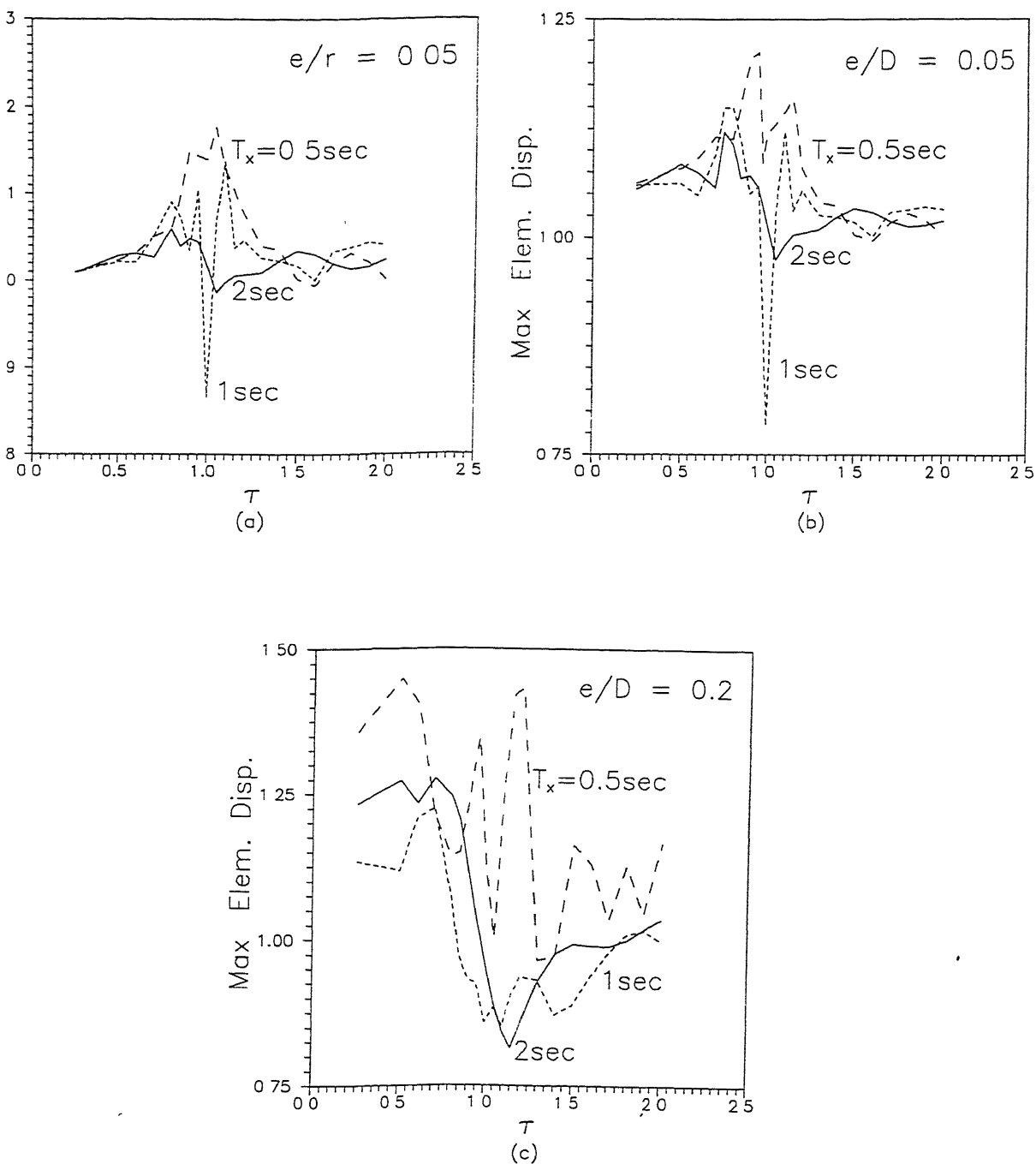


Figure 2.10 : Maximum normalized element displacement of four-element system under spectrum-consistent synthetic ground motion (a) $e/r=0.05$, (b) $e/D=0.05$, and (c) $e/D=0.20$.

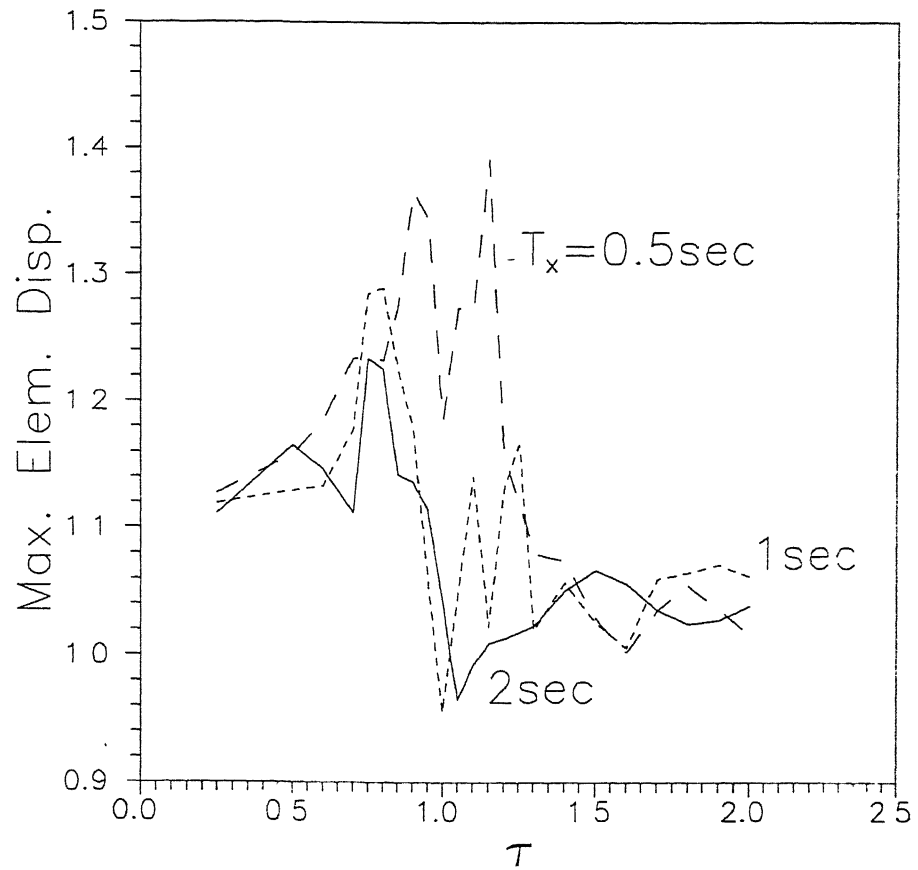
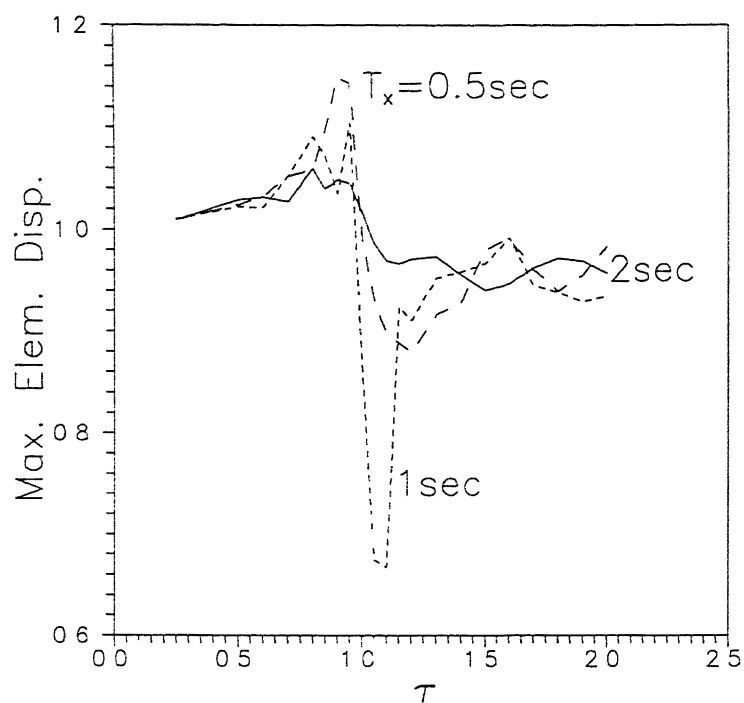
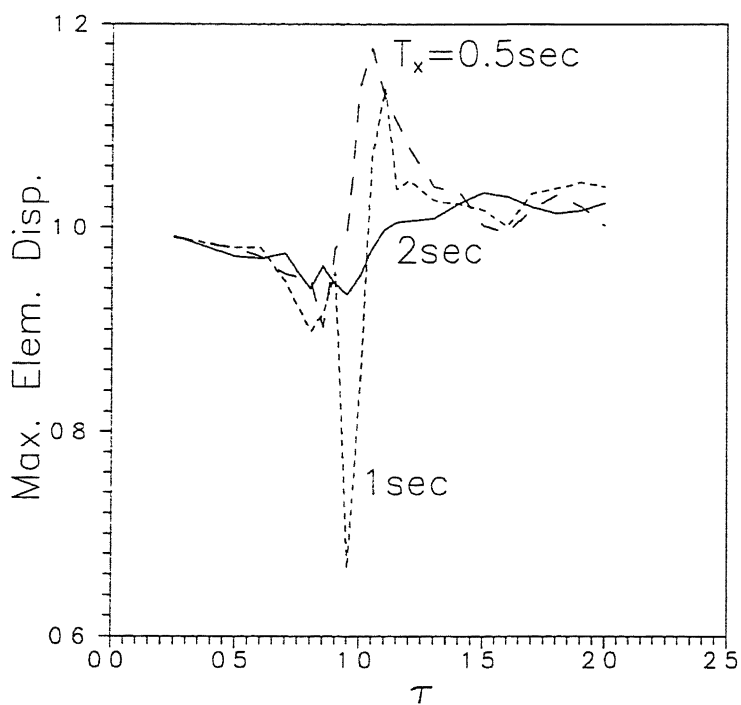


Figure 2.11 : Maximum normalized element displacement of two-element system ($e/D=0.05$) under spectrum-consistent synthetic ground motion.



(a) Flexible Element Displacement



(b) Stiff Element Displacement

Figure 2.12 : Maximum normalized element displacement of four-element system ($e/r=0.05$) under spectrum-consistent synthetic ground motion.

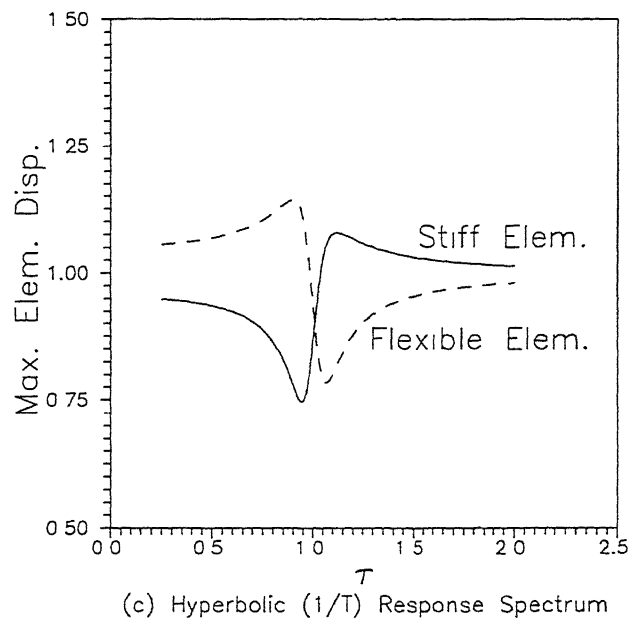
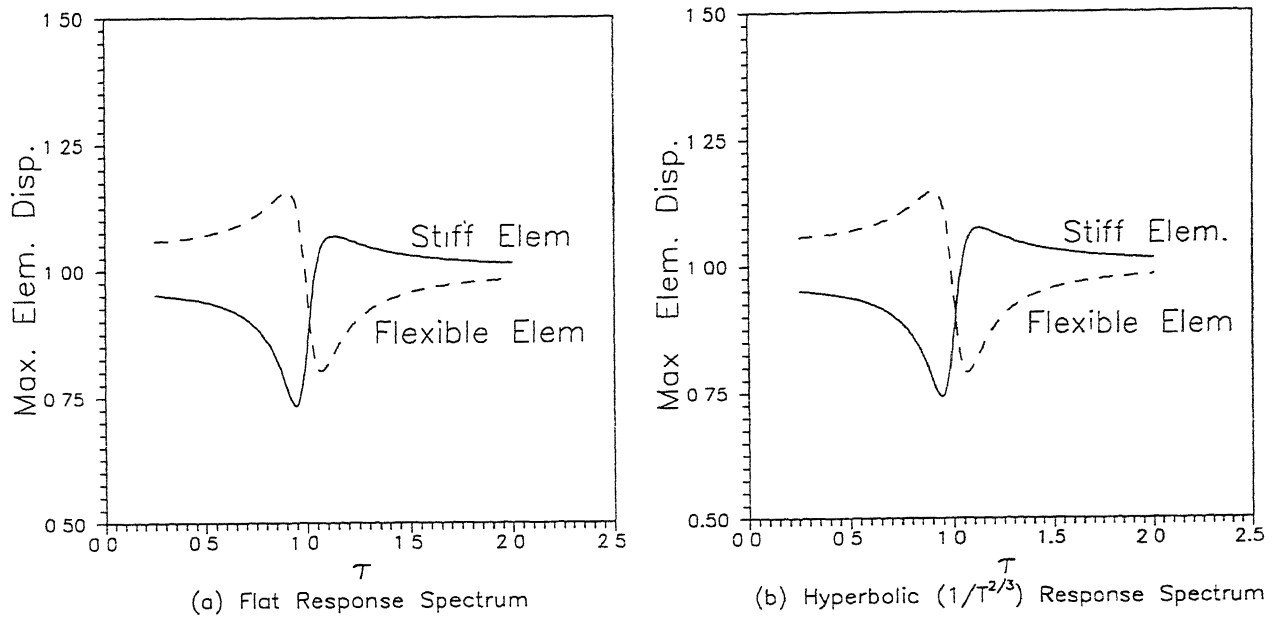


Figure 2.13 : Maximum normalized element displacement of four-element system ($e/D=0.05$) under idealized spectra.

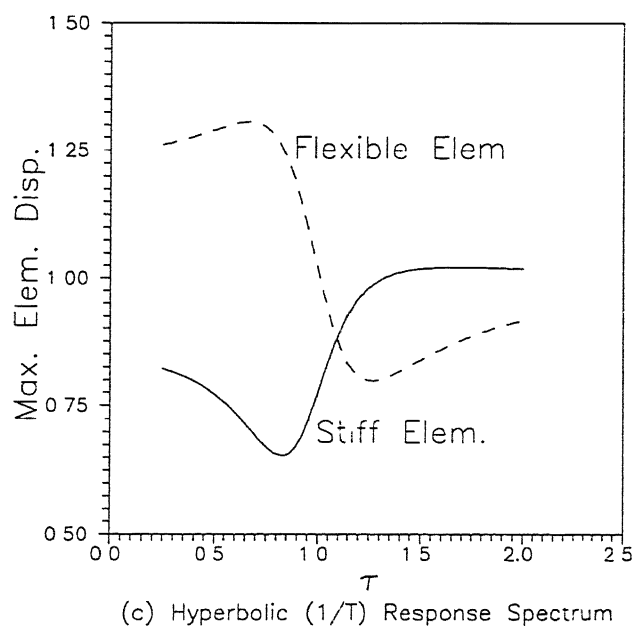
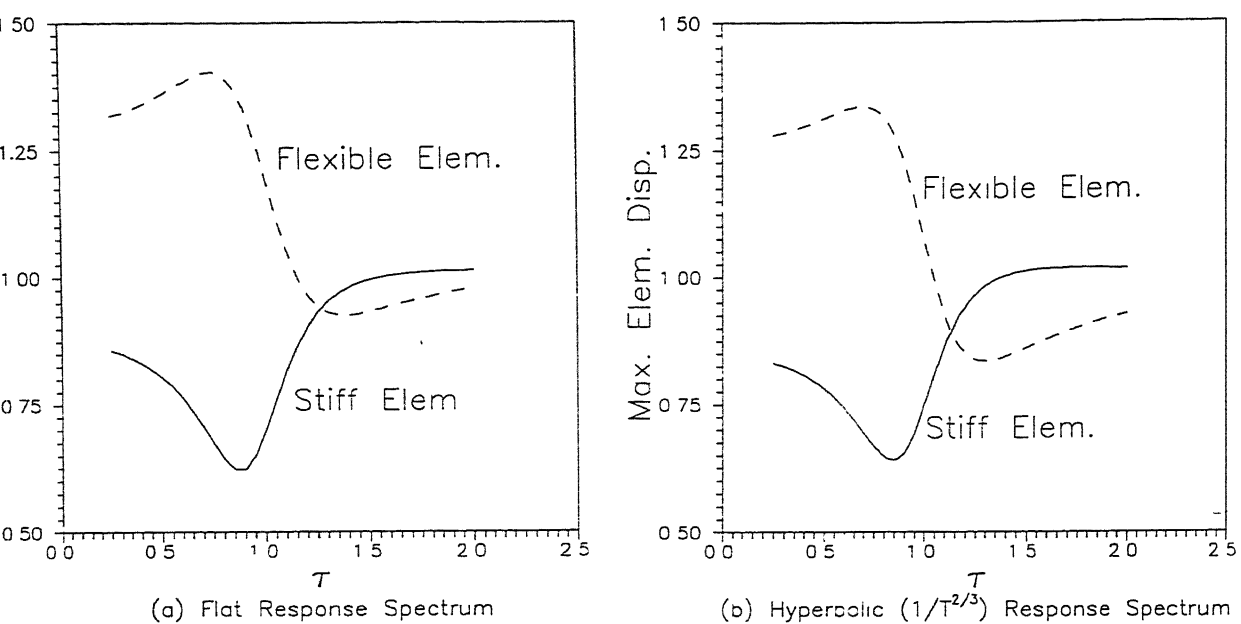
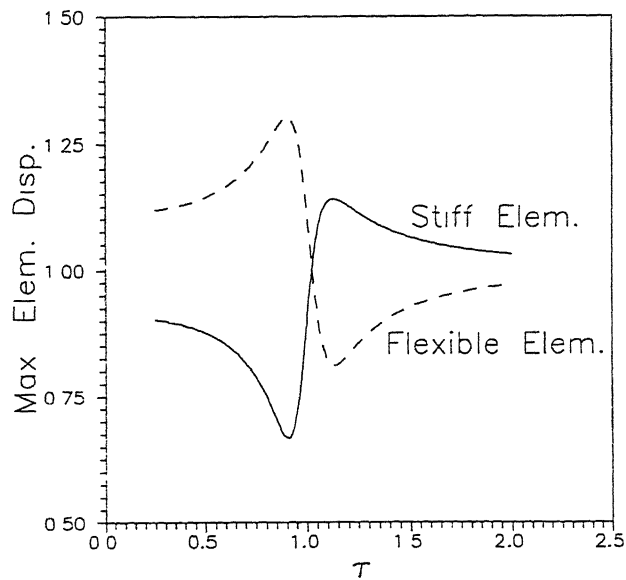
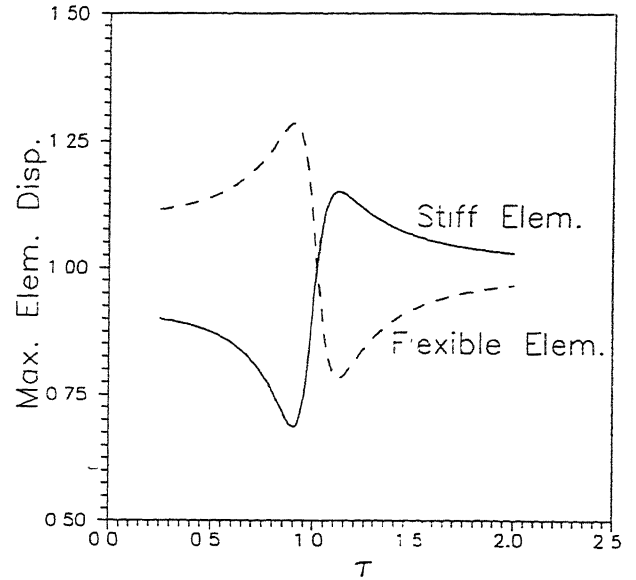


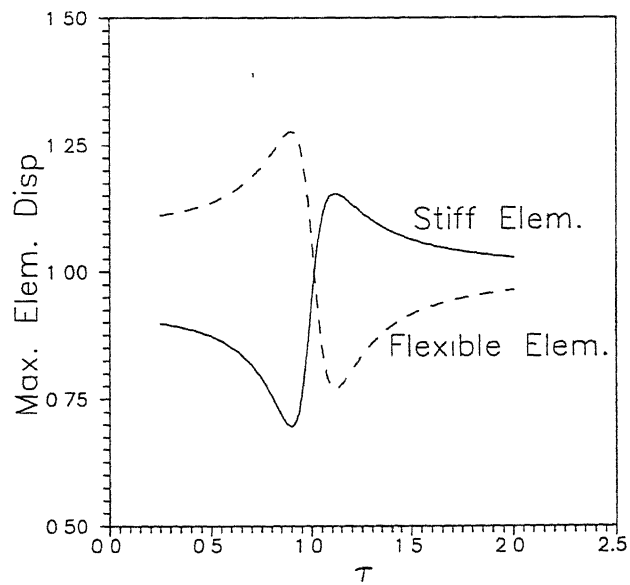
Figure 2.14 : Maximum normalized element displacement of four-element system ($e/D=0.20$) under idealized spectra.



(a) Flat Response Spectrum



(b) Hyperbolic $(1/T^{2/3})$ Response Spectrum



(c) Hyperbolic $(1/T)$ Response Spectrum

Figure 2.15 : Maximum normalized element displacement of two-element system ($e/D=0.05$) under idealized spectra.

CHAPTER 3

INELASTIC TORSIONAL RESPONSE

3.1 INTRODUCTION

This chapter aims at understanding the post-yield torsional behaviour of elevated water tanks. The prominence of lateral-torsional coupling in small-eccentricity systems under linear elastic conditions discussed in Chapter 2, is investigated in the nonlinear range also. While studying the linear elastic behaviour, it is observed that the torsional amplification is much larger in small-eccentricity systems than in large-eccentricity systems. It is expected that this torsional amplification due to closeness of uncoupled torsional and lateral natural periods, may not be as prominent once yielding occurs, since the system no longer retains the closeness of the uncoupled natural periods.

Numerous studies on nonlinear behaviour of systems with lateral-torsional coupling have been reported in the literature; a review of these studies is also available (Rutenberg, 1992). Most of these studies were restricted to response under recorded earthquake ground motions (or associated spectra), and of systems without strength deterioration. However, progressive strength deterioration in the reinforced concrete frame stagings of elevated water tanks may be important. Consider the columns of such stagings which yield due to lateral-torsional coupling caused by small accidental eccentricity. The columns may undergo continued strength deterioration in each new inelastic excursion resulting in large strength eccentricity. This may

place a large ductility demand on some members of the frame staging.

In this chapter, the inelastic responses of elevated water tanks under spectrum-consistent synthetic ground motions, and synthetic ground motions with large pulses characteristic of fault-parallel and fault-normal motions in the proximity of tectonic faults, are presented. The effect of strength deterioration is studied under the spectrum-consistent synthetic ground motions alone and not under near-fault ground motion pulses. The study under the typical near-fault synthetic ground motions is conducted to understand the behaviour of elevated water tanks located in the neighbourhood of major tectonic faults.

The amplification in torsional response due to lateral-torsional coupling with small eccentricity is reported to be absent in yielding systems with elasto-plastic behaviour for resisting elements (Tso and Sadek, 1985). This is attributed to considerable de-tuning of the uncoupled lateral and torsional time periods on yielding. In fact, two earlier studies (Irvine and Kountouris, 1980; Tso and Sadek, 1984) concluded that the peak ductility demand in small-eccentricity systems is similar to that in the symmetric systems.

Further, it has also been reported that including stiffness degrading characteristics in the element does not appreciably change the peak ductility demand in comparison with that obtained when elasto-plastic characteristics are considered (Tso and Sadek, 1985). However, the effects of strength deterioration on the inelastic response of eccentric systems with lateral-torsional coupling are yet to be addressed.

Thus, it seems that small-eccentricity systems, like elevated water tanks, may not have additional distress owing to the stiffness degrading behaviour of reinforced concrete members. However, in case of unsymmetrical yielding due to torsion, strength eccentricity may increase with the number of inelastic excursions due to the strength deteriorating property of reinforced concrete members. In this study, an investigation of this effect has been carried out for small-eccentricity systems. A simplified hysteresis model for strength-deterioration has been proposed and used in this study.

The ground motions generated near a fault consist of long duration impulse of low-frequency (acceleration pulse) perhaps with moderate peak acceleration, as against the large recorded peak accelerations with short duration impulse of high frequency (acceleration spike) characteristics of far-field ground motions. A recent study (Naeim, 1995) cautions that the former may result in significantly larger deformations due to the larger duration of pulses than the later. Rather than the magnitude of peak acceleration, the largest area under a single acceleration pulse and that under a single velocity pulse in the whole time-history may be more meaningful parameters to quantify this effect of pulse duration. In fact, the study (Naeim, 1995) also confirms the above-mentioned effect based on a detailed analysis of the 1994 Northridge earthquake records. The effect of these near-fault motions on small-eccentricity systems is also studied in this chapter.

3.2 SYSTEMS CONSIDERED

The idealized four-element and two-element systems, shown in Figure

2.3 and employed in the linear response analysis presented in Chapter 2, are also used here in the nonlinear response study.

For frame type stagings with low number of panels (say, four or lesser) and four columns, the two-element system reasonably approximates the nondimensionalized ratio of torsional and lateral stiffness $K_{\theta}/(K_x D^2)$ and nondimensionalized ratio of torsional and lateral strength $S_{\theta}/(S_x R_s)$. A detailed derivation of the ratio $S_{\theta}/(S_x R_s)$ of the torsional strength to the lateral strength is given in Appendix A. Also, the range of values that $(S_{\theta}/S_x R_s)$ may take for different stagings of varying number of columns and panels, is presented therein. As the numbers of panels and columns become large, the four-element system better represents the actual system as regards the ratios $K_{\theta}/(K_x D^2)$ and $S_{\theta}/(S_x R_s)$.

When one element in a two-element system yields, the system becomes a mechanism in so far as torsional response is concerned. So, there is no difference in the strength at which first yielding takes place and the strength of the system at which the whole system is converted into a mechanism. In fact, in a staging with four columns, the difference between the strength at which the first column yields and the strength at which the system becomes a mechanism due to yielding of two more columns is not much. On the other hand, the torsional indeterminacy of a staging with many columns is rightly reflected by a four-element system. Systems with higher redundancy in torsion are also considerably stiffer and stronger in torsion; the torsional effects are expected to be much less in such systems than those in systems with less torsional redundancy. Hence, a detailed study is conducted on idealized

two-element systems, followed by a limited study on four-element systems.

3.2.1 Nature of Eccentricity

Depending on the nature of the eccentricity, four cases arise in elevated water tanks, namely:

- (a) Strength-symmetric stiffness-symmetric tanks,
- (b) Strength-symmetric stiffness-eccentric tanks,
- (c) Strength-eccentric stiffness-symmetric tanks,
- and (d) Strength-eccentric stiffness-eccentric tanks.

In case (a), coupling of lateral and torsional motions does not arise. Cases (b) and (c) are most useful in drawing meaningful conclusions regarding the individual effects of strength and stiffness eccentricities on the behaviour of coupled systems. Case (d) reflects the combined effects of cases (b) and (c).

While studying case (b), a small stiffness eccentricity is introduced by increasing the stiffness of one lateral element and decreasing the stiffness of other lateral element by an equal amount. This ensures that the total lateral stiffness, K_x , in the x-direction in Figure 2.3 is kept same as that of the symmetric system. In real situations, the stiffness of the resisting elements of one side of a tank may be larger due to addition of stairs, etc., the stiffnesses of which are not usually considered in the design. Strength eccentricity is introduced by providing one of the lateral elements with lesser strength. So, the system with strength eccentricity has a slightly lesser overall lateral strength with respect to that of a similar

symmetric system. This may occur in reality due to faulty constructions. One would expect that the combined effect of stiffness eccentricity and reduced strength may considerably affect the performance of the system.

Alongside these strength-eccentric systems, strength-symmetric systems with the same overall lateral strength are also studied to isolate the impact of strength eccentricity. Let e_{strength} be the eccentricity due to strength. If D is the distance between the resisting elements as defined in Figures 2.3 and 3.1, then the normalized strength eccentricity is denoted by e_{strength}/D . As in Chapter 2, e denotes the stiffness eccentricity of the system. Since, the focus of present study is on investigation of effects of small eccentricity, both e/D and e_{strength}/D are taken as 0.05.

The present study considers that stiffness eccentricity arises from the noncoincidence of the centre of stiffness (CS) and the geometric centre (GC) of the resisting elements (see Figure 3.1a). However, even if CS is located at GC, eccentricity may arise if the centre of mass (CM) is located eccentrically with respect to GC due to the eccentric distribution of mass (see Figure 3.1b). The first type of eccentric systems are called stiffness-eccentric systems, while the second type are called mass-eccentric systems. In the latter case, the distances of lateral elements from the CM are unequal. One which is more distant from the CM will undergo less displacement when a static lateral load is applied at the CM; this is analogous to a stiff element. Similarly, the element nearer to the CM will undergo more displacement when a static lateral load is applied at the CM; this element is analogous to a flexible element. For a small eccentricity of $e/D=0.05$, the distance of

these two elements from CM varies only by about 10%. Therefore, this will change the contributions of torsional motion to element displacement in the same proportion. Hence, the effect of changing the distance of the element from CM on overall displacement may be even lesser. Therefore, no considerable departure from the observed behaviour of stiffness-eccentric systems is expected in mass-eccentric systems, when the eccentricity is small.

A stiffness-eccentric strength-symmetric system has its eccentricity effective in the linear elastic range and possibly in part of the inelastic range. When all the load-resisting elements are in the post-yield range, this eccentricity disappears. On the other hand, a stiffness-symmetric strength-eccentric system does not have any eccentricity in the linear elastic range; however, in the post-elastic range, when all the elements are yielded, then the strength eccentricity becomes effective. For a mass-eccentric system, the eccentric location of CM does not change even in the post-yield range. So, mass eccentricity is effective in linear elastic as well as completely yielded state of the system. From this consideration, such systems are similar to the stiffness-eccentric strength-eccentric systems, *i.e.*, case (d) systems. In view of these considerations, mass-eccentric systems are not separately studied in this chapter.

Under inelastic conditions in reinforced concrete members, stiffness degradation and strength deterioration may take place under the repeated events of yielding, unloading and reloading during earthquake response. To understand the effect of strength deterioration, behaviour of two-element systems under cases (b) and (c) is studied.

However, a limited study is conducted on the behaviour of four-element systems of case (b) alone subjected to bi-directional ground motion.

Stiffness-eccentric strength-symmetric systems undergo unsymmetrical yielding due to coupled lateral-torsional motion in the linear range. And, in stiffness-symmetric strength-eccentric systems, one element undergoes early yielding due to lesser strength. If such systems are subjected to characteristic fault-parallel or fault-normal ground motion pulses of large duration, then the yielded element may undergo large post-yield displacement even before the ground acceleration changes its direction. Even though systems of both case (b) and case (c) seem to be prone to this effect, only systems of case (b) are studied under typical near-fault synthetic ground motion pulses.

3.3 EQUATIONS OF MOTION AND GROUND MOTIONS USED

The equations of motion of the lateral-torsionally coupled systems in the nonlinear range can be represented as

$$\begin{bmatrix} m & 0 \\ 0 & mr^2 \end{bmatrix} \begin{Bmatrix} \ddot{u} \\ \ddot{\theta} \end{Bmatrix} + [C] \begin{Bmatrix} \dot{u} \\ \dot{\theta} \end{Bmatrix} + \{p\} = - \begin{bmatrix} m & 0 \\ 0 & mr^2 \end{bmatrix} \begin{Bmatrix} \ddot{u}_g(t) \\ 0 \end{Bmatrix}, \quad (3.1)$$

where u , \dot{u} and \ddot{u} are displacement, velocity and acceleration of CM, respectively; θ , $\dot{\theta}$, $\ddot{\theta}$ are rotational displacement, rotational velocity and rotational acceleration, respectively; $[C]$ is the damping matrix; and $\{p\}$ is the stiffness-related resisting force vector. $[C]$ is chosen such that the damping in each mode of the initial linear elastic system is 2% of the critical damping. The damping matrix so obtained is kept constant throughout the analysis. The stiffness of individual element changes as it undergoes yielding, which introduces nonlinearity in $\{p\}$.

The nonlinear matrix equation of motion (Eq.3.1) is numerically solved in the time domain by Newmark's β - γ Method using the iterative Modified Newton-Raphson technique. The Newmark's parameters are chosen as $\gamma=0.5$ and $\beta=0.25$. For systems with lateral natural period, $T_x=1$ sec and 2 sec, the time step for integration is taken as 0.01 sec, while for systems with $T_x=0.5$ sec, it is taken as 0.005 sec. The synthetic ground motion data are generated at a time increment of 0.01 sec. When time integration is carried out with a time step of 0.005 sec, accelerogram data generated at a time increment of 0.01 sec are linearly interpolated to obtain accelerations at every 0.005 sec. The convergence tolerances for iterations are taken as 1.0×10^{-7} N and 1.0×10^{-7} N.m for force and moment quantities, respectively. For all the systems studied having different natural periods, the mass is taken as 1 kg and the stiffnesses are adjusted accordingly to achieve the desired natural periods.

The synthetic ground motion of duration 20.48 secs, shown in Figure 2.5b and discussed in Section 2.4, is used in studying the effect of strength deterioration. Its response spectrum (Figure 2.5a) is consistent with the shape of usual design spectra. It is recognised that studies based on a single ground motion are not sufficient in establishing the exact nature of inelastic response. However, conclusions drawn from the study based on this single ground motion are broad reflections of the trends in the behaviour. While studying the response of four-element system under bi-directional ground motion, another synthetic ground motion (Figure 3.2a) of the same duration of 20.48 seconds is used along the axis of symmetry of the system. It has a similar response spectrum (Figure 3.2b) and same peak ground

acceleration, as that of the ground motion used in the principle direction of investigation (i.e., perpendicular to the axis of symmetry).

When a strike-slip occurs at a fault, ground motions developed in the vicinity have certain characteristic features. They consist of discrete pulses as shown in Figures 3.3a and 3.3b. In the direction parallel to the fault, the ground motion is such that there is a net residual slip (see the displacement pulse in Figure 3.3a). However, in the direction normal to the fault, the ground motion is such that there is no residual slip but there is a half-cycle displacement pulse, indicating a momentary opening and closing of the earth in slip region (see the displacement pulse in Figure 3.3b). For instance, the Port Hueneme earthquake of March 18, 1957 (NS component) (Figure 3.4) shows characteristics very similar to those of the fault normal motion. The magnitude and duration of these pulses vary depending on the slip characteristics. The duration of such a pulse in Port Hueneme earthquake was 1.5 sec (Figure 3.4). Also, these characteristic pulses decay with distance from the fault.

3.4 HYSTERESIS MODEL FOR STRENGTH DETERIORATION

A number of sophisticated strength-deteriorating hysteresis models are available in the literature for reinforced concrete members, e.g., three parameter model (Park *et al.*, 1987). However, in the present study, a simple strength-deteriorating hysteresis model is proposed which broadly reflects the overall lateral response of the reinforced concrete members. This simple model is considered convenient for

Understanding the behaviour qualitatively. Each time a member yields, some damage takes place, resulting in deterioration of its strength. The number of yield excursions regulates the extent of strength deterioration. For simplicity, the strength deterioration is considered as a regime-independent phenomenon in this model, i.e., the amount of plastic strain accumulated does not control the strength decay.

The hysteresis rules employed in this simplified strength deteriorating hysteresis model are as follows:

1. The backbone curve is elastic-perfectly plastic.
2. Each yielding on either side, positive side or negative side, causes a deterioration in the yield force by a definite fraction, δ , of the original (undeteriorated) yield force. This deterioration is effective only on the next plastic excursion, in either the positive side or the negative side.
3. If a yielding is followed by a small amount of unloading such that the current force after unloading is still higher than the new deteriorated strength after the last yielding, then a further loading will cause immediate yielding at the current force level itself.

A general force-displacement curve demonstrating the above hysteresis rules is shown in Figure 3.5. The loading starts from point "o" at which both the load and deformation are zero. Due to monotonic increase in the loading, the element yields at point "a" at which force is equal to F_y . Subsequent loading from "a" to "b" causes the yielding to continue. Unloading takes place from "b" to "c". On re-loading at "c", the element yields "d" at the lowered yield strength of $F_y(1-\delta)$, as

per hysteresis rule 2, since one yield excursion has taken place. Again, from "d" to "e", the element accumulates plastic strain on continued loading. From "e" to "f", unloading takes place. If at point "f", element is re-loaded, three possibilities exist, namely point "f" is at a force level below, at or above the new yield strength $F_y(1-2\delta)$. The first two cases are already described in moving from point "b" to "c" and from point "c" to "d". In the third case, re-loading at "f" causes an immediate yielding at that force level itself, as per hysteresis rule 3. Let the force level be $F_y(1-\delta-\delta^*)$, where $\delta^* < \delta$. Since $F_y(1-\delta-\delta^*) > F_y(1-2\delta)$, loading at point "f" causes immediate yielding upto point "g". If unloading takes place at "g", the element is loaded in the negative direction after crossing the zero force level. This continues upto point "h" at which the element undergoes yielding upto point "i" at a further deteriorated strength of $F_y(1-3\delta)$, as per hysteresis rule 2. Then, unloading at "i" causes zero-crossing and re-loading in the opposite direction until yielding of the element takes place at "j" at a yield strength of $F_y(1-4\delta)$, as per hysteresis rule 2.

Strength deterioration in reinforced concrete members largely depends on their detailing. A properly detailed member may exhibit a very small deterioration in strength, while a poorly detailed member exhibits a very large drop in strength under cyclic loading. However, most of the normally detailed reinforced concrete structures existing in practice exhibit considerable strength deterioration. Experimental studies are available on the load-deformation behaviour of reinforced concrete members (e.g., Brown and Jirsa, 1971; Wight and Sozen, 1975; Scribner and Wight, 1980; Ehsani and Wight, 1985, Saatcioglu and Ozcebe,

1989). These studies provide load-deformation curves for different specimens of reinforced concrete members with different detailing schemes. For the present study, these curves were carefully examined. Figure 3.6 shows the amount of strength-drop observed in the load-deformation curve of a specimen of reinforced concrete member used in one experimental study (Ehsani and Wight, 1985). The total drop in strength can be divided by the total number of yield excursions to get the average amount of strength deterioration in each yield excursion. In the data shown in Figure 3.6, the average rate of strength deterioration comes to be around 5%. From a number of such curves available in the literature (Brown and Jirsa, 1971; Wight and Sozen, 1975; Scribner and Wight, 1980; Ehsani and Wight, 1985; Saatcioglu and Ozcebe, 1989), it is found that in most cases, the average rate of deterioration, δ , in a single yield excursion is around 5% of the initial yield strength for ordinarily detailed reinforced concrete specimen. However, it may take a value of upto 10%.

In all the above experimental studies, the specimen are subjected to slow cyclic loading unlike the loading during an earthquake. A slower withdrawal of load may continue the plastic deformation for a long duration and hence the specimen may accumulate larger plastic strain. This in turn may lead to larger strength deterioration which may not take place in actual earthquake. On the other hand, the experimental cyclic loadings generally have many peaks of comparable magnitude as against the earthquake loadings which generally have only a few large peaks accompanied by numerous small peaks before and after them. It is difficult to conclude how truly δ obtained from slow cyclic loading

experiments represents the strength-drop per yield excursion in earthquake-type loading.

However, the present study relies on the values obtained above from the experimental curves. The values of δ used in this study are 0.0, 0.02, 0.05 and 0.1. In case of stiffness-eccentric systems with lateral natural period $T_x=0.5$ sec, a sample case of $\delta=0.08$ is also included. However, in case of bi-directional ground motion, only cases related to $\delta=0.05$ and 0.1 are considered.

3.5 DUCTILITY REDUCTION FACTOR, R_μ

Yielding is introduced in a structure when its strength is less than the maximum force that would be experienced by it if it were to remain elastic. The extent of inelasticity depends on the difference of this elastic strength demand and the lateral strength. The response reduction factor, R , which is the ratio of the maximum lateral force experienced by the structure if it were to remain elastic and the design lateral force for a system, is one way of quantifying this reduction. Building structures possess large redundancies, and hence, are assigned a large value of R (e.g., NEHRP provisions specify R as high as 8 for some building systems). However, the elevated water tank structures do not enjoy such a high degree of redundancy, and are assigned a significantly lower value of R (e.g., $R=2.5$ in NEHRP Recommended Provisions, 1991). Since, factors of safety are involved in the process of design, all structures including elevated water tanks will always possess significant overstrength over and above the design lateral force

(e.g., Jain and Navin, 1995). This implies that yielding will take place not at the design value of lateral force but at a higher value. A factor called the ductility reduction factor R_μ is defined in the literature as the ratio of the maximum lateral force that will be experienced by the structure if it were to remain elastic and the yield lateral force. So, the ductility reduction factor R_μ will be less than the response reduction factor R . This implies that R_μ for elevated water tanks will be less than 2.5. In the current study, two cases of $R_\mu=1$ and $R_\mu=2$ are considered, the former being the elastic case for the symmetric system.

3.6 EFFECT OF STRENGTH DETERIORATION

While presenting results, the maximum element displacement of the eccentric system is normalized with respect to the maximum element displacement of the corresponding symmetric system with same lateral natural period T_x .

3.6.1 Study of Two-Element Systems

A study on two-element system has been carried out for lateral natural period T_x of 0.5 sec, 1 sec and 2 sec, and rate of strength deterioration δ as 0.0, 0.02, 0.05 and 0.1. Both stiffness-eccentric strength-symmetric and stiffness-symmetric strength-eccentric systems have been analysed. The normalized maximum element displacement is presented as function of τ ($=T_\theta/T_x$) in Figures 3.7, 3.8 and 3.9 for stiffness-eccentric strength-symmetric systems, and in Figures 3.10, 3.11 and 3.12 for stiffness-symmetric strength-eccentric systems. Figure 3.10a presents the curves for lateral time period $T_x=0.5$ sec for

different values of δ . Some curves are not clear in Figure 3.10a owing to the scale chosen. Therefore, enlarged view of these curves are presented in Figure 3.10b. In each figure, two sets of graphs are provided corresponding to ductility reduction factor $R_\mu=1$ and $R_\mu=2$ used in designing the yield strength of the system. As discussed in section 3.2.1, the stiffness-symmetric strength-eccentric systems have slightly lesser overall lateral strength than that of the corresponding symmetric system; the element displacement of the latter is used for normalizing that of the former. Hence, Figures 3.10, 3.11 and 3.12 also present the results for symmetric systems with same overall lateral strength as that of stiffness-symmetric strength-eccentric systems. This enables one to clearly see the effect of strength eccentricity alone.

For stiffness-eccentric strength-symmetric systems, the normalized element displacement presented in Figures 3.7, 3.8 and 3.9 are same as the ratio of the maximum element ductility demand of these systems normalized with respect to the maximum element ductility demand of reference symmetric systems. This is because, in this case, elements in symmetric as well as eccentric systems have same yield strength. For stiffness-symmetric strength-eccentric systems, the displacement of either the normal-strength element or the reduced-strength element will govern the maximum value. In the first case, the normalized element displacement will be equal to the ratio of element ductility demand for eccentric versus symmetric systems. In the second case, the normalized element displacement will be marginally less than the ratio of ductility demands.

Figures 3.7 to 3.12 show that the effect of eccentricity on maximum

element displacement, and hence on ductility demand, increases with increasing rate of strength deterioration, δ . For a high rate of strength deterioration ($\delta=0.1$), except when $T_x=2$ sec, eccentric systems show a very high normalized element displacement. The maximum element displacement and ductility demand of eccentric systems is in many instances more than twice the element displacement and ductility demand of the reference symmetric systems. A large element displacement is also observed for $R_\mu=2$ when $\delta=0.05$. Since, a rate of strength deterioration of 0.05 is not unexpected in reinforced concrete members, such elevated water tanks cannot be relied upon for their post-elastic range performance. A small accidental eccentricity may create large inelastic displacements caused by torsion. Stiffness or strength unsymmetry causes early yielding of one of the elements. A higher rate of strength deterioration further lowers the strength of that element under repeated loading. This leads to a larger strength eccentricity resulting in an increase in element displacement, and hence, in the ductility demand. The effect may still be larger if both stiffness-eccentricity and strength-eccentricity occur together.

In Figures 3.10, 3.11 and 3.12, the normalized element displacements of the symmetric systems having same strength as that of stiffness-symmetric strength-eccentric systems are close to 1.0 (maximum range of variation is 0.8-1.3). Therefore, the large response in the eccentric systems in these figures is due to the torsional effect and not due to slightly lower overall lateral strength.

Comparing Figure 3.7 with Figure 3.10, Figure 3.8 with Figure 3.11, and Figure 3.9 with Figure 3.12, respectively, it is clear that

increased torsional response due to strength deterioration is more severe in the stiffness-symmetric strength-eccentric systems than in the corresponding stiffness-eccentric strength-symmetric systems. Thus, a structure with strength-eccentricity may be more vulnerable in torsion than the corresponding stiffness-eccentric structure.

The trends in the linear range behaviour seen in Chapter 2, of a minimum value of normalized element displacement at a natural period ratio $\tau \approx 1$, accompanied by a maximum value each on either side of it, is generally not observed in the inelastic range. The linear range amplification is basically due to the tuning of lateral and torsional natural periods before yielding. Since, considerable de-tuning occurs in the nonlinear range, the amplification recedes. However, many peaks are observed in the critical range of time period ratio from 0.7 to 1.25 ($0.7 < \tau < 1.25$); this is the range found critical in Chapter 2 for torsional response under elastic range. This may have serious implications for small-eccentricity systems like elevated water tanks having time period ratio within the critical range. This issue needs to be further studied for a large ensemble of ground motion time histories.

3.6.2 Study of Four-Element Systems

The idealized four-element systems discussed in Chapter 2 are also studied with small stiffness eccentricity and strength symmetry to investigate the inelastic behaviour. The variations in normalized maximum element displacement with τ under bi-directional synthetic ground motion for two values of rate of strength deterioration, $\delta=0.05$ and 0.1 , and $R_{\mu}=2$ are shown in Figure 3.13. To facilitate easy

comparison, the responses of the four-element system under uni-directional ground motion with $\delta=0.1$, are also presented. The curves marked 2D indicate the responses under bi-directional ground motion while those marked 1D indicate the responses under uni-directional ground motion. Three values of natural periods, $T_x=0.5$ sec, 1.0 sec and 2.0 sec, are considered.

As expected, the four-element system always shows a greater effect of torsion under bi-directional motion than under uni-directional ground motion. A four-element system has two additional elements with symmetric characteristics oriented parallel to the axis of symmetry in addition to the two elements with unsymmetric characteristics oriented perpendicular to the axis of symmetry. Under uni-directional ground motion, these additional elements primarily remain elastic. So, even if the stiffness in the direction of ground motion becomes zero because of the yielding of both the elements, the torsional resistance generally does not reduce below 50% of the original torsional stiffness.

However, the situation may be different, if a four-element system is subjected to bi-directional ground motions. In this case, the additional elements are also expected to exhibit considerable post-yield range response during ground shaking owing to the ground motion parallel to their orientation. So, under bi-directional ground motion, the torsional resistance may become zero during ground shaking depending on the correlation between the ground acceleration in two mutually perpendicular directions. Hence, as observed in the present study, an earlier study (Correnza and Hutchinson, 1994) using an elasto-plastic behaviour also showed that this drop in the torsional stiffness may

increase torsional response. Another reason of increasing response under bi-directional ground motion may be the introduction of unsymmetry in strength in the additional elements due to their unsymmetrical yielding and the subsequent deterioration in strength.

Further, if the curves of $\delta=0.1$ and 0.05 in Figure 3.11 are compared with the corresponding curves for two-element systems for $R_{\mu}=2$ in Figures 3.7, 3.8 and 3.9, it is confirmed that a four-element system exhibits a lesser effect of torsion than two-element systems. Such a behaviour can be explained physically. A two-element system becomes a mechanism under coupled lateral-torsional motion, if any one of the elements undergoes yielding, and hence, it exhibits a greater torsional response. On the other hand, a four-element system has greater torsional stiffness and strength, and also has more redundancy under coupled lateral-torsional motion; such systems show less torsional response as compared to two-element systems. This implies that the stagings with many panels and columns represented by four-element systems are less vulnerable to the effect of torsion even in the post-yield range.

Under bi-directional ground motion, four-element systems with $T_x=0.5$ sec and 1 sec, indicate element displacement and ductility demand which may be upto twice or more than that of the corresponding symmetric system; this has serious implications. Such a high displacement and ductility demand caused by torsion may not be acceptable as far as the detailing of load resisting elements is concerned.

Comparison of the element displacement curves in Figure 3.13 for systems with $\delta=0.1$ and 0.05 under bi-directional ground motions shows that the effect of torsion increases with rate of strength deterioration

in four-element systems also.

Even though the study on four-element system is limited to stiffness-eccentric strength-symmetric systems, it shows that torsional response may be a serious issue. The study on the two-element system shows that stiffness-symmetric strength-eccentric systems exhibit a greater effect of torsion as compared to stiffness-eccentric strength-symmetric systems. Same is expected in four-element systems also. Moreover, a still greater effect is expected if both stiffness eccentricity and strength eccentricity occur together.

3.7 BEHAVIOUR OF ELEVATED WATER TANKS LOCATED NEAR THE FAULTS

Consider a small-eccentricity system subjected to a pulse of duration T_1 longer than its lateral natural period T_x . If unsymmetrical yielding occurs in the initial stages of the pulse, the post-yield displacement may continue for a significant duration till the earthquake ground acceleration changes its direction. Thus, there may be a high ductility demand even in a small-eccentricity system. The present study is intended to study the performance of small-eccentricity systems under fault-parallel and fault-normal ground motions, which have characteristic pulses as shown in Figures 3.3a and 3.3b, respectively. The effect of the duration of pulses is also studied.

In the past, inelastic behaviour of eccentric systems under fault-normal ground motion has been reported (Goel and Chopra, 1990). However, that study concentrated only on large eccentricity systems with $e/r=0.5$, which are not uncommon in building systems. Inelastic behaviour of planar steel frames under fault-parallel and fault-normal ground

motions has also been reported (Murty and Hall, 1994). Similar collapse analyses of elevated water tanks supported on frame stagings may provide crucial inputs in their design.

3.7.1 Variation of Parameters

The natural period ratio, τ , is varied from 0.25 to 2. Four values of T_x/T_1 , namely 0.05, 0.5, 1.0 and 5, are considered. The case of $T_x/T_1=1.0$ is studied to investigate the possibility of amplification in displacement due to resonance-type condition. Two values of ductility reduction factor namely $R_\mu=1$ and $R_\mu=2$ are used to arrive at the yield strength of the systems. For all systems studied, eccentricity is taken as $e/D=0.05$, where D is the distance in plan between the resisting elements. Stiffness-eccentric strength-symmetric two-element systems alone are considered. Elasto-plastic behaviour is assumed for each lateral load-resisting elements.

3.7.2 Results and Discussion

Again, the maximum element displacement of the eccentric system is normalized with respect to the displacement of the corresponding symmetric system. The variation in this normalized maximum element displacement with τ , for different values of T_x/T_1 , under fault-parallel ground motion is presented in Figure 3.14. Similarly, the variation under fault-normal ground motion is presented in Figure 3.15.

Figures 3.14 and 3.15 show that the torsion effect increases the maximum element displacement by only a small amount: not more than around 20-25% (only under fault-parallel pulse with $T_x/T_1=0.05$ and $R_\mu=2$,

an increase of around 50% is observed). No considerable amplification is found even in case of $T_x/T_1=1.0$. Therefore, torsion does not seem to have severe effect on element ductility demand for near-fault motions. This does not imply that pulses of large duration are not detrimental for the tanks because Figures 3.14 and 3.15 present the values which are normalized with respect to the response of symmetric systems.

The variation of element displacement ductility demand of a symmetric system for $R_\mu=2$ with T_x/T_1 varying from 0.2 to 5 is shown in Figure 3.16. This figure shows that when the pulse duration T_1 is large, i.e., T_x/T_1 is small, the symmetric system itself produces a very high ductility demand. Ductility demand stabilizes at a value of around 2, when the pulse duration becomes less than the lateral natural period (i.e., $T_x/T_1 \geq 1$). So, a pulse of large duration may produce a large ductility demand in a system due to increased amplitude in lateral translation irrespective of symmetry or small eccentricity in it. Since, a pulse duration of around 2 sec is not unexpected, the elevated water tanks having lateral natural period less than 2 sec may have a problem of large ductility demand if situated near a fault. Large displacement may not be acceptable in elevated water tanks from the operational point of view. Moreover, such structures having large masses concentrated at considerable heights may undergo complete collapse due to secondary P- Δ effects.

3.8 CONCLUSIONS

In this chapter, the effect of torsion has been investigated under the inelastic range of response and with members having

strength-deteriorating properties. The study was focussed on the two-element systems, but a limited study was also conducted on the four-element systems. Also, the response of elasto-plastic two-element systems due to near-fault ground motions was studied. The salient conclusions of this chapter are as follows:

1. Two-element systems with small strength or stiffness eccentricity and with large strength deterioration ($\delta=0.10$) show very significant torsional response. For instance, the maximum element displacements as high as 30 times those for the symmetric but otherwise similar systems have been observed. As against this, the torsion caused only 20 to 40% increase in the element displacements under elastic response as seen in chapter 2.
 2. The torsional response is significant even with moderate strength deterioration ($\delta=0.05$) if the system is designed to undergo significant inelastic response, *i.e.*, systems designed for large R_{μ} . For instance when $R_{\mu}=2$ and $\delta=0.05$, torsional effect caused maximum element displacements which went as high as 5 times those of the corresponding symmetric systems.
 3. In general, systems with strength eccentricity show higher vulnerability to torsion than the stiffness-eccentric systems.
 4. In the inelastic response also many large response peaks are observed for τ in the range $0.7 < \tau < 1.25$; hence, systems should be designed so as to fall outside this range of τ . However, the minimum at $\tau \approx 1.0$ and a maximum on either side of $\tau=1.0$ are not generally observed in the inelastic response due to the detuning effect.
 5. Two-element systems show considerably more torsional response in the
-

inelastic range also, as against the four-element systems. This implies higher torsional vulnerability of tanks with low number of panels and columns.

6. In the inelastic range, the four-element systems show much more torsional response under bi-directional ground motion than under the uni-directional motion.
7. Torsional response is not significantly high under near-fault ground motions when the element response is elasto-plastic. Both symmetric and eccentric systems require large ductility when the pulse duration is larger than the lateral natural period.

The results of this chapter underline the fact that the reinforced concrete elevated tanks if designed with a large value of "response reduction factor" will be particularly vulnerable to torsional response caused by accidental eccentricity and with even moderate rate of strength-deterioration. Hence, such structures should be designed to respond elastically under earthquake ground motion; this is in line with the overall "response reduction factor" of about 2.5 (currently used in many codes, such as the NEHRP Recommended Provisions, 1991); when considering a overstrength factor of about 3.0 or more, this may generally lead to elastic response under the design earthquake motion. Similarly, tanks located near active faults may show a very large ductility demand if not designed to respond elastically.

3.9 REFERENCES

- Brown, R.H., and Jirsa, J.O., (1971), "Reinforced Concrete Beams Under Load Reversals," *ACI Journal*, Vol.68, No.3, May, pp 380-390.
- Clough, R.W., and Penzien, J., (1993), *Dynamics of Structures*, Second Edition, McGraw-Hill, Inc., USA.
-

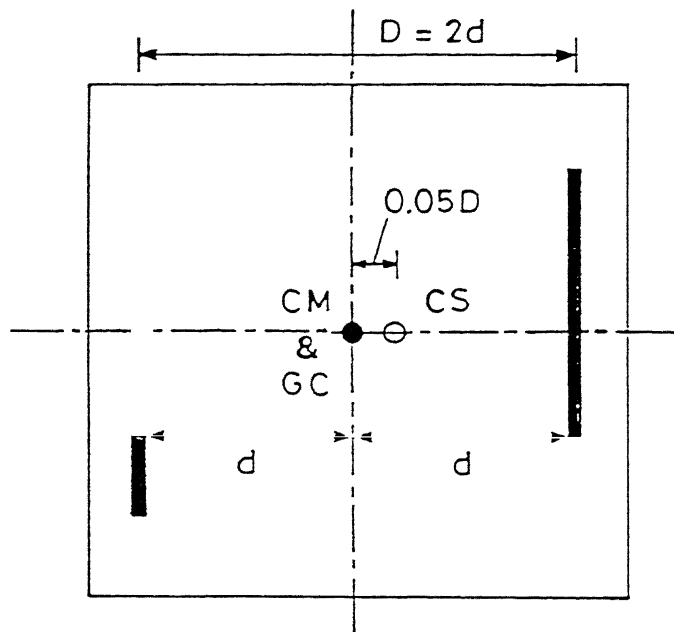
- Correnza, J.C., and Hutchinson, G.L., (1994), "Effect of Transverse Load-Resisting Elements on Inelastic Response of Eccentric-Plan Buildings," **Earthquake Engineering and Structural Dynamics**, Vol.23, No.1, pp 75-89.
- Ehsani, M.R., and Wight, J.K., (1985), "Exterior Reinforced Concrete Beam-to-Column Connections Subjected to Earthquake-Type Loading", **ACI Structural Journal**, Vol.82, No.4, pp 492-499.
- Goel, R.K., and Chopra, A.K., (1990), "Inelastic Seismic Response of One-storey, Asymmetric-Plan Systems: Effects of Stiffness and Strength Distribution," **Earthquake Engineering and Structural Dynamics**, Vol.19, No.7, pp 949-970.
- Irvine, H.M., and Kountouris, G.E., (1980), "Peak Ductility Demands in Simple Torsionally Unbalanced Building Models Subjected to Earthquake Ground Excitation," **Proceedings of Seventh World Conference on Earthquake Engineering**, Istanbul, Turkey, Vol.4, pp 117-120.
- Jain, S.K., and Navin, R., (1995), "Seismic Overstrength in Reinforced Concrete Frames," **Journal of Structural Engineering**, ASCE, Vol.121, No.3, pp 580-585.
- Murty, C.V.R., and Hall, J.F., (1994), "Earthquake Collapse Analysis of Steel Frames," **Earthquake Engineering and Structural Dynamics**, Vol.23, No.11, pp 1199-1218.
- Naeim, F., (1995), "On Seismic Design Implications of the 1994 Northridge Earthquake Records", **Earthquake Spectra**, Vol.11, No.1, pp 91-109.
- NEHRP 1991, "NEHRP Recommended Provisions for the Development of Seismic Regulations for New Buildings, (1992), Part I: Provisions," Report No. FEMA 222, **Federal Emergency Management Agency**, Washington, DC, USA, January.
- Park, Y.J., Reinhorn, A.M. and Kunnath, S.K., (1987), "IDARC: Inelastic Damage Analysis of Reinforced Concrete Frame-Shear Wall Structures," **Technical Report NCEER-87-0008**, National Centre for Earthquake Engineering Research, State University of New York at Buffalo, Red Jacket Quadrangle, Buffalo, NY14261, USA.
- Rutenberg, A., (1992), "Nonlinear Response of Asymmetric Building Structures and Seismic Codes: A State of the Art Review," **European Earthquake Engineering**, Vol.6, No.2, pp 2-19.
- Saatcioglu, M., and Ozcebe, G., (1989), "Response of Reinforced Concrete Columns to Simulated Seismic Loading," **ACI Structural Journal**, Vol.86, No.1, January-February, pp 3-12.
- Scribner, C.F., and Jirsa, J.O., (1980), "Reinforced Concrete Beams Under
-

Load Reversals," *Journal of Structural Engineering*, ASCE, Vol.106, No.ST4, pp 861-876.

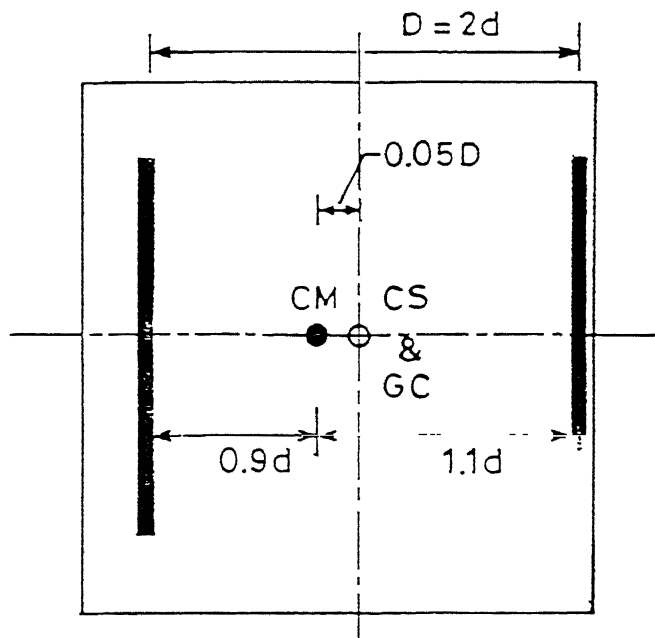
Tso, W.K., and Sadek, A.W., (1984), "Inelastic Response of Eccentric Buildings Subjected to Bidirectional Ground Motions," *Proceedings of Eighth World Conference on Earthquake Engineering*, San Francisco, Vol.4, pp 203-210.

Tso, W.K., and Sadek, A.W., (1985), "Inelastic Response of Simple Eccentric Structures," *Earthquake Engineering and Structural Dynamics*, Vol.13, No.2, pp 255-269.

Wight, J.K., and Sozen, M.A., (1975), "Strength Decay of RC Columns Under Shear Reversals," *Journal of Structural Division*, ASCE, Vol.101, No.ST5, pp 1053-1065.

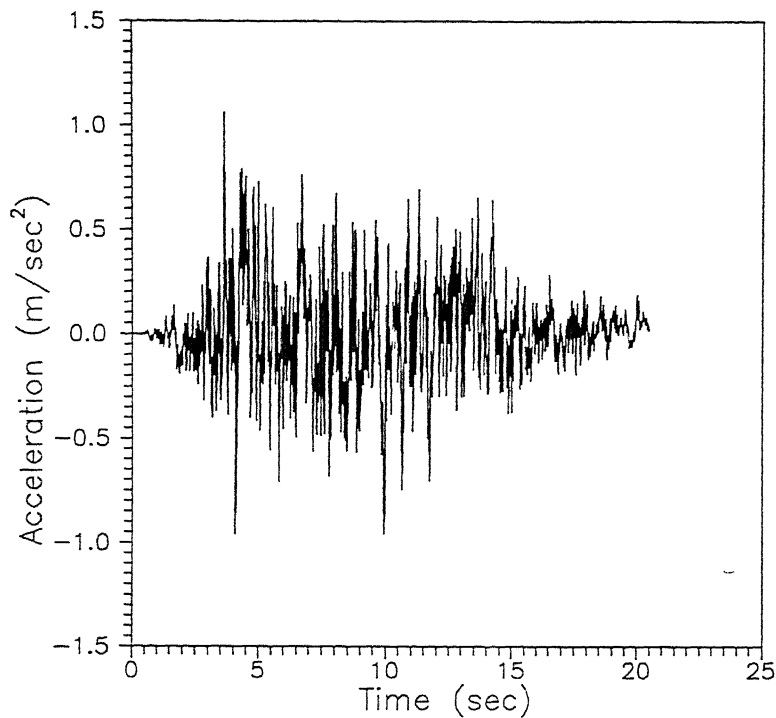


(a) Stiffness-eccentric system

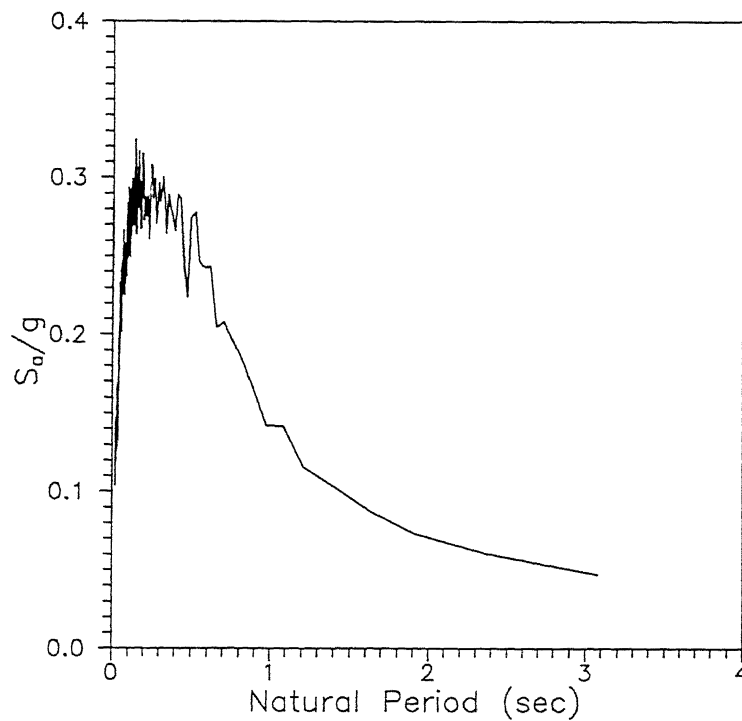


(b) Mass-eccentric system

Figure 3.1 : Different types of eccentric systems in linear range.



(a) Acceleration-Time History



(b) Response Spectrum

Figure 3.2 : Synthetic ground motion used along the axis of symmetry
(a) generated acceleration-time history, (b) response spectrum generated by the time history (2% damping).

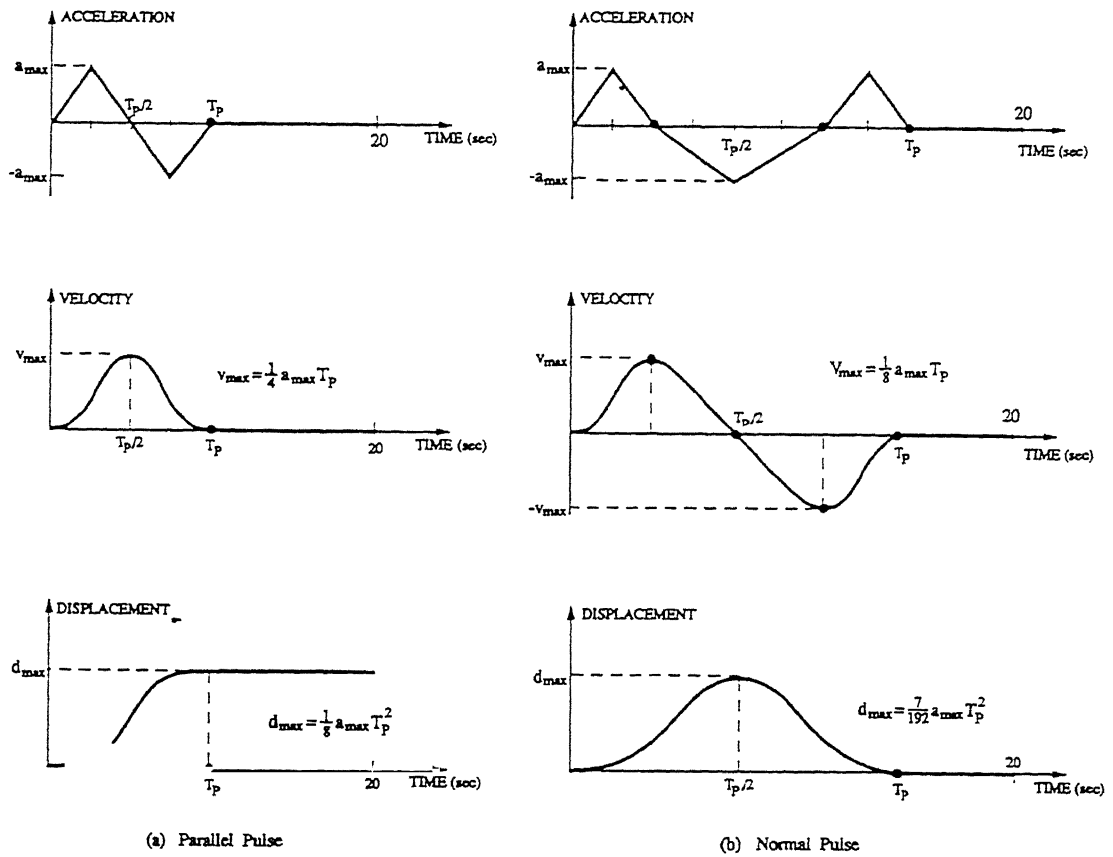


Figure 3.3 : Simulated near-fault ground motions in directions parallel and normal to a strike-slip fault (Murty and Hall, 1994).

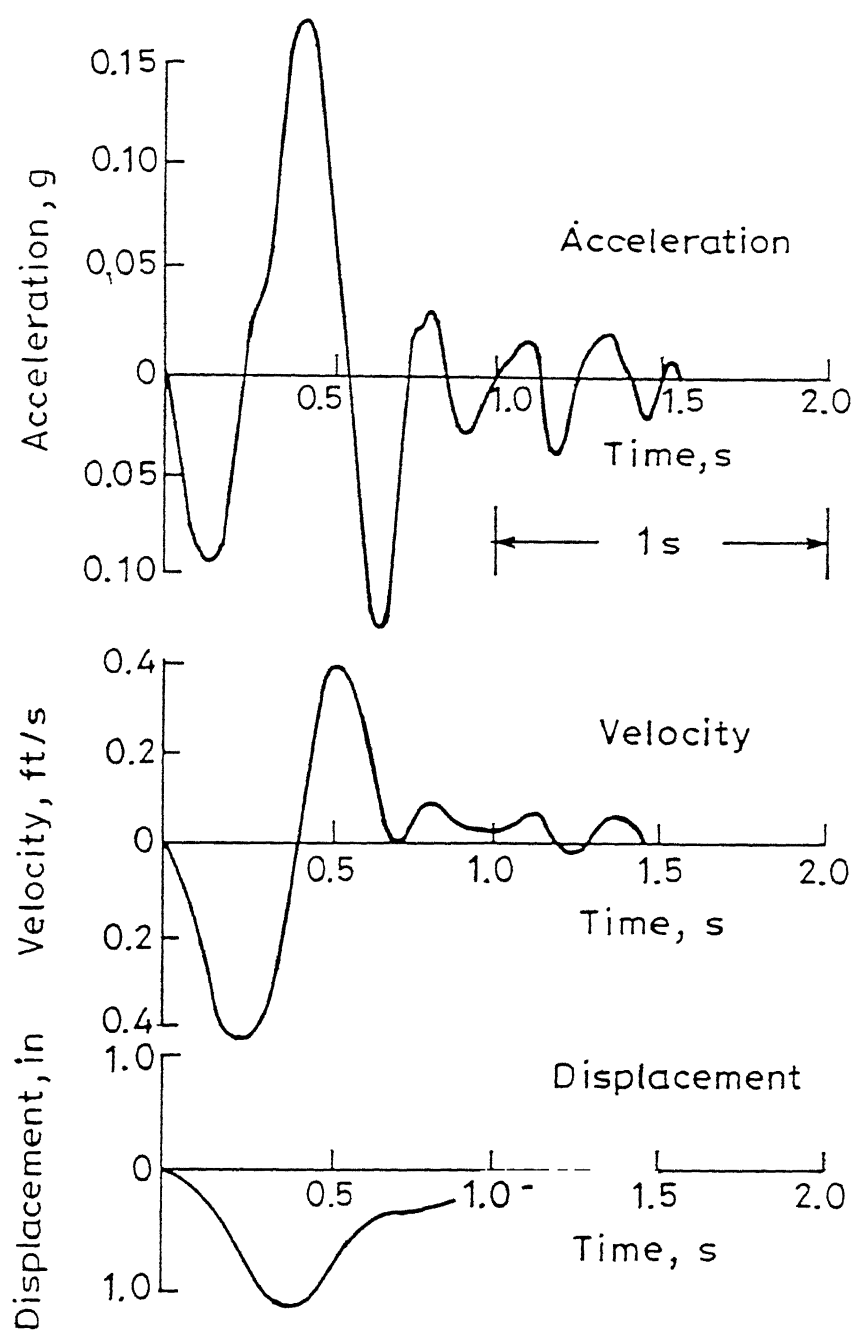


Figure 3.4 : Accelerogram from Port Hueneme earthquake, March 18, 1957 NS Component (Clough and Penzien, 1993).

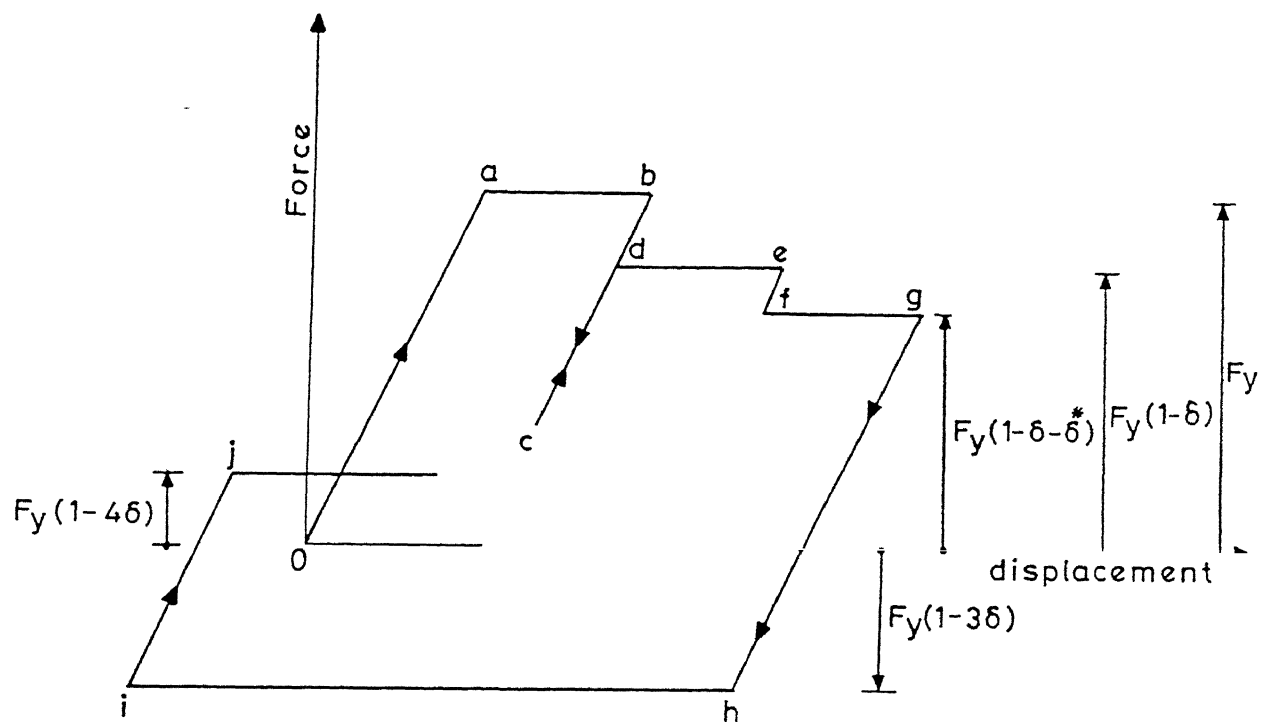


Figure 3.5 : General hysteresis loops based on the proposed simple strength-deteriorating hysteresis model.

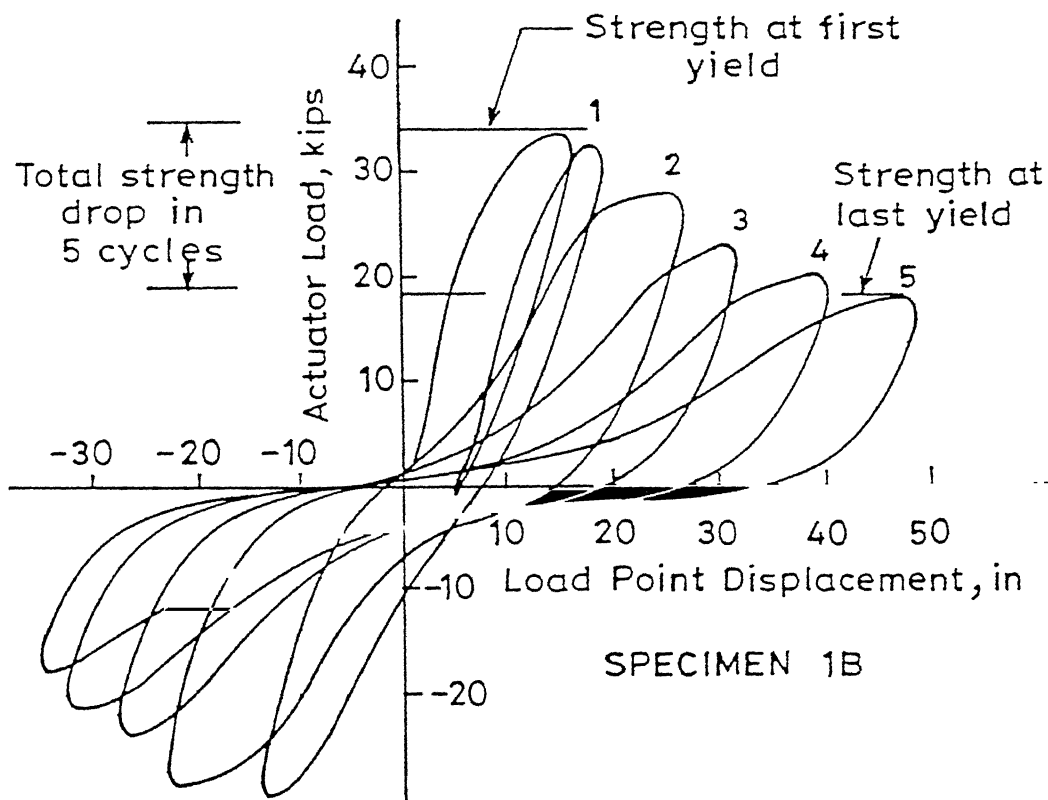


Figure 3.6 : Experimental load-deformation curve of a reinforced concrete member obtained under slow cyclic loading (Ehsani and Wight, 1985)

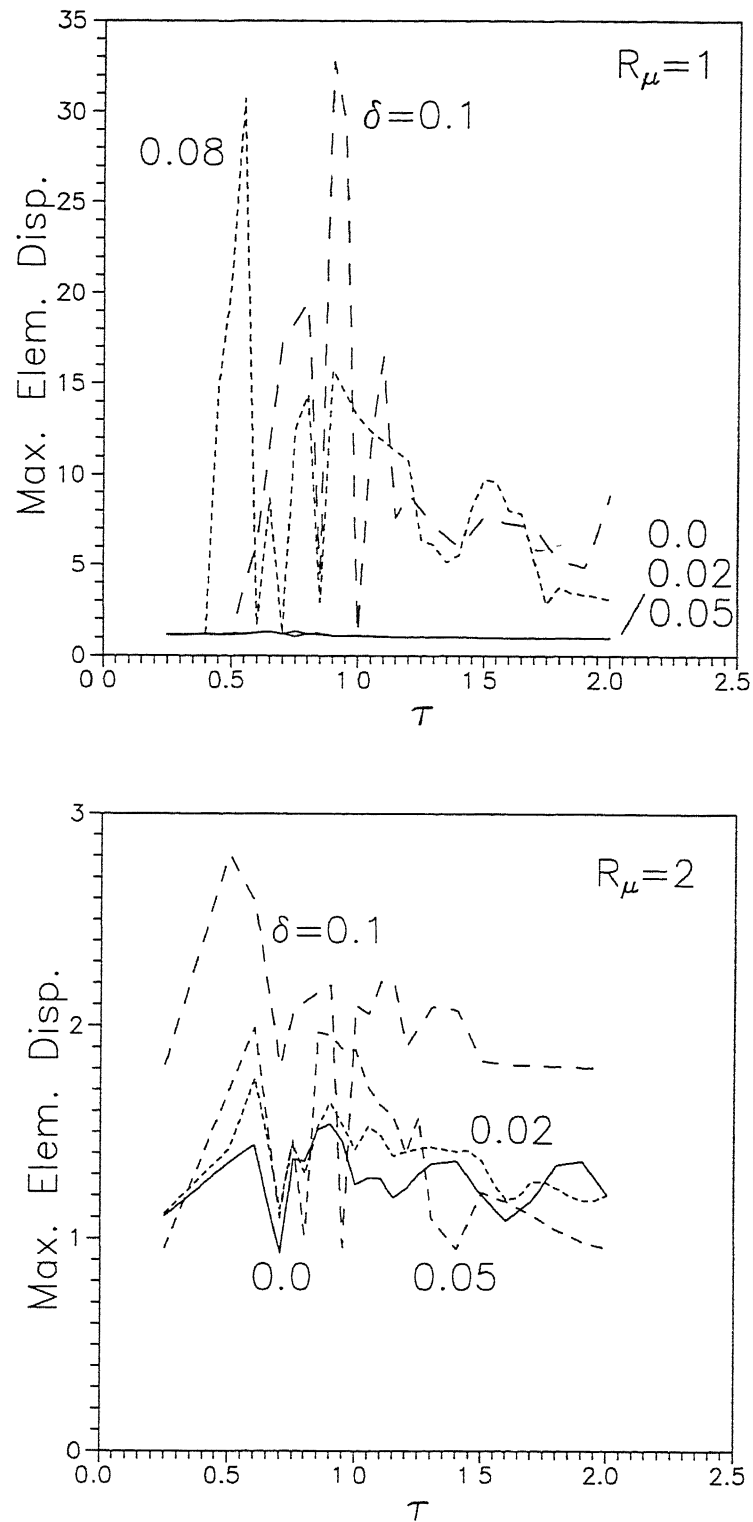


Figure 3.7 : Maximum normalized element displacement of stiffness-eccentric two-element system ($T_x = 0.5$ sec, $e/D=0.05$).

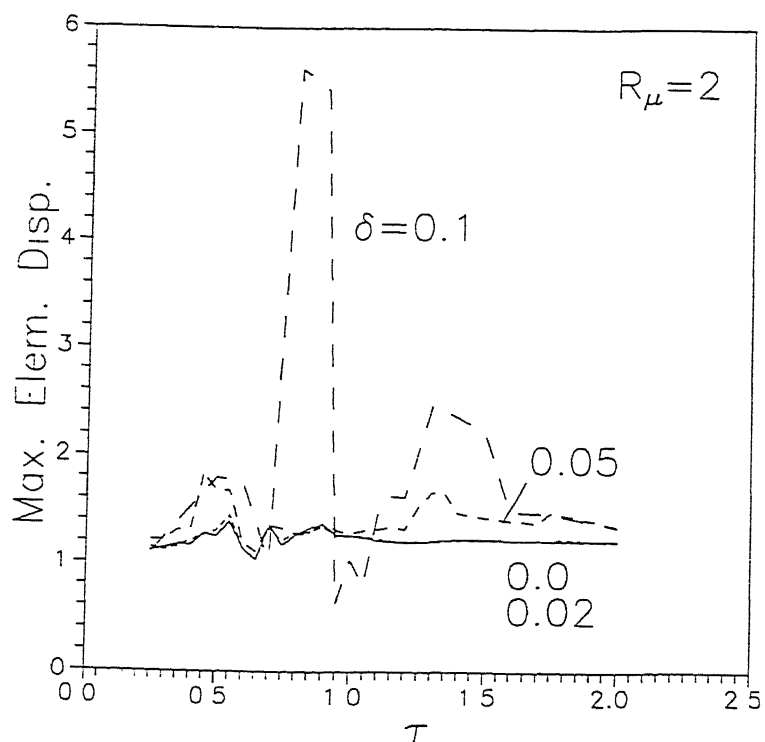
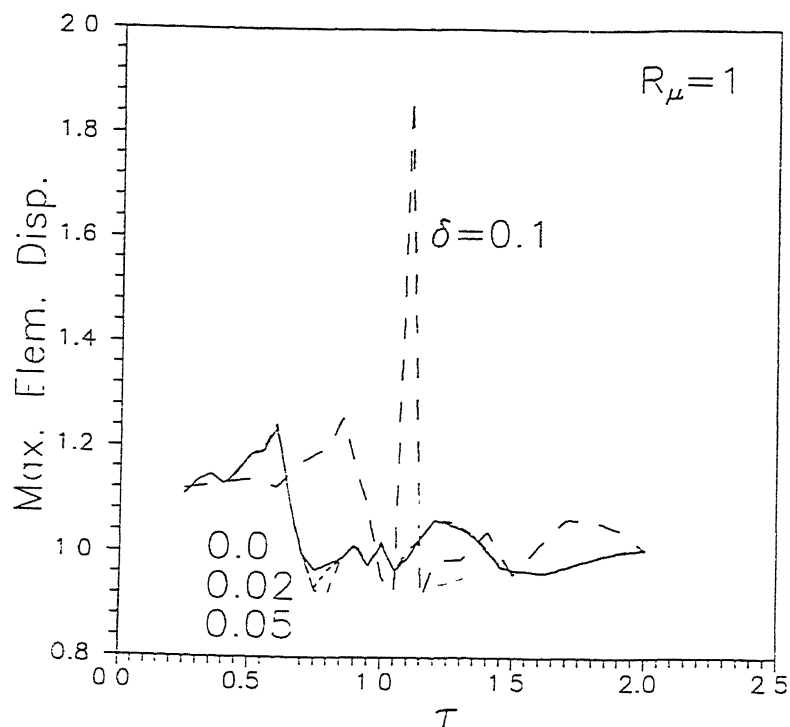


Figure 3.8 : Maximum normalized element displacement of stiffness-eccentric two-element system ($T_x = 1$ sec, $e/D=0.05$).

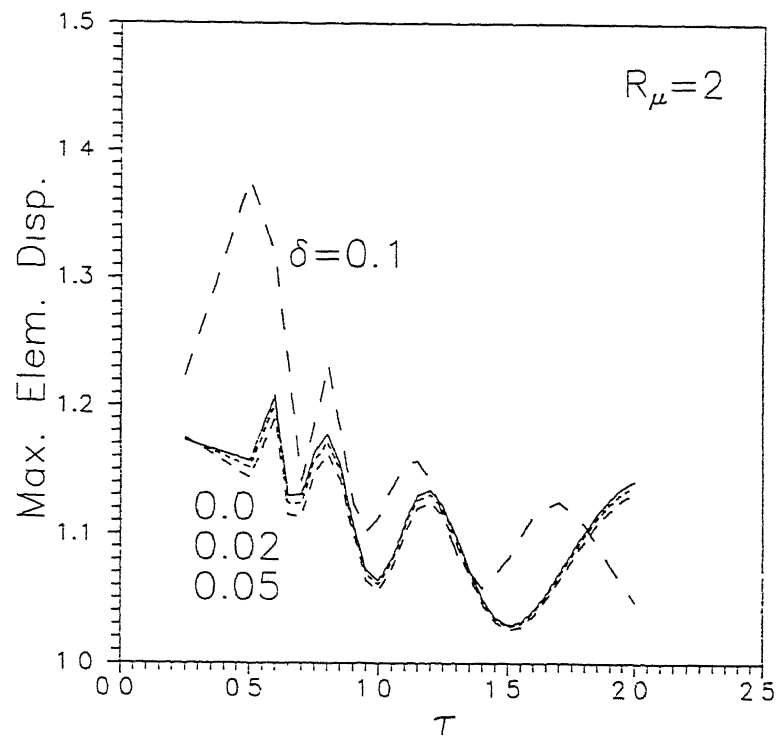
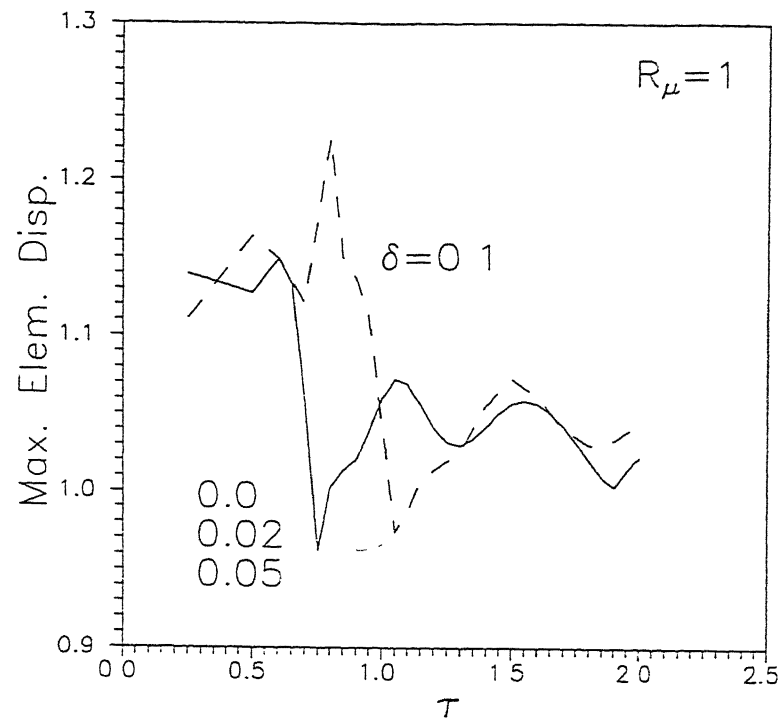


Figure 3.9 : Maximum normalized element displacement of stiffness-eccentric two-element system ($T_x = 2$ sec, $e/D=0.05$).

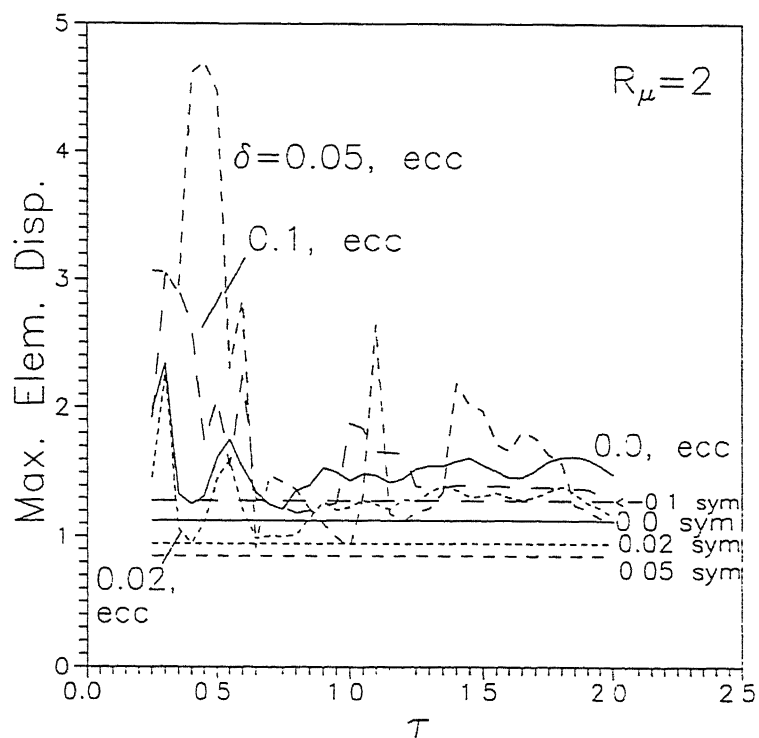
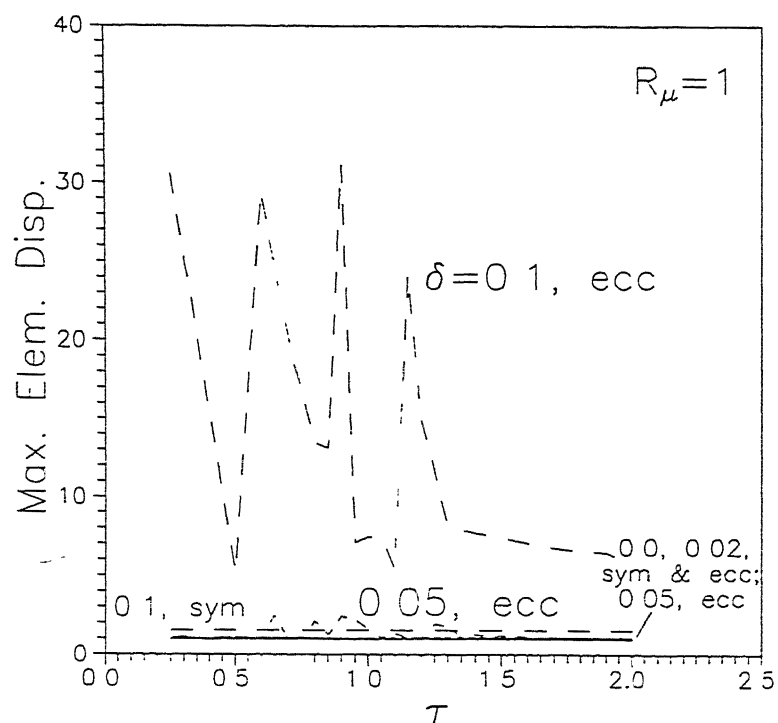


Figure 3.10a : Maximum normalized element displacement of stiffness-eccentric two-element system ($T_x = 0.5$ sec, $e_{\text{strength}}/D = 0.05$).

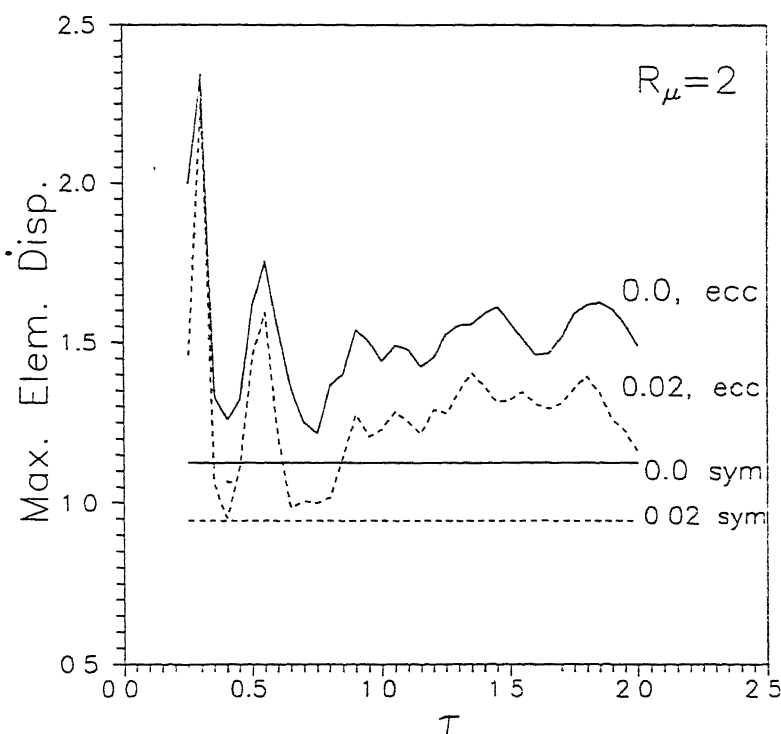
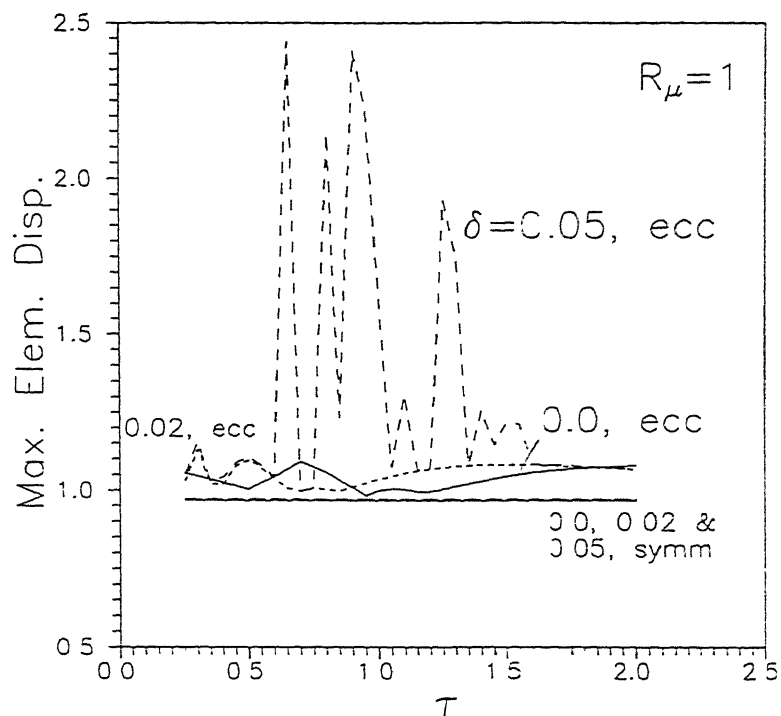


Figure 3.10b : Maximum normalized element displacement of strength-eccentric two-element system ($T_x = 0.5$ sec, $e_{\text{strength}}/D = 0.05$); enlarged view of the curves with some specific values of δ .

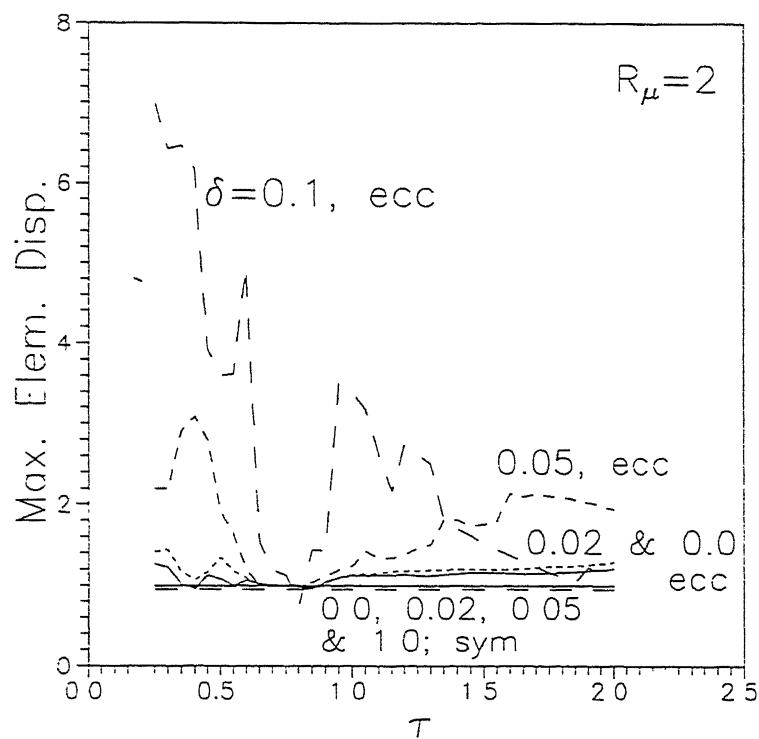
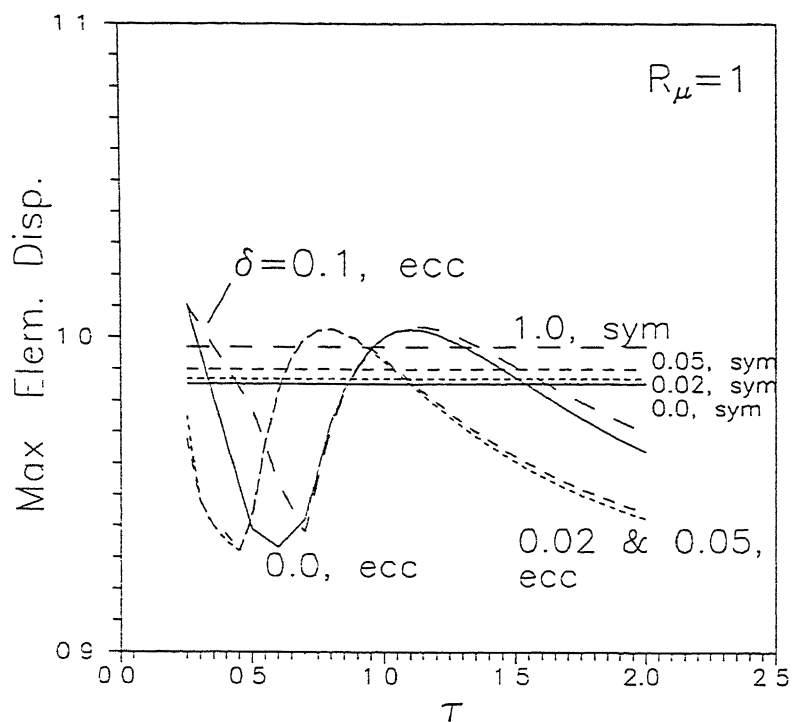


Figure 3.11 : Maximum normalized element displacement of strength-eccentric two-element system ($T_x = 1 \text{ sec}$, $e_{\text{strength}}/D = 0.05$).

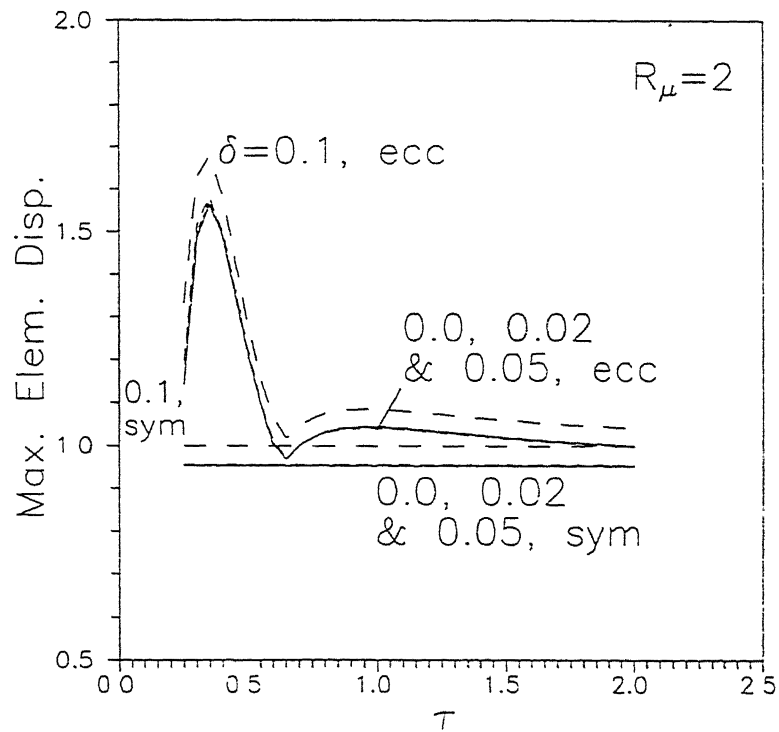
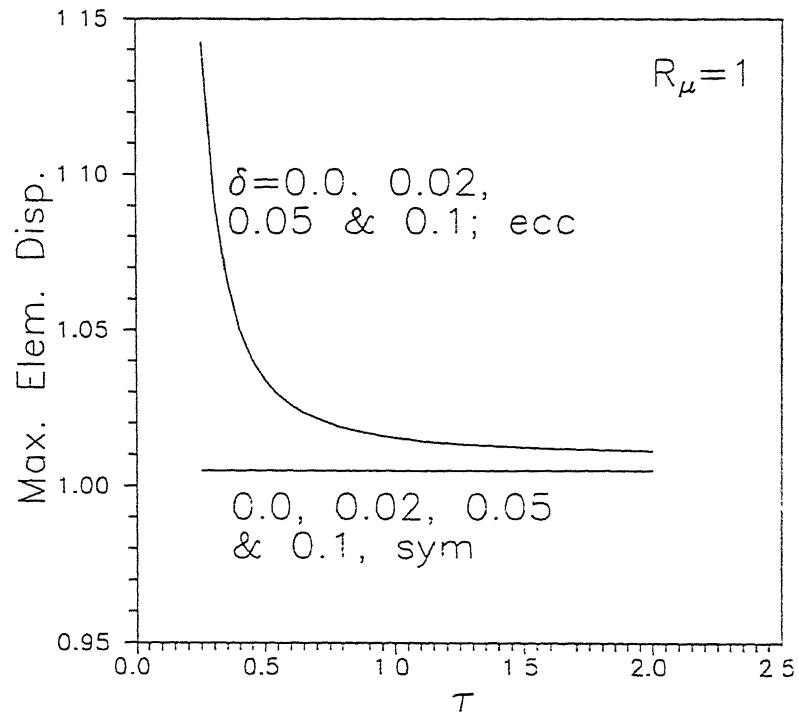


Figure 3.12 : Maximum normalized element displacement of strength-eccentric two-element system ($T_x = 2$ sec, $e_{\text{strength}}/D = 0.05$).

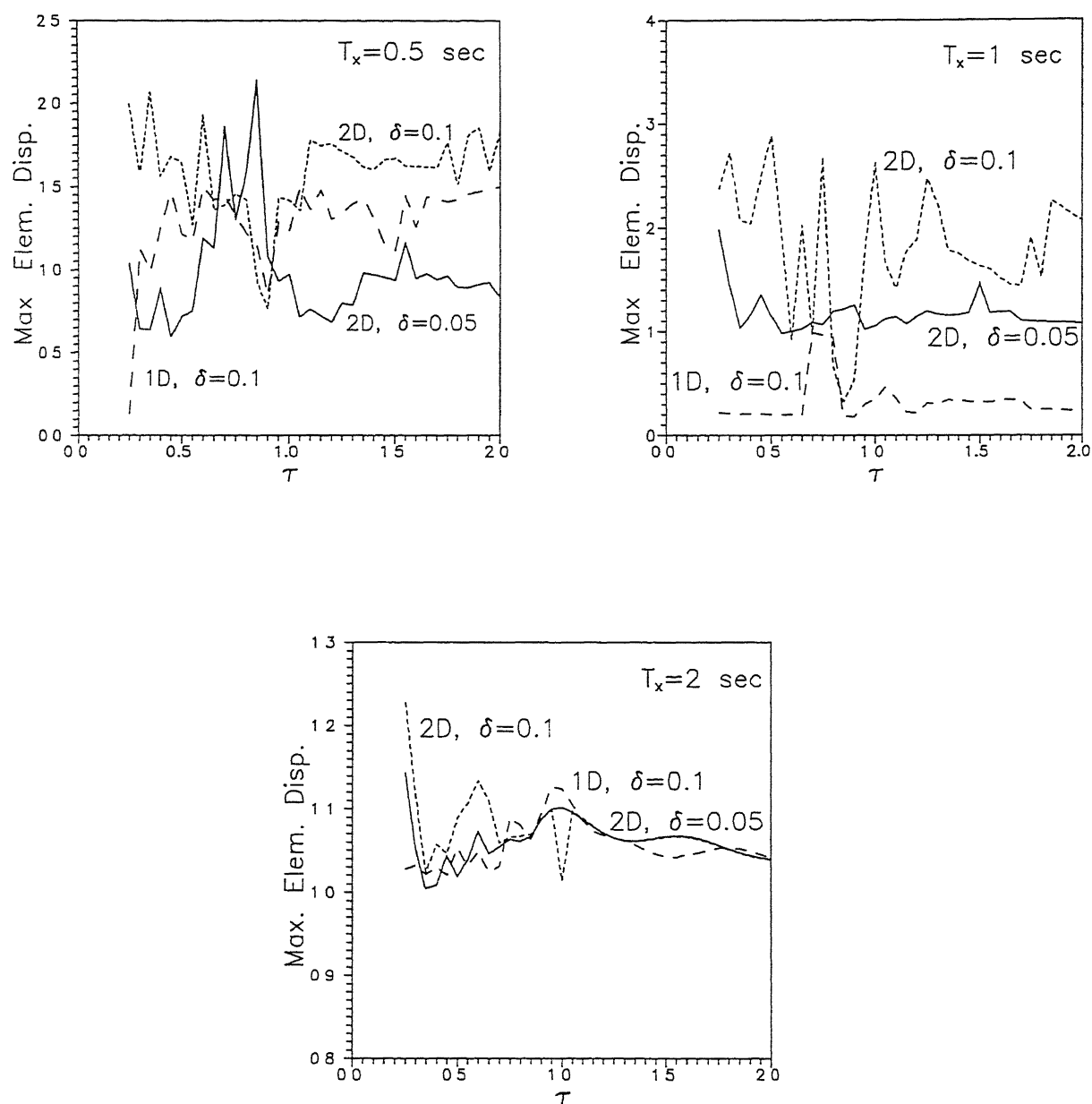


Figure 3.13 : Maximum normalized element displacement of stiffness-eccentric four-element system under bi-directional and uni-directional ground motions.

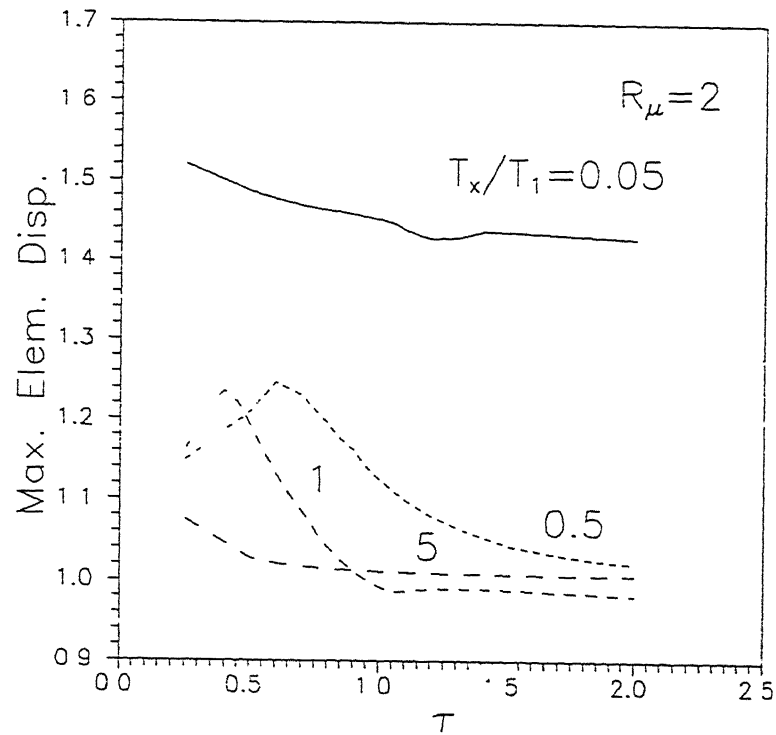
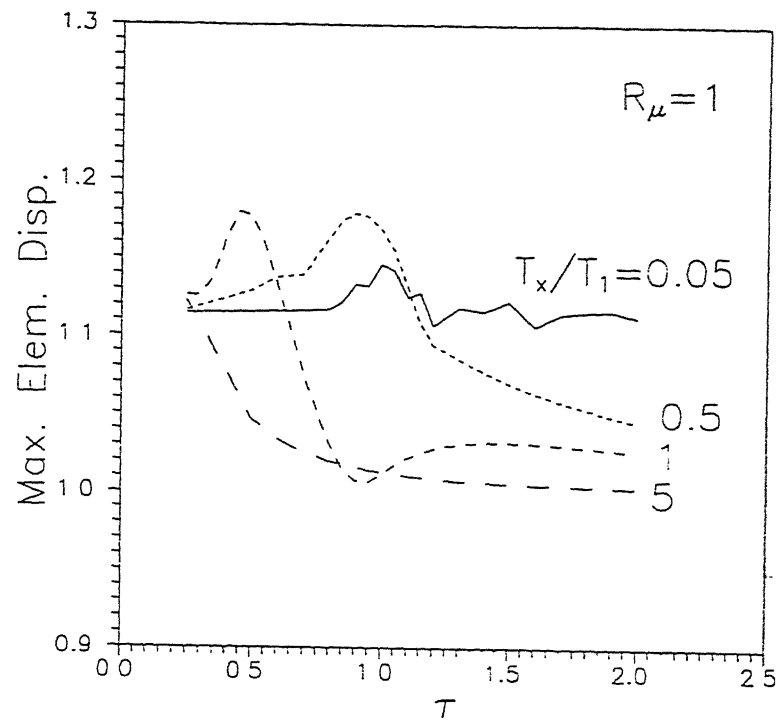


Figure 3.14 : Maximum normalized element displacement of stiffness-eccentric two-element system under fault-parallel ground motion ($e/D = 0.05$)

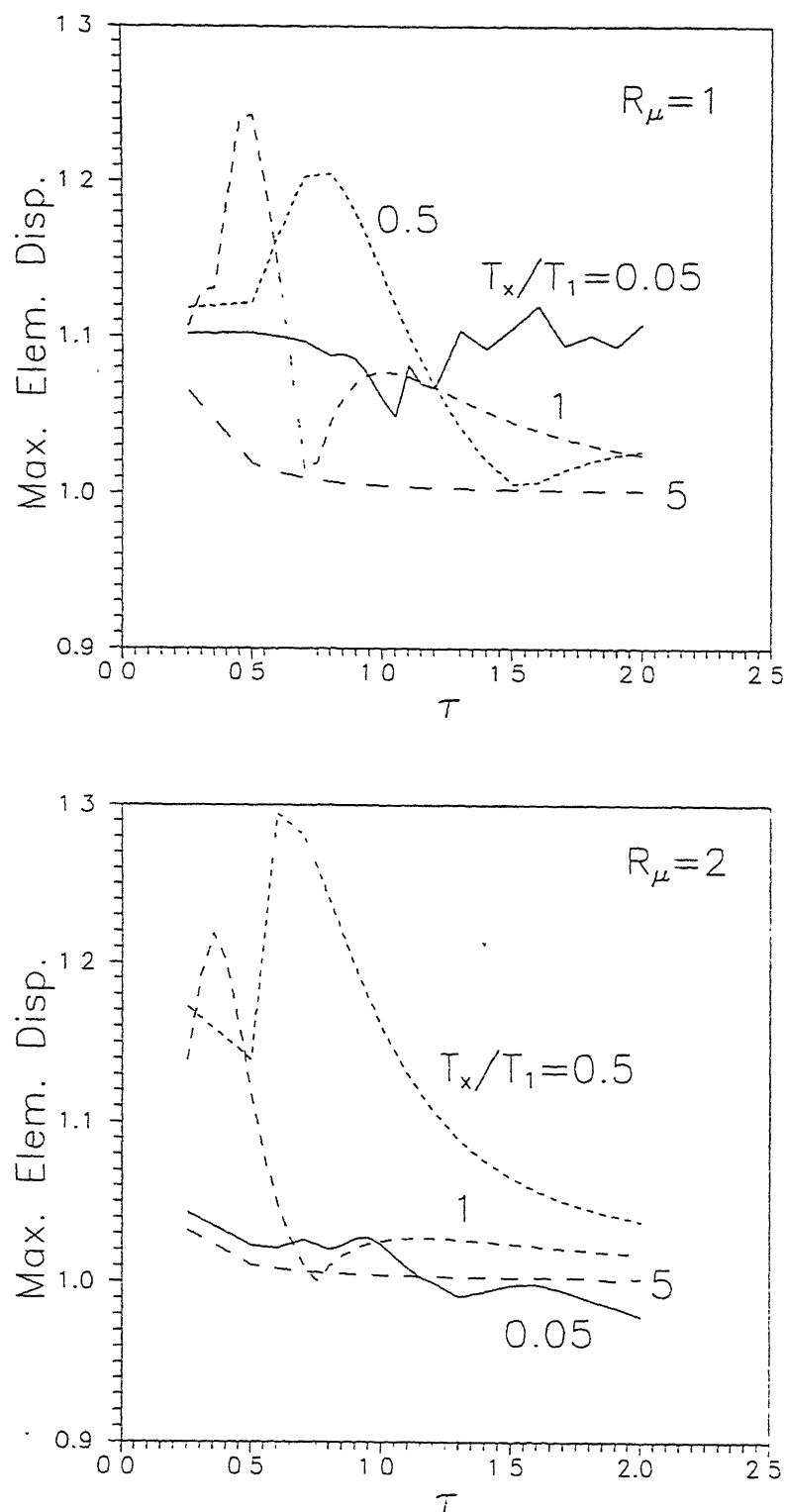


Figure 3.15 : Maximum normalized element displacement of stiffness-eccentric two-element system under fault-normal ground motion ($e/D = 0.05$)

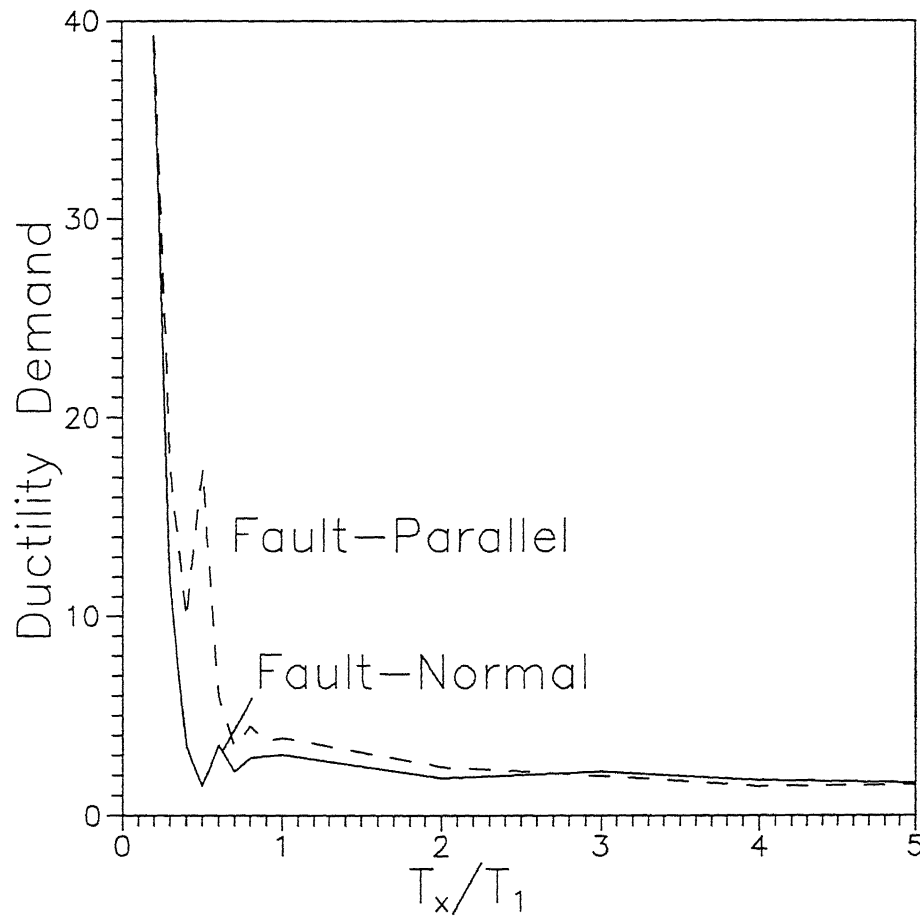


Figure 3.16 : Variation of element displacement ductility demand in symmetric systems under fault-parallel and fault-normal ground motions with different pulse durations.

CHAPTER 4

DYNAMIC CHARACTERISTICS OF THE BASIC STAGING CONFIGURATION

4.1 INTRODUCTION

It is observed in Chapter 2 that the small-eccentricity systems like elevated water tanks, exhibit amplified torsional response either in terms of rotation or element displacement if their natural period ratio is in the range $0.7 < \tau < 1.25$. Main objective of this chapter is to study the range of variation of τ for typical water tanks with RC moment-resisting frame staging. The stagings studied in this chapter have vertical columns resting on the perimeter of a circle (Figure 4.1). This configuration will be called as *basic configuration* in rest of this thesis. The range of τ has been studied using approximate closed-form expressions for lateral stiffness, K_x , torsional stiffness, K_θ , and time period ratio, $\tau = T_\theta / T_x$. An analytical expression is preferred since it facilitates to identify the influencing parameters as against the rigorous finite element method. Moreover, the analytical expression gives insight on the nature of variation of τ with various parameters. The number of panels, N_p , the number of columns, N_c , the relative stiffness of columns with respect to beams, K_r , and the ratio (ρ) of effective radius of gyration (R_{egyr}) to the radius of staging (R_s) are identified as the primary influencing parameters for τ .

When yielding starts in a structure, the plastic hinges should preferably be formed in beams rather than in columns. So, the ratio of the moment capacity of the columns and beams should be such that the

moment in beam first reaches the yield value. For frame staging, even if the formation of plastic hinges in columns is avoided under lateral force through design calculations, it needs to be seen if column hinges will not precede beam hinges under torsion. If the ratio of moments in columns and in beams under torsion is higher than that under lateral force, then yielding in columns may precede yield in beams under torsion as the staging members are generally proportioned for applied lateral force. In this chapter ratio (ϵ_M) of maximum bending moments' ratio of columns and beams under torsion and moment ratio under lateral force is used to assess this possibility.

4.2 ANALYTICAL EXPRESSIONS FOR CHARACTERISTIC QUANTITIES

4.2.1 Stiffness

The stiffness of RC axisymmetric frame-type staging shown in Figure 4.1, can be ascertained by three-dimensional analysis with the help of any finite element software. As an alternative, an approximate method for estimating the lateral stiffness of tank stagings with reasonable accuracy has been reported in the literature (Sameer and Jain, 1992). In this chapter, the method has been extended to estimate the torsional stiffness of tank stagings. The analytical formulation is based on following assumptions:

- (i) The staging behaviour is elastic and linear.
 - (ii) Centre line dimensions are used, neglecting the stiffness contribution of finite-sized end zones in beams and columns.
 - (iii) The columns in the bottom panel are fixed against translation and rotation at the footing. The columns in the top panel are fixed
-

against rotation at the ring beam of the tank.

- (iv) The torsional stiffness of the individual beams and columns is small.
- (v) The shear deformation in the columns is negligible.

4.2.1.1 Lateral Stiffness

The expression for lateral stiffness of the staging using a simplified Portal Method has been reported in the literature (Sameer and Jain, 1992). The salient steps in the derivation of the same are merely recollected in this section with a view to discuss in detail the implications of some of the assumptions made therein, in addition to introducing all the parameters of the problem at hand.

The lateral displacement of a column in bending is assumed to consist of two parts, namely (a) flexural deflection under constant shear, with its ends restrained against rotation, and (b) flexural deflection due to joint rotation. Consider the staging sub-assemblage shown in Figure 4.2. The lateral deflection, Δ_c , of a column, is

$$\Delta_c = 2 \frac{V(\frac{h}{2})^3}{3E_c I_c} + \frac{\theta_t h}{2} + \frac{\theta_b h}{2}, \quad (4.1)$$

in which V is the shear in column; E_c is the modulus of elasticity of the column material; I_c is the moment of inertia of the column cross section; h is the panel height; and θ_t and θ_b are the rotations of the top and bottom joints, respectively. These rotations are given by

$$\theta_t = \frac{V(h_a + h)}{2K_{\theta t}} \quad (4.2)$$

and $\theta_b = \frac{V(h_b + h)}{2K_{\theta b}} .$

In Eq.(4.2), h_a and h_b are the heights of the panels above and below the panel under consideration, respectively. Also, $K_{\theta t}$ and $K_{\theta b}$ are the rotational stiffnesses at top and bottom joints due to all beams meeting there. Rotational stiffness of a beam in the direction of the lateral force is obtained by multiplying its rotational stiffness in the direction of beam axis with $\cos^2 \alpha$, where α is the angle between the longitudinal axis of beam and the direction of lateral force. So, neglecting torsional stiffness of the individual beams,

$$\begin{aligned} K_{\theta t} &= 6 \sum k_{bt} , \\ \text{and } K_{\theta b} &= 6 \sum k_{bb} , \end{aligned} \quad (4.3)$$

where

$$\begin{aligned} \sum k_{bt} &= E_b \sum_{1}^{N_b} \frac{I_{bt}}{L} \cos^2 \alpha \\ \text{and } \sum k_{bb} &= E_b \sum_{1}^{N_b} \frac{I_{bb}}{L} \cos^2 \alpha , \end{aligned} \quad (4.4)$$

in which L is span of the beam; E_b is the modulus of elasticity of the beam material; N_b is number of beams meeting the column at the joint; and, I_{bt} and I_{bb} are the moments of inertia of the beams meeting the column at top and bottom joints, respectively.

From Eqs.(4.1), (4.2) and (4.3), the lateral stiffness of a column is

$$K_{\text{column}} = \frac{V}{\Delta_c} = \frac{12E_c I_c}{h^3} \left[\frac{1}{1 + 0.5 \frac{E_c I_c}{h^2} \left(\frac{h_a + h}{\sum k_{bt}} + \frac{h_b + h}{\sum k_{bb}} \right)} \right] \quad (4.5)$$

A direct expression for determination of panel stiffness, without calculating individual column stiffness, can be obtained by further

approximations. As a reasonable simplification, it is assumed that point of contraflexure of the beams is located at midspan. This implies that all joints rotate equally at any beam level. Hence, rotational stiffness of the staging at any beam level is approximated by adding rotational stiffness at all the joints at that level. Thus, the entire staging is modeled as a single equivalent column connected to a rotational spring at each beam level. The moment of inertia of the equivalent column is equal to the sum of moments of inertia of all the columns. Therefore, $\sum k_{bt}$ and $\sum k_{bb}$ in Eq.(4.5) are replaced by k_{st} and k_{sb} , the stiffnesses of the rotational springs at top and bottom of the panel considered, respectively. In fact, k_{st} and k_{sb} are equal to the sum of rotational stiffness of all beams at top and bottom of the panel, respectively. Thus, for a tank staging, the lateral stiffness of a panel due to flexural deformation of members is given by

$$K_{p(\text{lateral})} = \frac{12E_c I_s}{h^3} \left[\frac{1}{1 + 0.5 \frac{E_c I_s}{h^2} \left(\frac{h_a + h}{k_{st}} + \frac{h_b + h}{k_{sb}} \right)} \right], \quad (4.6)$$

where $I_s = \sum_{i=1}^N I_{c_i}$, in which N_c is the number of columns. Though approximate, this model has been found to give excellent results (Sameer and Jain, 1992). For tank stagings with equal panel height, identical columns and identical beams, k_{st} and k_{sb} are given by

$$\begin{aligned} k_{st} = k_{sb} &= \sum_{i=1}^{N_c} \sum_{j=1}^2 (k_{bt})_{ij} = \sum_{i=1}^{N_c} \sum_{j=1}^2 (k_{bb})_{ij} \\ &= \frac{E_b I_b}{L} \sum_{i=1}^{N_c} \sum_{j=1}^2 \cos^2 \alpha_{ij} = \frac{E_b I_b N_c}{L}, \end{aligned} \quad (4.7)$$

where N_c is the number of columns, and I_b is the moment of inertia of

each beam. From Eqs.(4.6) and (4.7), the lateral stiffness of each panel (due to bending deformation only) is

$$K_{p(\text{lateral})} = \frac{12E_c I_c N_c}{h^3} \frac{1}{1 + \gamma K_r}, \quad (4.8)$$

where $\gamma = \begin{cases} 2 & \text{for intermediate panels,} \\ 1 & \text{for top and bottom panels.} \end{cases}$

$$\text{and } K_r = \frac{E_c I_c / h}{E_b I_b / L}.$$

In Eq.(4.8), K_r is a stiffness related parameter which is a measure of the relative stiffness of columns with respect to that of beams.

To derive the lateral stiffness of the staging only due to axial deformation of columns, the axial force in columns is calculated by the Cantilever Method. Then, the lateral displacement of the staging under these axial loads in columns is calculated by the Castigliano's Theorem (Sameer and Jain, 1992). Using this, the staging stiffness, K_{axial} , due to axial deformation of columns, is obtained as

$$K_{\text{axial}} = \frac{1}{\frac{2}{N_c A_c E_c R_s^2} \sum_{i=1}^{N_p} H_i^2 h_i}, \quad (4.9)$$

where H_i is the height at which the lateral force acts, measured from the point of contraflexure of the panel i ; h_i is the height of the panel i ; A_c is cross-sectional area of each column; R_s is the staging radius; and N_p is the number of panels. Further, for equal panel heights, De Moivre's identity (Carmichael and Smith, 1962) and the assumption that lateral force acts at the top of the staging, gives

$$K_{\text{axial}} = \frac{6N_c A_c E_c R_s^2}{h^3 N_p (4N_p^2 - 1)}. \quad (4.10)$$

For deriving the total lateral bending stiffness of the staging, the individual panels are considered to be connected in series. The lateral stiffness due to flexural deformation of the entire staging is then combined in series with lateral stiffness due to axial deformation of columns, to obtain the overall lateral stiffness, K_x .

$$K_x = \frac{12E_c I_c N_c}{h^3} \left[\frac{1}{\frac{2I_c N_p (4N_p^2 - 1)}{A_c R_s^2} + N_p + 2(N_p - 1)K_r} \right] \quad (4.11)$$

4.2.1.2 Torsional Stiffness

The torque applied at centre of mass of the tank is resisted by the equal shear forces developed in all the columns, in the tangential direction (see Figure 4.3). Also, the lateral forces in all columns act at an angle $\alpha = \pi/N_c$ with respect to the beams meeting the corresponding columns. Therefore, all the columns contribute equally to torsional resistance. The torsional stiffness of a single panel is

$$K_{p(\text{torsional})} = N_c K_{\text{column}} R_s^2 \quad (4.12)$$

From Eqs. (4.12) and (4.5), and using $\alpha = \pi/N_c$, the torsional stiffness of a single panel is

$$K_{p(\text{torsional})} = \frac{\frac{12E_c I_c N_c R_s^2}{h^3}}{1 + \frac{\gamma K_r}{2 \cos^2\left(\frac{\pi}{N_c}\right)}} \quad (4.13)$$

Due to the axisymmetric nature of the loading in case of a torsional moment applied at the top of the staging, no axial force is developed in columns. The torsional stiffness, K_θ , of the whole staging

is calculated from torsional stiffness of individual panels, considering the individual panels to be connected in series. Hence,

$$K_{\theta} = \frac{12E_c I_c N_c R_s^2}{h^3} \left[\frac{1}{N_p + \frac{(N_p - 1) K_r}{\cos^2\left(\frac{\pi}{N_c}\right)}} \right] \quad (4.14)$$

The performance of the approximate method for lateral and torsional stiffnesses is presented for two example tanks. Details of the tanks considered are given in Table 4.1. Comparisons of the stiffnesses predicted by approximate method and those obtained from Finite Element Method are presented in Table 4.2. The approximate method shows very good accuracy.

4.2.2 Inertial Mass

The natural periods of the sloshing modes of vibration of elevated water tanks are usually quite large and the maximum response of staging is primarily governed by the impulsive mode. Hence, only the impulsive modes of vibration, in translation and torsion, are considered in this chapter. The water mass participating in the translational mode may be estimated by the expressions given in the literature (Housner, 1957). In the torsional mode, the shear stress between the tank walls and water is conceived to be inadequate to mobilize significant amount of liquid to vibrate with the tank in impulsive torsional mode. Hence, irrespective of whether the tank is full or empty, for torsional vibrations, the mass moment of inertia to be considered is only that due to the tank structure.

Effective radius of gyration, R_{egyr} , can be expressed in terms of the mass that participates in the lateral vibration, as

$$\begin{aligned} R_{\text{egyr}} &= \sqrt{\frac{I}{M_{\text{lateral}}}} = \sqrt{\frac{I}{M_{\text{torsional}}}} \sqrt{\frac{M_{\text{torsional}}}{M_{\text{lateral}}}} = \sqrt{\frac{I}{M_{\text{torsional}}}} \sqrt{\frac{M_{\text{empty}}}{M_{\text{lateral}}}} \\ &= R_{\text{gyr}} \sqrt{\frac{M_{\text{empty}}}{M_{\text{lateral}}}}, \end{aligned} \quad (4.15)$$

where I is the torsional mass moment of inertia of the empty tank; R_{gyr} is the usual radius of gyration of the tank in empty condition; M_{lateral} is the mass of tank structure plus the impulsive mass of liquid which takes part in the impulsive mode of lateral vibration; $M_{\text{torsional}}$ is the mass that participates in impulsive mode of torsional vibration; and M_{empty} is the mass of the tank structure alone. Since the water does not contribute to the impulsive mass in the torsional mode, $M_{\text{torsional}}$ is the same as M_{empty} .

4.2.3 Bending Moments and Shear Forces in Staging Members

The analytical method employed here to derive closed-form expressions for member forces under lateral load was recently proposed in literature (Sameer and Jain, 1994). This method is briefly discussed here and extended further to obtain the closed-form expressions for member forces under torsional moment. Here, the point of inflection for intermediate panels is assumed at mid-height of the panels, while for end-panels, its location is separately derived. The general assumptions made in the derivation of stiffness are also made here.

4.2.3.1 Under Lateral Force

4.2.3.1.1 Beams

Consider a vertical plane normal to the direction of lateral force and cutting any two beams (Figure 4.4). The shear force in both of them will be equal to the difference between the sum of axial forces in all columns located on one side of the plane in the panel above and that in the panel below the beam level under consideration. The shear in those beams will be maximum, for which the vertical plane will contain the bending axis of the whole staging with half the number of columns on either side of the plane (see Figures 4.5a(i) and 4.5b(i)). So, the largest shear, V_{bj} , in beams at beam level j , is

$$V_{bj} = \sum_{i=1}^{N_c/2} \frac{F_{i,j} - F_{i,j+1}}{2}, \quad (4.16)$$

where $F_{i,j}$ and $F_{i,j+1}$ are the axial forces in column i of panels j and $(j+1)$, respectively. By the Cantilever Method, axial force in column i of panel j is given by

$$F_{i,j} = \frac{2 P H_j x_i}{N_c R_s^2}, \quad (4.17)$$

where x_i is the distance of column i measured along the direction of lateral force, P , from the centre of the staging. Now, using Eq.(4.17) in Eq.(4.16) and simplifying using De Moivre's Identity (Carmichael and Smith, 1961),

$$V_{bj} = \frac{P Y_j}{N_c R_s} \operatorname{cosec}\left(\frac{\pi}{N_c}\right), \quad (4.18)$$

where

$$Y_j = H_j - H_{j+1},$$

in which H_j is the height of the point of application of lateral load from point of contraflexure in panel j . So, the largest moment, M_{bj} , in beams at level j , is

$$M_{bj} = \frac{P Y_j L}{2 N_c R_s} \operatorname{cosec} \left(\frac{\pi}{N_c} \right). \quad (4.19)$$

4.2.3.1.2 Columns

(a) Intermediate Panel

When the direction of lateral force is such that the two diametrically opposite columns are situated on the bending axis of the whole staging, these columns, with beams meeting at an angle of π/N_c with the direction of lateral force, carry the maximum shear force. The critical directions of lateral force are depicted in Figure 4.5. From the equilibrium of joints on these critical columns, the largest shear, V_c , in columns of intermediate panels is

$$V_c = \frac{2 \bar{V}_{bj} L}{h_j + h_{j+1}} \cos \left(\frac{\pi}{N_c} \right), \quad (4.20)$$

where h_j and h_{j+1} are the heights of panels j and $j+1$, respectively; and \bar{V}_{bj} is the shear force in the beams connected to the columns carrying largest shear. Deriving expressions for \bar{V}_{bj} in a similar manner as for V_{bj} , and substituting in Eq. (4.20),

$$V_c = \frac{P L}{N_c R_s} \cos \left(\frac{\pi}{N_c} \right) \cot \left(\frac{\pi}{N_c} \right). \quad (4.21)$$

Hence, the largest moment, M_{cj} , in the columns of panel j is

$$M_{cj} = \frac{P L h_j}{2 N_c R_s} \cos \left(\frac{\pi}{N_c} \right) \cot \left(\frac{\pi}{N_c} \right). \quad (4.22)$$

b) End Panels

Consider an end panel. The columns are assumed to be completely fixed against rotation at top ring beam level, and against rotation and translation at foundation level. All columns have equal restraint at the fixed-end. At the other ends, fixity against rotation depends on beam configurations. Because of this difference in end conditions of the columns in the end panels, a redistribution of shear takes place among the columns in the end-panels. From the equilibrium of joints, the bending moment, M_{cb} , in the critical column at the braced end in the end panel is

$$M_{cb} = \frac{2 P \bar{y}}{N_c} \cos^2 \left(\frac{\pi}{N_c} \right), \quad (4.23)$$

where \bar{y} is the distance of point of inflection of end panel from the braced end. It may be taken as $(3-K_r)h/6$ for a staging with equal panel heights (Sameer and Jain, 1994).

The largest moment, M_{cr} , of the column at the restrained end of the end panel consists of the fixed-end moment due to lateral displacement of the braced-end of the end-panel column and the released moment due to rotation of the braced end. So, M_{cr} and M_{cb} can be expressed as

$$M_{cb} = \frac{6 E I_c \Delta_c}{h^2} - \frac{4 E I_c \theta_c}{h}, \quad (4.24a)$$

$$M_{cr} = \frac{6 E I_c \Delta_c}{h^2} - \frac{2 E I_c \theta_c}{h}, \quad (4.24b)$$

and

$$M_{cr} = M_{cb} + \frac{2 E I_c \theta_c}{h}. \quad (4.24c)$$

Here, θ_c the rotation of the column at the braced end, can be determined by dividing the moment causing rotation of the joint, M_θ , by

the rotational stiffness, K_θ . Thus,

$$\theta_c = \frac{M_\theta}{K_\theta} = \frac{\frac{2PY_j}{N_c} \cos^2\left(\frac{\pi}{N_c}\right)}{\frac{12E_b I_b}{L} \cos^2\left(\frac{\pi}{N_c}\right)} = \frac{PY_j L}{6N_c E_b I_b} \quad (4.25)$$

Substituting Eq. (4.25) in Eq. (4.24) yields

$$M_{cr} = \frac{P}{N_c} \left[2 \bar{y} \cos^2\left(\frac{\pi}{N_c}\right) + \frac{Y_j}{3} K_r \right] \quad (4.26)$$

4.2.3.1.3 Bending Moments' and Shear Forces' Ratio

Staging structure can be designed in two possible ways: (1) The largest value of moments of members in intermediate and end panels are used and separate design are provided for members in intermediate and end panels. (2) The largest values of moments in columns and beams considering all the panels are used and the same design is provided in all the panels.

Consider the case where intermediate panels and end panels are separately designed. For a staging with equal panel heights, the ratio of largest column bending moments and beam bending moments are

$$M_{cj}/M_{bj} = \cos^2\left(\frac{\pi}{N_c}\right) \quad \text{for intermediate panels} \quad (4.27)$$

and

$$M_{cr}/M_{be} = 2 \left(\frac{3 - K_r}{6 - K_r} \right) \cos^2\left(\frac{\pi}{N_c}\right) + \frac{K_r}{3} \quad \text{for end panels.} \quad (4.28)$$

Consider the case of same design in all panels. In an intermediate panel, different columns have different rotational restraints at their two ends as the beams connected to each of them have different orientations with respect to the direction of lateral force. But, in an

end panel, all the columns have same end condition at one end. So, in end panel, the difference in largest and smallest shear force in columns will be less than that in an intermediate panel. Since, all the panels carry the same amount of shear, for column shear intermediate panels will govern design. Again, point of inflection in the end panel columns is closer to the braced end. So, the moments coming from the columns to the joints of end panels are less owing to the lesser maximum column shear and lower lever arm. Therefore, the moments in beams of end panels are lesser than the moments in beams of intermediate panel. However, it is not possible to say whether end panel or intermediate panel will govern the design for column moment; this is because in the end panels maximum column shear is lesser while lever arm for the moment at the restrained end is larger. If column moment in intermediate panel governs, then Eq.(4.27) gives the ratio of design moment in columns and in beams. If end-panel column governs, then ratio of design moments in columns and in beams is

$$M_{cr}/M_{bj} = \left(\frac{3 - K_r}{3} \right) \cos^2 \left(\frac{\pi}{N_c} \right) + \left(\frac{6 - K_r}{18} \right) K_r . \quad (4.29)$$

The ratio of shear force in column and that in beam is presented for the case of same design in all the panels. From the previous discussion, it is clear that largest shear in columns of intermediate panel will be more than that in end panel. Since, the largest moment in beams of intermediate panel always governs the design, the same will be true for largest shear in beams also. So, for a staging of equal panel heights, the ratio of design shear force in columns and in beams is

$$V_c/V_{bj} = \left(\frac{L}{h} \right) \cos^2 \left(\frac{\pi}{N_c} \right) \quad (4.30)$$

4.2.3.2 Under Torsional Moment

Due to axisymmetry of structural geometry and loading, all the member forces are also axisymmetric under applied torsional moment. Notation used in this sub-section is similar to that in the previous sub-section, except that a subscript "t" has been added to denote quantities under torsional moment.

4.2.3.2.1 Beams

Due to axisymmetry of structural geometry and loading, all the member forces are also axisymmetric under applied torsional moment. The bending moment, M_{bjt} , in all beams at a particular beam level j is equal, and from the equilibrium of joints,

$$M_{bjt} = \frac{V_{ct} Y_{jt}}{2 \cos\left(\frac{\pi}{N}\right)} \quad (4.31)$$

where Y_{jt} is the distance between points of inflection in panels j and $(j+1)$. If panels j and $(j+1)$ are intermediate panels then for a staging with equal panel heights h ,

$$Y_{jt} = h \quad (4.32a)$$

If either panel j or panel $(j+1)$ is an end panel, then

$$Y_{jt} = \frac{h}{2} + \bar{y}_t \quad (4.32b)$$

in which \bar{y}_t is the distance of the point of inflection in columns of end panel from the restrained end under applied torsion. \bar{y}_t is derived in a similar manner as was done in case of lateral force (Sameer and Jain, 1994), and is given by

$$\bar{y}_t = \frac{6 \cos^2\left(\frac{\pi}{N_c}\right) + K_r}{12 \cos^2\left(\frac{\pi}{N_c}\right)} h . \quad (4.33)$$

The shear force in beams, V_{bjt} , is given by

$$V_{bjt} = \frac{V_{ct} y_{jt}}{L \cos\left(\frac{\pi}{N_c}\right)} . \quad (4.34)$$

4.2.3.2.2 Columns

All columns in all panels carry equal shear force, V_{ct} , in resisting the torsional moment T ; the column shear force is given by (Figure 4.3)

$$V_{ct} = \frac{T}{N_c R_s} . \quad (4.35)$$

All the columns in a particular panel will carry the same moment, M_{cjt} , given by

$$M_{cjt} = V_{ct} y_{jt} , \quad (4.36)$$

where y_{jt} is the distance of point of inflection in columns in panel j from the end of panel. In a staging of equal panel height, h ,

$$y_{jt} = \frac{h}{2} \quad \text{in intermediate panels} \quad (4.37a)$$

For end panels, y_{jt} is given by

$$y_{jt} = \begin{cases} \bar{y}_t, & \text{for calculation of moment at the restrained end of the end panel} \\ h - \bar{y}_t, & \text{for calculation moment at the braced end of the end panel} \end{cases} \quad (4.37b)$$

Accuracy of all these approximate expressions has been tested against results from rigorous Finite Element Method for some example tanks. The comparison of the member forces under lateral load estimated by the approximate formulations with those from Finite Element Method is available in the literature (Sameer and Jain, 1994); error in the member

forces by the approximate method is within about 10%. The comparison for member forces under torsion is included in the present study. The details of the tanks considered are presented in Table 4.1, while the comparisons of the results from approximate expression and those from Finite Element Method are presented in Table 4.3. The percentage error in the estimates by the approximate methods is found to be within 5%.

4.2.3.2.3 Bending Moments' and Shear Forces' Ratios

For a staging with equal panel heights, the ratio of bending moment in columns and that in beams in the intermediate panel j , is

$$M_{cjt}/M_{bjt} = \cos\left(\frac{\pi}{N_c}\right), \quad (4.38)$$

while in the end panel, this ratio is

$$M_{crt}/M_{bet} = \frac{2 \left[6 \cos^2\left(\frac{\pi}{N_c}\right) + K_r \right] \cos\left(\frac{\pi}{N_c}\right)}{12 \cos^2\left(\frac{\pi}{N_c}\right) - K_r}, \quad (4.39)$$

where M_{crt} is the bending moment at the fixed end of the columns of end panel, and M_{bet} is the bending moment in the beams of end panel due to applied torsional moment.

The ratio of design shears, V_{ct}/V_{bjt} , of columns and beams for intermediate panels is

$$V_{ct}/V_{bjt} = \left(\frac{L}{h}\right) \cos\left(\frac{\pi}{N_c}\right) \quad (4.40)$$

4.3 NUMERICAL STUDY

4.3.1 Parameters Studied

4.3.1.1 Natural Period Ratio (τ)

The ratio, τ , of torsional natural period, T_θ , and lateral natural

period, T_x , is given by

$$\tau = \frac{T_\theta}{T_x} = \sqrt{\frac{I K_x}{K_\theta M_{\text{lateral}}}} = R_{\text{egyr}} \sqrt{\frac{K_x}{K_\theta}} \quad (4.41)$$

where I is the torsional mass moment of inertia of the empty tank; M_{lateral} is the mass of tank structure plus the impulsive mass of liquid which takes part in the fundamental impulsive mode of lateral vibration as already discussed in section 4.2.2; and R_{egyr} is the effective radius of gyration defined in Eq.(4.15).

Using Eq.(4.11) and Eq.(4.14), the ratio of lateral and torsional stiffness (K_x/K_θ), is given by

$$\frac{K_x}{K_\theta} = \frac{1}{R_s^2} \left[\frac{N_p + \frac{(N_p - 1) K_r}{\cos^2\left(\frac{\pi}{N_c}\right)}}{\frac{2I_c N_p (4N_p^2 - 1)}{A_c R_s^2} + N_p + 2(N_p - 1) K_r} \right] \quad (4.42)$$

The first term in the denominator is due to the axial flexibility of the columns. To reduce the parameters in Eq.(4.42), based on a few example tanks, $(I_c/A_c)/R_s^2$ is taken as 0.00125. This quantity will obviously vary for different tanks of varying configurations. But, the contribution of axial flexibility of columns on the overall lateral deflection of staging may be only 5% to 15% (Sameer & Jain, 1992). So, this assumption is not likely to affect the subsequent results significantly. Hence, using Eq.(4.42), Eq.(4.41) reduces to

$$\tau = \rho \sqrt{\frac{N_p + \frac{(N_p - 1) K_r}{\cos^2\left(\frac{\pi}{N_c}\right)}}{0.0025N_p (4N_p^2 - 1) + N_p + 2(N_p - 1)K_r}} \quad (4.43)$$

where $\rho = R_{\text{egyr}}/R_s$. It may be noticed that the ratio of torsional to lateral time period depends primarily on ρ , N_p , N_c and K_r .

4.3.1.2 Ratio of Member Forces' Ratios under Torsion and Lateral Force

Elevated water tank stagings are generally designed under lateral force only. If the ratio of moments in columns and in beams under torsion is higher than that under applied lateral force, then plastic hinging in columns is likely to precede that in beams. To investigate this issue, ratio (ϵ_M) of bending moments' ratio in columns and beams and that under lateral force is derived. Similarly, the ratio (ϵ_V) of shear forces' ratio of columns and beams under torsion to that under lateral force is also derived to see the shear vulnerability of columns under applied torsion.

4.3.1.2.1 Ratio of Bending Moments' Ratio

If different designs are to be provided in intermediate and end panels, then the ratio, ϵ_M , of the ratio of column and beam moments under torsional moment and that under lateral force, is

$$\epsilon_M = \begin{cases} \frac{(M_{cjt}/M_{bjt})}{(M_{cj}/M_{bj})} = \frac{1}{\cos\left(\frac{\pi}{N_c}\right)} & \text{for intermediate panels} \quad (4.44) \end{cases}$$

$$\epsilon_M = \begin{cases} \frac{(M_{crt}/M_{bet})}{(M_{cr}/M_{be})} = \frac{\frac{6\cos^2\left(\frac{\pi}{N_c}\right) + K_r}{12\cos^2\left(\frac{\pi}{N_c}\right) - K_r} \cos\left(\frac{\pi}{N_c}\right)}{\frac{3-K_r}{3-K_r} \cos^2\left(\frac{\pi}{N_c}\right) + \frac{K_r}{6}} & \text{, for end panels} \quad (4.45) \end{cases}$$

If same design is provided in all the panels, then under applied

lateral force, beam design will always be governed by the intermediate panels while column moment may be governed by either end panels or intermediate panels. If column moment in intermediate panel governs, then ϵ_M for intermediate panels is given by Eq.(4.44) and ϵ_M for end panel is given by

$$\epsilon_M = \frac{(M_{crt}/M_{bet})}{(M_{cj}/M_{bj})} = \frac{6 \cos^2\left(\frac{\pi}{N_c}\right) + K_r}{\left[12 \cos^2\left(\frac{\pi}{N_c}\right) - K_r\right] \cos\left(\frac{\pi}{N_c}\right)}, \quad (4.46)$$

When column moment of end panels governs the design under lateral force, then for intermediate panels

$$\epsilon_M = \frac{(M_{cjt}/M_{bjt})}{(M_{cr}/M_{bj})} = \frac{\cos\left(\frac{\pi}{N_c}\right)}{\frac{3-K_r}{3} \cos^2\left(\frac{\pi}{N_c}\right) + \frac{6-K_r}{18} K_r}, \quad (4.47)$$

and end panels

$$\epsilon_M = \frac{(M_{crt}/M_{bet})}{(M_{cr}/M_{bj})} = \frac{\frac{36 \cos^2\left(\frac{\pi}{N_c}\right) + 6K_r}{12 \cos^2\left(\frac{\pi}{N_c}\right) - K_r} \cos\left(\frac{\pi}{N_c}\right)}{(6-K_r)}. \quad (4.48)$$

Clearly, ϵ_M depends only on N_c and K_r and is independent of N_p .

4.3.1.2.2 Ratio of Shear Forces' Ratios

Shear forces in both columns and beams are always greater in intermediate panel than those in end panels. If same shear design is provided in all panels, then the ratio, ϵ_V , of the ratio of column and beam shear forces under torsion and that under lateral force, is

$$\epsilon_V = \frac{V_{ct}/V_{bjt}}{V_c/V_{bj}} = \frac{1}{\cos\left(\frac{\pi}{N_c}\right)}. \quad (4.49)$$

4.3.2 Ranges of Parameters Studied

A parametric study is conducted to study the effects of ratio, ρ , of effective radius of gyration (R_{egyr}) to radius of staging (R_s), number of panels N_p , number of columns N_c , and ratio of flexural stiffness parameters of columns and beams (K_r) on the natural period ratio, τ .

The ratio of structural mass of the container to the mass of water in tank-full condition may take values from 0.25 for large tanks, to 0.5 for small tanks. If one-third the mass of the supporting structure is also considered, then this ratio will increase somewhat. Hence, a range of 0.25 to 0.75 is considered in this study. The height-to-radius ratio of the container may vary from 0.5 to 2. For these values, assuming the roof, wall and floor thickness to be same, the radius of gyration of the empty tank is 0.82 and 0.91 times the radius of the container, respectively. On the other hand, the ratio of impulsive mass to the total mass of liquid takes values of 0.29 and 0.81, respectively. Even though the ratio of radii of the container to the staging is usually kept in the range of 1.30 to 1.5 (Krishna and Jain, 1977; Dayaratnam, 1986), it may vary from 1.0 to 1.75. Considering all these values, ρ may vary from 0.8 to 1.59 for tank-empty condition, and from 0.44 to 1.22 for tank-full condition. Hence, in the subsequent parametric study, ρ is taken to vary between 0.5 and 1.5.

Numbers of panels N_p considered are 4, 6 and 8, while numbers of columns considered are 4, 6, 8 and 10. However, the results of stagings with 4 and 8 panels, and 4 and 10 columns alone are presented here to indicate the trends. The parameter, $K_r = (E_c I_c / h) / (E_b I_b / L)$, reflects the

relative stiffness of columns with respect to that of beams, and can vary widely; hence, K_r is taken as 0.25, 1.0 and 4.0.

4.4 RESULTS & DISCUSSIONS

4.4.1 Study of Stiffness Ratio K_θ/K_x

K_θ/K_x is calculated from Eq.(4.42) considering the term due to axial flexibility of columns in the denominator as $0.0025N_p(4N_p^2-1)$. For stagings with less number of panels and columns, this ratio approaches $D^2/4$ where $D (=2R_s)$ is the diameter of the staging. For instance, K_θ/K_x is $1.02(D^2/4)$ for $N_p=4$, $N_c=4$ and $K_r=4$. For stagings with considerably large number of panels and columns, this ratio approaches $D^2/2$. For example, K_θ/K_x becomes $0.89(D^2/2)$ for $N_p=8$, $N_c=10$ and $K_r=4$; and $0.94(D^2/2)$ for $N_p=8$, $N_c=20$ and $K_r=4$. So, the two-element idealized systems used in Chapters 2 and 3, which have a K_θ/K_x as $D^2/4$, model the stiffness ratio of stagings with small number of panels and columns. Similarly, the four-element systems used in Chapter 2 and 3 model the stiffness ratio of stagings with large number of panels and columns.

4.4.2 Study of Natural Period Ratio (τ)

4.4.2.1 Effect of ρ

The variation in natural period ratio, τ , with the ratio of effective radius of gyration to the radius of staging, ρ , for different combination of N_p , N_c and K_r is shown in Figure 4.6. For given values of N_p , N_c and K_r , the variation of τ with ρ is linear. As discussed in sub-section 4.3.2, for most stagings the ρ will lie in the range 0.5 to 1.5. For this range of ρ , the value of τ varies from 0.4 to 1.5 in

Figure 4.6. This implies that most ordinary tanks on frame stagings are likely to have the value of τ in the range $0.7 < \tau < 1.25$ either in the tank-empty or in tank-full condition; the variation in τ between tank-empty and tank-full conditions has been discussed in the next sub-section. Therefore, most elevated tanks of the basic configuration are vulnerable to large torsional response due to proximity of lateral and torsional periods.

4.4.2.2 Effect of Depth of Water (h_w)

Elevated water tanks are not always completely empty or completely full. At the time of earthquake, a tank may have any intermediate depth of water. Since, the depth of water (h_w) in tank changes the effective radius of gyration, it also changes the natural period ratio, τ . Figure 4.7 shows the variation of τ with depth of water (h_w); τ has been normalized with the natural period ratio at tank-empty condition, τ_{empty} , and h_w is expressed as a fraction of radius of container (R_c). For low-capacity tanks, i.e., tanks with structural mass of about 0.75 times the water mass in tank-full condition, τ/τ_{empty} for tank-full condition is about 0.85 when $h_w/R_c = 0.5$, and about 0.72 when $h_w/R_c = 2.0$; low-capacity tanks are more likely to have a higher h_w/R_c ratio. For large-capacity tanks, i.e., tanks with structural mass of about 0.25 times water mass in tank-full condition, τ/τ_{empty} is about 0.68 and 0.49 for $h_w/R_c = 0.5$ and 2.0, respectively; the large-capacity tanks generally have low h_w/R_c ratio. Therefore, natural period ratio at tank-full condition can be considerably less than that at tank-empty condition. Efforts must be made to configure the staging such that

natural period ratio at both tank-empty and tank-full conditions lies outside the region $0.7 < \tau < 1.25$.

4.4.3 Effect of Different Design Parameters on τ

As seen above, a very large number of tanks will have τ in the range $0.7 < \tau < 1.25$. The questions arise how feasible it is to configure the staging so that τ is not in this range, and what parameters have more significant bearing on τ . This section addresses these questions.

Substituting $\rho = R_{\text{egyr}}/R_s$ in Eq.(4.41), τ can be expressed as $\rho \cdot R_s \sqrt{(K_x/K_\theta)}$. The height and radius of container are generally fixed from the view point of container design. Once container radius is fixed, the staging radius is by and large fixed. Therefore, scope of changing ρ by changing these quantities is quite limited. So, the possibility of changing τ by changing N_p , N_c and K_r needs to be seen. From Figure 4.6, it is observed that as N_p and N_c come close to each other (see curves for $N_p=4$ and $N_c=4$; and, $N_p=8$ and $N_c=10$), the effect of K_r on τ becomes very subdued. To study this effect more clearly, the variation of nondimensional stiffness ratio parameter, $R_s \sqrt{K_x/K_\theta}$, with N_c/N_p ratio is plotted in Figure 4.8 for $N_p=4, 6$ and 8 .

It is seen from Figure 4.8 that the curves for different K_r cross each other near $N_c/N_p=1$. This implies that if number of panels and number of columns are close to each other, then the relative stiffness of columns with respect to beams does not considerably affect $R_s \sqrt{K_x/K_\theta}$ and τ . It can also be noticed when N_c/N_p is small, an increase in N_c causes a sharp reduction in $R_s \sqrt{K_x/K_\theta}$ and hence in τ . This trend is very prominent for curves with $N_p=4$ while much subdued for curves with $N_p=8$.

For large values of N_c/N_p , the curves show a saturating trend implying no considerable change in $R_s \sqrt{K_x/K_\theta}$ and τ , due to a change in the number of columns. It is obvious that there is a very limited scope for configuring the tank staging so as to avoid the range $0.7 < \tau < 1.25$.

4.4.4 Adequacy Under Torsion, of Staging Members Designed for Lateral Force Alone

4.4.4.1 Adequacy of Design for Flexure

Numerical values of the ratio (ϵ_M) of the ratio of column and beam moments under torsion and that under lateral force given by Eqs.(4.44) to (4.48) are presented in Table 4.4. All the values are greater than 1.0 which implies that the columns are more vulnerable to hinging under torsion motion than under lateral motion. Generally, ratio ϵ_M increases with increase in column stiffness over the beam stiffness and with reduction in the number of columns. In four-column stagings, the columns may be significantly more vulnerable to hinging prior to beams under the applied torsion. The value of ϵ_M is as high as 18.0 which implies a serious problem of column hinging under torsion. It may be advisable that in the seismic design and detailing of frame stagings based on the "capacity design principles", the failure mechanism under torsion should also be considered together with the lateral-failure mechanism.

4.4.4.2 Adequacy of Design for Shear

As seen in Eq.(4.49), the ratio ϵ_v is always greater than 1.0; it varies from 1.41 for four-column stagings to 1.0 for stagings with very large number of columns. Again, this implies that in four-column stagings, the columns are more vulnerable to damage in shear occurring

prior to that in beams due to the effect of torsional motion.

4.5 CONCLUSIONS

In this chapter, the basic stiffness characteristics of basic configuration of frame stagings have been studied with a view to assess the vulnerability of such tanks to large torsional response. The important conclusions arrived at in this chapter are as follows:

1. Frame stagings with low number of columns and panels have the stiffness ratio (K_{θ}/K_x) approaching $D^2/4$ while the stiffness ratio for those with large number of columns and panels approaches $D^2/2$. Thus, these can be adequately modelled by the two-element and the four-element systems, respectively, used in Chapters 2 and 3. Chapters 2 and 3 showed that the two-element systems are more vulnerable to large torsional response; hence, stagings with less number of columns and panels are also more vulnerable to large torsional response.
 2. For most of the usual tank stagings with basic configuration, the natural period ratio (τ) may lie in the range $0.7 < \tau < 1.25$; this is the range in which large torsional response occurs.
 3. The value of natural period ratio (τ) may vary significantly between the tank-empty and tank-full conditions. Hence, in seismic design efforts should be made to ensure that the ratio τ does not lie in the critical range in either of the two conditions.
 4. There is only a limited scope for changing τ by modifying the number of columns (N_c), number of panels (N_p), and the relative stiffness of column over that of the beam (K_r). Therefore, in general, it may be
-

better to adopt a configuration other than the basic configuration; this issue has been addressed in the next chapter.

5. The force resultants in different members under applied torsion moment and under applied lateral load are such that under torsional motion the system is more vulnerable to column failure (flexural or shear) preceding the beam failure. The capacity design procedures for such stagings need to explicitly account for this fact.

4.6 REFERENCES

- Dayaratnam,P., (1986), **Design of Reinforced Concrete Structures**, Third Edition, Oxford and IBH Publishing Co. Pvt. Ltd., New Delhi, India.
- Elorduy,J. and Rosenblueth,E., (1968), "Torsional Sismicas en Edificios de un piso," **Segundo Congreso Nacional de Ingenieria Sismica**, Veracruz, Mexico.
- Goel,R.K., and Chopra,A.K., (1992), "Inelastic Seismic Response of One Story Asymmetric Plan Systems: Effects on Stiffness and Strength Distribution," **Earthquake Engineering and Structural Dynamics**, Vol.19, No.7, pp 949-970.
- Green,B.N., (1978), **Earthquake Resistant Building Design and Construction**, Van Norstrand Reinhold Company, New York.
- Housner,G.W., (1957), "Dynamic Pressures on Accelerated Fluid Containers," **Bulletin of Seismological Society of America**, Vol.47, pp 15-35.
- Jain,S.K., Murty,C.V.R., Chandak,N., Seeber,L., and Jain,N.K., (1994), "The September 29, 1993, M6.4 Killari, Maharashtra, Earthquake in Central India," **EERI Newsletter**, Vol.28, No.1, January, pp 1-8.
- Krishna,J., and Jain,O.P., (1977), **Plain and Reinforced Concrete**, Vol.II, Nem Chand and Bros., Roorkee, India.
- Kan,C.L., and Chopra,A.K., (1977), "Effects of Torsional Coupling on Earthquake Forces in Buildings," **Journal of Structural Engineering Division, ASCE**, Vol.103, No.ST4, pp 805-819.
- Lin,B.C., and Papageorgiou,A.S., (1989), "Demonstration of Torsional Coupling Caused by Closely Spaced Periods-1984 Morgan Hill Earthquake Response of Santa Clara County Building," **Earthquake Spectra**, Vol.5, No.3, August, pp 539-556.
-

- Ramiah,B.K., and Gupta,D.S.R.M., (1966), "Factors Affecting Seismic Design of Water Towers," *Journal of the Structural Division, ASCE*, Vol.92, No.ST4, August, pp 13-27.
- Sameer,U.S., and Jain,S.K., (1992), "Approximate Methods for Determination of Time Period of Water Tank Stagings," *The Indian Concrete Journal*, Vol.66, No.12, December, pp 691-698.
- Sameer,U.S., and Jain,S.K., (1994), "Lateral-Load Analysis of Frame Stagings for Elevated Water Tanks," *Journal of Structural Engineering, ASCE*, Vol.120, No.5, May, pp 1375-1394.
- Shepherd,R., (1973), "The Seismic Response of Elevated Water Tanks Supported on Cross Braced Towers," *Proceedings of Fifth World Conference on Earthquake Engineering*, 25-29 June, Rome, pp 640-649.
- SP:22-1982, (1982), *Explanatory Handbook for Codes on Earthquake Engineering: IS:1893-1975 and IS:4326-1976*, Bureau of Indian Standards, New Delhi.
- Steinbrugge,K.V., (1970), "Earthquake Damage and Structural Performance in the United States," Chapter 9, *Earthquake Engineering*, Editor: Robert Wiegel, Prentice-Hall Inc., Englewood Cliffs, New. Jersey, USA.
- Steinbrugge,K.V., and Moran,D.F., (1954), "An Engineering Study of the the South California Earthquake of July 21, 1952 and its Aftershocks," *Bulletin of the Seismological Society of America*, Vol.44, Appendix R, pp 436-453.
- Tso,W.K., and Dempsey,K.M., (1980), "Seismic Torsional Provisions for Dynamic Eccentricity," *Earthquake Engineering and Structural Dynamics*, Vol.8, No.3, pp 275-289.
-

Table 4.1: Details of the Tanks Analyzed.

Items	Example Tanks	
	SP22 Example Tank (no diagonal braces)	Text Book Tank
(1)	(2)	(3)
Staging Radius (mm)	4,500	3,375
Number of Panels	4	4
Panel Height (mm)	4,000	4,540
Beam Size (mm)	200 x 500	400 x 500
Column Size (mm)	diameter 520	460 x 460
Modulus of Elasticity (N/mm^2)	20,000	25,500

Table 4.2: Performance of Proposed Approximate Expressions in Predicting Stiffness for Basic Configuration (Fig.4.1).

Example Tanks	SP22 Example (no diagonal braces)	Text Book Tank
(1)	(2)	(3)
Lateral Flexural Stiffness (N/mm)		
Exact	8,130	7,698
Approximate	8,088	7,694
Error (%)	-0.5	3.3
Lateral Stiffness due to Axial Deformation of Columns (N/mm)		
Exact	277,800	62,112
Approximate	256,400	60,606
Error (%)	-7.7	-2.4
Torsional Stiffness (10^{11} N.mm)		
Exact	2.48	1.27
Approximate	2.37	1.25
Error (%)	-4.5	-1.8

Table 4.3(a) : Performance of Proposed Approximate Expressions in Predicting Shear Forces and Bending Moments in Columns Under Applied Torsion Motion.

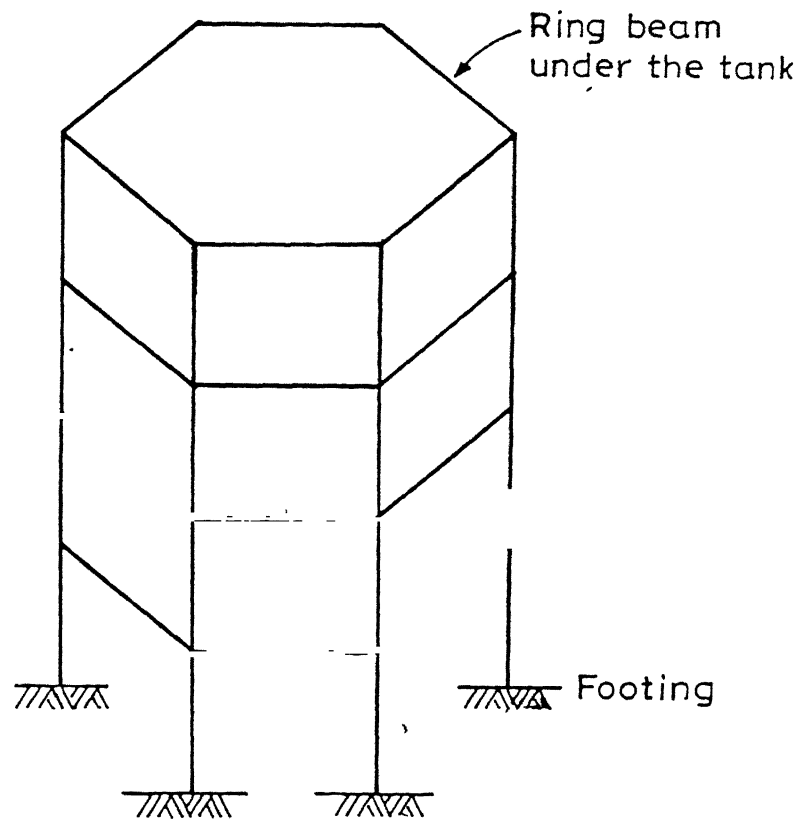
Tank	Panel	Design Shear (N)			Design Moment (10^6 N.mm)		
		Exact	Approx.	Error(%)	Exact	Approx.	Error(%)
(1)	(2)	(3)	(4)	(5)	(6)	(7)	(8)
SP22	4	27,480	27,780	1.0	69.05	71.64	3.8
	3	27,430	27,780	1.0	53.44	55.56	2.3
	2	27,430	27,780	1.0	53.45	55.56	2.3
	1	27,480	27,780	1.0	60.04	71.64	3.8
Text Book	4	49,380	49,380	0.0	127.60	128.69	0.9
	3	49,380	49,380	0.0	111.16	112.10	0.8
	2	49,380	49,380	0.0	111.16	112.10	0.8
	1	49,380	49,380	0.0	127.60	128.69	0.9

Table 4.3(b): Performance of Proposed Approximate Expressions in Predicting Shear Forces and Bending Moments in Beams Under Applied Torsion Motion.

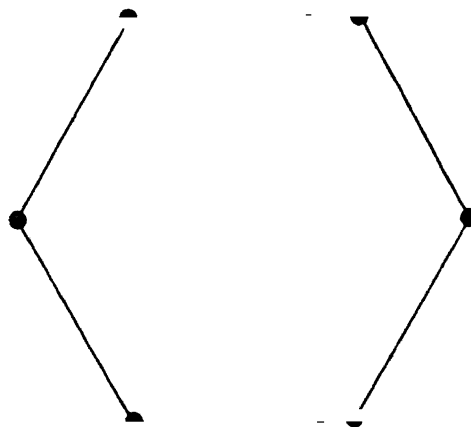
Tank	Beam Level	Design Shear (N)			Design Moment (10^6 N.mm)		
		Exact	Approx.	Error(%)	Exact	Approx.	Error(%)
(1)	(2)	(3)	(4)	(5)	(6)	(7)	(8)
SP22	3	31,230	29,870	4.4	53.78	51.43	4.4
	2	33,530	34,920	4.0	57.73	60.13	4.0
	1	31,230	29,870	4.4	53.78	51.43	4.0
Text Book	3	71,720	71,030	-1.0	121.03	119.86	-1.0
	2	76.060	76,710	0.8	128.36	129.44	0.8
	1	71,720	71,030	-1.0	121.03	119.86	-1.0

Table 4.4 : ϵ_M for Different Values of N_c and K_r (Values are Independent of N_p)

K_r	N_c	Separate Design for Intermediate & End Panels		Same Design for All Panels, Intermediate Panel Columns Govern		Same Design for All Panels, End Panel Columns Govern	
		Intermediate Panel	End Panel	Intermediate Panel	End Panel	Intermediate Panel	End Panel
		$\frac{M_{cjt}/M_{bjt}}{M_{cj}/M_{bj}}$	$\frac{M_{crt}/M_{bet}}{M_{cr}/M_{be}}$	$\frac{M_{cjt}/M_{bjt}}{M_{cj}/M_{bj}}$	$\frac{M_{crt}/M_{bet}}{M_{cj}/M_{bj}}$	$\frac{M_{cjt}/M_{bjt}}{M_{cr}/M_{bj}}$	$\frac{M_{crt}/M_{bet}}{M_{cr}/M_{bj}}$
(1)	2	(3)	(4)	(5)	(6)	(7)	(8)
0.25	4	1.41	1.42	1.41	1.60	1.31	1.49
	6	1.16	1.17	1.16	1.25	1.13	1.23
	8	1.08	1.10	1.08	1.16	1.07	1.15
	10	1.05	1.07	1.05	1.13	1.05	1.12
1.0	4	1.41	1.54	1.41	2.26	1.16	1.85
	6	1.16	1.28	1.16	1.59	1.11	1.53
	8	1.08	1.20	1.08	1.43	1.09	1.45
	10	1.05	1.17	1.05	1.37	1.08	1.41
4.0	4	1.41	5.9	1.41	9.90	2.55	17.82
	6	1.16	5.05	1.41	3.93	4.45	15.14
	8	1.08	5.63	1.08	3.16	5.78	16.88
	10	1.05	6.10	1.05	2.89	6.65	18.30

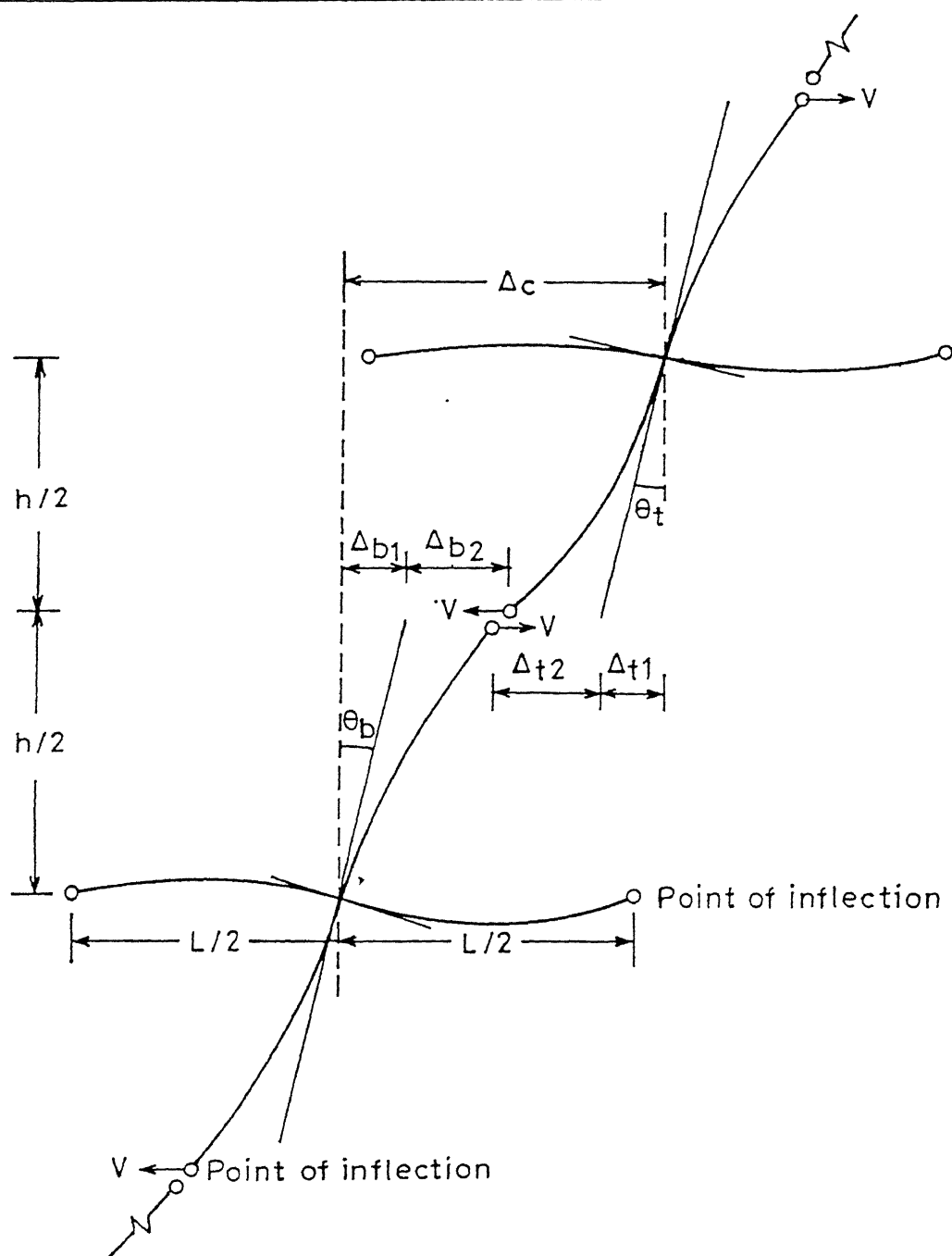


(a) Isometric view



(b) Plan

Figure 4.1 : A typical staging with basic configuration.



$$\Delta_{b1} = \theta_b \frac{h}{2} , \Delta_{t1} = \theta_t \frac{h}{2}$$

$$\Delta_{b2} = \Delta_{t2} = \frac{V(h/2)^3}{3E_c I_c}$$

$$\Delta_c = \Delta_{b1} + \Delta_{b2} + \Delta_{t1} + \Delta_{t2}$$

Figure 4.2 : Staging sub-assemblages showing deflection between successive joints due to bending of beams and columns (Sameer and Jain, 1992).

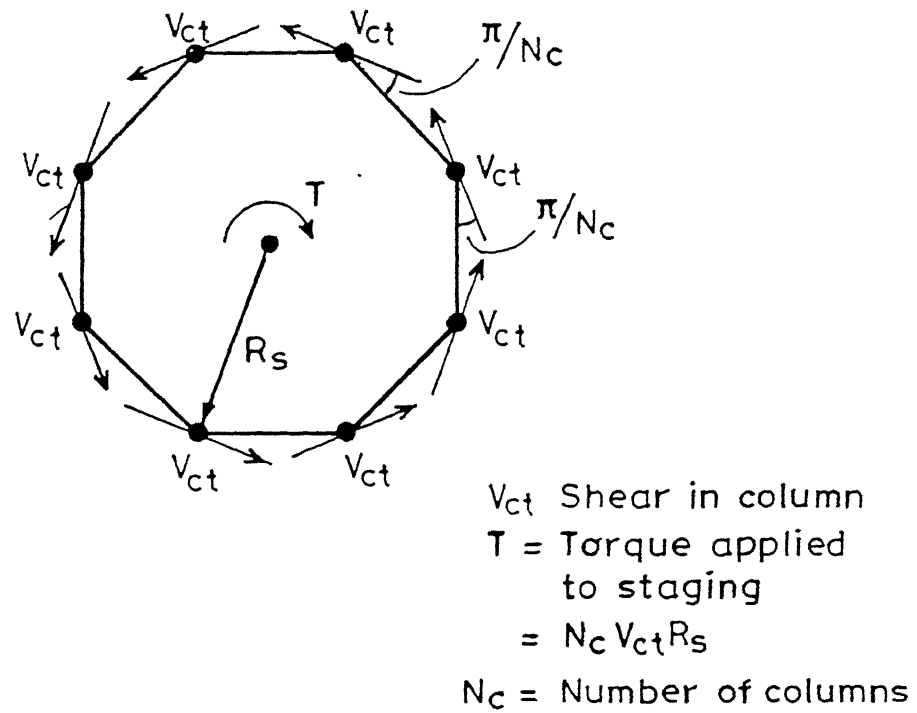
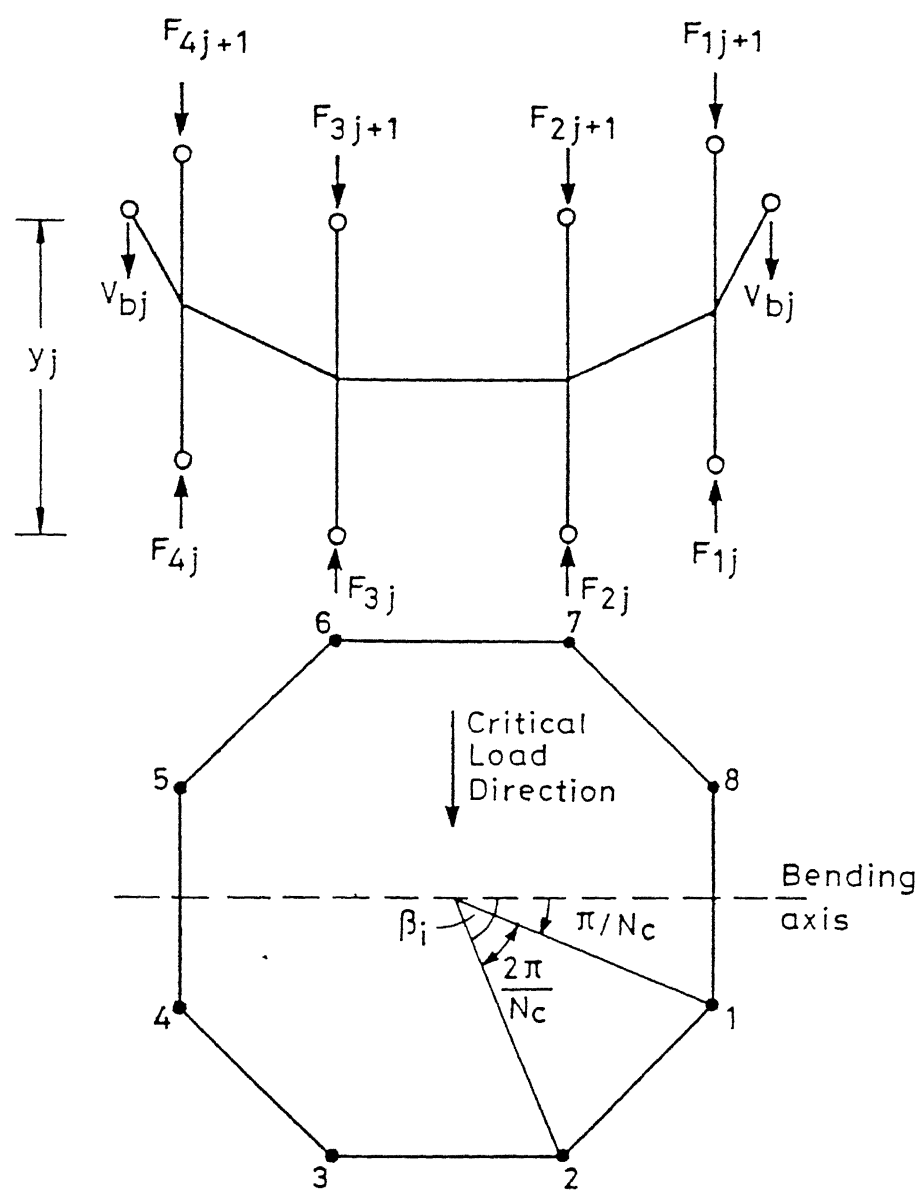


Figure 4.3 : Development of torsional resistance in typical frame-type staging.



$$V_{bj} = \frac{(F_{1j} + F_{2j} + F_{3j} + F_{4j}) - (F_{1j+1} + F_{2j+1} + F_{3j+1} + F_{4j+1})}{2}$$

Figure 4.4 : Determination of shear forces in beams.

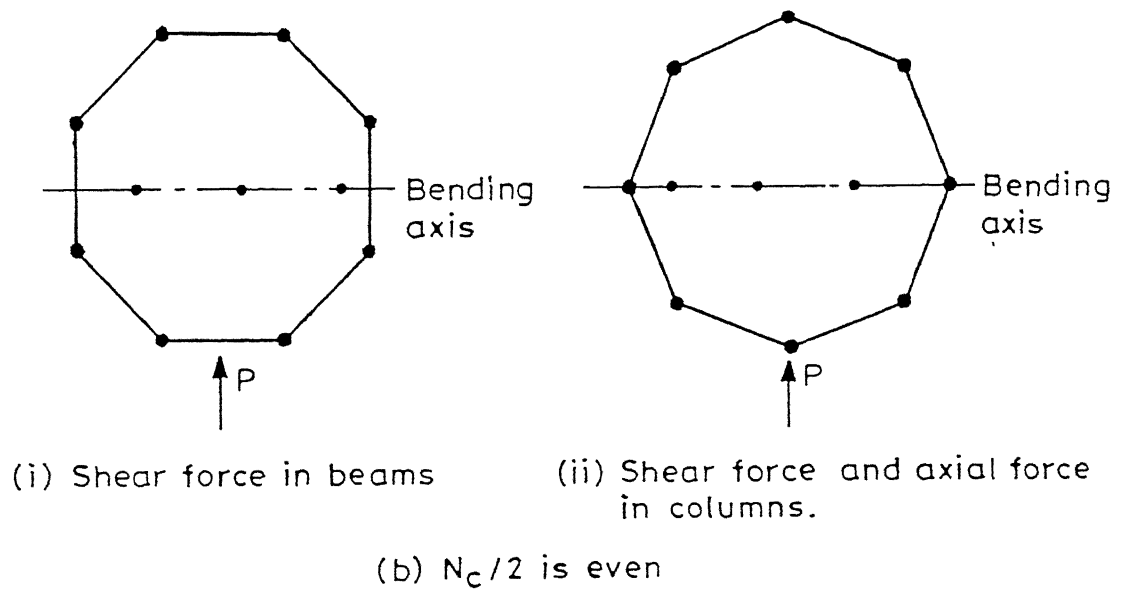
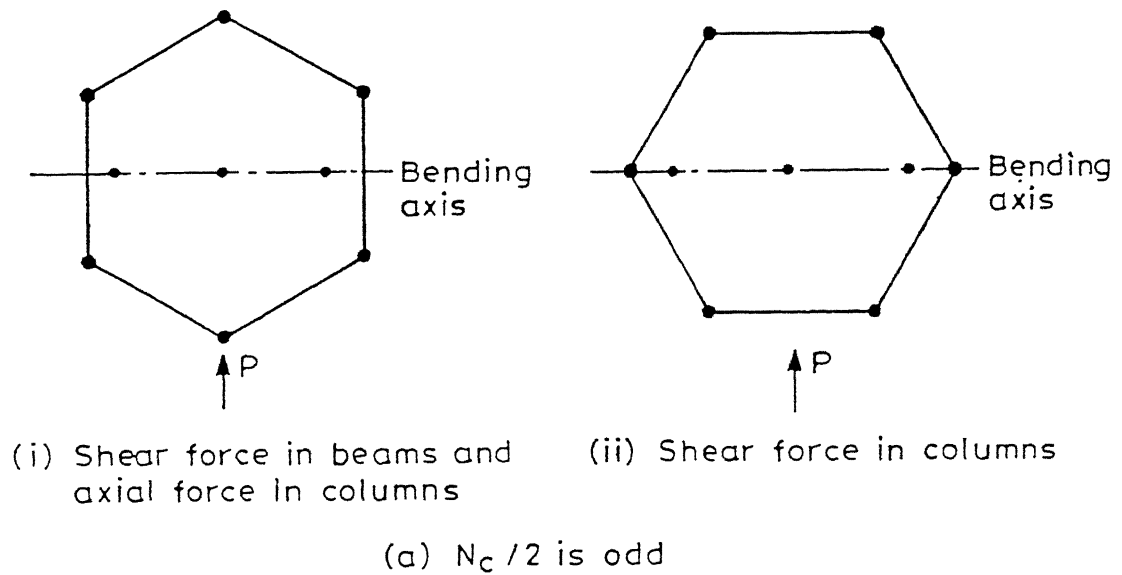


Figure 4.5 Critical direction for forces in beams and columns
(Sameer and Jain, 1994).

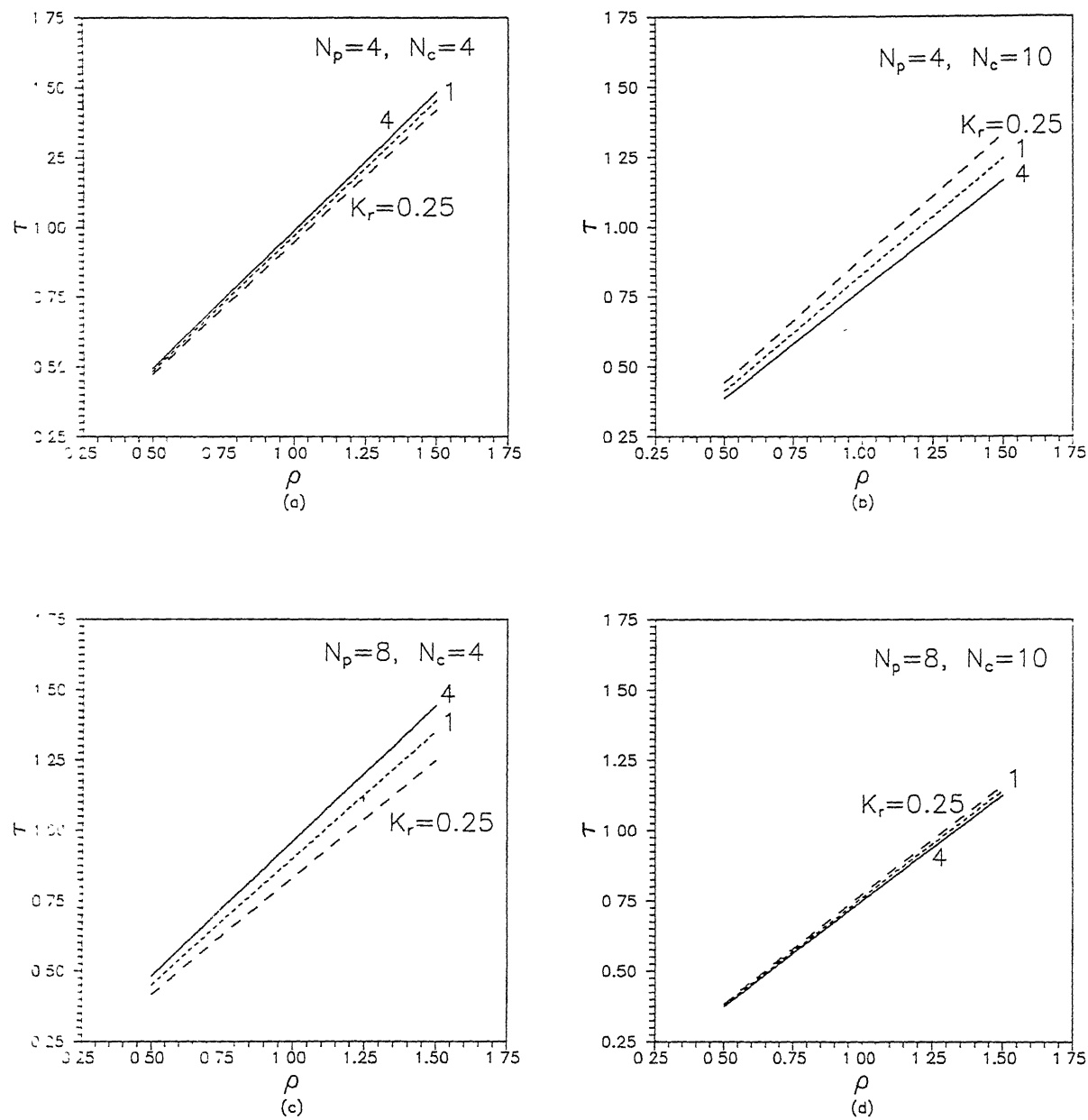


Figure 4.6 : Variation of natural period ratio, τ ($= T_{\theta}/T_x$), with ρ ($= R_{\text{egyr}}/R$).

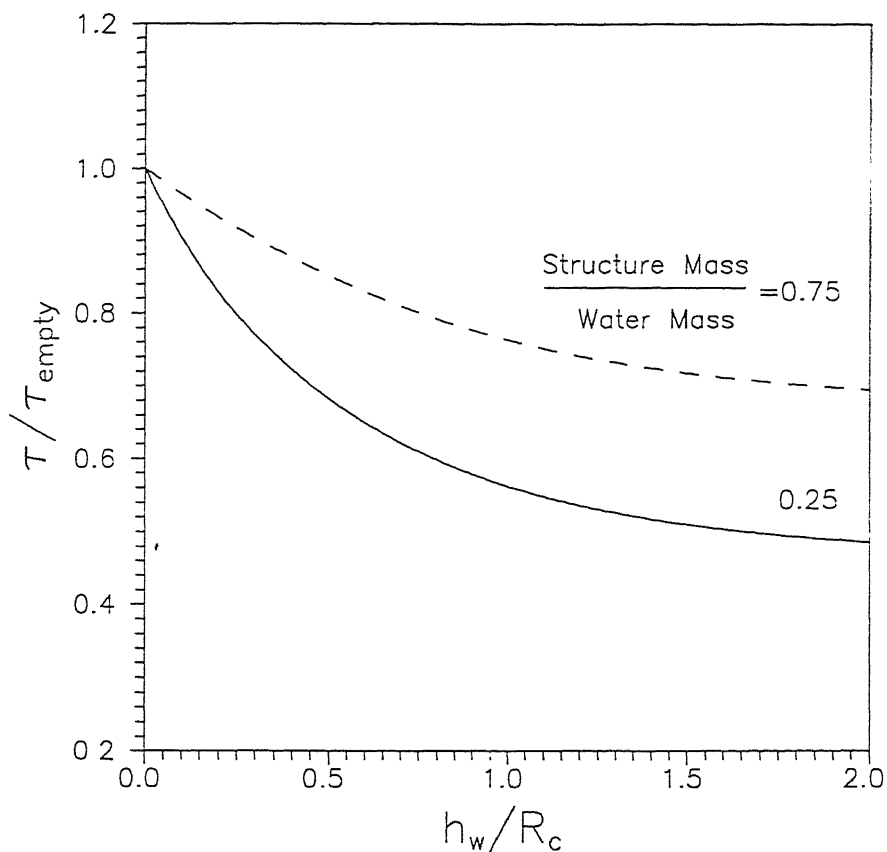


Figure 4.7 : Variation of natural period ratio (τ) with depth of water, h_w . Natural period ratio (τ) is normalized with natural period ratio (τ_{empty}) at tank-empty condition. Water depth is normalized with radius of container (R_c).

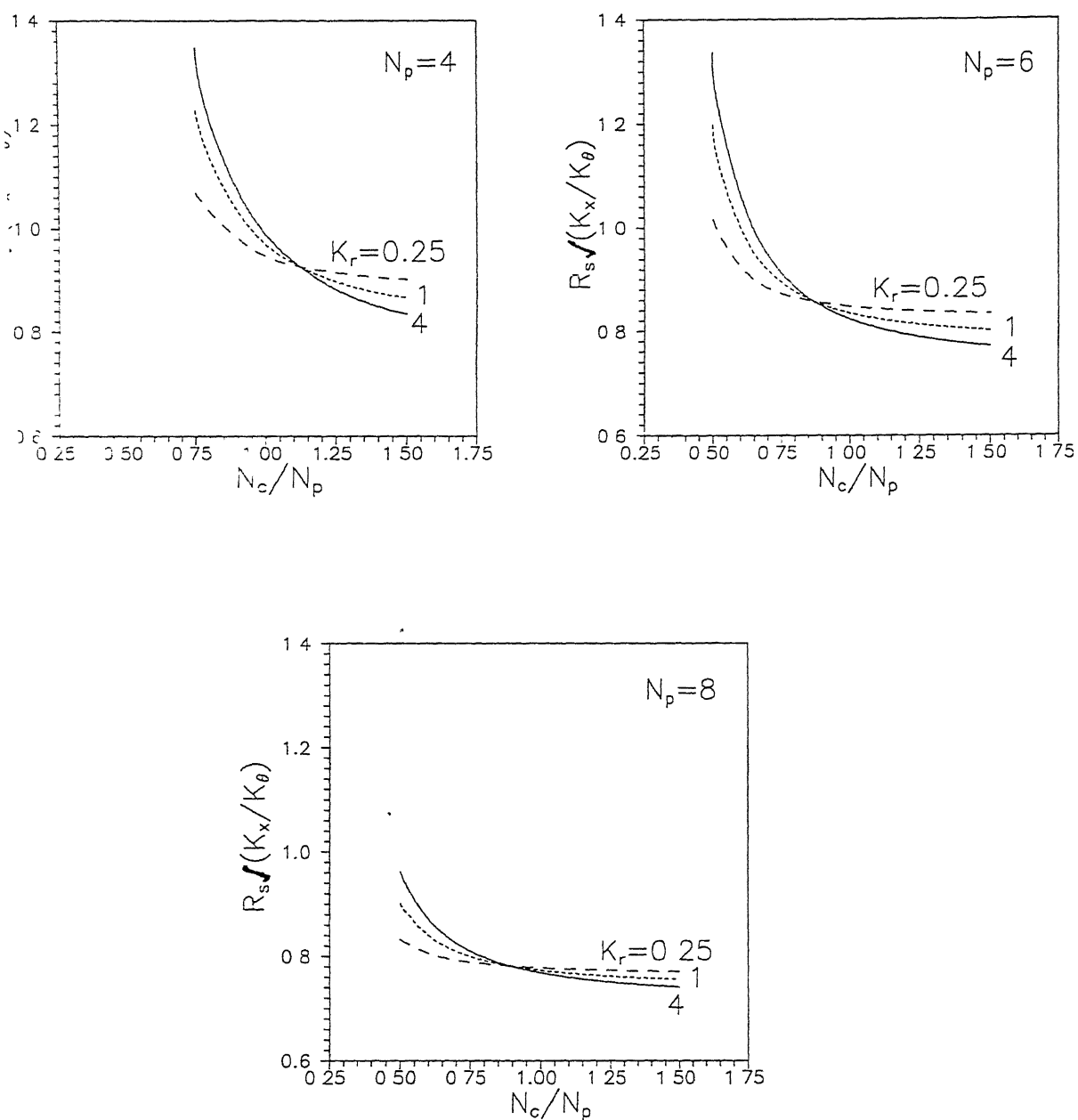


Figure 4.8 : Variation of nondimensional stiffness ratio parameter $R_s \sqrt{(K_x/K_\theta)}$ with N_c/N_p (a) $N_p = 4$, (b) $N_p = 6$, (c) $N_p = 8$.

CHAPTER 5

ALTERNATE STAGING CONFIGURATIONS TO REDUCE TORSIONAL COUPLING

5.1 INTRODUCTION

It is seen in the previous chapters that elevated water tanks of basic configuration (Figure 4.1) are prone to large torsional response due to accidental eccentricity since the natural period ratio (τ) may often lie in the range $0.7 < \tau < 1.25$. Since the magnitude and direction of eccentricity is not known because of the accidental nature, it is difficult to take care of this problem by conventional increased strength design. It was also seen in Chapter 4 that the period ratio (τ) can be adjusted only to a limited extent by adjusting the number of panels N_p , number of columns N_c , and the parameter K_r related to the bending stiffness of columns and beams.

In this chapter, alternative staging configurations are studied with a view to move the natural period ratio away from the critical range. The alternative configuration studied are those which can be achieved by some modifications to the basic configuration; for instance by (a) adding radial beams at the levels of circumferential beams, (b) adding the radial beams and a central column, (c) having two concentric rows of columns connected through radial beams, and (d) adding diagonal braces (Figures 5.1 and 5.2). As compared to the basic configuration, first three of these configurations have larger torsional-to-lateral natural period ratio (τ) while the addition of diagonal braces reduces the natural period ratio (τ).

Approximate closed-form expressions for torsional and lateral stiffnesses of these configurations are derived. Panel heights are assumed identical, even though the procedure outlined here is general enough and can be extended for stagings with unequal panel heights. A parametric study is conducted for the alternate configurations, to understand the effect of the various parameters on τ .

5.2 STAGING WITH RADIAL BEAMS

Addition of the radial beams to the basic staging configuration provides increased lateral stiffness with hardly any change in the torsional stiffness. Therefore, the natural period ratio (τ) is increased. Addition of the radial beams may also be feasible for retrofitting the existing elevated water tanks.

5.2.1 Lateral Stiffness

5.2.1.1 Due to Bending Deformation of Staging Members

To account for the radial beams, k_{st} and k_{sb} in Eq.(4.6) are replaced by $k_{st} + k_{srt}$ and $k_{sb} + k_{srb}$, respectively. Here, k_{srt} and k_{srb} are the sum of rotational stiffness in the direction of lateral force of all radial beams at all the top and bottom joints of the panel considered. Assuming that all the radial beams have their points of inflection at the centre of the staging circle,

$$k_{srt} = k_{srb} = \sum_{i=1}^{N_c} k_{brt} = \sum_{i=1}^{N_c} k_{brb} = \frac{E_b I_{br}}{2R_s} \sum_{i=1}^{N_c} \cos^2 \beta_i = \frac{E_b I_{br} N_c}{4R_s}, \quad (5.1)$$

where k_{brt} and k_{brb} are the rotational stiffness of individual radial

beams at top and bottom joints, respectively; β_i is the angle made by radial beam i with direction of lateral force; and I_{br} is the moment of inertia of the cross section of the radial beam. Let the ratio of moments of inertia of radial and circumferential beams, I_{br}/I_b be denoted by δ_0 . Using Eq.(4.6) and $R_s = (L/2)\sin(\pi/N_c)$, the lateral panel stiffness due to bending for a staging with equal panel heights, identical columns, and identical radial beams is given by

$$K_{p(lateral)} = \frac{\frac{12E_c I_c N_c}{h^3}}{1 + \frac{\gamma K_r}{1 + 0.5\delta_0 \sin\left(\frac{\pi}{N_c}\right)}} \quad , \quad (5.2)$$

where

$$\gamma = \begin{cases} 2, & \text{for intermediate panels} \\ 1, & \text{for topmost and bottommost panels.} \end{cases}$$

5.2.1.2 Due to Axial Deformation of Staging Columns

The expression for staging stiffness due to axial deformation in columns is same as that for the basic staging configuration, given by (Eq.4.10), i.e.,

$$K_{axial} = \frac{6N_c A_c E_c R_s^2}{h^3 N_p (4N_p^2 - 1)} \quad . \quad (5.3)$$

5.2.2 Torsional Stiffness

Torsional stiffness of the individual radial beams about their longitudinal axes is small and hence neglected. Therefore, addition of radial beams does not change torsional stiffness of the staging and the torsional panel stiffness is same as that for the basic configuration given by Eq. (4.13), i.e.,

$$K_{p(\text{torsional})} = \frac{\frac{12E_c I_c N_c R_s^2}{h^3}}{1 + \frac{\gamma K_r}{2 \cos^2 \left(\frac{\pi}{N_c} \right)}} \quad (5.4)$$

5.2.3 Natural Period Ratio (τ_{rb})

The total lateral stiffness of staging can be obtained by combining the stiffnesses due to flexural and axial deformations considered in series. Since the objective of this study is only to observe the variation in natural period ratio due to addition of radial beams, the stiffness contribution due to bending deformation alone is considered in the calculation of τ . The lateral stiffness of the staging with radial beams (K_x)_{rb} is obtained by combining the panel stiffnesses considered in series, and is given by

$$(K_x)_{rb} = \frac{12E_c I_c N_c}{h^3} \left[\frac{1}{N_p + \frac{2(N_p - 1)K_r}{1 + 0.5 \delta_0 \sin \left(\frac{\pi}{N_c} \right)}} \right] \quad (5.5)$$

The alternate staging configuration is compared with the corresponding basic staging configuration having the same N_p , N_c and K_r . Hence, the lateral stiffness of the basic staging configuration K_x considering bending deformations alone is obtained from Eq.(4.11) by dropping the axial deformation terms as

$$K_x = \frac{12E_c I_c N_c}{h^3} \left[\frac{1}{N_p + 2(N_p - 1)K_r} \right] \quad (5.6)$$

Since, the torsional stiffness and the mass and rotational inertia are the same for the alternate as well as the basic configuration, the ratio

of the natural period ratio (τ_{rb}) of the staging with radial beams and the natural period ratio (τ) of the staging with basic configuration is

$$\frac{\tau_{rb}}{\tau} = \sqrt{\frac{(K_x)_{rb}}{K_x}} = \sqrt{\frac{N_p + 2(N_p - 1)K_r}{2(N_p - 1)K_r}} \cdot \sqrt{N_p + \frac{1}{1 + 0.5 \delta_0 \sin\left(\frac{\pi}{N_c}\right)}} \quad (5.7)$$

5.2.4 Results and Discussion

Accuracy of the approximate analytical expressions for lateral stiffness has been verified through two example tanks given in Table 4.1 to which radial beams were added. The lateral stiffnesses from Eqs. (5.2) and (5.4) are compared in Table 5.1 with the FEM solution, denoted as the exact solution. The analytical expressions are found to give very reasonable estimates.

To study the effect of radial beams, τ_{rb} is plotted as a function of $K_r = (E_c I_c / h) / (E_b I_b / L)$ for different values of N_p and N_c (Figure 5.3). All radial and circumferential beams are assumed to have identical cross sections, i.e., $\delta_0 = 1$. The introduction of radial beams increases the natural period ratio by 2% to 14%, depending on N_p , N_c and K_r . The increase will be more if one uses radial beams of larger cross-section. As K_r increases, i.e., as the columns become stiffer with respect to the beams, (τ_{rb}/τ) increases; the rate of increase is larger at small values of K_r and becomes marginal beyond K_r around 1.5. In the basic staging configuration, the columns farther away from the bending axis of the entire staging, share less shear due to lack of adequate framing action in the direction of lateral force through the circumferential beams. The radial beams increase the participation of these columns by facilitating

frame action in the direction of lateral force.

Radial beams are more effective in increasing the natural period ratio of stagings with lesser number of columns. As the number of columns increase, span of the circumferential beams decreases and hence, their stiffness with respect to radial beams increases; this results in lower influence of radial beams.

5.3 STAGING WITH RADIAL BEAMS AND A CENTRAL COLUMN

The additional central column and the radial beams (Figure 5.1b) make negligible contribution to the torsional stiffness of the staging, but increase the lateral stiffness.

5.3.1 Lateral Stiffness

5.3.1.1 Due to Bending Deformation of Staging Members

The lateral stiffness may be considered separately due to (a) the circumferential columns and (b) the central column. The central column is also assumed to be rotationally restrained at top ring beam level and at the foundation. Fixity at ring beam level can be achieved by connecting the central column to the ring beam through deep radial beams. The central column provides only lateral stiffness and does not carry any axial load. The points of inflection of all radial beams are assumed to be at mid-span. Span of radial beams in this case is one half of that in the absence of central column. Therefore, the rotational stiffness of radial beams can be obtained by substituting $(2R_s)$ in place of $(4R_s)$ in Eq.(5.1), i.e.,

$$k_{srt} = k_{srb} = \frac{E_b I_{br} N_c}{2R_s} . \quad (5.8)$$

Hence, the panel stiffness due to circumferential columns becomes

$$K_{\text{circ.cols}} = \frac{\frac{12E_c I_c N_c}{h^3}}{1 + \frac{\gamma K_r}{1 + \delta_0 \sin\left(\frac{\pi}{N_c}\right)}} . \quad (5.9)$$

The stiffness of the central column in a panel, $K_{\text{cent.col.}}$, is obtained from Eq.(4.5) by replacing $\sum k_{bt}$ and $\sum k_{bb}$ with k_{srt} and k_{srb} , respectively, given by Eq.(5.8). Thus,

$$K_{\text{cent.col.}} = \frac{\frac{12\phi E_c I_c N_c}{h^3}}{N_c + \frac{\gamma \phi K_r}{\delta_0 \sin\left(\frac{\pi}{N_c}\right)}} , \quad (5.10)$$

where ϕ is the ratio of the moment of inertia of central column to that of the circumferential columns. The total lateral panel stiffness due to bending deformation, $K_{p(\text{lateral})}$, is the sum of $K_{\text{circ.cols.}}$ and $K_{\text{cent.cols.}}$ given by Eqs.(5.9) and (5.10), respectively.

5.3.1.2 Due to Axial Deformation of Columns

The expression for stiffness of the staging due to axial deformation in columns is same as that for the basic staging configuration, given by Eq.(5.3).

5.3.2 Torsional Stiffness

Since both the radial beams and the central column do not contribute any significant torsional stiffness, the expression for

torsional stiffness of a panel given by Eq.(4.13) for a staging with basic configuration, is also valid for this staging.

5.3.3 Natural Period Ratio (τ_{rbcc})

The panel stiffnesses due to circumferential columns are combined considering them to be in series to obtain contribution of the circumferential columns to the staging stiffness. This is then added to the similar contribution of the central column. In the process, the compatibility condition of equal lateral displacement in all columns at different beam levels is violated. Thus, the overall lateral stiffness of staging with radial beams and a central column, $(K_x)_{rbcc}$, is

$$(K_x)_{rbcc} = \frac{12E_c I_c N_c}{h^3} \left[\frac{1}{N_p + \frac{2(N_p-1)K_r}{1+\delta_0 \sin\left(\frac{\pi}{N_c}\right)}} + \frac{\phi}{N_p N_c + \frac{2(N_p-1)\phi K_r}{\delta_0 \sin\left(\frac{\pi}{N_c}\right)}} \right] \quad (5.11)$$

As in the previous section, here also the terms due to axial deformation of columns have been dropped. The torsional stiffness, the mass and the rotational inertia are the same in this and the basic configuration. Hence the ratio of natural period ratio of staging with radial beams with a central column (τ_{rbcc}) and that of staging with basic configuration (τ) is obtained using Eqs.(5.11) and (5.6)

$$\frac{\tau_{rbcc}}{\tau} = \sqrt{\frac{(K_x)_{rbcc}}{K_x}} = \sqrt{\frac{N_p + 2(N_p-1)K_r}{N_p + \frac{2(N_p-1)K_r}{1+\delta_0 \sin\left(\frac{\pi}{N_c}\right)}} + \frac{\phi \left(N_p + 2(N_p-1)K_r \right)}{N_p N_c + \frac{2(N_p-1)\phi K_r}{\delta_0 \sin\left(\frac{\pi}{N_c}\right)}}} \quad (5.12)$$

5.3.4 Results and Discussion

The analytical expressions for stiffnesses provide reasonable estimates as per the comparisons given in Table 5.2 for the two example tanks of Table 4.1 to which radial beams and central column are added.

Figure 5.4 shows the effect of radial beams and a central column on the natural period ratio. Here, all radial and circumferential beams are assumed to have identical cross sections, i.e., $\delta_0=1$. Also, all the columns are assumed to have identical cross-sections, i.e., $\phi=1$. The trends in the variation are same as observed in Figure 5.3 without the central column. However, the present configuration leads to more significant increase in the natural period ratio. The increase ranges from 9% to 47%; this can be further increased by having larger size for radial beams. Therefore, this configuration can be effectively used to configure stagings away from the critical region of natural period ratio.

5.4 STAGING WITH TWO CONCENTRIC ROWS OF COLUMNS WITH CIRCUMFERENTIAL AND RADIAL BEAMS

In this configuration (Figure 5.1c) two concentric row of columns are provided with equal number of columns (N_c) in each row. Radial beams only connect the outer and inner columns and do not extend to the centre of the staging. The inner row of columns contributes both the lateral stiffness as well as the torsional stiffness. The columns of inner row also are assumed to be fixed at the footing level against displacement and rotation, and at the top-ring beam level against rotation. In the procedure followed here lateral stiffness of the entire staging due to

outer and inner row of columns is estimated separately and then combined by considering the two rows of columns to be in parallel. This same procedure followed for the torsional stiffness also. This violates the compatibility of equal displacement between the joints of the inner and outer rows.

5.4.1 Lateral Stiffness

5.4.1.1 Due to Bending Deformation of Staging Members

Let μ be the ratio of radii of inner and outer concentric rows of columns. Then, the length of the radial beams connecting two concentric circular rows of columns is $(1-\mu)R_s$. To obtain the panel stiffness $K_{po(lateral)}$ due to outer circular row, k_{st} and k_{sb} in Eq.(4.6) are replaced by $(k_{st}+k_{srt})$ and $(k_{sb}+k_{srb})$, respectively, where

$$k_{st} = k_{sb} = \frac{E_b I_b N_c}{L} \quad \text{and} \quad (5.13)$$

$$k_{srt} = k_{srb} = \frac{E_b I_{br} N_c}{2(1-\mu)R_s}.$$

Thus,

$$K_{po(lateral)} = \frac{\frac{12E_c I_c N_c}{h^3}}{1 + \frac{\gamma K_r}{\delta_0 \sin\left(\frac{\pi}{N_c}\right) + \frac{1}{1-\mu}}} \quad (5.14)$$

In Eq.(5.14), N_c denotes the number of columns in a single circular row and not the total number of columns.

The length of the inner circumferential beams is μL , where L is length of the outer circumferential beams. To obtain the panel stiffness

$K_{pi(lateral)}$ due to the inner circular staging, k_{st} and k_{sb} in Eq.(4.6) are replaced by $(k_{st}+k_{srt})$ and $(k_{sb}+k_{srb})$, respectively, where

$$k_{st} = k_{sb} = \frac{E_b I_b N_c}{\mu L} \quad (5.15)$$

and

$$k_{srt} = k_{srb} = \frac{E_b I_{br} N_c}{2(1-\mu)R_s}.$$

Thus,

$$K_{pi(lateral)} = \frac{\frac{12\eta E_c I_c N_c}{h^3}}{-1 + \frac{\eta K_r}{\delta_1 + \frac{\delta_0 \sin\left(\frac{\pi}{N_c}\right)}{\mu + (1-\mu)}}} \quad (5.16)$$

In Eq.(5.16), η is the ratio of moments of inertia of columns in the inner and outer circular staging frames; and δ_1 is the ratio of moments of inertia of circumferential beams in the inner and outer circular staging frames.

5.4.1.2 Due to Axial Deformation of Staging Columns

Staging stiffness due to axial deformation of columns is calculated separately for outer and inner rows of columns; the procedure followed is same as that adopted in Chapter 4. The terms contributed by the inner and outer rows are then combined considering them to be in parallel; this gives

$$K_{axial} = \frac{6N_c A_c E_c R_s^2 (1+\eta_1 \mu^2)}{h_p^3 N_p (4N_p^2 - 1)} \quad (5.17)$$

In Eq.(5.17), η_1 is the ratio of the cross sectional areas of columns of

inner and outer circular rows of columns, respectively.

5.4.2 Torsional Stiffness

For outer circular staging frame, the torsional stiffness of panel is same as that given by Eq.(4.13). However, for inner circular staging frame, K_r , I_c , and R_s in Eq.(4.13) are replaced by $\mu\eta K_r/\delta_1$, ηI_c and μR_s , respectively. Hence, the panel stiffnesses of outer and inner circular staging frames, respectively, are

$$K_{po(\text{torsional})} = \frac{\frac{12E_c I_c N_c R_s^2}{h^3}}{1 + \frac{\gamma K_r}{2\cos^2\left(\frac{\pi}{N_c}\right)}} \quad (5.18)$$

and

$$K_{pi(\text{torsional})} = \frac{\frac{12\eta E_c I_c N_c R_s^2 \mu^2}{h^3}}{1 + \frac{\gamma \mu \eta K_r}{2\delta_1 \cos^2\left(\frac{\pi}{N_c}\right)}} \quad (5.19)$$

5.4.3 Natural Period Ratio (τ_{2crc})

For the present purpose, terms in lateral stiffness due to axial deformation of columns are ignored. The stiffness terms due to outer and inner circular row of columns are combined to obtain the overall lateral staging stiffnesses $(K_x)_{2crc}$ as

$$(K_x)_{2crc} = \frac{12E_c I_c N_c}{h^3} \left[\frac{1}{N_p + \frac{2(N_p-1)K_r}{\delta_0 \sin\left(\frac{\pi}{N_c}\right)} + \frac{\eta}{N_p + \frac{2(N_p-1)\eta K_r}{\delta_1 \delta_0 \sin\left(\frac{\pi}{N_c}\right)} + \frac{\mu}{\mu + \frac{(1-\mu)}{(1-\mu)}}} \right], \quad (5.20)$$

and the torsional stiffness of staging, $(K_{\theta})_{2crc}$, as

$$(K_{\theta})_{2crc} = \frac{12E_c I_c N_c}{h^3} \left[\frac{1}{N_p + \frac{(N_p - 1)K_r}{\cos^2\left(\frac{\pi}{N_c}\right)}} + \frac{\eta \mu^2}{N_p + \frac{(N_p - 1)\eta K_r \mu}{\delta_1 \cos^2\left(\frac{\pi}{N_c}\right)}} \right]. \quad (5.21)$$

So, the natural period ratio τ_{2crc} is given by

$$(\tau)_{2crc} = \left(\frac{T_{\theta}}{T_{x'}} \right)_{2crc} = \rho \sqrt{\frac{(K_{x'})_{2crc}}{(K_{\theta})_{2crc}}}. \quad (5.22)$$

Thus, the ratio of τ_{2crc} of staging with two concentric rings of columns and τ of staging with basic configuration is given by

$$\frac{\tau_{2crc}}{\tau} = \sqrt{\frac{(K_{x'})_{2crc}/(K_{\theta})_{2crc}}{K_{x'}/K_{\theta}}}. \quad (5.23)$$

5.4.4 Results and Discussion

The analytical expressions for stiffness are verified through the two example tanks of Table 4.1 to which an inner row of columns is added. The values estimated by the proposed approximate expressions are found to match very well with the finite element results (Table 5.3).

For the parametric study on effect of two rows of columns on the natural period ratio, all radial and circumferential beams are assumed to have identical cross section ($\delta_0 = \delta_1 = 1$), all outer and inner columns are also assumed to have identical cross section ($\eta = 1$). The ratio of radii of inner and outer rows of columns (μ) is taken as 0.2, 0.4, 0.6 and 0.8.

Figure 5.5 shows the variation of natural period ratio normalized with that for the basic configuration. It is obvious that the natural

period ratio is significantly higher, even upto 100%, for stagings with the two rows of columns over that for basic staging. The ratio (τ_{2crc}/τ) generally increases with reduction in μ , i.e., as the radius of inner row reduces. This is because with low inner radius the torsional stiffness contributed by the inner row reduces significantly.

5.5 STAGING WITH DIAGONAL BRACES

The effect of addition of diagonal braces to frame-type stagings is studied in this section. Diagonal braces induce truss action in the staging in addition to the existing frame action.

Generally, two cross braces are provided in each bay of each panel as shown Figure 5.2 Under lateral load, one of them is in tension and the other in compression. The diagonal braces can be of small diameter steel rods. The contribution of the diagonal braces carrying tension is only considered, as the braces carrying compression generally buckles easily and hence, contribute very less to the stiffness. However, in practice the diagonal braces of small diameter rods may be pretensioned to avoid compression buckling. Diagonal braces of reinforced concrete can also be provided which will add very considerable stiffness. These cases where both tension and compression braces contribute stiffness are not covered in the present study. However, the present treatment can be easily extended to cover such situations.

In the present study, the stiffness due to truss action mobilized by the diagonal braces is derived separately and then it is added with the stiffness due to frame action of the staging without diagonal braces. Since the diagonal braces predominantly induce truss action in

the staging, the frame action developed by them has been neglected. The approximate procedure used in the past (Ramiah and Gupta, 1966; SP:22-1982; Arya and Ajmani, 1989) for estimating stiffness of such stagings, consider columns and horizontal beams to be axially rigid in comparison to the diagonal braces. Consequently, these methods neglect the effect of axial deformations of columns and beams in deriving the stiffness, as shown in Figure 5.6a. The approximate method proposed in this study eliminates this assumption by considering the axial deformations in beams and columns, as shown in Figure 5.6b.

5.5.1 Stiffness Contributed by Truss Action of Staging Members

5.5.1.1 Lateral Stiffness

In a staging composed of N_c bays and N_p panels, each bay is oriented at an angle different from the direction of lateral force. If K is the in-plane lateral stiffness of each bay including all the panels, then the stiffness of bay j in the direction of lateral force is $K \cos^2 \phi_j$, where ϕ_j is the angle between the plane of bay j and the direction of lateral force. The lateral force, P , is carried by the different bays in the ratio of their lateral stiffness. So, force P_j carried by bay j is

$$P_j = \frac{P \cos^2 \phi_j}{\sum_{i=1}^c \cos^2 \phi_j} = \frac{2P \cos^2 \phi_j}{N_c} . \quad (5.24)$$

The force P_j is approximate because individual bays do not have the same stiffness when they act together. The axial forces in columns change as a result of mutual interaction among the bays.

The column j is common to both bay $(j-1)$ and bay j . Under a lateral force P applied at staging top, column j attracts compressive force C in bay j and tensile force T in bay $(j-1)$, given by

$$C = \frac{2P(N_p+1-i)\tan\theta_i\cos\phi_j}{N_c} \quad (5.25)$$

and

$$T = \frac{2P(N_p-i)\tan\theta_i\cos\phi_{j-1}}{N_c}, \quad (5.26)$$

where θ_i is the inclination of brace in panel i with horizontal. So, the net axial compressive force, F_{cij} , in column j of panel i is

$$F_{cij} = \frac{2P \tan\theta_i \left[(N_p+1-i)\cos\phi_j - (N_p-i)\cos\phi_{j-1} \right]}{N_c}. \quad (5.27)$$

If a lateral force P is applied at a height h_0 from the top of the staging, it is equivalent to a lateral force P and a moment Ph_0 acting at staging top. The additional increase in axial compressive force in column j due to moment Ph_0 is $(2P/N_c)(h_0/L)(\cos\phi_j - \cos\phi_{j-1})$. Hence, the net axial force in column j of panel i is

$$F_{cij} = \frac{2P}{N_c} \left[\left\{ (N_p+1-i)\tan\theta_i + \frac{h_0}{L} \right\} \cos\phi_j - \left\{ (N_p-i)\tan\theta_i + \frac{h_0}{L} \right\} \cos\phi_{j-1} \right]. \quad (5.28)$$

The total axial strain energy, U_c , stored in all columns is

$$U_c = \sum_{j=1}^{N_c} \sum_{i=1}^{N_p} \frac{4P^2 h_i^2}{2N_c^2 A_c E_c} \left[\left\{ (N_p+1-i)\tan\theta_i + \frac{h_0}{L} \right\}^2 \cos^2\phi_j - 2 \left\{ (N_p+1-i)\tan\theta_i + \frac{h_0}{L} \right\} \left\{ (N_p-i)\tan\theta_i + \frac{h_0}{L} \right\} \cos\phi_j \cos\phi_{j-1} + \left\{ (N_p-i)\tan\theta_i + \frac{h_0}{L} \right\}^2 \cos^2\phi_{j-1} \right]. \quad (5.29)$$

Therefore,

$$\begin{aligned} \frac{\partial U_c}{\partial P} = & \sum_{j=1}^{N_c} \sum_{i=1}^{N_p} \frac{4Ph_i}{N_c^2 A_c E_c} \left[\left\{ (N_p+1-i) \tan \theta_i + \frac{h_0}{L} \right\}^2 \cos^2 \phi_j \right. \\ & - 2 \left\{ (N_p+1-i) \tan \theta_i + \frac{h_0}{L} \right\} \left\{ (N_p-i) \tan \theta_i + \frac{h_0}{L} \right\} \cos \phi_j \cos \phi_{j-1} \\ & \left. + \left\{ (N_p-i) \tan \theta_i + \frac{h_0}{L} \right\}^2 \cos^2 \phi_{j-1} \right] . \end{aligned} \quad (5.30)$$

Simplifying Eq.(5.30) using De Moivre's identity (Carmichael and Smith, 1962),

$$\frac{\partial U_c}{\partial P} = F_1 P , \quad (5.31)$$

where

$$\begin{aligned} F_1 = & \sum_{i=1}^{N_p} \frac{4 h_i}{N_c^2 A_c E_c} \left[2N_c \sin^2 \left(\frac{\pi}{N_c} \right) \left\{ (N_p-i) \tan \theta_i + \frac{h_0}{L} \right\}^2 \right. \\ & \left. + 2N_c \sin^2 \left(\frac{\pi}{N_c} \right) \tan \theta_i \left\{ (N_p-i) \tan \theta_i + \frac{h_0}{L} \right\} + \frac{N_c}{2} \tan^2 \theta_i \right] . \end{aligned}$$

The force carried by diagonal brace j of panel i is $(2P/N_c) \cos \phi_j \sec \theta_i$. So, the total axial strain energy, U_{db} , stored in all of the diagonal braces is

$$U_{db} = \sum_{j=1}^{N_c} \sum_{i=1}^{N_p} \frac{4P^2}{N_c^2} \cos^2 \phi_j \sec^2 \theta_i \frac{L_{0i}}{2A_0 E_0} ,$$

where L_{0i} is the length of diagonal brace of panel i , A_0 is the cross section area, and E_0 is the modulus of elasticity of the material of the diagonal braces. Using De Moivre's identity (Carmichael and Smith, 1962),

$$U_{db} = \sum_{i=1}^{N_p} \frac{2P^2}{N_c} \sec^2 \theta_i \frac{L_{0i}}{2A_0 E_0}, \quad (5.32)$$

and

$$\frac{\partial U_{db}}{\partial P} = F_2 P, \quad (5.33)$$

where

$$F_2 = \sum_{i=1}^{N_p} \frac{2}{N_c} \sec^2 \theta_i \frac{L_{0i}}{A_0 E_0}.$$

The axial force in beams in bay j in panel i is $(2P/N_c) \cos \phi_j$. So, using De Moivre's identity (Carmichael and Smith, 1962), the axial strain energy, U_b , stored in all beams is

$$U_b = \sum_{j=1}^{N_c} \sum_{i=1}^{N_p-1} \frac{4P^2}{N_c^2} \cos^2 \phi_j \frac{L}{2A_b E_b} = \frac{(N_p-1)LP^2}{N_c A_b E_b}, \quad (5.34)$$

where A_b is the cross section area of the beams. The strain energy stored in the beams located above the top panel is not considered, as these beams are assumed to be infinitely rigid. From Eq.(5.34)

$$\frac{\partial U_b}{\partial P} = F_3 P, \quad (5.35)$$

where

$$F_3 = \frac{2(N_p-1)L}{N_c A_b E_b}.$$

Hence, the total lateral displacement, δ_{lt} , caused by the lateral force P applied at centre of mass, considering the truss action alone is

$$\delta_{lt} = \frac{\partial U_c}{\partial P} + \frac{\partial U_{db}}{\partial P} + \frac{\partial U_b}{\partial P} = (F_1 + F_2 + F_3)P. \quad (5.36)$$

Therefore, the lateral stiffness, K_{tx} , due to truss action is

$$K_{tx} = \frac{1}{F_1 + F_2 + F_3}. \quad (5.37)$$

If all panels are of equal height, h , then Eq.(5.37) reduces to

$$K_{tx} = \frac{\frac{N_c A_0 E_0}{2N_p L_0} \cos^2 \theta_v}{1 + C_1 K_{arc} + C_2 K_{arb}}, \quad (5.38)$$

where θ_v is the common angle of inclination of diagonal braces in each panel in vertical plane. K_{arc} and K_{arb} represent the relative axial stiffness of diagonal braces with respect to that of columns and beams, respectively, given by

$$K_{arc} = \frac{A_0 E_0 / L_0}{A_c E_c / h}$$

and $K_{arb} = \frac{A_0 E_0 / L_0}{A_b E_b / L}$.

Also,

$$C_1 = \left\{ \frac{4(N_p^2 - 1)}{3} \sin^2 \left(\frac{\pi}{N_c} \right) + 1 \right\} \sin^2 \theta_v + (N_p + 1) \left(\frac{h_0}{L} \right) \sin 2\theta_v \sin^2 \left(\frac{\pi}{N_c} \right) + 4 \left(\frac{h_0}{L} \right)^2 \cos^2 \theta_v \sin^2 \left(\frac{\pi}{N_c} \right) \quad (5.39a)$$

and

$$C_2 = \frac{(N_p - 1)}{N_p} \cos^2 \theta_v. \quad (5.39b)$$

If lateral force, P , is applied at the top of the staging, then C_1 simplifies to

$$C_1 = \left\{ \frac{4(N_p^2 - 1)}{3} \sin^2 \left(\frac{\pi}{N_c} \right) + 1 \right\} \sin^2 \theta_v \quad (5.40)$$

5.5.1.2 Torsional Stiffness

If a torsional moment, T , is applied at top of the staging, then all bays share equal torsional shear force, F , given by

$$F = \frac{T}{N_c R_s \cos\left(\frac{\pi}{N_c}\right)} . \quad (5.41)$$

The axial compressive force, F_{ci} , in a column in panel i , is

$$F_{ci} = \frac{T \tan\theta_i}{N_c R_s \cos\left(\frac{\pi}{N_c}\right)} , \quad (5.42)$$

and the axial tensile force, F_{dbi} , in a diagonal brace in panel i , is

$$F_{dbi} = \frac{T \sec\theta_i}{N_c R_s \cos\left(\frac{\pi}{N_c}\right)} , \quad (5.43)$$

and the axial compressive force, F_b , in a beam, is

$$F_b = \frac{T}{N_c R_s \cos\left(\frac{\pi}{N_c}\right)} . \quad (5.44)$$

Therefore, axial strain energy, U_t , of the whole staging under torsional moment is

$$\begin{aligned} U_t &= \sum_{j=1}^{N_c} \sum_{i=1}^{N_p} \frac{T^2}{N_c^2 R_s^2 \cos^2\left(\frac{\pi}{N_c}\right)} \left[\frac{L_{0i} \sec^2\theta_i}{2A_0 E_0} + \frac{h_i \tan^2\theta_i}{2A_0 E_0} + \frac{L}{2A_b E_b} \right] \\ &= \sum_{i=1}^{N_p} \frac{T^2}{N_c^2 R_s^2 \cos^2\left(\frac{\pi}{N_c}\right)} \left[\frac{L_{0i} \sec^2\theta_i}{2A_0 E_0} + \frac{h_i \tan^2\theta_i}{2A_0 E_0} + \frac{L}{2A_b E_b} \right] . \end{aligned} \quad (5.45)$$

The beams at the top of the staging do not contribute to the strain energy as they are assumed to be rigid. And, hence, the rotation, θ_t , is given by

$$\theta_t = \frac{\partial U_t}{\partial T} = \sum_{j=1}^{N_c} \sum_{i=1}^{N_p} \frac{T}{N_c R_s \cos^2\left(\frac{\pi}{N_c}\right)} \left[\frac{L_{0i} \sec^2\theta_i}{A_0 E_0} + \frac{h_i \tan^2\theta_i}{A_c E_c} + \frac{L}{A_b E_b} \right] . \quad (5.46)$$

Therefore, the torsional stiffness, $K_{t\theta}$, of the complete staging due to

truss action is

$$K_{t\theta} = \frac{T}{\theta_t} = \sum_{i=1}^{N_p} \frac{N_c R_s^2 \cos^2 \left(\frac{\pi}{N_c} \right)}{\frac{L_{0i} \sec^2 \theta_i}{A_0 E_0} + \frac{h_i \tan^2 \theta_i}{A_c E_c} + \frac{L}{A_b E_b}} \quad (5.47)$$

If all panels are of equal height, then putting $h_i = h$ and $\theta_i = \theta_v$ in Eq.(5.47) gives

$$K_{t\theta} = \frac{\frac{A_0 E_0}{L_0} N_c R_s^2 \cos^2 \theta_v \cos^2 \left(\frac{\pi}{N_c} \right)}{N_p \left[1 + K_{arc} \sin^2 \theta_v + K_{arb} \frac{N_p^{-1}}{N_p} \cos^2 \theta_v \right]} \quad (5.48)$$

5.5.2 Total Stiffness of the Staging

5.5.2.1 Total Lateral Stiffness

The total lateral stiffness K_{bx} , of staging with diagonal braces is

$$K_{bx} = K_{tx} + K_x, \quad (5.49)$$

where K_x is the lateral stiffness due to frame action without considering the effect of diagonal braces and is given by Eq.(5.6).

5.5.2.2 Total Torsional Stiffness

The total torsional stiffness, $K_{b\theta}$, of a staging with diagonal braces is

$$K_{b\theta} = K_{t\theta} + K_\theta, \quad (5.50)$$

where K_θ is the torsional stiffness due to frame action without considering the effect of diagonal braces, and given by Eq.(4.14).

5.5.3 Natural Period Ratio (τ_b)

The natural period ratio (τ_b) of the staging with diagonal braces

divided by the natural period ratio (τ) of the basic configuration, is

$$\frac{\tau_b}{\tau} = \frac{T_{b\theta}/T_{bx}}{T_\theta/T_x} = \sqrt{\frac{K_{bx}/K_{b\theta}}{K_x/K_\theta}}, \quad (5.51)$$

where $T_{b\theta}$ and T_{bx} are the torsional and lateral natural periods, respectively, of the staging with diagonal braces. K_x/K_θ is obtained, from Eq.(4.42) dropping the contribution of axial deformation, as

$$\frac{K_x}{K_\theta} = \frac{1}{R_s^2} \left[\frac{N_p + \frac{(N_p - 1)K_r}{\cos^2\left(\frac{\pi}{N_c}\right)}}{N_p + 2(N_p - 1)K_r} \right]. \quad (5.52)$$

5.5.4 Results and Discussions

5.5.4.1 Expressions for Stiffnesses

The lateral and torsional stiffnesses of the two example tanks of Table 4.1 have been provided with diagonal braces and the stiffness calculated by the existing and proposed approximate methods. These are compared with the stiffnesses obtained by the FEM, termed as the exact solution (Table 5.4). The three types of braces considered are of 18mm diameter mild steel rods, 50mm diameter mild steel rods, and hypothetical braces with the cross section and material properties, *i.e.*, $A_c E_c$ and $E_c I_c$, respectively, same as those of columns.

The existing approximate procedure causes significant error in estimation of stiffness as the brace stiffness is increased. On the other hand, the proposed procedure works very well irrespective of the bracing stiffness. The error is within 10% when the lateral load is applied at top of staging, upto 22% when the load is applied at centre of mass, and within 5% for torsional stiffness. The increased error when

lateral load is applied at centre of mass is perhaps due to the assumption that each bay shares the moment Ph_0 in the same proportion as in case of lateral load P .

5.5.4.2 Effect of Addition of Diagonal Braces

A limited parametric study is presented here to show the effect of addition of diagonal braces on the natural period ratio. To limit the number of variables in this parametric study, a fictitious situation is considered wherein (a) all columns and beams have same cross-section, and (b) column length h and beam length L are equal. This implies $K_r=1$ and $K_{arc}=K_{arb}$. Moreover, the lateral load is assumed to be applied at staging top. With these considerations, K_{bx} and $K_{b\theta}$ simplify to

$$K_{bx} = \frac{12E_c I_c N_c}{h^3} \left[\frac{1}{3N_p - 2} + K_{arc} \frac{\left(\frac{h}{r_{cgyr}}\right)^2 \cos^2 \theta_v}{24N_p (1 + (C_1 + C_2) K_{arc})} \right] \quad (5.53)$$

and

$$K_{b\theta} = \frac{12E_c I_c N_c}{R_s^2 h^3} \left[\frac{1}{N_p + \frac{(N_p - 1)}{\cos^2 \left(\frac{\pi}{N_c}\right)}} + K_{arc} \frac{\left(\frac{h}{r_{cgyr}}\right)^2 \cos^2 \theta_v \cos^2 \left(\frac{\pi}{N_c}\right)}{12N_p \left[1 + \left\{ \frac{N_p - 1}{N_p} \cos^2 \theta_v + \sin^2 \theta_v \right\} K_{arc} \right]} \right], \quad (5.54)$$

where r_{cgyr} is the radius of gyration of the columns.

From Eq.(5.51), the parameters involved are N_p , N_c , K_{arc} , $(h/r_{cgyr})^2$ and θ_v . Since, it has been assumed that $h=L$, it implies that $\theta_v=45^\circ$. Since the diagonal braces are generally less stiff than columns and beams, K_{arc} is varied from 0 to 0.5. For elevated water tank

stagings, usually panel height varies from 3000 mm to 6000 mm and column diameter from 400 mm to 700 mm. Thus, $(h/r_{cgyr})^2$ takes values from about 300 to 3600. Only these extreme two values of $(h/r_{cgyr})^2$ are considered in the present study.

The variation of τ_b/τ with K_{arc} for extreme values of $(h/r_{cgyr})^2$ is presented in Figure 5.7. It is seen that τ_b/τ is always less than 1 implying that addition of diagonal braces decreases natural period ratio with respect to that of the stagings of basic configuration. Among the cases studied here, a maximum decrease of around 60% in natural period ratio of basic configuration is observed. The natural period ratio decreases as the axial stiffness of diagonal braces increases (K_{arc} large). Obviously, the ratio h/r_{cgyr} does not seem to have much bearing on τ_b/τ . The limited study presented here gives a qualitative idea about the effect of addition of diagonal braces on natural period ratio.

5.6 APPROACH FOR REDUCING TORSIONAL EFFECTS

The problem of closely-spaced lateral and torsional periods in frame stagings of basic configuration can be addressed in design by adjusting the parameters of the staging and/or by using one of the alternative configuration discussed in this chapter. A step-by-step procedure to achieve this is as follows:

1. The tank container is configured based on the considerations of container design. The staging radius is decided on the basis of container dimensions. The parameter $\rho (=R_{cgyr}/R_s)$ is calculated for tank-empty and tank-full conditions; for this the impulsive mass of water needs to be calculated using say Housner's analog model.

2. Choose the number of panels (N_p) and number of columns (N_c) in the usual manner and proportion the columns and beams for design gravity and lateral loads. It should be kept in view that tanks supported on stagings with more number of panels and more number of columns are less prone to torsional effects.
3. The torsional and lateral natural periods may be calculated, using the approximate expressions developed in this thesis. The ratio of these periods (τ) for tank-full and for tank-empty conditions should be checked to see if these lie in the critical range of $0.7 < \tau < 1.25$.
4. If the natural period ratio (τ) lies outside the critical region under both tank-empty and tank-full conditions, the staging configuration chosen is not expected to have significant torsional vibrations due to accidental eccentricity. If not, three distinct cases may arise (Figure 5.8):

Case 1: The natural period ratio (τ) is in critical region under tank-empty condition and not in the tank-full condition. In this case, it may be appropriate to reduce the time period ratio, i.e., decrease the torsional stiffness or increase the lateral stiffness. This can be done to a limited extent by changing N_p , N_c , or K_r . Figures 4.6 and 4.8 can be used as a guide. Else, one may introduce diagonal braces which will reduce τ .

Case 2: The natural period ratio (τ) lies in the critical region under both tank-empty and tank-full conditions. In this case, one can either reduce τ or increase τ so that it lies outside the critical region. One can achieve this by any of the four

alternate configurations discussed in this chapter.

Case 3: The natural period ratio (τ) lies in the critical region under tank-full condition but not under tank-empty condition.

In this case, it may be worthwhile to increase the values of τ by either changing N_p , N_c , and K_r , or by introducing any of the first three alternative configurations discussed in this chapter, i.e., with radial beams, with radial beams and central column, and with an additional circular row of columns.

5.7 SUMMARY AND CONCLUSIONS

The problem of closely-spaced torsional and lateral natural period in basic configuration may lead to large torsional response due to accidental eccentricity. This problem can be dealt with to some extent by changing the number of columns, number of beams, and the relative stiffness of columns and beams. However, it may be necessary to change the staging configuration such that the natural period ratio in tank-empty and tank-full conditions lies outside the critical region. In this chapter, four alternative configurations are studied: stagings with radial beams, stagings with radial beams and a central column, stagings with two circular rows of columns, and stagings with diagonal braces. Of these, the first three configurations are shown to have higher natural period ratio than that of the corresponding basic configuration, and the fourth configuration has a lower value. These can be usefully employed in staging design to avoid large torsional response. Approximate expressions for lateral and torsional stiffness

have been derived in this chapter which may prove useful in initial design. The efficacy of these approximate procedures has been tested on a number of staging configurations, results for two of those are presented. It is seen that the approximate procedures give very close estimates for stiffness. The alternate configurations discussed in this chapter are also useful for retrofitting the existing tanks, particularly the configurations with radial bracing only, and those with diagonal bracings.

5.8 REFERENCES

- Arya, A.S., and Ajmani, J.L., (1989), *Design of Steel Structures*, Nem Chand and Brothers, Roorkee, India.
- Carmichael, R.D., and Smith, R., (1962), *Mathematical Tables and Formulas*, Dover Publications, Inc., New York.
- Ramiah, B.K., and Gupta, D.S.R.M., (1966), "Factors Affecting Seismic Design of Water Towers," *Journal of Structural Division, Proceedings of ASCE*, Vol. 92, No. ST4, August, pp 13-27.
- SP22-1982, (1982), *Explanatory Handbook on Codes for Earthquake Engineering: IS:1893-1975 and IS:4326-1976*, Bureau of Indian Standards, New Delhi.
-

Table 5.1 : Performance of Proposed Approximate Expressions for Lateral Stiffness of Staging Radial Beams*

Effect due to	Tank	Lateral Stiffness (kN/m)		
		Exact Method	Proposed Approximate Method	% Error
(1)	(2)	(3)	(4)	(5)
Flexural Deformation of Columns	SP22 Example (no diagonal braces)	9,904	9,386	-5.2
	Text Book Example	10,309	10,171	-1.3
Axial Deformation of Columns	SP22 Example (no diagonal braces)	237,200	256,400	8.1
	Text Book Example	62,100	60,600	-2.4

* Radial beams have same cross-section as circumferential beams.

Table 5.2 : Performance of Approximate Expressions for Lateral Stiffness of Staging with Radial Beams and a Central Column*

Effect due to	Tank	Lateral Stiffness (kN/m)		
		Exact Method	Proposed Approximate Method	% Error
(1)	(2)	(3)	(4)	(5)
Flexural Deformation of Columns	SP22 Example (no diagonal braces)	12,128	11,730	-3.3
	Text Book Example	13,396	13,271	-0.9
Axial Deformation of Columns	SP22 Example (no diagonal braces)	249,000	256,400	3.0
	Text Book Example	61,800	60,600	-1.9

* Radial beams have same cross-section as circumferential beams.
Size of central column is same as of outer columns.

Table 5.3 : Performance of Proposed Approximate Expressions for Stiffness of Staging with Two Concentric Rows of Columns*

Effect due to	Tank	Lateral Stiffness (kN/m)		
		Exact Method	Proposed Approximate Method	% Error
(1)	(2)	(3)	(4)	(5)
Lateral Stiffness (kN/m)				
Flexural Deformation of Columns	SP22 Example (no diagonal braces)	27,615	26,824	-2.9
	Text Book Example	24,307	23,187	-4.6
Axial Deformation of Columns	SP22 Example (no diagonal braces)	331,300	320,500	-3.3
	Text Book Example	72,900	75,800	-4.0
Torsional Stiffness (kN m)				
Flexural Deformation of Columns	SP22 Example (no diagonal braces)	332,700	319,100	-4.1
	Text Book Example	168,400	164,200	-2.5

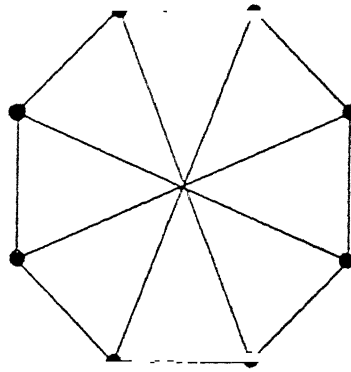
* All columns are identical and all beams are identical. Radius of inner row of columns is one half of the outer radius.

Table 5.4 : Performance of Proposed Approximate Expressions for Stiffness of Staging with Diagonal Braces

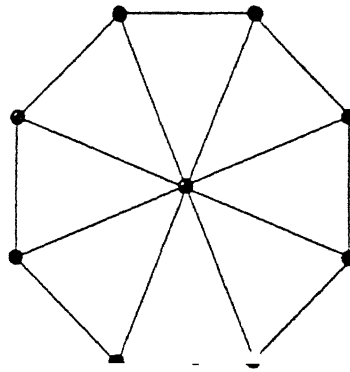
Tank	Diagonal Braces	Lateral Stiffness (kN/m)				
		Exact Method	Existing Approximate Method		Proposed Approximate Method	
			Absolute	% Error	Absolute	% Error
(1)	(2)	(3)	(4)	(5)	(6)	(7)
(a) LOAD APPLIED AT THE TOP OF THE STAGING						
SP22 Example	18mm ϕ	12,348	12,398	0.4	12,285	0.5
	50mm ϕ	34,775	41,346	18.9	35,598	2.4
	HB*	113,912	350,680	207.9	116,771	2.5
Text Book Example	18mm ϕ	10,173	10,872	6.9	10,818	6.3
	50mm ϕ	21,505	27,808	29.3	23,106	7.4
	HB*	62,189	262,886	322.7	67,963	9.3
(b) LOAD APPLIED AT CM LEVEL						
SP22 Example	50mm ϕ	19,146	27,422	43.2	22,635	18.2
	HB*	45,977	262,500	470.9	56,285	22.4

Tank	Diagonal Braces	Torsional Stiffness (10^5 kNm)				
		Exact Method	Existing Approximate Method		Proposed Approximate Method	
			Absolute	% Error	Absolute	% Error
(1)	(2)	(3)	(4)	(5)	(6)	(7)
SP22 Example	18mm ϕ	4.03	3.86	-4.2	3.84	-4.6
	50mm ϕ	13.23	13.86	4.8	12.96	-2.0
	HB*	66.23	120.80	82.4	65.44	-1.4
Text Book Example	18mm ϕ	1.71	1.68	-1.6	1.68	-1.7
	50mm ϕ	4.45	4.58	2.7	4.41	-1.0
	HB*	27.43	44.74	63.1	27.06	-1.4

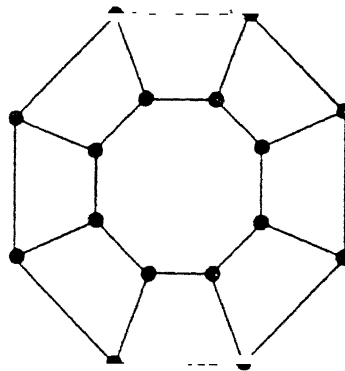
* Hypothetical brace; same section and material as that of columns



(a) Staging with radial beams



(b) Staging with radial beams
and a central column



(c) Staging with two-concentric rows
of columns, circumferential beams
and radial beams

Figure 5.1 : Plans of alternate staging configurations which increase natural period ratio, τ .

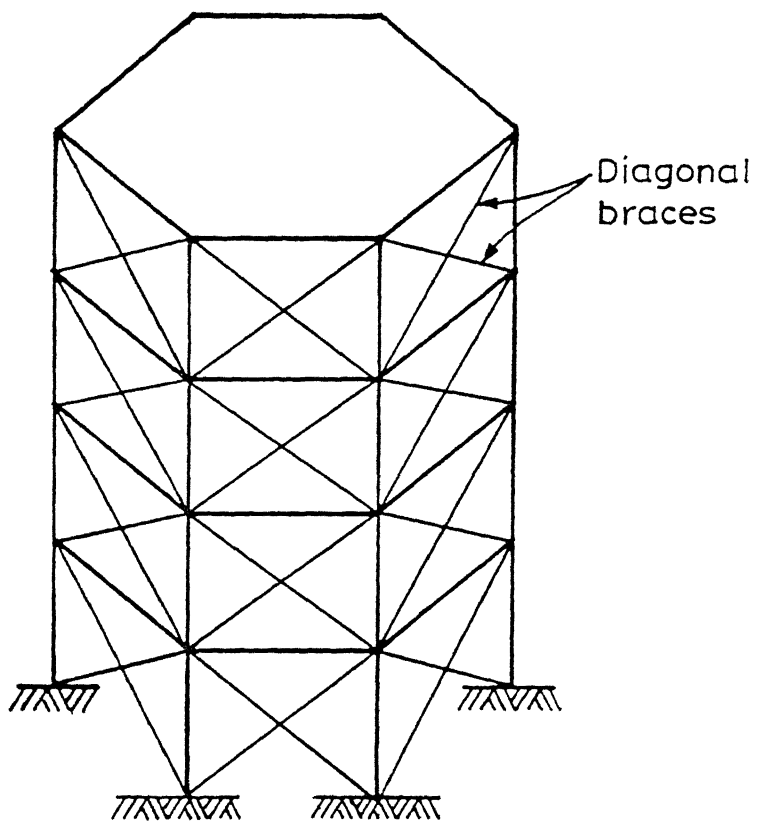


Figure 5.2 : Alternate configuration which decreases natural period ratio, τ .

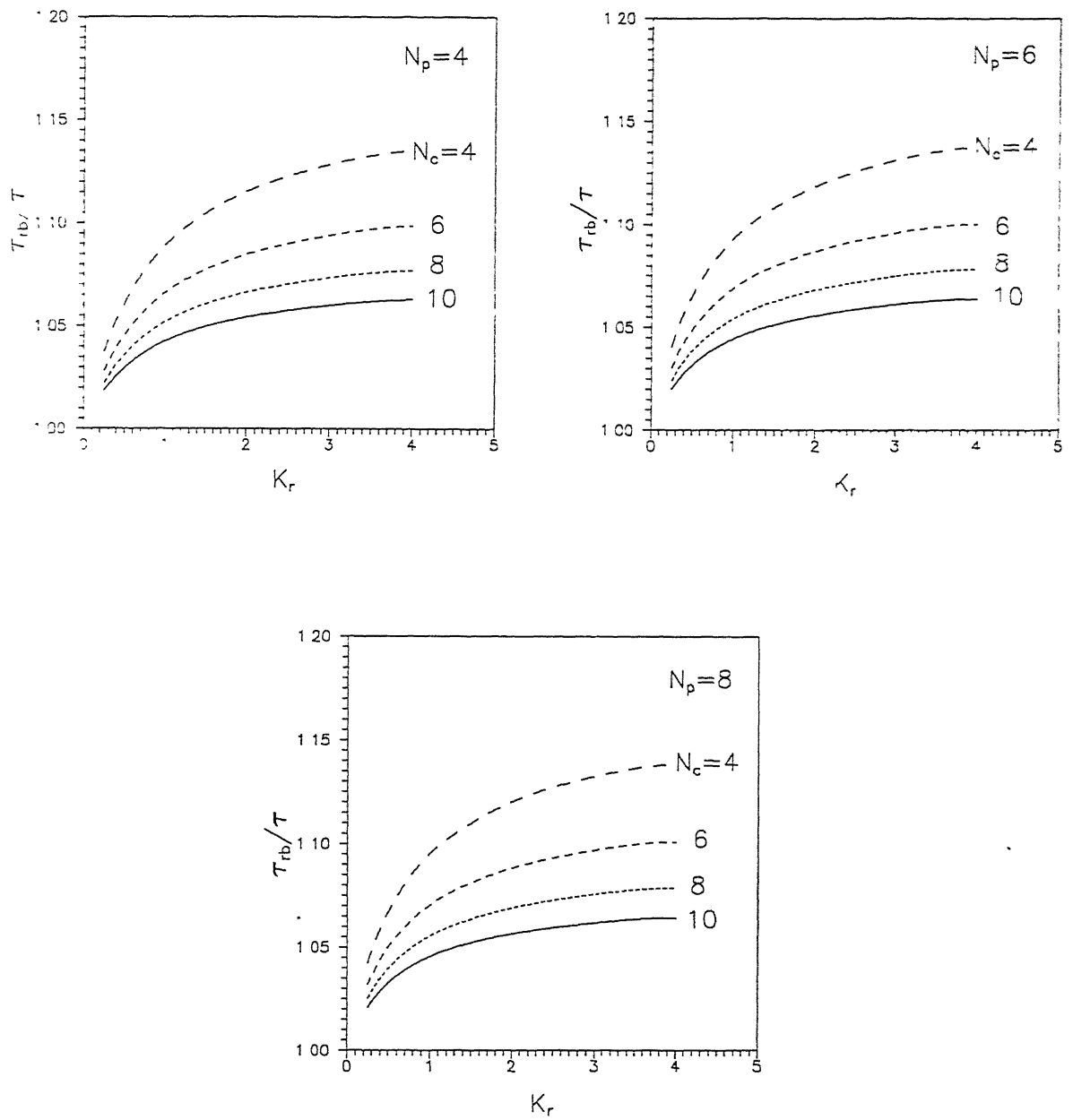


Figure 5.3 : Effect of radial beams on natural period ratio.

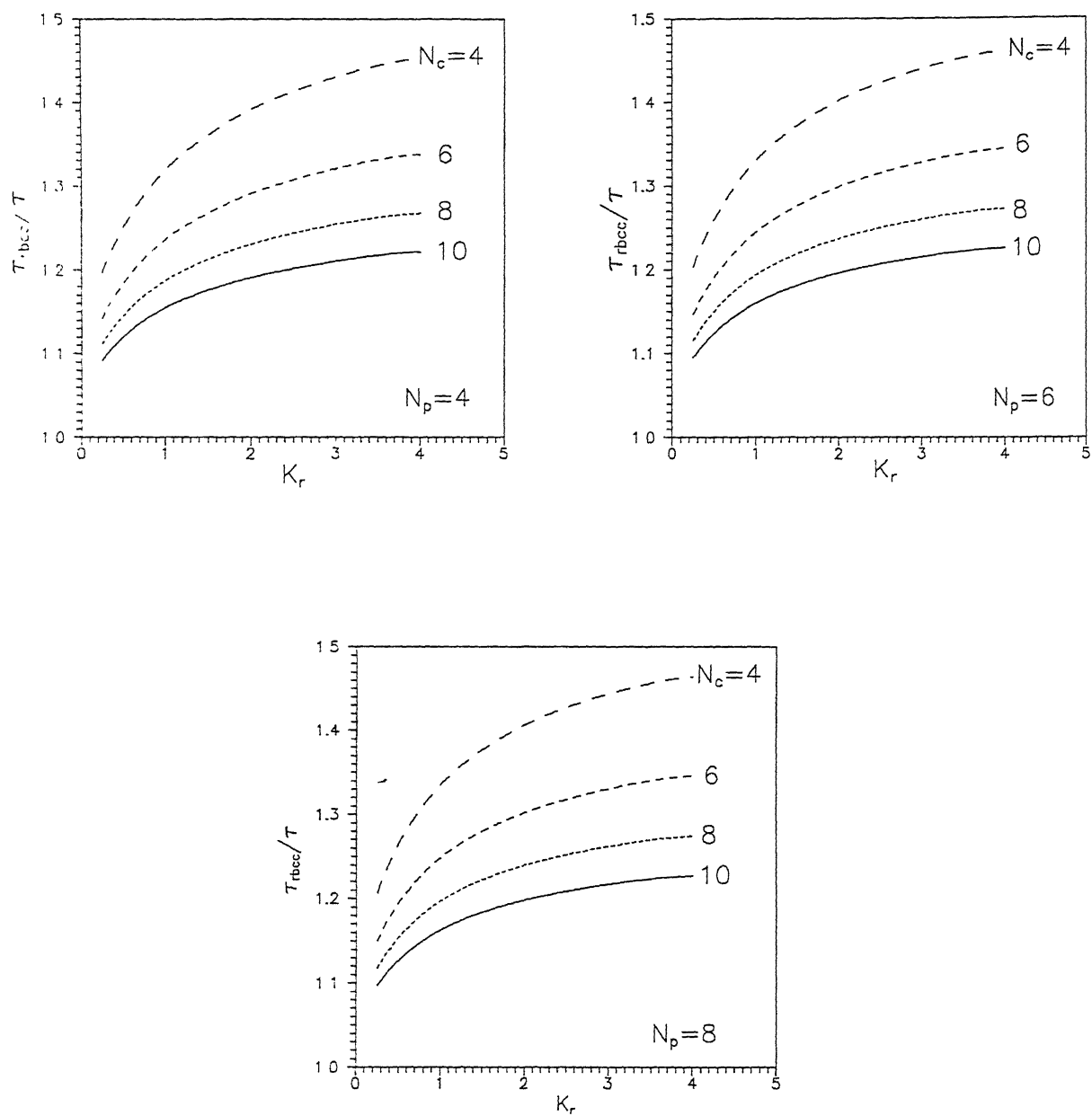


Figure 5.4 : Effect of radial beams and a central column on natural period ratio.

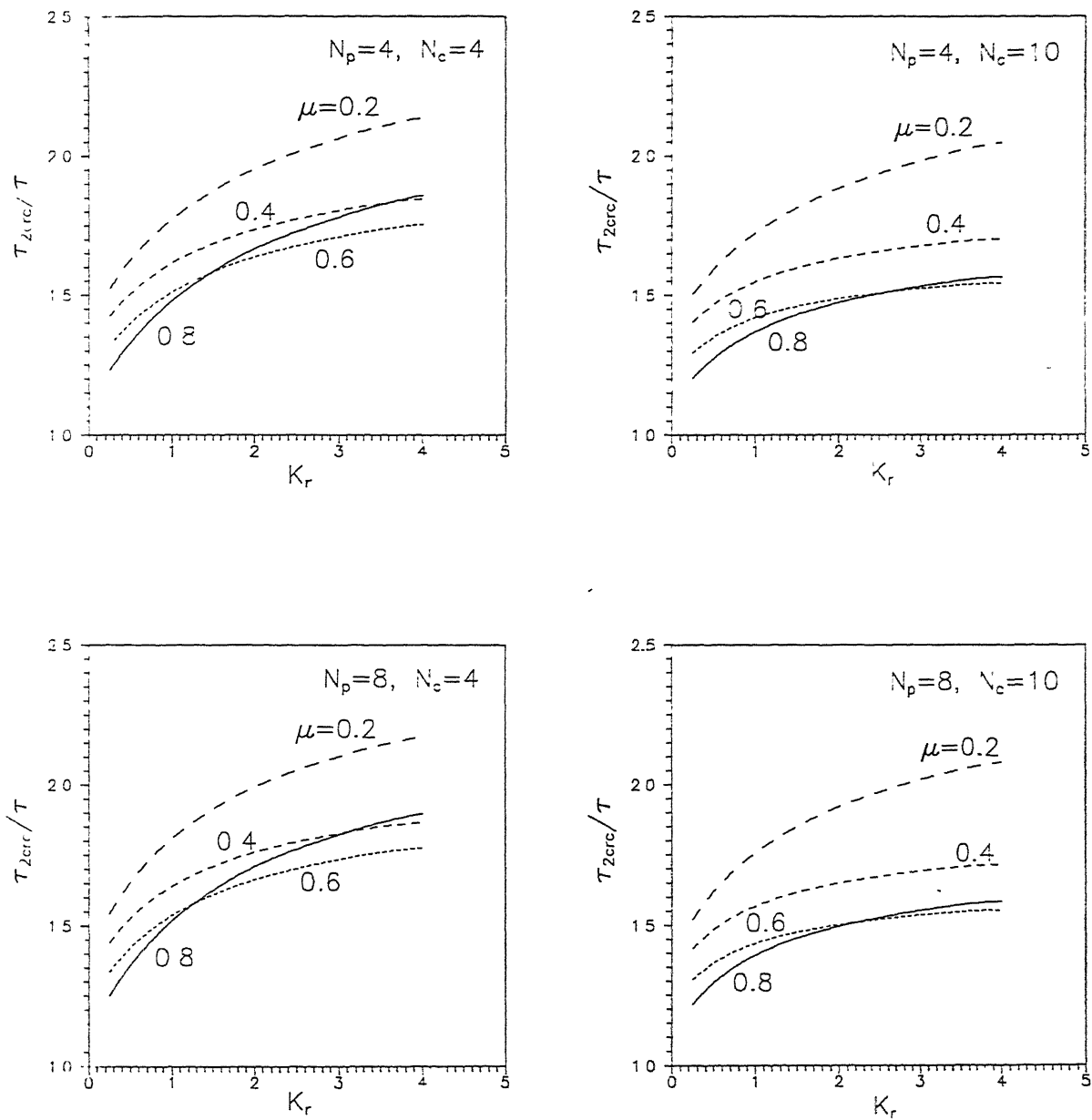
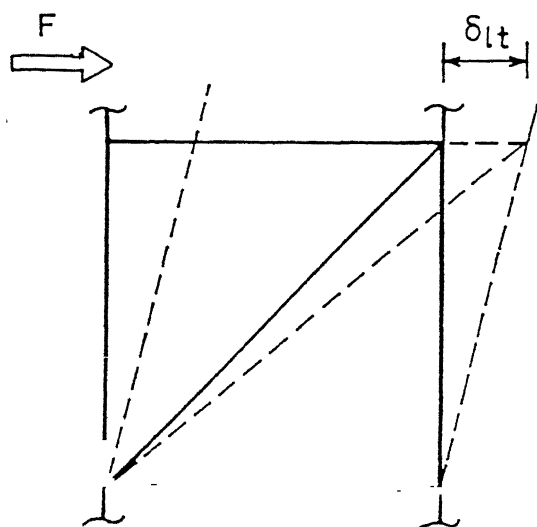
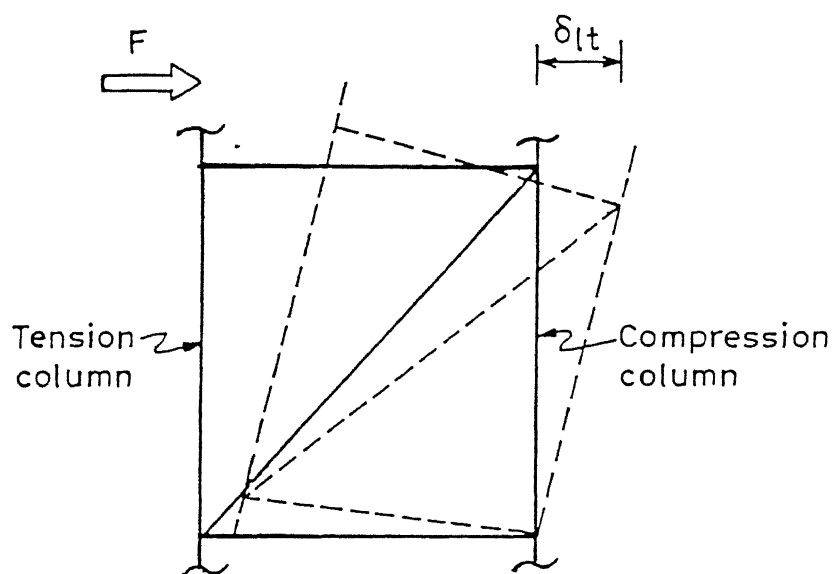


Figure 5.5 : Effect of an additional inner row of columns on natural period ratio.



(a) Existing approximate method
(Arya and Ajmani, 1989; Ramiah and Gupta, 1966)



(b) Proposed approximate method

Figure 5.6 : Relative deformation within a panel with diagonal braces.

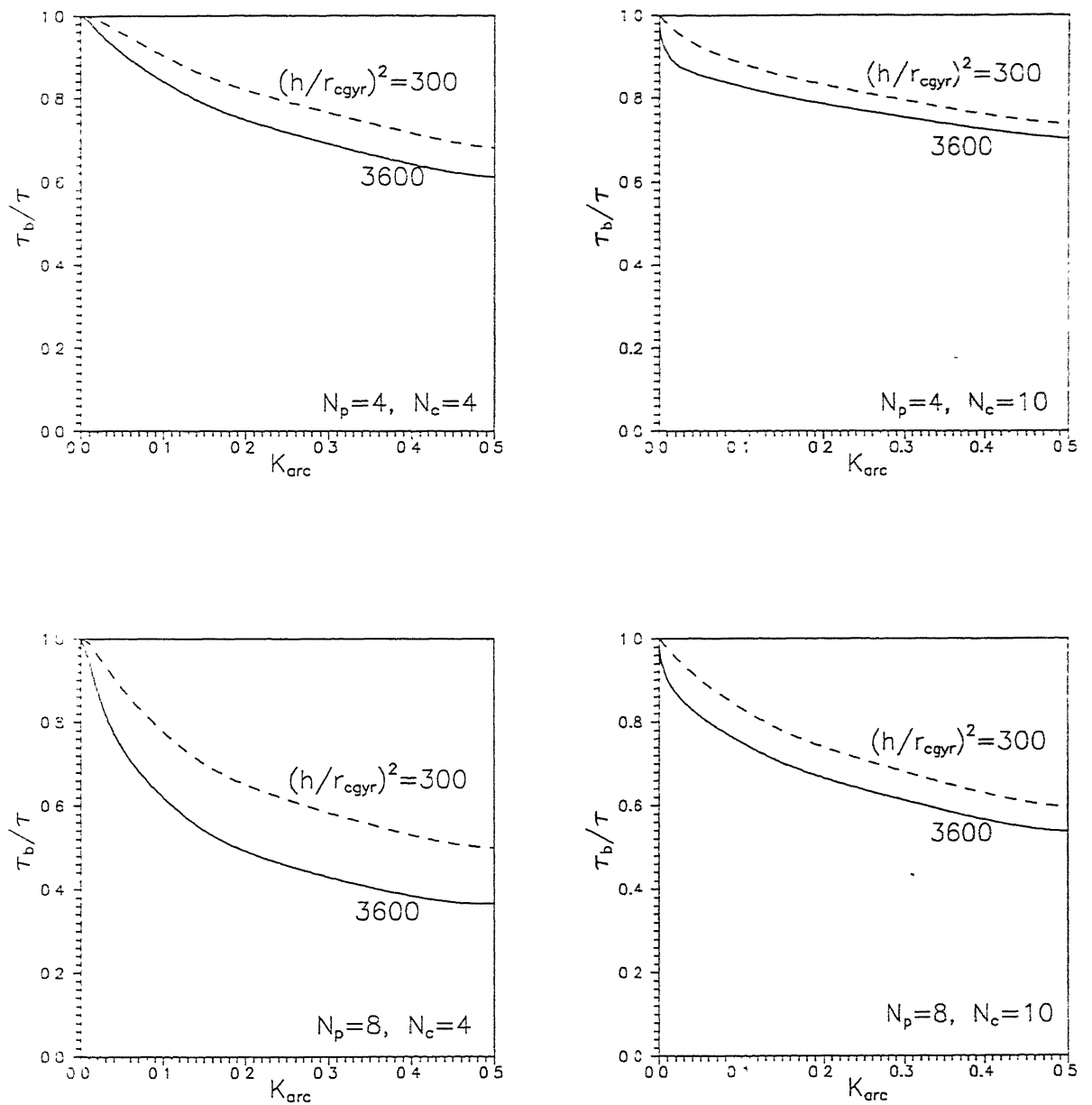


Figure 5.7 : Effect of diagonal braces on natural period ratio.

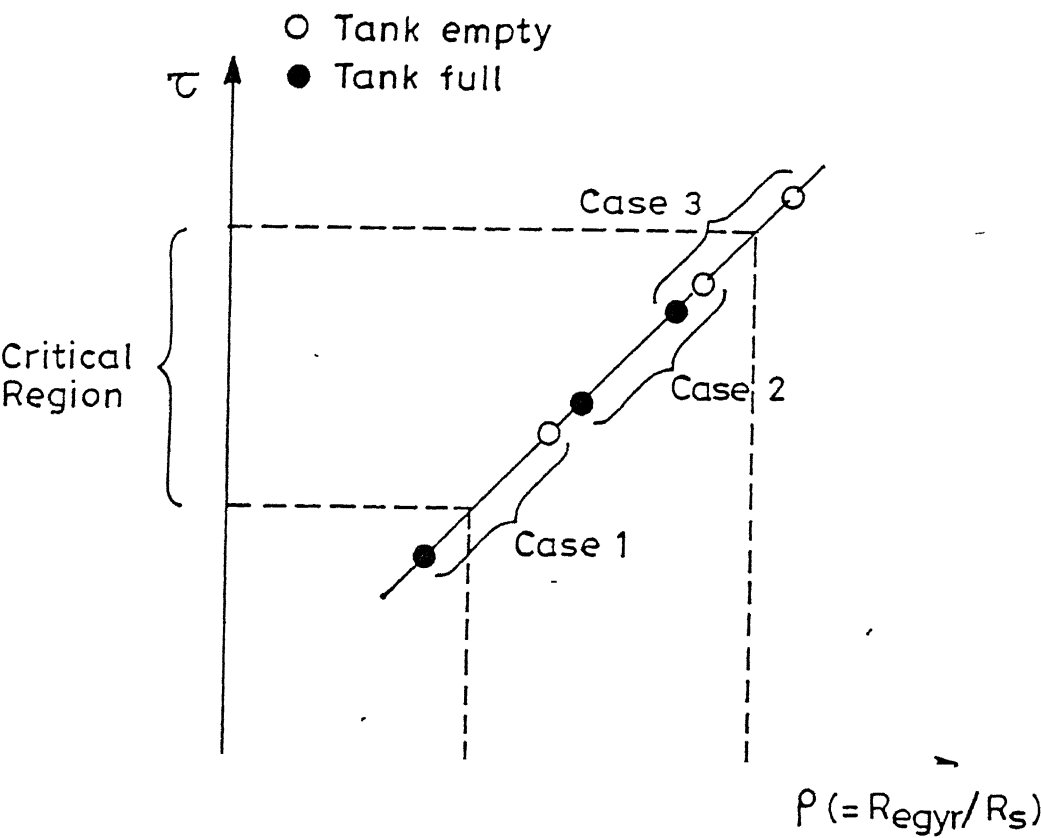


Figure 5.8 : Schematic of τ - ρ space showing the possible cases of vulnerability under tank-full and tank-empty conditions.

CHAPTER 6

SUMMARY AND CONCLUSIONS

6.1 SUMMARY

Torsional failure of elevated water tanks has been observed during past earthquakes. However, not much research has been conducted on this issue. The objectives of the present study are to better understand the behaviour and suggest means of overcoming the torsional failure in elevated water tanks. In particular, the present work is focussed on the study of reinforced concrete elevated water tanks supported on axisymmetric frame-type stagings.

The elevated water tanks are idealized as a simple one-storey lateral-torsional coupled systems, consisting of two or four lateral force-resisting elements depending on their torsional-to-lateral stiffness ratio. The linear responses of these idealized systems are studied under various representative ground motions. Responses under harmonic ground motions are analytically obtained, while those under spectrum-consistent synthetic ground motions are calculated by numerically integrating governing matrix equation. The CQC technique is used to combine the modal responses under idealized spectra, namely flat and hyperbolic spectra.

Inelastic response of the idealized systems is also studied under synthetic ground motions consistent with a typical design spectrum. For this purpose, an elastic-perfectly plastic but strength-deteriorating hysteresis behaviour is assumed in the individual lateral

force-resisting elements to model the progressive damage of reinforced concrete members. Inelastic responses under characteristic near-fault ground motions are also studied using an elastic-perfectly plastic behaviour for lateral force-resisting elements.

Reinforced concrete elevated water tanks supported on stagings with a single circular row of columns with circumferential beams at discrete levels, are very frequent in practice. Approximate analytical expressions for stiffness and member forces of such structures under lateral load is available in the literature. The present study extends this formulation to derive the expressions under torsional moment. Using these, an expression for torsional-to-lateral natural period ratio, τ , is derived. A parametric study is conducted to study the variations in τ with different parameters. A comparison of the member forces under torsional moment with those under lateral force, is made to check the adequacy of the members that are designed for a design lateral force, when the tank is subjected to torsion.

Four alternate staging configurations are proposed to reduce the effect of torsional coupling. Expressions for their lateral and torsional stiffnesses are also derived. Using these expressions, a parametric study is conducted for each of these alternate staging configurations to study the possible change in natural period ratio, τ .

6.2 CONCLUSIONS

Linear torsional response analyses of the idealized systems show that the element displacement versus torsional-to-lateral period ratio (τ) response has a minimum near $\tau=1$ and a maximum each on either side of

this minimum. These peaks of maxima usually lie within the range $0.7 < \tau < 1.25$. The element displacement under torsional coupling also depends on the torsional-to-lateral stiffness ratio in addition to the other parameters well-established in the literature. As a result, the torsional response of two-element systems having lower non-dimensionalized stiffness ratio, $K_\theta / (K_x D^2)$, and representing tanks on four columns and less number of panels is much higher than that of the four-element systems.

In the post-elastic range, the element displacement in small eccentricity systems is large with respect to symmetric systems, if the rate of strength deterioration is high. Even with a moderate rate of strength deterioration, the element displacement is large, if the structure is designed to respond inelastically with a ductility reduction factor of 2 or more. Idealized systems with two elements, representing staging with small number of panels and columns, are found to be more vulnerable to torsional response amplification than idealized systems with four elements representing stagings with many panels and columns. Also, the four-element idealized systems are more vulnerable under bi-directional ground motions as compared to that under uni-directional ground motion. Since, detuning of the torsional and lateral natural periods takes place in the post-elastic range, the particular trend of minimum element displacement at $\tau \approx 1$ with a maximum each on either side of it is not observed.

The study of the idealized systems subjected to near-fault characteristic ground motion pulses shows that the elevated water tanks may exhibit a very high ductility demand, irrespective of the existence

or otherwise of small eccentricity in them, if the duration of such pulses is larger than the lateral natural period of the tank.

Study of axisymmetric frame-type stagings with usual range of parameters for reinforced concrete water tanks shows that most such tanks may have the natural period ratio (τ) within the identified critical range. The study of the member forces shows that under torsional motion, the columns sustain higher force resultants *vis-a-vis* beams than under lateral motion. This problem is again more serious for four-column stagings as compared to stagings with large number of columns. This implies that large rotation of the tank may cause columns to yield prior to beams resulting in an early collapse.

Adopting suitable alternate staging configurations may change the natural period ratio so as to significantly reduce the torsional coupling. It is observed that addition of radial beams with or without a central column or the addition of another concentric circular row of columns within the staging increase τ , while addition of diagonal braces to the staging decreases τ . The parametric study conducted provides a suitable basis to identify an appropriate alternate staging configuration for a given case. Some of the alternate staging configurations proposed are also useful for retrofitting existing elevated water tanks to reduce the torsional coupling problem.

The study clearly underlines the potential of large torsional response due to accidental eccentricity even in this otherwise axi-symmetric structure. The four-column stagings are found to be particularly vulnerable to large torsional response. The tanks need to be detailed to minimize strength deterioration under cyclic response.

Also, these structures should be designed to respond more or less elastically under severe earthquake motions, *e.g.*, with low response reduction factor, to eliminate the possibility of high ductility demand in members due to small eccentricity or near-fault ground motion. To avoid the torsional amplification problem in the linear range, the frame stagings should be configured such that the natural period ratio (τ) is not in the range $0.7 < \tau < 1.25$.

The approximate formulations outlined for calculating torsional and lateral stiffness are reasonably accurate, and hence can be used in design, particularly at the initial stages. These formulations may also be used to cross-check the computer-based results obtained by the Finite Element Method.

6.3 RECOMMENDATIONS FOR FUTURE RESEARCH IN THIS AREA

The present study is a limited effort to understand and to try and solve the practical problem of torsional failure of elevated water tanks. The following studies may be useful to better address the vulnerability of elevated water tanks due to torsional coupling:

- (i) The post-elastic range behaviour can be studied under a large ensemble of earthquake data to confirm the trends observed in the present study.
 - (ii) Ambient vibration tests may be performed to obtain natural period ratio, τ , of a large number of existing elevated water tanks.
 - (iii) A detailed study needs to be made on the time period ratio of elevated water tank supported on (a) frame stagings with battered columns, and (b) cylindrical shaft.
-

- (iv) A rigorous finite element model of the actual inelastic dynamic response of elevated water tanks supported on axisymmetric frame type stagings may be made. Detailed modelling of member behaviour and consideration of secondary effects, may lead to a better understanding of the actual process of failure under torsional coupling.
-

APPENDIX A

TORSIONAL-TO-LATERAL STRENGTH RATIO

A.1 GENERAL

The ratio of the torsional strength, S_{θ} , to the lateral strength, S_x , influences the post-yield response of a lateral-torsionally coupled system. It is of interest to see how well the strength ratios (S_{θ}/S_x) of the idealized two-element and four-element coupled systems reflect the strength ratio of frame stagings of basic configuration. Herein, the values of strength ratio are estimated for frame-type stagings.

S_{θ} and S_x are estimated by carrying out plastic analysis using the failure mechanism method. The location of plastic hinges is decided based on moment capacities of columns *versus* beams at a given joint. The effect of axial load on bending moment capacity of the column is neglected in this analysis. Also, it is assumed that no column undergoes yield due to large axial force. These assumptions are reasonable for stagings in high seismic regions where column moments due to the lateral force are large and the columns are designed to undergo tension failure.

Depending on the plastic moment capacity of column (M_{pc}) and the plastic moment capacity of beam (M_{pb}), the plastic hinges may occur either in the columns or in the beams. Thus, the relative proportioning of strength of columns and beams plays a vital role to decide the failure mechanism. At the foundation and top ring beam levels, complete plastic hinges always occur at the column ends.

The relative proportions of moment capacities of columns and beams

are decided at the design stage. Three relative proportioning of column and beam are considered as follows.

- (a) The moment capacity in columns and beams are in the proportion of the bending moments derived by the approximate method of analysis under lateral load (Sameer and Jain, 1994), *i.e.*,

$$M_{pc} = M_{pb} \cos^2 \left(\frac{\pi}{N_c} \right), \quad (A.1)$$

- (b) The columns and beams may have the same moment capacities, *i.e.*,

$$M_{pc} = M_{pb}. \quad (A.2)$$

In this case, due to beam orientations, the hinges will form in beams prior to the columns, *i.e.*, strong-column weak-beam design.

- (c) The columns have half as much moment capacity as the beams, *i.e.*,

$$M_{pc} = 0.5M_{pb}. \quad (A.3)$$

This is the case of weak-column strong-beam design. For a four-column staging, Eq.(A.1) also reduces to Eq.(A.3).

A.2 ANALYSIS

A.2.1 Derivation of Lateral Strength (S_x)

Depending on the direction of the lateral load, the location of plastic hinges and the failure mechanism may change. The direction of lateral force may coincide with the line joining two diagonally-opposite columns (Figure 4.5a(i) and 4.5b(ii)). Or, the direction of lateral force may be such that it is perpendicular to the diagonally-opposite circumferential beams (Figure 4.5a(ii) and 4.5b(i)). For example, in a six-column staging, two different mechanisms (Figure A.1) develop depending on the direction of lateral force. These mechanisms correspond to the relative moment capacities given by Eq.(A.1). In the first case,

except for the two farthest columns from the bending axis, all other columns develop plastic hinges at all joints (Figure A.1a). In the second case, except in the four columns which are farthest from the bending axis, plastic hinges develop in all columns at all joints.

In plastic analysis, to write the expression for work done, the component of plastic moment in the direction of hinge rotation is required. In beams, since the moments act on the vertical plane passing through the longitudinal axis of beam, the component effective in the direction of lateral force can be derived. In columns, the plane of action of the plastic moments developed are not explicitly known. So, its component acting in the direction of lateral force cannot be derived. The following two extreme cases of plastic moment of columns M^* effective in the direction of lateral load are considered:

$$(i) \quad M^* = M_{pc} , \quad (A.4)$$

$$\text{and} \quad (ii) \quad M^* = 0.5 M_{pc} , \quad (A.5)$$

The first case will clearly overestimate the value of S_x while the second case appears more reasonable. Considering all the above aspects, the expression for lateral strength (S_x) is derived.

A.2.2 Derivation of Torsional Strength (S_θ)

Two failure mechanisms are possible under torsional moment. For designs given by Eq.(A.1) and Eq.(A.3), the panel-sway mechanism develops wherein all the columns of a single panel develop plastic hinges at their both ends and create a mechanism (Figure A.2(a)). For the design given by Eq.(A.2), the beams develop plastic hinges at the two ends at all intermediate beam levels and the columns develop hinges

at the foundation and the top ring beam levels (Figure A.2b). These are used for estimating the torsional strength (S_θ).

A.3 RESULTS

The expressions for S_θ/S_x are derived for the general case of a staging with N_p panels and N_c columns, considering the relative moment capacities of columns and beams and the column moment effective in the direction of lateral force. These expressions are given in the following. R_s is the radius of the staging.

A.3.1 Design with $M_{pc} = M_{pb} \cos^2\left(\frac{\pi}{N_c}\right)$

Case (i) : $M^* = M_{pc}$

$$\frac{S_\theta}{S_x} = \begin{cases} \frac{N_p}{1 + \frac{(N_p-1)(N_c-2)}{N_c} + \frac{2(N_p-1)\sin\left(\frac{\pi}{N_c}\right)}{N_c \cos^2\left(\frac{\pi}{N_c}\right)}} R_s, & \text{for lateral load passing through two diametrically opposite columns} \\ \frac{N_p}{1 + \frac{(N_p-1)(N_c-4)}{N_c} + \frac{2(N_p-1)\sin\left(\frac{2\pi}{N_c}\right)}{N_c \cos^2\left(\frac{\pi}{N_c}\right)}} R_s, & \text{for lateral load perpendicular to two circumferential beams} \end{cases} \quad (A.7)$$

Case (ii) : $M^* = 0.5 M_{pc}$

$$\frac{S_\theta}{S_x} = \begin{cases} \frac{N_p}{1 + \frac{0.5(N_p-1)(N_c-2)}{N_c} + \frac{2(N_p-1)\sin\left(\frac{\pi}{N_c}\right)}{N_c \cos^2\left(\frac{\pi}{N_c}\right)}} R_s, & \text{for lateral load passing through two diametrically opposite columns} \\ \frac{N_p}{1 + \frac{0.5(N_p-1)(N_c-4)}{N_c} + \frac{2(N_p-1)\sin\left(\frac{2\pi}{N_c}\right)}{N_c \cos^2\left(\frac{\pi}{N_c}\right)}} R_s, & \text{for lateral load perpendicular to two circumferential beams} \end{cases} \quad (A.8)$$

A.3.2 Design with $M_{pc} = M_{pb}$

For such a design of relative column and beam moment capacities, the equilibrium of the joints suggests that no plastic hinges will be formed in the columns, except at the top ring beam and foundation levels. At the top ring beam and foundation levels, M^* is always equal to M_{pc} . Hence, $M^* = 0.5M_{pc}$ need not be considered. And, S_θ/S_x is given by:

$$\frac{S_\theta}{S_x} = \begin{cases} \frac{(N_p - 1)N_c \cos\left(\frac{\pi}{N_c}\right) + N_c}{2(N_p - 1)\operatorname{cosec}\left(\frac{\pi}{N_c}\right) + N_c} R_s, & \text{for lateral load passing through two diametrically opposite columns} \\ \frac{(N_p - 1)N_c \cos\left(\frac{\pi}{N_c}\right) + N_c}{2(N_p - 1)\cot\left(\frac{\pi}{N_c}\right) + N_c} R_s, & \text{for lateral load perpendicular to two circumferential beams} \end{cases} \quad (A.9)$$

A.3.3 Design with $M_{pc} = 0.5M_{pb}$

Case (i): $M^* = M_{pc}$

$$\frac{S_\theta}{S_x} = \begin{cases} \frac{N_p}{1 + \frac{(N_p - 1)(N_c - 2)}{N_c} + \frac{4(N_p - 1)\sin\left(\frac{\pi}{N_c}\right)}{N_c}} R_s, & \text{for lateral load passing through two diametrically opposite columns} \\ \frac{N_p}{1 + \frac{(N_p - 1)(N_c - 4)}{N_c} + \frac{4(N_p - 1)\sin\left(\frac{2\pi}{N_c}\right)}{N_c}} R_s, & \text{for lateral load perpendicular to two circumferential beams} \end{cases} \quad (A.10)$$

Case (ii): $M^* = 0.5 M_{pc}$

$$\frac{S_\theta}{S_x} = \begin{cases} \frac{N_p}{1 + \frac{(N_p - 1)(N_c - 2)}{2N_c} + \frac{4(N_p - 1)\sin\left(\frac{\pi}{N_c}\right)}{N_c}} R_s, & \text{for lateral load passing through two diametrically opposite columns} \\ \frac{N_p}{1 + \frac{(N_p - 1)(N_c - 4)}{2N_c} + \frac{4(N_p - 1)\sin\left(\frac{2\pi}{N_c}\right)}{N_c}} R_s, & \text{for lateral load perpendicular to two circumferential beams} \end{cases} \quad (A.11)$$

A.4 COMMENTS

The expressions presented in section A.3.1 and A.3.3 are not valid for four-column stagings. Under these two designs of $M_{pc} = M_{pb} \cos^2\left(\frac{\pi}{N_c}\right)$ and $M_{pc} = 0.5 M_{pb}$, panel sway mechanisms occur in four-column stagings under lateral force as well as torsional moment.

Table A.1 shows the limiting values of S_θ/S_x ratio when $N_c=4$, $N_p=1$ and when $N_p \rightarrow \infty$, $N_c \rightarrow \infty$ for the three possible designs of relative column and beam moment capacities corresponding to the two cases of effective column moment in the direction of lateral force. It is obvious that the ratio (S_θ/S_x) approaches R_s for low number of columns and panels; this is same as for the two-element systems. For stagings with large number of columns and panels, the strength ratio is R_s^* when M is assumed equal to M_{pc} in weak-column designs. However, this situation is hypothetical since the moment component in the direction of rotation is going to be less than the moment capacity. With $M^* = 0.5M_{pc}$ assumption the strength ratio is $2R_s$ while for strong-column weak-beam designs it is $1.57R_s$. Value of $2R_s$ matches with that for the four-element systems studied in Chapter 3. Hence, the two- and four-element systems studied in Chapter 3 seem to reasonably well model the strength ratio of realistic stagings with small number of columns/panels and large number of columns/panels, respectively.

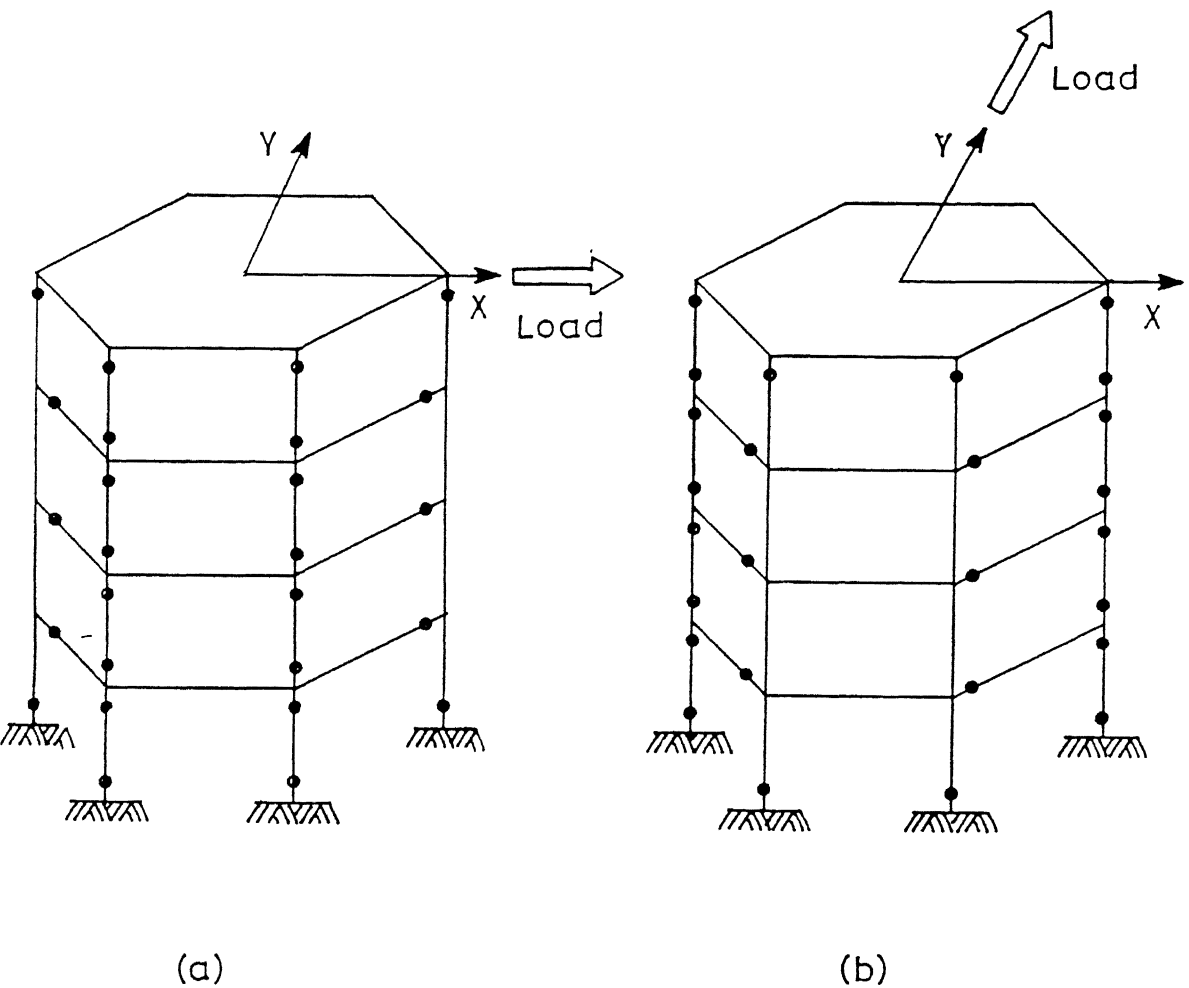
A.5 REFERENCE

Sameer, U.S., and Jain, S.K., (1994), "Lateral-Load Analysis of Frame Stagings for Elevated Water Tanks," *Journal of Structural Engineering*, ASCE, Vol.120, No.5, May, pp 1375-1394.

Table A.1 : Limiting Values of Strength Ratio (S_{θ}/S_x) for Different Designs Considered.

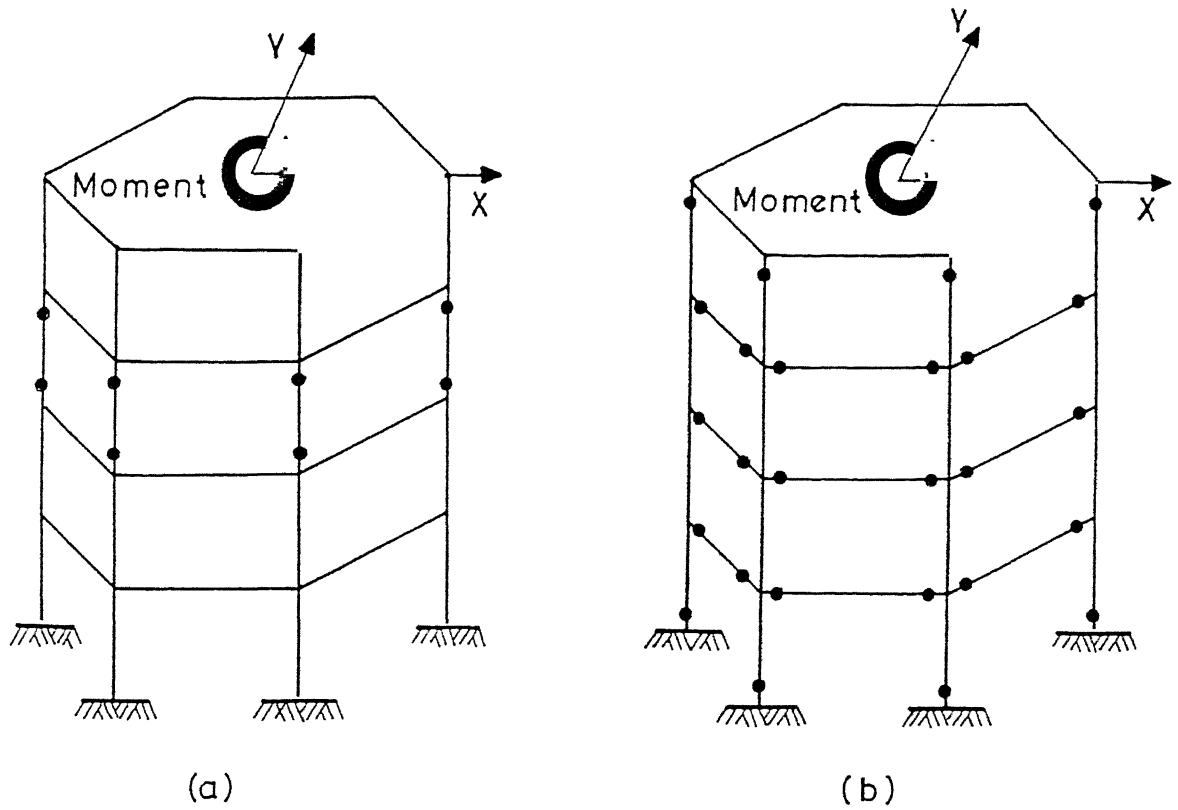
Beam-Column Design	Torsional-to-Lateral Strength Ratio (S_{θ}/S_x)			
	$N_c=4$ and $N_p=1$		$N_c \rightarrow \infty$ and $N_p \rightarrow \infty$	
	$M^* = M_{pc}$	$M^* = 0.5M_{pc}$	$M^* = M_{pc}$	$M^* = 0.5M_{pc}$
$M_{pc} = M_{pb} \cos^2\left(\frac{\pi}{N_c}\right)$	R_s	††	R_s	$2R_s$
$M_{pc} = M_{pb}$	R_s	††	R_s	$2R_s$
$M_{pc} = 0.5M_{pb}$	R_s	††	$\frac{\pi}{2} R_s$	††

†† Column moment always acts in the direction of lateral force.
Hence, the case of $M^* = 0.5M_{pc}$ does not arise.



Plastic hinges are shown by dots (•) on the members

Figure A.1 : Two possible mechanisms in tank stagings due to two different orientations of lateral load.



Plastic hinges are shown by dots (•) on the members

Figure A.2 : Two possible mechanisms in tank stagings due to torsional moment.

Δ 22910

22910
Date Slip

Date Slip

This book is to be returned on the
date last stamped.

This image shows a single sheet of white paper with horizontal blue or grey ruling lines. A vertical line runs down the center of the page, creating two equal-width columns. The lines are evenly spaced and extend across the entire width and height of the page. There is no handwriting or other markings on the paper.

CE-1995-D-DUT-TOR



A121910